LBL--27155

DE89 012995

A Molecular Genetic Analysis of Carotenoid Biosynthesis and the Effects of Carotenoid Mutations on other Photosynthetic Genes in *Rhodobacter capsulatus*

by

Gregory Aleksandr Armstrong
(Ph.D. Thesis)

Chemical Biodynamics Division
Lawrence Berkeley Laboratory
1 Cyclotron Road
Berkeley, California 94720

April 1989

DISCLAIMER

This work was supported by the U.S. Department of Energy under Contract No. DE-AC03-76SF00098

A molecular genetic analysis of carotenoid biosynthesis and the effects of carotenoid mutations on the photosynthetic phenotype of Rhodobacter capsulatus

by

Gregory Aleksandr Armstrong

Abstract

Rhodobacter capsulatus, a metabolically versatile purple, non-sulfur photosynthetic bacterium, provides an attractive system for genetic and biochemical studies of carotenoid biosynthesis. The nine known R. capsulatus carotenoid genes are contained within the 46 kilobase (kb) photosynthesis gene cluster. An 11 kb subcluster containing eight of these genes has been cloned and its nucleotide sequence determined. A new gene, crtK , has been located in the middle of the subcluster. The carotenoid gene cluster contains sequences homologous to Escherichia coli σ^{70} promoters, rho-independent transcription terminators, and prokaryotic transcriptional factor binding sites. The phenotypes and genotypes of ten transposon Tn5.7 insertion mutations within the carotenoid gene cluster have been analyzed, by characterization of the carotenoids accumulated and high resolution mapping of the Tn5.7 insertions. The enzymatic blockages in previously uncharacterized early carotenoid mutants have been determined using a new in vitro synthesis system, suggesting specific roles for the CrtB and CrtE gene products. The expression of six of the eight carotenoid genes in the cluster is induced upon the shift from dark chemoheterotrophic to anaerobic photosynthetic growth. The magnitude of the induction is equivalent to that of genes encoding structural photosynthesis polypeptides, although the carotenoid genes are induced earlier after the growth shift. Different means of regulating photosynthesis genes in R. capsulatus are discussed, and a rationale for the temporal

pattern of expression of the carotenoid genes during photosynthetic adaptation is presented. Comparison of the deduced amino acid sequences of the two dehydrogenases of the R. capsulatus carotenoid biosynthesis pathway reveals two regions of strong similarity. The effect of carotenoid mutations on the photosynthetic phenotype has been studied by examining growth rates, pigments, pigment-protein complexes and gene expression for a complete set of carotenoid mutants. The pigment synthesis gene cluster of Erwinia herbicola, a gram-negative nonphotosynthetic bacterium, provides a second model system for carotenoid biosynthesis. The E. herbicola genes, resident in E. coli, have been shown to direct the synthesis of carotenoids derived from phytoene by the use of chemical inhibitors of carotenoid biosynthesis.

I dedicate this thesis to my mother and the memory of my father

Acknowledgments

I would like to acknowledge the contributions of the many people who have not only made this work possible, but who are also friends, and who have helped to make this a safe, sane and fun thesis!

To those who along the way have taught a naive chemist something about molecular genetics and biochemistry, including particularly Francesca Leach, Kris Zsebo, and Yu Sheng Zhu, I give my thanks. I wish to acknowledge Marie Alberti for the contribution of her invaluable expertise and ability in DNA sequencing and for her incredible energy, her unflagging optimism and her constant thoughtfulness. Without Marie's efforts much of the work presented here would not have been possible. I also acknowledge all of my lab comrades for their stimulating discussions and ideas. I would like to especially thank Dave Cook for sharing the broad scope of his thinking and for his help in the design and execution of the aerobic to photosynthetic shift experiments, and Francesca for her constant friendship, advice, and for the initial subcloning of the R. capsulatus photosynthesis genes. I also thank Arno Schmidt for his insights and understanding, as well as his contribution of the development of the in vitro carotenoid biosynthesis system and the analysis of the R. capsulatus blue-green mutants.

I thank John Hearst, Ken Sauer, and Willi Gruissem for their critical comments on this thesis and John for guiding my research, while granting the freedom which allowed my interests to evolve and mature scientifically. I feel very fortunate to have worked under John's direction and to have been exposed to his constant fascination and excitement with science. I thank him not only for his scientific support but for his interest in his students as human beings, and for recognizing that the most important aspects of life lie outside the lab.

I thank all of my friends for making my time in Berkeley much more than a scientific undertaking, especially Gerry and Bernie (who have always known when to explore Death

Valley), Karen (who knows when to drop in unexpectedly), Tina (who has made possible many adventures with her unbridled enthusiasm), Michel and Karin (who know a good cup of coffee when they see it). These friends and many others have always known when to call, when to visit, or when to plan a trip to revive a weary researcher. I reserve a special and unique thanks for Catharina Maulbecker, who has been both my toughest critic and my greatest friend and with whom I have learned so much about myself and the world during the last five years. Finally, I thank my mother for her advice, understanding and support of my efforts through a decade of college.

Table of contents

Chapter 1: Introduction to the study of carotenoids, using Rhodobacter capsulatus and Erwinia herbicola as model systems

I. A review of carotenoids, their distribution and biosynthesis

"There would be no photosynthesis as we now recognize it were it not for the presence of carotenoids!" (Cogdell and Frank, 1987).

The term carotenoid is used to refer to any member of a large class of naturally distributed isoprenoid pigments. Over 500 different carotenoids have now been identified and the number continues to grow (Britton, 1983). Most carotenoids are composed of a linear C_{40} hydrocarbon backbone containing a series of conjugated double bonds. The backbone is constructed from eight C_5 isoprenoid units. The number of double bonds in the polyene system gives particular carotenoids their characteristic colors and absorption spectra, as exemplified in Fig. 1-1 for phytoene and lycopene, two important and widely distributed compounds. Carotenoids which are derivatized with oxygen-containing functions, such as hydroxy, methoxy, oxo or epoxy groups, aldehydes or carboxylic acids, are termed xanthophylls (Britton, 1983). Carotenoids also exist as esters or glycosides.

The C_{40} carotenoid backbone is sometimes further extended to give C_{45} or C_{50} species, or shortened yielding apocarotenoids or norcarotenoids (Goodwin, 1980; Britton, 1983; Bramley and Mackenzie, 1988). Some nonphotosynthetic bacteria also synthesize C_{30} carotenoids derived from the C_{15} precursor FPP rather than the normal C_{20} precursor GGPP (Fig. 1-2). These carotenoid variants will not be further discussed here.

All photosynthetic organisms from bacteria through algae to higher plants synthesize carotenoids. Carotenoids are also produced by some nonphotosynthetic bacteria, fungi, and red yeasts (reviewed in Goodwin, 1980). About 1×10^8 tons of carotenoids

Figure 1-1. Structures and spectra of phytoene and lycopene isolated from radish (spectra from Grumbach, 1983). Spectra were taken in petroleum ether. Note the red-shifting of the characteristic three peak carotenoid absorption spectrum as the number of conjugated double bonds increases from three in phytoene to eleven in lycopene. Lycopene has a reddish-orange color while phytoene absorbs only in the UV.

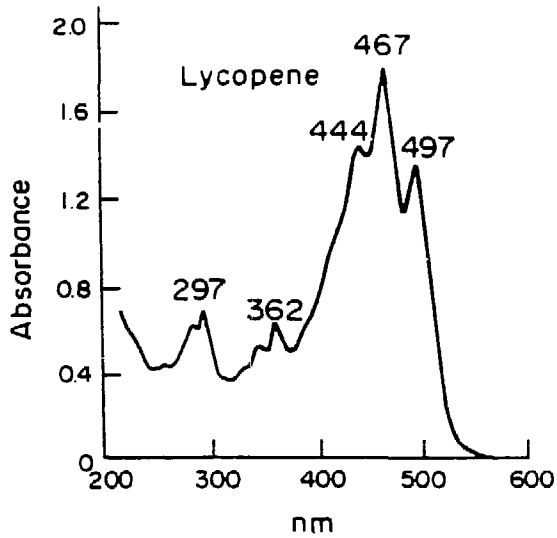
Lycopene
467
444
497
297
362
Absorbance
2.0
1.6
1.2
0.8
0.4
0
200
300
400
500
600
nm

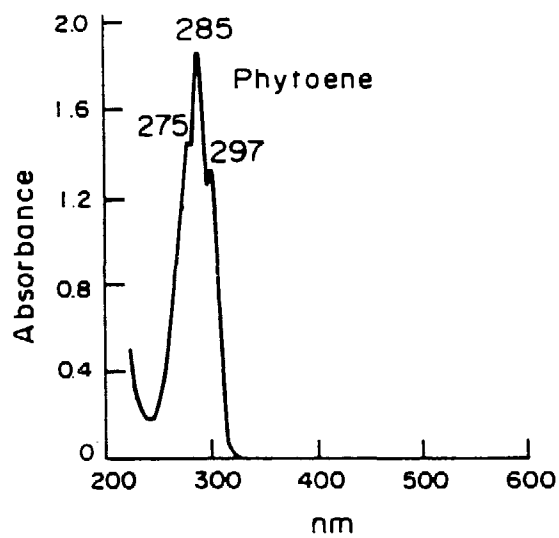
285
Phytoene
275
297
Absorbance
2.0
1.6
1.2
0.8
0.4
0
200
300
400
500
600
nm

Figure 1-2. The general carotenoid biosynthetic pathway from the condensation of IPP to the formation of cyclic carotenes based on reviews by Goodwin (1980) and Bramley and Mackenzie (1988). Compounds from IPP to GGPP are used in other branches of isoprenoid metabolism, including the synthesis of Chl and Bchl (Britton, 1983). Phytoene and some of the other early C_{40} carotenoids occur as cis isomers in some organisms, although the majority of carotenoids are found as the all-trans isomers (Goodwin, 1980; Britton, 1983). ζ-carotene is the usual intermediate, although 7, 8, 11, 12-tetrahydrolycopene occurs in certain photosynthetic bacteria (Goodwin, 1980). Compounds with heptaene or longer chromophores absorb at visible wavelengths (Britton, 1983). Abbreviations used in this figure and throughout the text are: IPP, isopentenyl pyrophosphate; DMAPP, dimethylallyl pyrophosphate; GPP, geranyl pyrophosphate; FPP, farnesyl pyrophosphate; GGPP, geranylgeranyl pyrophosphate; PPPP, prephytoene pyrophosphate.

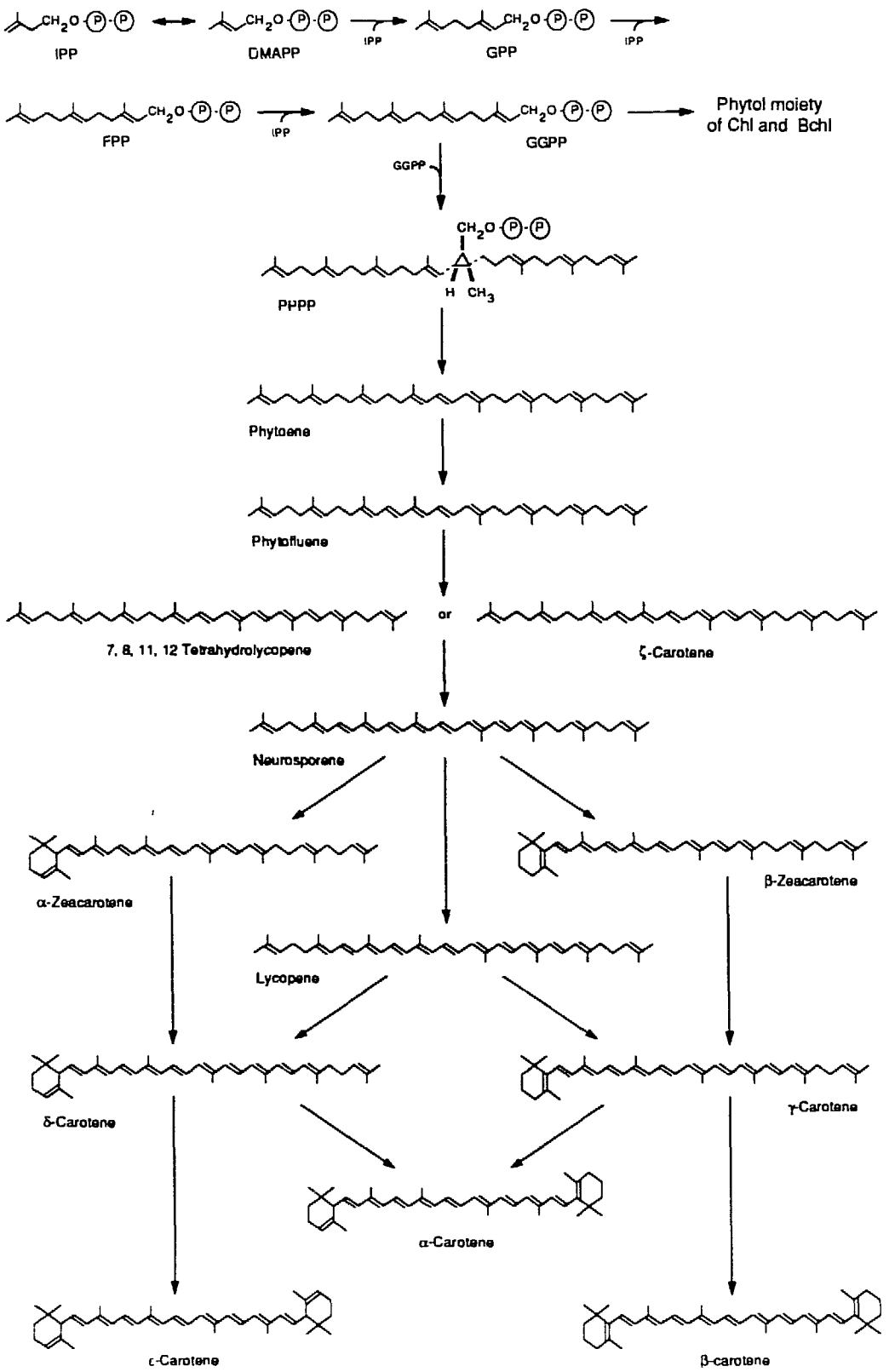
IPP
DMAPP
IPP
GPP
IPP
FPP
IPP
GGPP
Phytol moiety of Chl and Bchl
GGPP
PPPP
Phytoene
Phytofluene
7, 8, 11, 12 Tetrahydrolycopene
or
ζ-Carotene
Neurosporene
α-Zeacarotene
β-Zeacarotene
Lycopene
δ-Carotene
γ-Carotene
α-Carotene
ε-Carotene
β-carotene

per year are produced worldwide by carotenogenic organisms (Kläui, 1982). Xanthophylls derived from α- and β-carotene constitute the bulk of naturally accumulated carotenoid species. Carotenoids give many flowers and fruits their characteristic yellow and red colors (Bramley and Mackenzie, 1988). Xanthophylls are believed to serve as the precursors of abscisic acid, an important plant hormone (Gamble and Mullet, 1986). In a variety of noncarotenogenic organisms, including birds, fish, insects and crustaceans, carotenoids and their derivatives also function as pigments (Kläui, 1982; Britton, 1983), although they are often modified after ingestion (Davies, 1985). In mammals, which cannot synthesize carotenoids, β-carotene and related carotenoids with a similar half-structure (ie. β-zeacarotene, γ-carotene, and α-carotene; Fig. 1-2) serve as precursors of vitamin A, retinal, retinol and retinoic acid (Pitt, 1971; Frickel, 1985).

In all carotenogenic organisms, both photosynthetic and nonphotosynthetic, carotenoids protect against in vivo photooxidation produced by the combination of light, oxygen and endogenous photosensitizers (Krinsky and Deneke, 1982; Fig. 1-3). In nonphotosynthetic bacteria or fungi known endogenous photosensitizers are porphyrins, such as protoporphyrin IX or cytochromes (Tuveson et al., 1988). Carotenoids also offer protection against damage caused by free radicals (Krinsky and Deneke, 1982; Mathews-Roth, 1987; Fig. 1-3).

In photosynthetic organisms the ubiquitous carotenoid pigments serve two roles. They protect against photooxidative damage caused by excited state triplet chlorophyll (Chl) or bacteriochlorophyll (Bchl), or by singlet oxygen generated by the excited triplets. Carotenoids with nine or more conjugated double bonds quench excited state singlet oxygen and protect against Chl a photobleaching efficiently (Krinsky, 1979). Aside from their protective role, carotenoids harvest light in the range of 450-570 nm where Chl or Bchl-protein complexes do not absorb strongly, and surrender the collected energy to antenna Chl or Bchl molecules via singlet-singlet energy transfer (Cogdell and Frank, 1987).

Figure 1-3. Protective reactions of carotenoids against photosensitizing molecules. The boxed reaction (above) shows a general scheme for the generation of an excited state photosensitizing molecule, S*, by a photon. Some proportion of the population of excited state singlet molecules undergo intersystem crossing, indicated by the dotted line, yielding excited state triplets. Carotenoids (CRT) are capable of (**1**) quenching the S* triplet directly, (**2**) quenching excited state singlet oxygen generated by the S* triplet, or (**3**) quenching radical species generated by the S* triplet. In reactions (**1**) and (**2**) the resulting excited state CRT triplet has a lifetime of 7-8 microseconds both in solution and in bacterial photosynthetic reaction centers (Taremi et al., 1989), and thus decays rapidly back to the ground state. In reaction (**3**) a highly delocalized and unreactive carbon-centered radical species is generated.

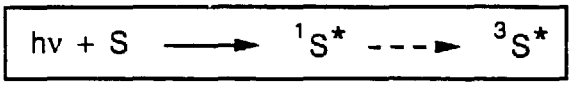
hv + S
1S*
3S*

(1)

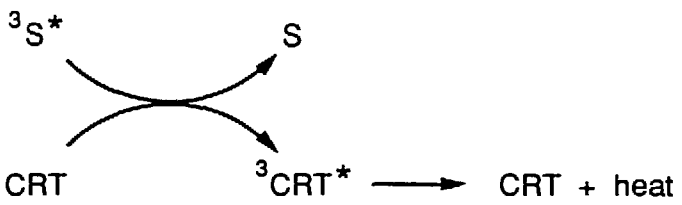
3S*
S
CRT
3CRT*
CRT + heat

(2)

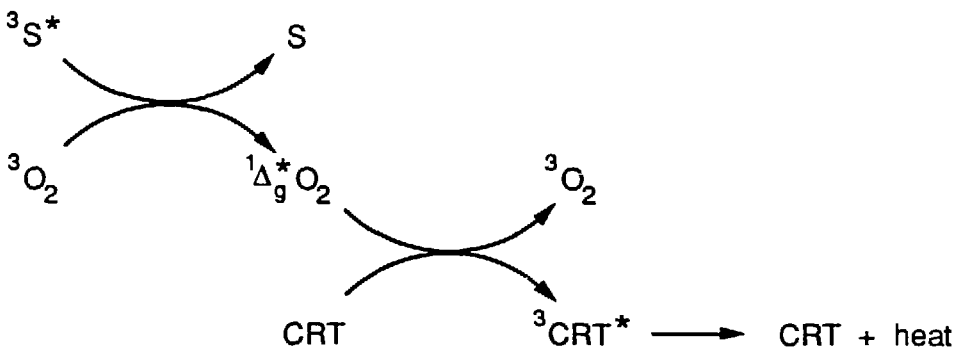
3S*
S
3O2
1Δg*O2
3O2
CRT
3CRT*
CRT + heat

(3)

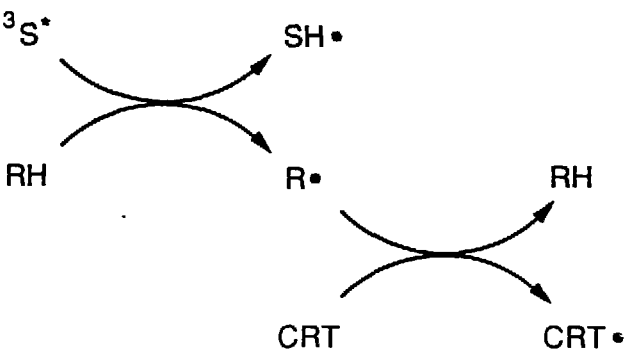
3S*
SH•
RH
R•
RH
CRT
CRT•

Commercial interest in carotenoids arises from several sources. Because carotenoids are highly colored, non-toxic compounds (Mathews-Roth, 1987) they are considered desirable as coloring agents (Kläui, 1982). In addition, the flesh and eggs of poultry and fish assume colors characteristic of the dietary carotenoids available (Kläui, 1982). Carotenoids color the feathers of flamingos, the scales of goldfish and the flesh of salmon, to give a few examples (Britton, 1983). The red color of cooked lobster results from the heat denaturation of an astaxanthin carotenoprotein in the shell, and liberation of the free carotenoid, whose absorption maxima are almost 100 nm blue-shifted with respect to the carotenoprotein complex (Britton, 1983).

β-carotene and canthaxanthin are currently the focus of interest as anti-cancer agents. Given as dietary supplements to mice these carotenoids offer protection against UV-B induced skin tumors (Mathews-Roth, 1982). High doses of β-carotene have also been used effectively as a therapy for human patients suffering from erythropoietic protoporphyria, a disease characterized by sensitivity to visible light (Mathews-Roth, 1987).

One of the major classes of herbicides, typified by Norflurazon (SAN 9789), targets carotenoid biosynthesis (Ridley, 1982). These herbicides inhibit the dehydrogenation of phytoene to phytofluene. Phytoene, the first C_{40} carotenoid, has only three conjugated double bonds (Fig. 1-2) and hence is not effective at protection against photooxidative damage. Thus, application of these bleaching herbicides to crops leads to photodestruction of Chl and photooxidative killing because of the lack of colored carotenoid quenchers (Ridley, 1982).

Carotenoids are lipophilic molecules and thus usually reside in hydrophobic environments, either in protein complexes shielded from solvent or in the lipid bilayer (Britton, 1983). Carotenoids can exist in water soluble form either complexed with protein, or as polar glycosides. In higher plants, carotenoids are found in photosynthetic tissues (described below) and in the chromoplasts of fruits, flowers and roots (Goodwin,

1980). The localization of carotenoids in photosynthetic membranes has been reviewed (Siefermann-Harms, 1985). They are found in protein complexes containing Chl or Bchl, such as the photosynthetic reaction center, where the primary photochemistry of membrane charge separation occurs, and the light-harvesting antenna complexes. Membrane-bound higher plant Chl-protein complexes contain non-covalently bound carotenoids in situ. Bchl-protein complexes of photosynthetic bacteria also bind carotenoids non-covalently in situ (Webster et al., 1980), although reduced amounts of carotenoids are synthesized during aerobic respiratory growth in the absence of photosynthetic pigment-protein complexes (Marrs, 1982). The question of carotenoid localization in Bchl$^-$ mutants of R. capsulatus which lack stable pigment-binding protein complexes (Zsebo and Hearst, 1984; Tadros et al., 1984; Klug et al., 1985; Klug et al., 1986), or in aerobic cultures has not been addressed. A carotenoprotein has been isolated, however, from Rhodospirillum rubrum, a related photosynthetic bacterium (Schwenker et al., 1974). The harsh solubilization techniques sometimes required for the isolation of pigment-protein complexes in other photosynthetic organisms can lead to the artifactual release of carotenoids from photosynthetic complexes (Siefermann-Harms, 1985). Soluble carotenoproteins lacking Chl have been found in some cyanobacteria and green algae. An example of a dimer of a soluble 23 kDa polypeptide binding roughly 44 carotenoid molecules has recently been described in Anacystis nidulans (Diverse-Pierluissi and Krogmann, 1988). Some cyanobacterial cytoplasmic membrane fractions, as well as higher plant chloroplast envelope membranes also contain carotenoids, but it is not known in all cases whether these pigments are protein-associated (Siefermann-Harms, 1985). In at least one case a carotenoid binding protein has been isolated from a cyanobacterial cytoplasmic membrane preparation from photoautotrophic cells (Bullerjahn and Sherman, 1986). The light-harvesting antenna complexes of higher plant, algae and cyanobacteria bind xanthophylls preferentially, while the reaction center prefers carotenes as a general rule (Siefermann-Harms, 1985). Carotenoid glycosides are found in cyanobacteria and

nonphotosynthetic bacteria (Britton, 1983), but are not widely distributed in purple or green photosynthetic bacteria (Schmidt, 1978). In nonphotosynthetic bacteria, carotenoids are found in the cytoplasmic membrane or cell wall (Goodwin, 1980; Britton, 1983). The fungi Phycomyces and Neurospora accumulate carotenoids in their mycelia and sporangiophores (Cerda-Olmedo, 1987; Nelson et al., 1989), as well as in their mitochondria (Goodwin, 1980).

Despite the crucial role of carotenoids in photooxidative protection, no carotenoid gene sequences from any organism have been reported, nor have the molecular mechanisms regulating carotenogenesis been elucidated. Light has been shown to regulate the accumulation of carotenoids in higher plants, algae, fungi and nonphotosynthetic bacteria (reviewed in Harding and Shropshire, 1980; Cerda-Olmedo, 1987) but the mechanism of light-mediated induction of carotenoid biosynthesis remains unknown (Bramley and Mackenzie, 1988). Genes involved in carotenoid biosynthesis have been mapped to chromosomal locations in the photosynthetic bacteria Rhodobacter capsulatus (Yen and Marrs, 1976; Taylor et al., 1983, Zsebo and Hearst, 1984; Giuliano et al., 1986, 1988), and Rhodobacter sphaeroides (Pemberton and Harding, 1986), the nonphotosynthetic bacterium Myxococcus xanthus (Balsalobre et al., 1987) and the fungi Phycomyces blakesleeanus (reviewed in Cerda-Olmedo, 1987) and Neurospora crassa (reviewed in Bramley and Mackenzie, 1988). A cluster of genes which directs the synthesis of yellow pigments, presumed to be carotenoids, has been cloned from the nonphotosynthetic bacterium Erwinia herbicola and expressed in the gram-negative nonphotosynthetic bacterium Escherichia coli (Perry et al., 1986). The introduction of these putative carotenoid biosynthesis genes into E. coli confers resistance against damage caused by the combination of near-UV radiation and membrane-directed phototoxic molecules (Tuveson et al., 1988). Gene specific probes which would facilitate the study of carotenoid gene expression have been lacking in any of these organisms, however.

No enzymes involved in the biosynthesis of carotenes have been purified to

homogeneity with one exception. Dogbo et al. (1988) have recently purified a bifunctional enzyme catalyzing the two step synthesis of phytoene from GGPP via PPPP from red pepper chromoplasts (Fig. 1-2). Cell-free carotenoid synthesizing extracts have been reported from a variety of organisms (reviewed in Bramley, 1985). Purification of carotenoid enzymes has, however, been hindered in many cases by their rapid loss of activity upon separation from a membrane environment, thus preventing detailed biochemical studies.

II. Rhodobacter capsulatus as a model system for carotenoid biosynthesis in photosynthetic organisms

Rhodobacter capsulatus, a purple non-sulfur photosynthetic bacterium (formerly Rhodopseudomonas capsulata, Imhoff et al. (1984)) offers the best characterized system among photosynthetic organisms for studies of carotenoid biosynthesis genes (Bramley and Mackenzie, 1988). R. capsulatus is found naturally in local water accumulations and sewage ponds (Weaver et al., 1975). This gram-negative bacterium, is a facultative phototroph whose metabolic versatility has proven extremely valuable in studies of photosynthesis and nitrogen fixation, providing extraordinary insights into these processes with applications to other organisms (reviewed in Scolnik and Marrs, 1987). Purple non-sulfur photosynthetic bacteria such as the closely related species Rhodobacter sphaeroides (formerly Rhodopseudomonas sphaeroides, Imhoff et al. (1984)) and others such as Rhodopseudomonas viridis and Rhodospirillum rubrum have also been extensively studied using a barrage of biophysical, biochemical and genetic techniques. R. capsulatus remains, however, the photosynthetic bacterium most amenable to study by genetic and molecular biological approaches (Scolnik and Marrs, 1987). The structural and functional relationships between the photosynthetic reaction center of purple non-sulfur bacteria and

the photosystem II (PS II) reaction center of oxygen evolving photosynthetic organisms have recently been reviewed (Michel and Deisenhofer, 1988).

R. capsulatus grows chemoheterotrophically by respiration when oxygen is abundant. Upon a reduction of the oxygen tension in the growth medium, either in the presence or absence of light, R. capsulatus induces an intracytoplasmic membrane system containing photosynthetic pigment-protein complexes (Drews and Oelze, 1981). Photosynthetic growth does not occur, however, in the absence of light. The induction of the photosynthetic apparatus triggers the expression of genes encoding three major membrane-bound pigment-protein complexes (Clark et al., 1984; Klug et al., 1985), namely the photochemical reaction center (RC), and the two light-harvesting antennae, LH-I (also B870) and LH-II (also B800-850) (Drews, 1985). Lowering of oxygen tension in the growth medium to less than a few percent also substantially increases the rate of synthesis of the carotenoid and Bchl photopigments (Schumacher and Drews, 1978; Biel and Marrs, 1985). A similar result is observed upon shifting cells from dark respiratory to anaerobic photosynthetic growth (Kaufmann et al., 1982). A shift in light intensity under anaerobic photosynthetic conditions also changes the cross-section of the photosynthetic membrane and consequently affects Bchl and carotenoid accumulation (Golecki et al., 1980). R. capsulatus is also capable of anaerobic respiratory growth in the dark, but requires an appropriate carbon source and an accessory oxidant, such as dimethyl sulfoxide or trimethylamine-N-oxide, to act as a terminal electron acceptor in place of oxygen (Yen and Marrs, 1977; Schultz and Weaver, 1982). Under these conditions, cells gratuitously synthesize the components of the photosynthetic apparatus (Yen and Marrs, 1977; Scolnik et al., 1980b). Although R. capsulatus is capable of surviving strictly by fermentation of fructose in the absence of exogenous oxidants, the growth rate under these conditions is extremely slow (Schultz and Weaver, 1982). Thus, mutants of R. capsulatus which lack the ability to photosynthesize are most easily cultivated using either dark aerobic respiration or dark anaerobic respiration conditions in the presence of an accessory

oxidant.

The Bchl and carotenoid pigments synthesized during reduction of oxygen tension in the medium are non-covalently associated with the RC, LH-I and LH-II antenna complexes. The structure and organization of the photosynthetic apparatus of purple non-sulfur bacteria has been recently reviewed (Drews, 1985). The R. capsulatus RC consists of three subunits, often termed H (heavy), M (medium) and L (light) for their apparent molecular weights of 28, 24, and 21 kDa on SDS polyacrylamide protein gels. LH-I consists of two hydrophobic polypeptides of apparent molecular weights of 12 and 7 kDa termed α and β, respectively. LH-II is composed of three hydrophobic polypeptides of apparent molecular weights of 14, 10 and 8 kDa, denoted α, β, and γ, respectively. All of these polypeptides, except for the H subunit of the RC and the γ polypeptide of LH-II, bind pigment cofactors. The genes for all the components of the RC, LH-I and LH-II of R. capsulatus have been isolated and sequenced (Youvan et al., 1984a; Youvan and Ismail, 1985), with the exception of the gene encoding the γ polypeptide of LH-II (Youvan and Ismail, 1985).

The two antenna complexes are found in molar excess over the RC in the photosynthetic membrane. The ratio of the LH-II:LH-I antenna complexes varies inversely with light intensity, while the ratio of LH-I:RC remains constant (Aagaard and Sistrom, 1972; Drews and Oelze, 1981). The molar ratio of Bchl specific to LH-II and LH-I per mol of RC is 80-40:20:1 at low light intensities in R. capsulatus (Drews, 1985). The absorption spectra of both Bchl and carotenoids complexed with protein is typically red-shifted with respect to the free pigment. In wildtype photosynthetically grown cultures of R. capsulatus, carotenoid absorption maxima from pigment-protein complexes occur from about 450 to 510 nm (Scolnik et al., 1980b), and are red-shifted about 20 nm with respect to the maxima of organic extracts of carotenoids (Cogdell and Frank, 1987).

The RC of all examined species of wildtype photosynthetic bacteria contains one specifically bound carotenoid molecule (reviewed in Cogdell and Frank, 1987).

Biophysical studies on RC preparations from carotenoidless strains have shown that the carotenoid is not required for the primary electron transfer reactions of photosynthesis. A high resolution X-ray crystal structure of the R. viridis RC has recently been determined (Deisenhofer et al., 1984; Deisenhofer et al., 1985; Michel et al., 1986; Deisenhofer and Michel, 1988). This work was the basis for the award of the 1988 Nobel Prize in Chemistry to Drs. Deisenhofer, Huber, and Michel, both for their contributions to photosynthesis as well as for solving the first high-resolution X-ray crystal structure of a membrane-bound complex. The high resolution X-ray crystal structures of the R. sphaeroides RC complexes from strains R-26 (carotenoidless) and 2.4.1 (wildtype carotenoid) have recently been determined (Allen et al., 1987a; Allen et al., 1987b; Yeates et al., 1987; Allen et al., 1988; Komiya et al., 1988; Yeates et al., 1988). The location and conformation of the RC carotenoid molecule have been defined in the R. viridis and R. sphaeroides X-ray crystal structures although some uncertainty remains in these determinations. The 1,2-dihydroneurosporene carotenoid molecule in the R. viridis RC appears to be 13-cis, with an out-of-plane twist (Deisenhofer and Michel, 1988). The carotenoid molecule (spheroidene) in the R. sphaeroides 2.4.1 wildtype RC lies within 3.5 Å of ten, mostly aromatic, amino acid residues from the M subunit and is situated between helices B and C in a similar location to the R. viridis RC carotenoid (Yeates et al., 1988). No charged amino acid residues are found within 10 Å of the R. sphaeroides RC carotenoid. The conformation of the carotenoid is bent, consistent with an internal cis double bond, as had been previously proposed based on spectroscopic data (see below). A comparison of sequence homologies between the M subunit of the bacterial RC from R. sphaeroides, R. capsulatus, R. rubrum, R. viridis, the green photosynthetic bacterium Chloroflexus auranticus, and the D2 polypeptide of the alga Chlamydomonas reinhardtii, shows that none of the ten amino acids located within 3.5 Å of the R. sphaeroides RC carotenoid was absolutely conserved (Komiya et al., 1988). Of these ten residues, only Gly-162 and His-182 were conserved in all of the purple bacterial RC sequences.

Recent studies have examined the conformation of RC carotenoids either in situ or of the extracted species using resonance Raman, electronic absorption, ESR and ^{1}H-NMR spectroscopy. Carotenoids can be also reconstituted into reaction centers from carotenoidless mutant strains (Chadwick and Frank, 1986; Cogdell and Frank, 1987). Chadwick and Frank (1986) have suggested that the carotenoids isomerize from all-trans to a cis conformation upon reconstitution, with a possible out-of-plane twist deduced from the ESR zero-field splitting parameters of carotenoids reincorporated into the R. sphaeroides RC. Polar groups on the carotenoid appear to aid in the reconstitution (Chadwick and Frank, 1986), although no obvious interaction occurs in the wildtype R. sphaeroides RC between the terminal methoxy group of spheroidene (Fig. 1-5) and neighboring amino acid residues (Yeates et al., 1988). The carotenoid extracted from the R. sphaeroides RC of either the wildtype strain 2.4.1 (Lutz et al., 1987), which accumulates spheroidene, or the mutant G1C (Koyama et al., 1988), which accumulates neurosporene, has been shown to be largely if not exclusively in a 15-cis conformation and may be subject to some out-of-plane twisting in situ. Isomerization of the 15-cis species to the all-trans species occurs if photosensitizing Bchl is not rigorously removed from the extracted carotenoids.

Carotenoids in the LH complexes appear to be in an all-trans conformation, in contrast to the RC carotenoids (Cogdell and Frank, 1987). Koyama et al. (1988) have also shown that the neurosporene extracted from G1C light harvesting complexes exists in the all-trans conformation, by the same procedures used to study the RC carotenoid. Both the R. capsulatus LH-I and LH-II carotenoids are capable of energy transfer with an efficiency of 60-70% to the Bchl in these antenna complexes (Scolnik et al., 1980b). Values ranging between 60-100% efficiency of energy transfer have been reported in R. sphaeroides (Cogdell and Frank, 1987). The efficiency of singlet-singlet energy transfer to the antenna Bchl is not, however, strongly influenced by the type of carotenoid present in the antenna.

Several different Bchl:carotenoid ratios have been reported for both the R. sphaeroides

and R. capsulatus LH complexes, although the more rigorous studies have been performed in the former organism. Two Bchl per one carotenoid molecule are found in the R. capsulatus LH-I α and β monomer, in contrast to the R. sphaeroides ratio of two Bchl to two carotenoids (Drews, 1985). The ratio of Bchl to carotenoid in the R. sphaeroides LH-II complex has recently been unequivocally demonstrated to be 2:1, resolving a persistent conflict in the literature (Evans et al., 1988). This data supports a model originally proposed by Kramer et al. (1984) on the basis of fluorescence polarization and linear dichroism measurements in R. sphaeroides, which suggested a minimal LH-II structure of $(\alpha\beta)_2$ with six Bchl and three carotenoids. Although both 3:1 (Drews, 1985) and 2:1 ratios have been reported for the R. capsulatus LH-II complex, the similarities between the pigment-protein complexes in R. capsulatus and R. sphaeroides have led Evans et al. (1988) to propose that 2:1 is probably the correct ratio for the former organism as well. A very recent review has further modified the proposal of Kramer et al. (1984), suggesting that the minimal LH-II unit in R. sphaeroides consists of $(\alpha\beta)_3$ containing nine Bchl and six carotenoids (1.5:1), although the evidence justifying this proposal was not presented (Hunter et al., 1989). The molar ratio of Bchl:carotenoid in whole cells grown under either high light or low light regimes, in which either LH-I or LH-II is the dominant antenna complex, respectively, ranges from about 1:1 in the former case to 2:1 in the latter case in both R. capsulatus (Golecki et al., 1980) and R. sphaeroides (Sistrom, 1978; Hunter et al., 1988). These results have not been reconciled with the proposed ratios for the isolated complexes of R. capsulatus.

Spheroidene is the major carotenoid found in strictly anaerobic photosynthesizing cultures of wildtype Rhodobacter, while its 2-oxo derivative, spheroidenone, predominates in the presence of oxygen (Goodwin, 1980). Wildtype R. capsulatus grown under anaerobic, photosynthetic conditions accumulates spheroidene, spheroidenone and hydroxyspheroidene in a ratio of 83.6:11.5:4.9 (Scolnik et al., 1980b). Schmidt (1978) reported very similar ratios along with the occurrence of other minor carotenoid species.

Hunter et al. (1988) have also reported an asymmetry in the ratio of spheroidene to spheroidenone present in the different pigment-protein complexes isolated from photosynthetically grown cultures of R. sphaeroides. Isolated LH-I or RC complexes were enriched about 5-fold in the molar ratio of spheroidenone:spheroidene versus the isolated LH-II complex, while chromatophores from a RC^+ $LH\text{-}I^+$ $LH\text{-}II^-$ mutant showed a 10-fold enrichment in spheroidenone compared to wildtype chromatophores in which LH-II is the dominant antenna complex (Hunter et al., 1988). Evans et al. (1988) determined spheroidene:spheroidenone ratios for both isolated the LH-II complex and whole cells from the wildtype. They observed a 5-fold excess of spheroidenone to spheroidene in whole cell extracts versus the isolated LH-II complex. Thus, in cultures of wildtype R. sphaeroides there may be a preference for the binding of spheroidene versus spheroidenone in the LH-II complex. Aerobic chemoheterotrophic cultures of R. sphaeroides accumulated mainly spheroidenone and neurosporene in a ratio of 95:5 (Evans et al., 1988).

R. capsulatus provides an excellent model system to study carotenoid biosynthesis for several reasons. First, all of this bacterium's known carotenoid genes lie within a 46 kilobase (kb) photosynthetic gene cluster derived from the bacterial chromosome and carried on the R-prime plasmid pRPS404 (Marrs, 1981). Although pRPS404 complements all known mutations blocking carotenoid or Bchl biosynthesis, the photosynthetic pigments are not produced in E. coli strains bearing this plasmid. The photosynthetic gene cluster includes at least 9 carotenoid (crt) and 11 Bchl (bch) biosynthetic genes, along with the pufQBALMX and puhA operons (Fig. 1-4, 3-7) (Yen and Marrs, 1976; Taylor et al., 1983; Zsebo and Hearst, 1984; Youvan et al., 1984a; Bauer et al., 1988; Chapter 3). The designations pufB, pufA, pufL, pufM and puhA replace the previously used lhpA, lhpB, rxcA, rxcC and rxcB (Fig. 1-4), respectively (Kaplan and Marrs, 1986). pufQ encodes a polypeptide required for Bchl biosynthesis

Figure 1-4. Map of the 46 kb photosynthesis gene cluster of R. capsulatus (from Zsebo and Hearst, 1984). Genes for the reaction center polypeptides (rxc) and light-harvesting I antenna polypeptides (lhp) have since been renamed (see text). Carotenoid biosynthesis genes (crt) and bacteriochlorophyll biosynthesis genes (bch) are located in the middle of the gene cluster. XhoI and BglII restriction sites are shown by X and B, respectively. The locations of Tn5.7 insertion mutations generated within the gene cluster are indicated by numbers at the end of the vertical lines below the genes. Possible directions of transcription based on complementation studies are indicated above the genes by arrows, although more recent DNA sequencing (M. Alberti, unpublished data) indicates that the directions of transcription are contrary to those postulated in this figure for the bchA, bchC and bchI, bchD regions.

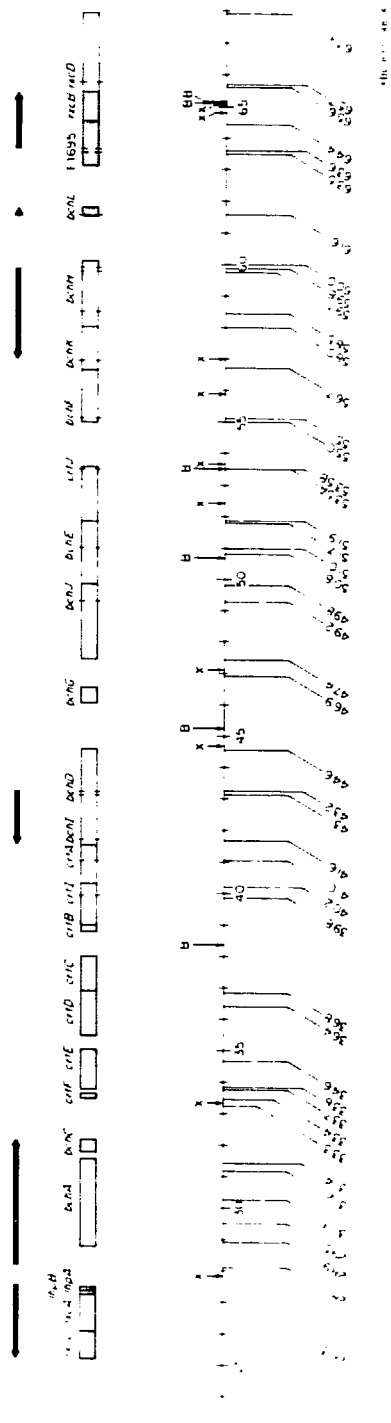

which is proposed to function as a Mg tetrapyrrole-binding carrier polypeptide (Bauer and Marrs, 1988) or alternatively as the pigment-binding polypeptide for a novel Bchl species (Klug and Cohen, 1988). pufB and pufA encode the β and α subunits, respectively, of the LH-I antenna complex, while pufL, pufM and puhA encode the L, M and H subunits, respectively, of the RC. pufX, formerly C2397 (Zsebo and Hearst, 1984) encodes a polypeptide required for maintenance of the proper LH-II:LH-I stoichiometry (Klug and Cohen, 1988). The pucBA operon encoding the LH-II β, α polypeptides, respectively, maps outside the photosynthetic gene cluster, while the gene encoding the LH-II γ polypeptide has not yet been located (Youvan and Ismail, 1985).

R. capsulatus synthesizes carotenoids using a modified spirilloxanthin pathway (Schmidt, 1978). The pyrophosphate precursors of the carotenoids (Fig. 1-5), arise through the condensation of the C_5 isoprenoid building block, IPP, with its isomer DMAPP to give GPP, followed by two successive additions of IPP yielding FPP and GGPP, respectively. All of the pyrophosphate intermediates up to and including GGPP are also used in other branches of isoprenoid biosynthesis. FPP is a precursor of squalene and steroids while GGPP is used in the synthesis of phytohormones such as gibberellins, and the phytyl side chains of quinones such as ubiquinone and plastoquinone (Bramley and Mackenzie, 1988). Carotenoid and Chl/Bchl biosynthesis are linked because GGPP is also used in the synthesis of the esterifying phytyl or geranylgeranyl side chains of Chl/Bchl (Figs. 1-2, 1-6). The Bchl biosynthetic pathway from addition of Mg to protoporphyrin IX, to Bchl a is shown in Fig. 1-6. R. capsulatus and R. sphaeroides synthesize Bchl a, while R. viridis synthesizes Bchl b (Jones, 1978). Bchl a from R. sphaeroides is esterified with a phytyl group (Evans et al., 1988).

The tail-to-tail condensation of two molecules of the C_{20} intermediate, GGPP produces PPPP (Fig. 1-2), the first reaction in the isoprenoid biosynthetic pathway considered to be unique to the production of carotenoids (Britton, 1983). PPPP undergoes a stereospecific conversion to either 15-cis or all-trans-phytoene, the first C_{40}

Figure 1-5. The revised R. capsulatus carotenoid biosynthetic pathway. Trivial names for the carotenoids are used here and throughout the text. Semisystematic names for the carotenoids have been given in Scolnik et al. (1980a) and Giuliano et al. (1986). Assignments of genetic loci to biochemical functions in the pathway are based on in vivo intermediate accumulation in crt mutants or on in vitro biochemical defects in cell-free carotenoid synthesizing extracts. Biochemical functions have been proposed for crtB and crtE (Chapter 4, Table 4-3), crtI (Giuliano et al., 1986), and crtC, crtD, crtF and crtA (Scolnik et al., 1980a). crtK has been recently identified by DNA sequence analysis (Chapter 3) and is tentatively placed on the pathway on the basis of our interpretation of mutational data (Giuliano et al., 1988). 7, 8, 11, 12-tetrahydrolycopene has been shown as an intermediate in the R. capsulatus carotenoid pathway (Giuliano et al., 1986, 1988) on the basis of studies in related photosynthetic bacteria (Schmidt, 1978). ζ-carotene has also been suggested as a possible intermediate in R. capsulatus (Giuliano et al., 1986). Deuterium labelling studies have also directly confirmed the conversion of neurosporene to hydroxyspheroidene in Rhodobacter sphaeroides by incorporation of ^{2}H during the hydration of the C-1, 2 and C-1', 2' double bonds of neurosporene and spheroidene, respectively (Patel et al., 1983). Reactions for which no genetic locus has been assigned are indicated by (?). Boxes indicate the major wildtype carotenoids, spheroidene and spheroidenone, accumulated during anaerobic photosynthetic and aerobic respiratory growth, respectively. Abbreviations used in this figure are as in Fig. 1-2.

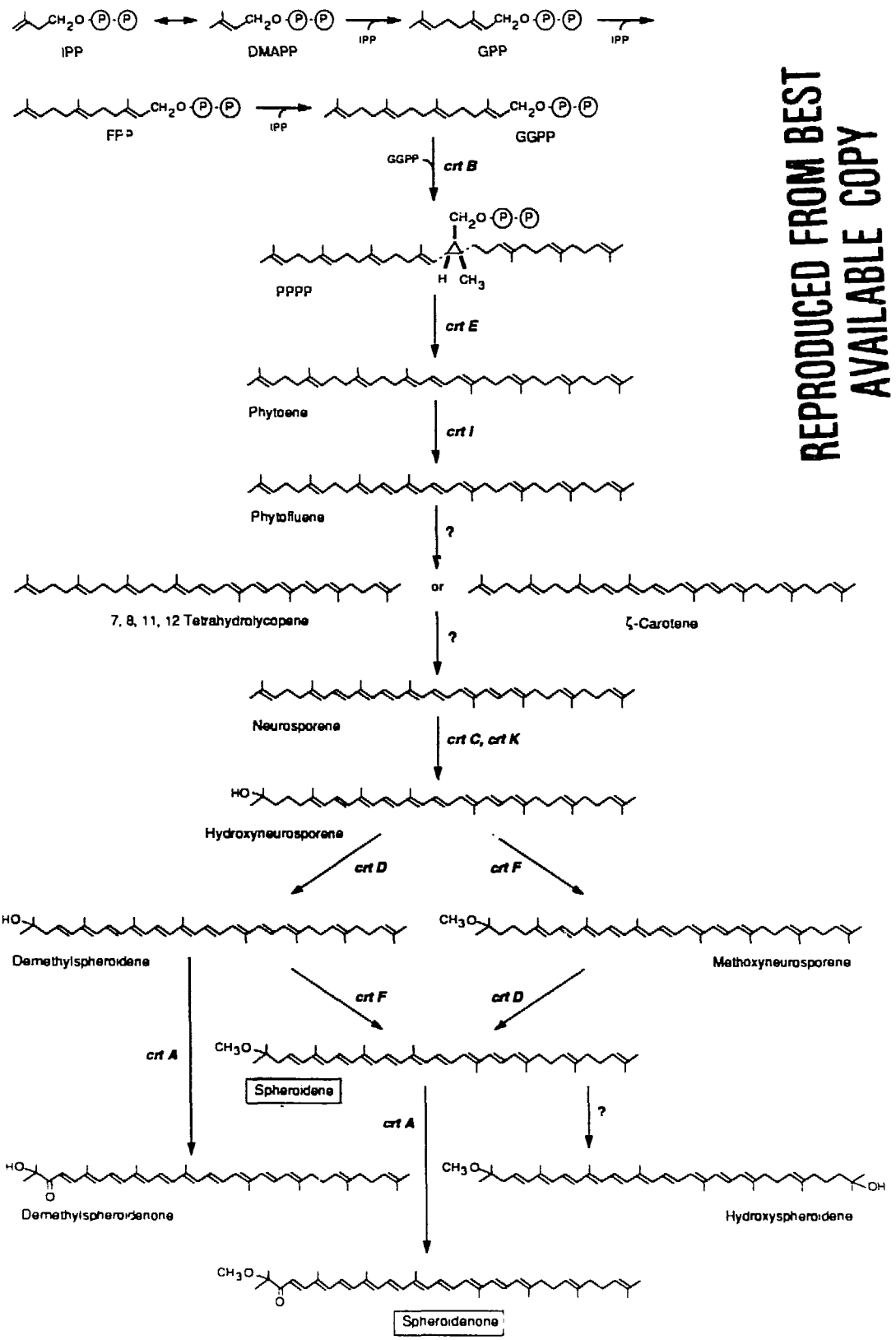

Figure 1-6. The pathway of bacteriochlorophyll biosynthesis from protoporphyrin IX onwards (from K. Zsebo, Ph.D. thesis, 1984). Protoporphyrin IX is an intermediate common to both heme and Chl/Bchl biosynthesis (reviewed in Jones, 1978; Britton, 1983). In the former case iron is inserted into the tetrapyrrole ring system, while in the latter case magnesium is inserted. Intermediates in the pathway and assignments of genetic loci to specific biochemical functions are as presented in Biel and Marrs (1983). Additional genetic loci involved in Bchl biosynthesis, bchI, bchJ, bchK and bchL (Fig. 1-4) identified by Zsebo and Hearst (1984), are not included on the biosynthetic grid as the precursors accumulated by these mutants have not been identified. Addition of the phytyl sidechain to bacteriochlorophyllide a, the last reaction in the synthesis of Bchl a in R. capsulatus, requires the presence of an isoprenoid pathway active up to the C_{20} intermediate GGPP (Fig. 1-5), which is used in the synthesis of phytol (Goodwin, 1980; Britton, 1983).

Bacteriochlorophyll Synthesis

Protoporphyrin IX to Bacteriochlorophyll *a*

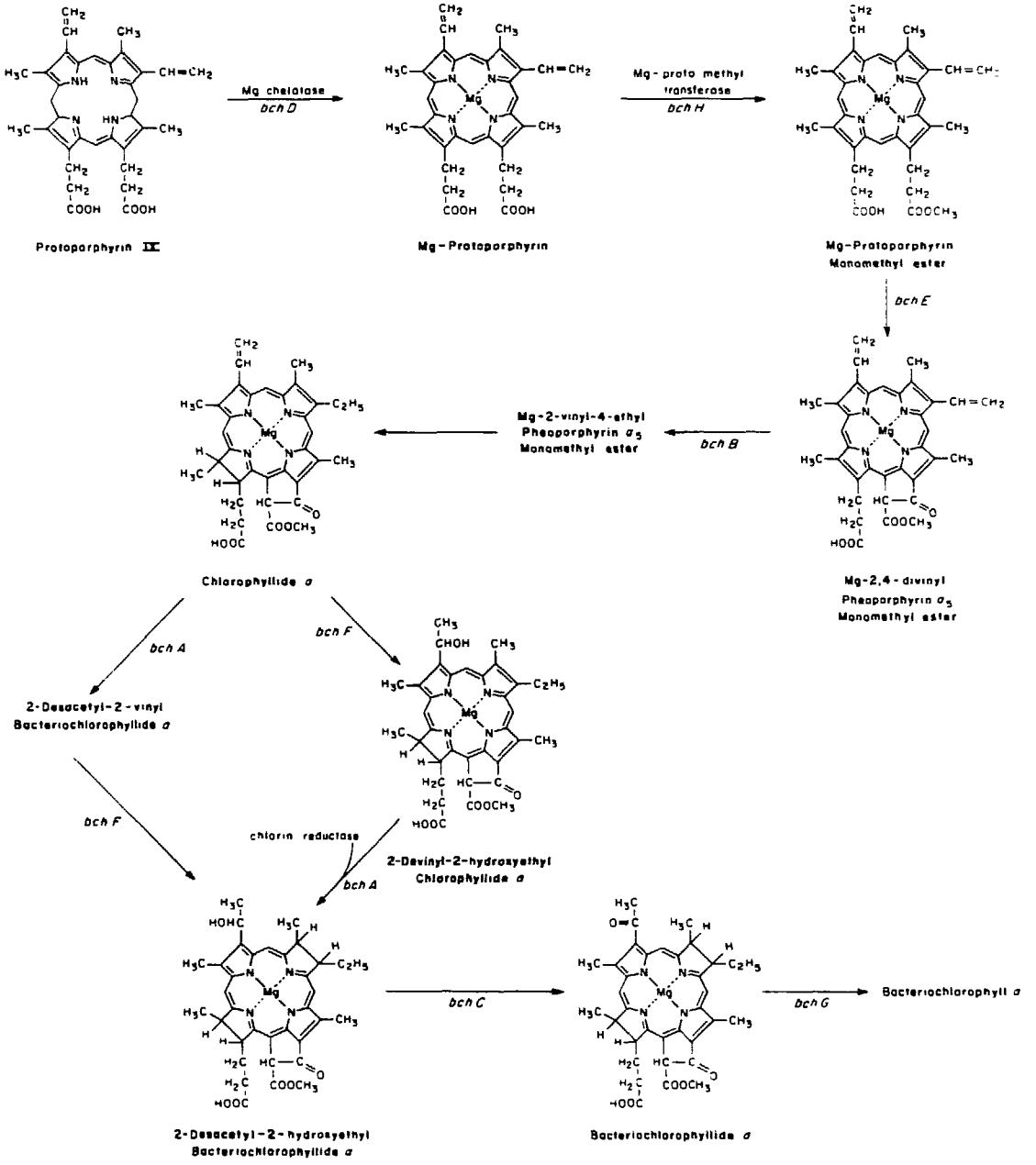

carotenoid. 15-cis-phytoene predominates in higher plants, alga and fungi, while both isomers occur in different species of bacteria, sometimes simultaneously in the same species (reviewed in Goodwin, 1980 and Bramley and Mackenzie, 1988). R. capsulatus accumulates roughly a 1:1 mixture of the 15-cis and the all-trans isomers in both dark aerobic and anaerobic photosynthetic cultures (A. Connor and G. Britton, personal communication; Chapter 4). Following three successive dehydrogenations which produce neurosporene, an intermediate common to many carotenogenic organisms (Fig. 1-2), the additional hydration, methylation and dehydrogenation reactions of the R. capsulatus pathway lead to carotenoids found only in photosynthetic bacteria (Fig. 1-5). Spheroidene and spheroidenone are the major end products accumulated in wildtype cultures of Rhodobacter (Schmidt, 1978), their relative ratios being determined by the availability of oxygen in the growth medium. Smaller amounts of other carotenoids also accumulate (Schmidt, 1978; Scolnik et al., 1980b; Evans et al., 1988).

Evidence for the proposed R. capsulatus carotenoid biosynthetic pathway is based on the accumulation of identified intermediates by R. capsulatus mutants for all compounds from neurosporene onwards (Fig. 1-5) (Yen and Marrs, 1976; Scolnik et al., 1980a). In addition, kinetic studies of intermediate synthesis upon removal of carotenoid biosynthesis inhibitors from cell cultures of R. sphaeroides and R. rubrum have suggested reaction sequences (reviewed in Schmidt, 1978 and Goodwin, 1980). Deuterium labelling studies have also directly confirmed the conversion of neurosporene to hydroxyspheroidene in R. sphaeroides by incorporation of ^{2}H during the hydration of the C-1, 2 and C-1', 2' double bonds of neurosporene and spheroidene, respectively (Patel et al., 1983). S-adenosyl methionine provides the methyl group used in the conversion of hydroxyneuroporene and demethylspheroidene to methoxyneurosporene and spheroidene, respectively, in R. capsulatus (Scolnik et al., 1980) and in R. sphaeroides (Singh et al., 1973). Spheroidene is converted to spheroidenone by the addition of an oxo group derived from molecular oxygen, as shown by ^{18}O-labelling experiments in R. sphaeroides (Shneour, 1962).

The early portion of the pathway from phytoene to neurosporene has been less firmly established because no R. capsulatus mutants accumulating phytofluene, ζ-carotene, or 7, 8, 11, 12-tetrahydrolycopene have been observed. It has been suggested in purple non-sulfur photosynthetic bacteria (Liaaen-Jensen et al., 1961; Marrs, 1982) and in other systems (Bramley and Mackenzie, 1988) that phytoene dehydrogenase performs several consecutive dehydrogenations. 7, 8, 11, 12-tetrahydrolycopene has been assumed to be an intermediate in recent studies of R. capsulatus carotenoid biosynthesis (Scolnik et al., 1980a; Giuliano et al., 1986, 1988), based on studies in other photosynthetic bacteria (reviewed in Schmidt, 1978). Some bacteria and fungi accumulate both ζ-carotene and 7, 8, 11, 12-tetrahydrolycopene (Goodwin, 1980). Recent data using an in vitro cell-free carotenoid synthesis system leave open the possibility that ζ-carotene may be the actual intermediate in R. capsulatus (Giuliano et al., 1986).

A variety of photosynthetically viable carotenoid biosynthesis transposon (Tn5.7), interposon and point mutants are available and are readily identified by their altered pigmentation (Yen and Marrs, 1976; Scolnik et al., 1980a; Zsebo and Hearst, 1984; Giuliano et al., 1986, 1988). These mutants have allowed the mapping of the crt genes on pRPS404 by genetic and physical techniques (Yen and Marrs, 1976; Taylor et al., 1983; Zsebo and Hearst, 1984; Giuliano et al., 1988; Chapter 4), as well as the assignment of biochemical functions to some of the crt gene products based on the accumulation of carotenoid intermediates in vivo or in vitro (Scolnik et al., 1980a; Giuliano et al., 1986; Chapter 4).

The carotenoid content of members of the family Rhodospirillaceae has been known to depend on oxygen tension and light since the classic kinetic studies of Cohen-Bazire et al. (1957). These authors showed that the rates of both Bchl and carotenoid synthesis are increased by downshifts in light intensity, and that the ratio of Bchl to carotenoid is increased by the decrease in illumination. In shifts of cultures from dark aerobic to anaerobic photosynthetic growth, the rates of synthesis for Bchl and carotenoids increased

during the period before cellular growth had resumed, a result also obtained with R. capsulatus (Kaufmann et al., 1982). Introduction of oxygen into continuously illuminated anaerobic cultures led to an immediate cessation of Bchl and carotenoid synthesis, an effect which could be reversed by removal of oxygen from the medium (Cohen-Bazire et al., 1957). Schumacher and Drews (1978), and Biel and Marrs (1985) observed that a reduction of oxygen tension in dark grown cultures of R. capsulatus was sufficient to stimulate the rates of both carotenoid and Bchl synthesis. Biel and Marrs (1985) have proposed that oxygen does not directly regulate carotenoid biosynthesis as Bchl$^-$ strains show little increase in carotenoid accumulation upon a reduction of oxygen tension, while the wildtype exhibits roughly a 3-fold increase. These authors proposed that the synthesis of Bchl or some other photosynthetic membrane component is required for the stimulation of carotenoid accumulation.

Although the regulation of the R. capsulatus carotenoid biosynthesis genes has been previously studied during both steady-state respiratory and photosynthetic growth (Zhu and Hearst, 1986) and during shifts between these growth modes (Clark and Marrs, 1984; Klug et al., 1985; Zhu et al., 1986; Zhu and Hearst, 1988) in no previous cases have gene-specific DNA probes been used. These previous reports have indicated 2-fold or smaller changes in carotenoid gene expression in response to changes in the environmental stimuli of oxygen and light. The statement has appeared in the literature recently that the R. capsulatus carotenoid genes are not regulated (Giuliano et al., 1986), although this position has now been modified (Giuliano et al., 1988). The relatively modest changes in crt gene expression observed in several studies have been interpreted as a transcriptional response to boost carotenoid biosynthesis for photooxidative protection (Zhu and Hearst, 1986; Zhu et al., 1986). Unfortunately, gene-specific probes for crt genes have not previously been available in Rhodobacter, nor in any other carotenogenic organism, thus complicating the interpretation of these experiments.

III. The cloned pigment genes of Erwinia herbicola expressed in Escherichia coli, as a model system for carotenoid biosynthesis in nonphotosynthetic organisms

Erwinia herbicola is a gram-negative nonphotosynthetic bacterium found in a variety of environments, including plant surfaces in association with diseased tissue (Perry et al., 1986). Certain strains of this phytopathogenic bacterium are also capable of providing nucleation sites for ice crystal formation on plant tissues, leading to an increased chance of frost damage to crops (Orser et al., 1985). Many epiphytic strains of E. herbicola found in aerial plant parts produce yellow pigments (Perry et al., 1986). The E. herbicola pigment genes have been cloned and expressed in E. coli (Perry et al., 1986; Tuveson et al., 1988). Although the structures of these pigments have not yet been established, the available data are consistent with the notion that these pigments are carotenoids, specifically some type of xanthophylls (Tuveson et al., 1988).

The E. herbicola carotenoid genes expressed in E. coli provide an ideal model system for the study of carotenoid biosynthesis genes from a nonphotosynthetic organism. The defined nature of the DNA and polypeptides required for carotenoid biosynthesis, and the ease of genetic manipulations and the isolation of mutations within the E. herbicola pigment genes resident in E. coli, may be used to great advantage. The comparison of amino acid sequences of the carotenoid gene products from E. herbicola and R. capsulatus should illuminate the similarities and differences between carotenoid biosynthetic enzymes from these distantly related nonphotosynthetic and photosynthetic prokaryotes. The evolutionary relationships between E. coli, E. herbicola, and R. capsulatus are shown in Fig. 1-7.

Figure 1-7. Time scale of the evolution of eubacteria, mitochondria and chloroplasts. The phylogenetic tree is based primarily on 16 S rRNA comparisons, and also on immunological similarities of alkaline phosphatase and tryptophan biosynthesis enzymes (from Wilson, et al., 1987). Escherichia coli and Erwinia herbicola (upper right) are much more closely related than are Rhodobacter capsulatus and E. coli. R. capsulatus and R. sphaeroides belong to the upper of the two branches denoted Rhodopseudomonas. Letters indicate calibrated branch points in the evolutionary tree.

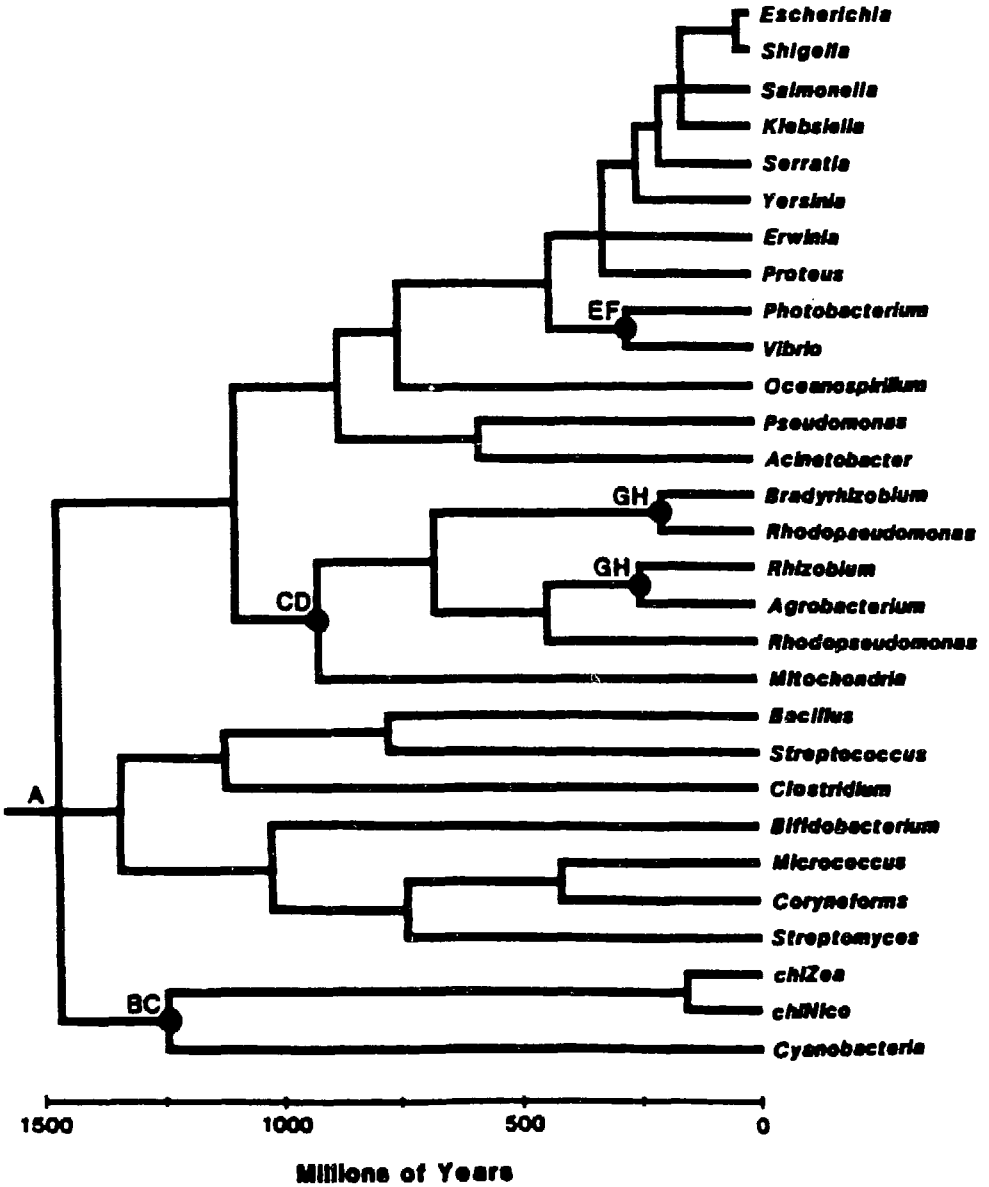

IV. Overview of the thesis

Chapters 2 and 4 describe the characterization of carotenoid biosynthesis mutants of R. capsulatus using both genetic and biochemical techniques. Chapter 2 focuses on the effects of carotenoid mutations on the expression of other genes involved in photosynthesis, the accumulation of photosynthetic pigment-protein complexes, and the growth properties of the mutants. Chapter 3 describes the cloning, sequencing and evaluation of the DNA sequence of a gene cluster containing eight of the nine known R. capsulatus carotenoid biosynthesis genes. Chapter 4 builds on the results of Chapter 3 to correlate the phenotypes of transposon insertion mutants blocked in carotenoid biosynthesis with the genotypes, based on high resolution mapping of the transposon insertions. In addition, biochemical functions are proposed for three gene products required early in the carotenoid biosynthetic pathway, based on the accumulation of carotenoid precursors in cell-free carotenoid synthesizing extracts. Chapter 5 describes the preliminary characterization of E. herbicola pigment genes maintained in E. coli as a model system for the study of carotenoid biosynthesis genes from a nonphotosynthetic bacterium. Results of chemical inhibition of pigment synthesis are given, along with evidence that E. herbicola synthesizes carotenoids derived from phytoene. Chapter 6 describes the regulation of the genes in the R. capsulatus carotenoid biosynthesis gene cluster during the metabolic shift from dark aerobic (respiratory) growth to anaerobic photosynthetic growth, in comparison to genes encoding structural photosynthetic polypeptides and a cytochrome complex. Chapter 7 examines the nature of the protein products of the carotenoid biosynthesis genes deduced from the nucleotide sequence (Chapter 3) in comparison to carotenoid biosynthetic enzymes in other systems. A comparison is presented between the deduced amino acid sequences of the two dehydrogenases of the R. capsulatus biosynthetic pathway. Chapter 8 summarizes the major results of the thesis and suggests possible future experiments.

Chapter 2: Effect of carotenoid mutations on the photosynthetic phenotype of R. capsulatus

I. Introduction

During anaerobic photosynthetic growth R. capsulatus synthesizes three photosynthetic pigment-protein complexes, each of which binds Bchl and carotenoids. These complexes are termed the RC (reaction center), LH-I or B870, and LH-II or B800-850 (light harvesting I and II antennae) (reviewed in Drews, 1985). B870 and B800-850 indicate the wavelengths in nm of the major near-IR (NIR) absorption maxima of bound Bchl in the two complexes (Drews and Oelze, 1981). The ratio of Bchl specific for LH-I per mol of RC is roughly 20:1 (Drews, 1985) and remains constant under different light intensities (Aagaard and Sistrom, 1972; Drews and Oelze, 1981), while the ratio of Bchl specific for LH-II per mol of RC is variable, ranging between 80-40:1 at low light intensities (Drews, 1985). At very high light intensities almost no LH-II is present (Drew and Oelze, 1981). LH-II is thus the dominant spectrally absorbing Bchl-protein complex under the illumination regimes considered here, masking both the absorbance of LH-I and to an even greater extent that of the RC, which has a maximal NIR absorbance at about 802 nm (Drews and Oelze, 1981).

The RC consists of three subunits, H, L and M, the latter two of which bind all of the Bchl and carotenoid pigment cofactors (Drews, 1985). LH-I and LH-II each contain two hydrophobic transmembrane polypeptides, denoted α and β, which bind the Bchl and carotenoid cofactors. The genes encoding the three RC subunits and the LH-I polypeptides have been isolated and sequenced (Youvan et al., 1984a, b), as have the genes for the LH-II α and β polypeptides (Youvan and Ismail, 1985). The R. capsulatus LH-II complex also contains a third polypeptide denoted γ which does not bind pigments

and whose function is not known (Drews, 1985). The gene encoding this polypeptide has not been isolated (Youvan and Ismail, 1985).

Mutants of R. capsulatus producing either LH-I or LH-II as the sole antenna complex and synthesizing either wildtype or neurosporene-type carotenoids have been studied (Scolnik et al., 1980b). An LH-II$^-$ mutant shows a blue-shifted chromatophore carotenoid absorption spectrum and the loss of the LH-II Bchl absorption maxima, in comparison to the wildtype strain accumulating the same carotenoid. The LH-I component absorbs at 880 nm in the LH-II$^-$ mutant. Similarly, RC$^-$ LH-I$^-$ mutants show a red-shifted carotenoid absorption spectrum, with no LH-I shoulder on the remaining LH-II Bchl absorptions. Thus, shifts in the absorption maxima of total chromatophore carotenoids or total chromatophore Bchl may be used to detect changes in the ratios of the LH-II and LH-I antenna complexes.

A variety of carotenoid biosynthesis mutants (crt) of R. capsulatus (Yen and Marrs, 1976; Scolnik et al., 1980a; Zsebo and Hearst, 1984; Klug et al., 1985; Giuliano et al., 1986, 1988) and R. sphaeroides (Griffiths and Stanier, 1956; Sistrom et al., 1956; Cohen-Bazire et al., 1957; Segen and Gibson, 1971) have been described. These mutants continue to produce Bchl and retain the ability to grow photosynthetically. Blue-green mutants which lack colored carotenoids have been most extensively studied. Mutations blocking colored carotenoid synthesis entirely have a pleiotropic effect on the R. capsulatus LH-II complex. Both the LH-II Bchl absorptions (Scolnik et al., 1980b; Zsebo and Hearst, 1984) and the γ polypeptide (Zsebo and Hearst, 1984) are absent in these blue-green mutants. Several carotenoidless mutants have been shown to incorporate reduced amounts the LH-II α polypeptide into the membrane (Tadros et al., 1984; Klug et al., 1984). Some R. capsulatus blue-green mutants have the LH-II β polypeptide in the membrane while others do not (Marrs, 1982). The question of whether carotenoid mutations affect mRNA accumulation for the β and α pigment-binding polypeptides of LH-II, has been previously addressed only in two blue-green mutants in which the crt

genetic lesion has not been defined (Klug et al., 1984; Klug et al., 1985). These polypeptides are encoded by the puc operon, which is unlinked to the R. capsulatus photosynthesis gene cluster (Youvan et al., 1985).

Thus, although certain aspects of photosynthesis and gene expression in crt mutants have been investigated in the above mentioned studies, a comprehensive comparison of growth rates, absorption properties of pigment-protein complexes, and expression of the genes encoding the structural photosynthetic polypeptides has not been carried out in any purple non-sulfur photosynthetic bacterium using the entire range of available crt mutants. We describe in detail in this chapter the photosynthetic phenotypes of R. capsulatus strains carrying mutations in crtA, B, C, D, E, F, I and J, in comparison to the wildtype.

The major carotenoid in anaerobic photosynthetic cultures of wildtype R. capsulatus is spheroidene (Fig. 1-5). Under the same growth conditions crtA mutants also accumulate spheroidene, crtC mutants accumulate neurosporene, crtD mutants accumulate neurosporene, hydroxyneurosporene and methoxyneurosporene, and crtF mutants accumulate demethylspheroidene (Yen and Marrs, 1976; Scolnik et al., 1980a), in addition to other minor carotenoid species (Schmidt, 1978; Scolnik et al., 1980b). crtB, crtE, crtI and crtJ mutants have a blue-green phenotype during photosynthetic growth, resulting from the absence of colored carotenoids and the continued synthesis of Bchl (Yen and Marrs, 1976; Zsebo and Hearst, 1984). crtI mutants have recently been shown to accumulate phytoene, the first C_{40} carotenoid (Giuliano et al., 1986; Chapter 4). The phytoene precursors accumulated in crtB, crtE and crtJ mutants have also been identified (Chapter 4).

II. Materials and methods

Growth and maintenance of the bacteria

The R. capsulatus crt mutants and wildtype strains used in this study are described in Table 2-1. Cells were grown in RCV minimal medium (Weaver et al., 1975) under anaerobic photosynthetic conditions (Chapter 4, Materials and methods) and used for growth rate measurements, cell titer determinations, and isolation of pigments, chromatophores and RNA. For growth of strain Y68 the RCV medium was supplemented with tryptophan (see Chapter 4, Materials and methods). Cells were harvested during mid-log phase growth, except in growth rate experiments, where OD_{680} measurements were made with a Bausch and Lomb Spectronic 21 colorimeter until cultures reached stationary phase.

Determination of cell titers

Viable cell titers were determined by plating assays to measure colony-forming-units/ml (CFU). 0.1 to 0.2 ml of 10^6-fold dilutions from mid-log phase cultures of the R. capsulatus wildtype and crt mutants prepared from samples of known absorbance at 680 nm were plated onto RCV agar plates. Six plates were used for each plating assay and three or four independent assays were performed for each strain. Bacteria were grown for several days in a 32ºC incubator and the colonies were counted.

Pigment extractions, chromatophore isolation and visible-NIR spectroscopy

Total photosynthetic pigments were extracted by using a mixture of acetone:methanol (7:2) as originally described by Cohen-Bazire et al. (1957). Approximate Bchl:carotenoid molar ratios (Table 2-2) were determined as follows. The extinction coefficient used for extracted Bchl was 76 mM^{-1} cm^{-1} at 772 nm, as determined by Clayton (1966) in

acetone:methanol (7:2). Extinction coefficients for extracted carotenoids were 156 mM^{-1} cm^{-1} at 437 nm for neurosporene-type carotenoids in petroleum ether, as calculated from the values of Sunada and Stanier (1965), and 149 mM^{-1} cm^{-1} at 453 nm for spheroidene-type carotenoids in acetone, as calculated by Evans et al. (1988). The former carotenoid extinction coefficient was used for Y68 (crtC) and PBR510 (crtD) extracts, and the latter value used for PY1291, PSB211 (both crtF), KZR9A12 (crtA) and SB1003 (wildtype) extracts. Carotenoid and Bchl concentrations were determined at their respective λ_{max} absorbances in our solvent system. Pigment extracts were dried under a stream of nitrogen and resuspended in ethyl ether:methanol (7:2) for spectral scans. Chromatophore vesicles derived from the intracytoplasmic photosynthetic membrane were isolated as described by Youvan et al. (1983). Concentrations of chromatophores were normalized on the basis of total crude chromatophore protein using a modified Lowry protein assay (Zhu et al., 1986). Spectra of both the extracted pigments and the normalized chromatophore samples were recorded using a Varian 2300 spectrophotometer.

Isolation of RNA, dot blot and Northern blotting procedures

Total RNA was isolated from mid-log phase photosynthetic cultures of R. capsulatus using the method of Zhu and Kaplan (1985), adapted for 15 ml cultures. RNA concentrations were normalized by several rounds of hybridization with pRC1 (courtesy of G. Drews), a cosmid probe containing a cloned set of R. capsulatus rRNA genes (Yu et al., 1982), using dot blots (1-5 ng total RNA per dot) prepared from dilutions of the RNA stocks. Dot blots probed for mRNAs contained about 2 µg of total RNA per dot, with side-by-side duplicate dots made for each probing. The RNA dot blotting procedure of Schloss et al. (1984) was followed, using a Gene Screen nylon membrane for all hybridizations except with the LH-II oligonucleotide probe, in which case nitrocellulose was used. Northern blots were performed by electrophoresis of denatured RNA through 1.2 % agarose gels containing 6 % formaldehyde (Maniatis et al., 1982) and subsequent

blotting to either Gene Screen or nitrocellulose membranes as described in Zhu and Hearst (1986) and noted above.

Labelling of probe DNA, detection of mRNA species and quantitation of dot blots

The functions of the pufQBALMX operon gene products have been described in Chapter 1. The M13 probes specific for mRNAs from the LH-I α subunit (encoded by pufA), RC-L (encoded by pufL), and RC-H (encoded by puhA) have been described (Zhu and Hearst, 1986) and were generated during the sequencing of these genes (Youvan et al., 1984a). The LH-I α probe hybridizes to 0.5 kb pufBA and 2.6 kb pufBALMX mRNAs, while the RC-L probe hybridizes only with the pufBALMX mRNA. Both of these mRNA species are long-lived processing products of an unstable 3.4 kb transcript covering the entire pufQBALMX operon (Chen et al., 1988; Adams et al., 1989). Since the molar ratio of the pufBA to pufBALMX mRNAs is about 9:1 (Belasco et al., 1985), most of the mRNA hybridizing to the LH-I α probe corresponds to the pufBA species. The M13 probe for PufQ (encoded by pufQ) was generated during the sequencing of this region and has been described in Zhu and Hearst (1988). The M13 probe for ORF J mRNA was generated during the sequencing of this region (M. Alberti, unpublished data; Chapter 3). The 15-mer oligonucleotide probe for the LH-II β subunit, which hybridizes to pucBA mRNA, has been previously described (Zhu and Hearst, 1986). M13 probes were labelled by primer extension as described in Chapter 4 (Materials and methods). The LH-II oligonucleotide was labelled at the 5' end by a polynucleotide kinase reaction with 50 μCi 5'-[γ-^{32}P]ATP (5000 Ci/mmol) (Zhu and Hearst, 1986). pRC1 was labelled by nick-translation with 50 μCi 5'-[α-^{32}P]dATP (400 Ci/mmol) using a kit and protocol supplied by Bethesda Research Laboratories and [α-^{32}P]dATP from Amersham. Procedures for probing of RNA blots are as described in Maniatis et al. (1982). Dot blots were quantitated subsequent to hybridization and autoradiography by excision of the dots and

scintillation counting in 5 ml of Opti-fluor (Packard Co.) using a Packard model 3385 scintillation counter.

III. Results

A. Growth rates and cellular light scattering

The doubling times of carotenoid mutants grown under photosynthetic conditions (5 W/m^2) range between 3.8 and 17.7 hours. In contrast, the two wildtype strains have an average doubling time of 3.3 hours (Table 2-1). Only the green crtD mutant PBR510 has a doubling time statistically equivalent to that of the wildtype strains (3.8 $\pm$ 0.5 hours). The doubling times of blue-green mutants (crtB, E, I and J) ranged from 6.9 to 17.7 hours. The two crtF mutants showed doubling times of 6.2 and 7.9 hours. The green crtC mutant had a doubling time of 4.1 hours, slightly longer than that of the wildtype strains.

Plating assays to determine the viable cell titer per OD at 680 nm were performed (Table 2-4). Cohen-Bazire et al. (1957) suggested the utility of optical density measurements made at 680 nm as a means of determining cell titers by light scattering, avoiding wavelengths at which pigment-protein complexes absorb. Substantial variations were observed in the viable cell titer between the carotenoid biosynthesis mutants and the wildtype strain. These differences indicate the need for caution in interpreting experiments comparing different strains of bacteria normalized on the basis of light scattering measurements. In general, the carotenoid mutants having the longest doubling times showed the greatest light scattering on a per cell basis. We propose that this effect arises from differences in the average cell size of these mutants compared to the wildtype. This issue will be addressed further in the Discussion.

B. Pigments and pigment-protein complexes

Total pigments were extracted from photosynthetically grown cultures of the wildtype and carotenoid mutants. Absorption spectra of the pigment extracts revealed differences in Bchl:carotenoid molar ratios between the mutants accumulating colored carotenoids and

Table 2-1. Properties of *R. capsulatus* strains used in this study[a]

Strain[b]	Genotype[c]	Relevant phenotype and reference[d,e,f]	Doubling time in hours ± mean S.D.[g]
B100		Wildtype pigments, (1)	3.4 ± 0.2
SB1003	*rif*-10	Wildtype pigments, (2)	3.2 ± 0.1
KZR9A12	*crtA*Ω(41.0::Tn5.7) *rif*-10	Yellow-brown, (3)	5.4 ± 1.0
W4	*crtB4*	Blue-green, (2)	12.3 ± 3.0
Y68	*crtC68 str-2 trpA20*	Green, Str^r, Trp^-, (2)	4.1 ± 0.5
PBR510	*crtD223 rif*-10	Green, (4)	3.8 ± 0.5
KZR8A1[e]	*crtE*Ω(34.6::Tn5.7) *rif*-10	Blue-green, (4)	17.7 ± 3.0
PY1291	*crtF129*	Muddy brown, (5)	6.2 ± 0.8
PSB211	*crtF21*	Muddy brown, (5)	7.9 ± 2.0
KZR9F4[e]	*crtI*Ω(39.8::Tn5.7) *rif*-10	Blue-green, (3)	12.6 ± 2.0
KZR9E3[e]	*crtJ*Ω(53.5A::Tn5.7) *rif*-10	Blue-green, (3)	6.9 ± 0.4

[a] abbreviations used in this table are: Rif, rifampicin; Str, streptomycin; Trp, tryptophan

[b] nomenclature for KZR strains was developed in Zsebo and Hearst (1984), KZR strains and PBR510 are derived from SB1003

[c] strains carrying the *rif*-10 allele are Rif^r

[d] color phenotypes reflect aerobic growth on agar plates; wildtype pigmentation is reddish-brown under these conditions and yellow-brown under anaerobic photosynthetic conditions

[e] these strains may carry the *crtD223* allele masked by an earlier blockage in carotenoid biosynthesis

[f] references are: (1) Marrs (1981), (2) Yen and Marrs (1976), (3) Zsebo and Hearst (1984), (4) Chapter 4, (5) Scolnik et al. (1980)

[g] based on 4 to 8 independent determinations using photosynthetically grown cultures (see Materials and methods)

the wildtype (Fig. 2-1). These differences were estimated as described in Table 2-2. PSB211 and PY1291, both crtF mutants, exhibited 2 to 4-fold depressions in the wildtype Bchl:carotenoid ratio of 1.48:1 (Table 2-2). Pigment ratios in PBR510 and KZR9A12 were similar to the wildtype, while Y68 (crtC) showed a slight increase in Bchl:carotenoid.

Chromatophore spectra of pigment-protein complexes isolated from photosynthetically grown cells show that mutations in crtB, E, I and J eliminate the LH-II Bchl absorption maxima found in the wildtype grown under our conditions at 800 and 857 nm (Fig. 2-2, Table 2-3). In addition, these mutations shift the red-most absorption maximum from 857 nm to 871-872 nm. Chromatophores containing pigment-protein complexes of other R. capsulatus blue-green mutants, including a phytoene accumulating strain, have similarly been shown to have red-most absorption maxima at 872 nm (Scolnik et al., 1980b). This is due to the background of LH-I absorption unmasked by the pleiotropic loss of LH-II absorption in the absence of colored carotenoids. RC absorption is negligible because of the molar excess of LH-I to RC (Drews, 1985), although in the case of the crtE mutant (KZR8A1) the small absorption at 800 nm may be due to the maximum of RC Bchl absorption (Drews and Oelze, 1981). Peak shifting of the red-most absorption to intermediate values between 857 and 872 nm (Table 2-3) indicates that crtC (Y68) and crtF (PY1291 and PSB211) mutants may have a reduced ratio of LH-II to LH-I, relative to the wildtype. In addition, mutants of R. capsulatus containing only LH-I or LH-II and wildtype carotenoids have been shown to have antenna carotenoid absorption maxima differing by about 10 nm (Scolnik et al., 1980b). The wildtype strain with both LH-I and LH-II complexes has carotenoid absorption maxima at intermediate values resulting from the superposition of the absorbances from both sets of chromatophore carotenoids, although LH-II is the dominant contributor. Thus, the loss of the characteristic three peak absorption spectrum for bulk antenna carotenoids in the crtF mutant strains also indicates a reduced LH-II:LH-I ratio, where both complexes contribute more equally to the total

Figure 2-1 A-C. Spectra of organic extracts of total photosynthetic pigments (Bchl and carotenoids) from carotenoid mutants taken in diethyl ether:methanol (7:2). **(A)** shows spectra from Y68 (crtC) and PBR510 (crtD), both of which accumulate neurosporene-type carotenoids and exhibit blue-shifted carotenoid absorptions, relative to the wildtype. **(B)** shows spectra from PSB211 and PY1291 (both crtF). **(C)** shows the absorption spectra from KZR9A12 (crtA) and SB1003 wildtype. Note the decrease in the relative ratio of Bchl:carotenoid absorbances in PY1291 versus wildtype, obvious upon comparison of the Bchl absorption at 766 nm and the carotenoid absorption bands from 400-500 nm. Absorption maxima of the organic extracts and the molar ratios of Bchl:carotenoid are given in Table 2-2. Isolated Bchl a absorbs at 358, 575 and 772 nm in diethyl ether (Britton, 1983).

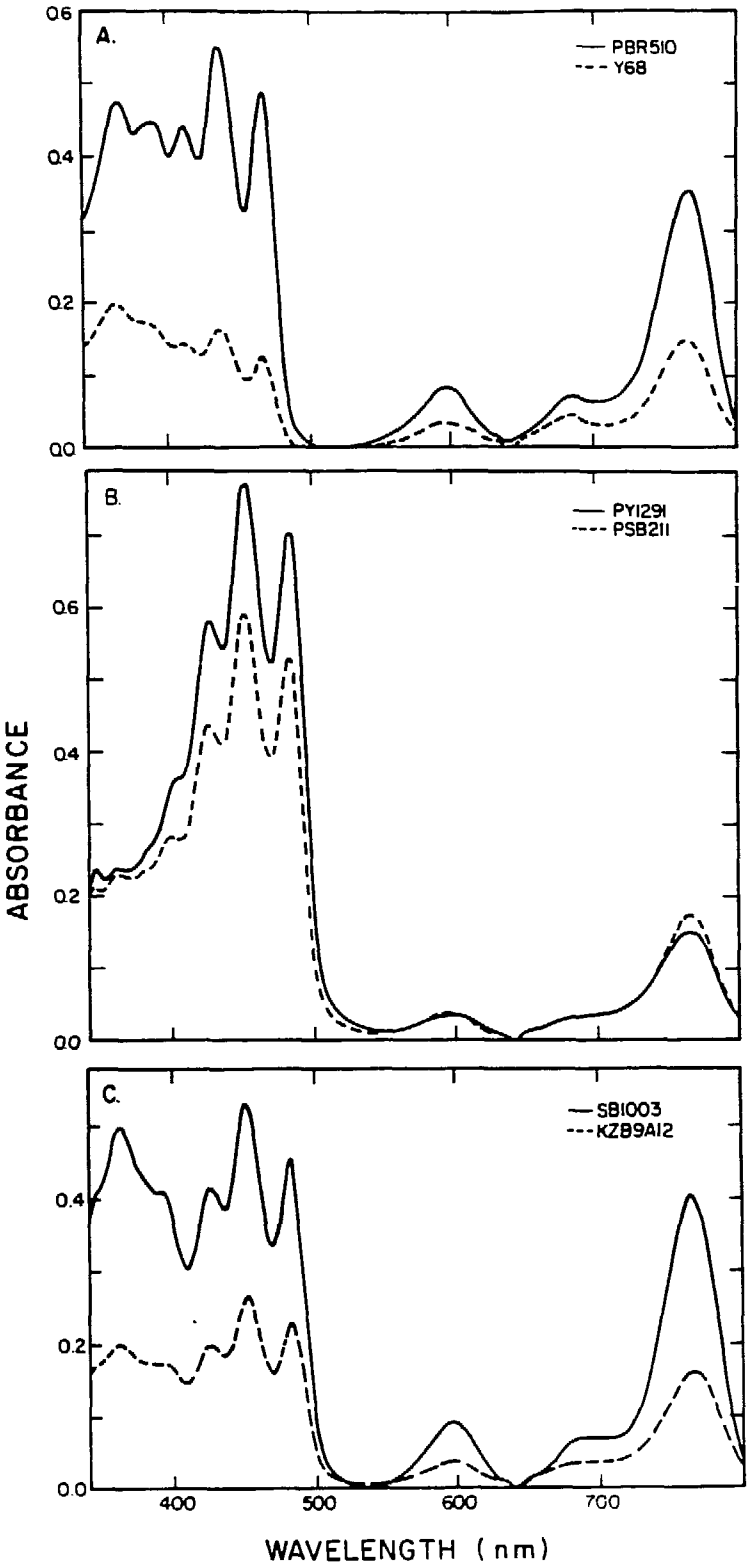
A.
PBR510
Y68
B.
PY1291
PSB211
C.
SB1003
KZB9A12
ABSORBANCE
WAVELENGTH (nm)
0.0
0.2
0.4
0.6
400
500
600
700

Table 2-2. Absorption maxima and molar Bchl to carotenoid ratios in organic extracts[a]

Strain[b]	Carotenoid maxima (nm)[c]	Bchl maximum (nm)	Estimated molar ratio of Bchl:carotenoid[d]
PBR510	414, 436, 466	766	1.32 : 1
Y68	411, 436, 466	766	1.90 : 1
PY1291	427, 452, 483	765	0.35 : 1
PSB211	426, 451, 483	766	0.87 : 1
SB1003	426, 451, 482	766	1.48 : 1
KZR9A12	426, 451, 482	766	1.15 : 1
LH-II[e]	- - - - -	- - -	1.85: 1
LH-I[e]	- - - - -	- - -	0.91: 1

[a] spectra shown in Fig. 2-1

[b] the blue-green mutants, which do not accumulate visibly absorbing carotenoids, have been omitted

[c] blue-shifting of the PBR510 and Y68 absorptions relative to other strains results from the accumulation of carotenoids with a nonaene rather than decaene chromophore

[d] extinction coefficients for pigments are given in Materials and methods

[e] data taken from Golecki et al. (1980) using an R. capsulatus wildtype strain grown under either high or low light regimes where LH-I or LH-II, respectively, are the dominant antenna complexes

Figure 2-2 A-D. Chromatophore spectra of pigment-protein complexes in carotenoid biosynthesis mutants and the wildtype. Strains and their genotypes are indicated in each panel. Equal chromatophore concentrations normalized to total chromatophore protein were used. (**A**) W4 and KZR8A1 both lack LH-II absorptions at 800 and 857 nm and show red-shifted NIR maxima due the remaining LH-I complex. KZR8A1, in addition, shows a small absorption at 800 nm, indicative of the RC absorption maximum. The absorption spectrum of chromatophores from strain KZR9F4 (crtI) was essentially superimposable on the W4 absorption spectrum (data not shown). In the case of KZR9E3 (crtJ), the NIR maximum was about 84% of the intensity of the same absorption in the W4 spectrum, but the maxima occurred at identical wavelengths (data not shown). Note the absence of carotenoid absorptions in the 400-550 nm region. (**B**) PBR510 shows essentially wildtype NIR absorption maxima. Y68 shows some red-shifting of the LH-II absorption maximum, indicating a reduction in the ratio of LH-II:LH-I relative to the wildtype. Both PBR510 and Y68 show blue-shifted carotenoid absorption maxima due to the accumulation of neurosporene-type carotenoids. (**C**) PSB211 and PY1291 both exhibit varying degrees of red-shifting of the LH-II 857 nm absorption maximum. In addition, the distinct three peak carotenoid absorption profile is replaced by a broad shoulder in these strains. Both of these spectral features indicate severe reductions in the ratio of LH-II:LH-I. (**D**) KZR9A12 and SB1003 wildtype both show similar absorption maxima across the spectrum, although the magnitude of the KZR9A12 absorptions is 3-fold lower. The absorption maxima of the chromatophore preparations are given in Table 2-3.

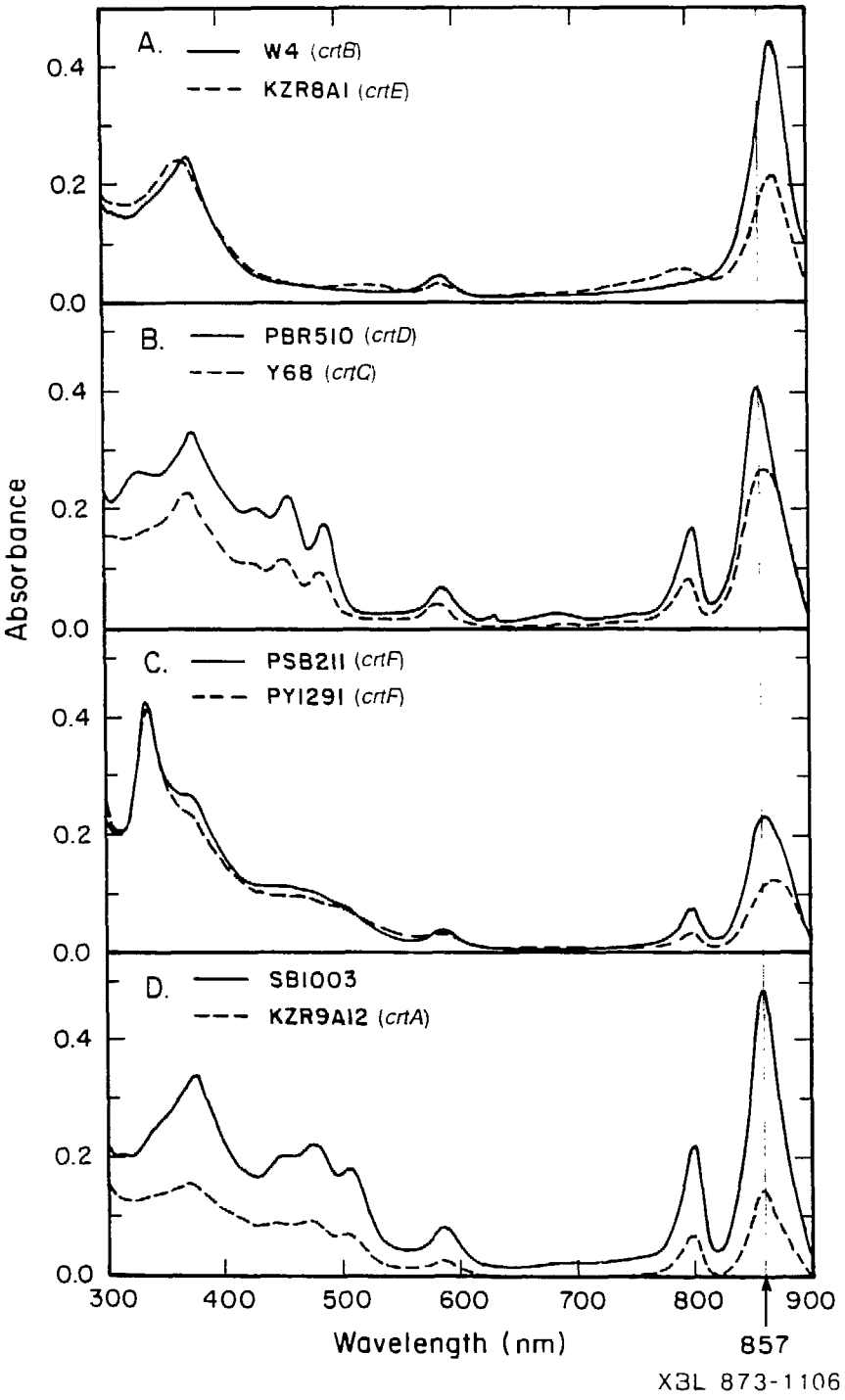
A.
W4 (crtB)
KZR8A1 (crtE)
B.
PBR510 (crtD)
Y68 (crtC)
C.
PSB211 (crtF)
PY1291 (crtF)
D.
SB1003
KZR9A12 (crtA)
Absorbance
0.0
0.2
0.4
300
400
500
600
700
800
900
Wavelength (nm)
857
X3L 873-1106

Table 2-3. Absorption maxima of Bchl and carotenoids in chromatophore pigment-protein complexes[a]

Strain	Carotenoid maxima (nm)[b,c]	NIR BChl maxima (nm)[d]
W4	- - - -	872
KZR8A1	- - - -	800, 872
KZR9F4	- - - -	872
KZR9E3	- - - -	871
PBR510	426, 453, 485	799, 855
Y68	428, 455, 486	800, 863
PY1291	~450 to 500	799, 869
PSB211	~450 to 500	800, 860
SB1003	447, 474, 505	800, 857
KZR9A12	445, 472, 504	800, 857

[a] spectra are shown in Fig. 2-2

[b] blue-green strains show no carotenoid absorption maxima

[c] PY1291 and PSB211 lack the characteristic three peak carotenoid absorption pattern but show a broad shoulder in the indicated region

[d] LH-II absorbs at ~800, ~857 nm; LH-I absorbs at ~872 nm; the RC absorbs also at ~800 nm but is masked by LH-II and LH-I absorptions except in the KZR8A1 chromatophore spectrum

chromatophore carotenoid spectrum. crtD (PBR510) and crtA (KZR9A12) mutants show magnitude of the absorption maxima at 800 and 857 nm is reduced about 3-fold. The absorption maxima of the chromatophore preparations are given in Table 2-3.

C. Expression of genes encoding the RC, LH-I and LH-II complexes, PufQ, and ORF J

Northern blot analysis of various sections of the photosynthetic gene cluster of R. capsulatus has revealed the presence of a relatively large amounts of a stable 0.4 kb mRNA species originating from the region of ORF J (Fig. 2-3ABC). Although the length of this mRNA species is insufficient to encode the entire ORF J, the mRNA may represent a stable processing product of a longer transcript originating from a promoter 3' to the translational stop of crtF (Fig. 2-3C, see Discussion).

Northern and dot blots of total RNA extracted from mid-log phase photosynthetic cells were probed for pufBALMX (LH-I β and α, RC-L and RC-M, PufX) and puhA (RC-H) mRNAs (Figs. 2-4, 2-5) using gene-specific M13 single-stranded DNA probes (Materials and methods). mRNA levels for these genes differ among the mutants, but appear to be coordinately regulated as shown by the quantitation of dot blots probed for pufA, pufL, and puhA mRNAs (Fig. 2-6). mRNA accumulation was reduced by a factor of up to 2 in some of the crt mutants, although the crtD mutant PBR510 and the crtE mutant KZR9E3 show no apparent reduction of mRNA accumulation. The latter example indicates that colored carotenoids are not required for accumulation of wildtype levels of LH-I and RC mRNA. mRNA for the pucBA operon (LH-II) (Figs. 2-5, 2-6) was more severely affected by crt mutations and showed a 2-4 fold reduction in both the dot and Northern blots in all the mutants, with the exception of the crtD mutant. The pattern of LH-II mRNA accumulation between the mutants did not always coincide with the variation in LH-I and RC mRNA accumulation. The blue-green crtJ mutant, with wildtype levels of all other mRNAs probed for, showed a 2-fold reduction in LH-II mRNA, for example.

Figure 2-3 A-C. Identification of a stable mRNA species originating from the BamHI-J fragment of pRPS404. (**A**) shows the determination of the size of the mRNA species by comparison of Northern blots probed with either pFL227, a plasmid containing the BamHI-J fragment, or with M13 subclone T319 which hybridizes to 0.5 kb pufBA and 2.6 kb pufBALMX mRNA species (Belasco et al., 1985; Zhu and Hearst, 1986). Both blots were prepared from the same agarose gel using 15 μg total RNA per lane from cultures of SB1003 and KZR8A1 (crtE). The size of the mRNA hybridizing to the BamHI-J fragment was estimated to be 0.4 kb. (**B**) shows the localization of this mRNA species to a region bordering the crt gene cluster, close to the BamHI-J/BamHI-C junction, using single-stranded M13 probes hybridized against 5 μg of total RNA per lane. Only probe XX6 hybridized to the 0.4 kb mRNA. (**C**) shows the location and directionality of the M13 probes (Solid arrows) used to map the 0.4 kb transcript (estimated position shown by a broken arrow), with respect to the position of ORF J, an open reading frame identified from the DNA sequence of the BamHI-J (Fig. 3-7) and BamHI-C fragments (M. Alberti, unpublished data). ORF J may be part of an operon required for Bchl biosynthesis (Chapter 3). -500 and 500 indicate the number of bp into the BamHI-J and BamHI-C fragments, respectively from the BamHI site at bp 1. The initial localization of the 0.4 kb mRNA to the BamHI-J fragment was performed in collaboration with F. Leach (U. of California, Berkeley).

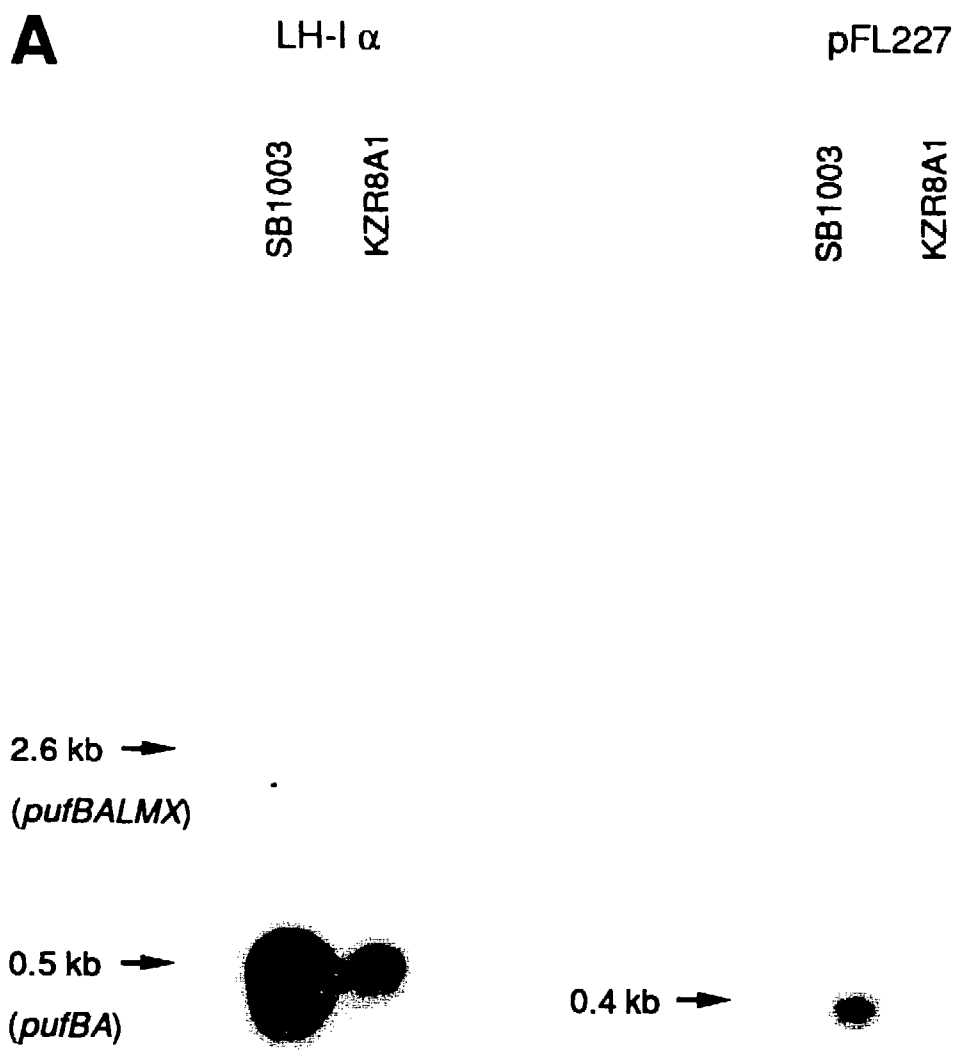
A
LH-I α
pFL227
SB1003
KZR8A1
SB1003
KZR8A1
2.6 kb
(pufBALMX)
0.5 kb
(pufBA)
0.4 kb

B

SS7 XX6 S465 S456 T451

0.4 kb →

C

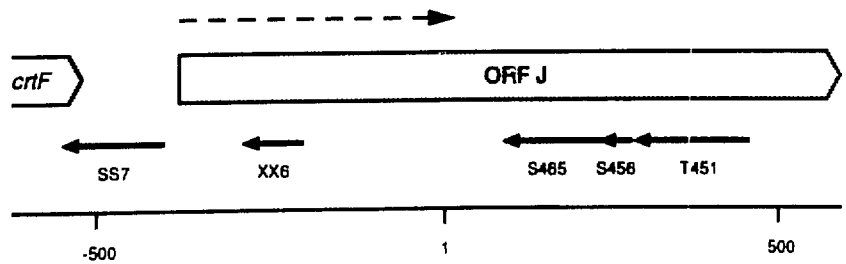

Figure 2-4 A-E. Northern blots of mRNA species derived from the puf, puh, puc, or ORF J operons, using probes for LH-I α, RC-L, RC-H, LH-II β and ORF J. 5 μg of total RNA (10 μg for the puhA and ORF J probes) from each strain was electrophoresed through agarose and blotted. Autoradiography exposure times differ between blots. Probes for mRNA species originating from puf transcripts hybridize to either (**A**) 0.5 and 2.6 kb mRNAs (covering pufBA and pufBALMX, respectively), or (**B**) only the latter species depending on the probe used (Zhu and Hearst, 1986). The stoichiometry of the 0.5 to 2.6 kb species is about 9:1 (Materials and methods). The 0.5 kb mRNA actually consists of two species of 0.49 and 0.50 kb (Belasco et al., 1985). The pucBA operon probe hybridizes to a 0.5 kb mRNA (**C**) (Zhu and Hearst, 1986), which has more recently been shown to consist of two distinct mRNAs of very similar sizes (505 and 491 bp) (Zucconi and Beatty, 1988). The puhA operon probe hybridizes to mRNAs of 1.4 and 1.2 kb (**D**) (Zhu and Hearst, 1986). The localization of the ORF J 0.4 kb mRNA (**E**) is described in Fig. 2-3. Note that the pattern of expression of mRNA species differs depending on the strain probed, but that puf (RC-L and LH-I α) and puh (RC-H) mRNAs are coordinately expressed, and that hybridization patterns to a given mRNA species correlate closely with the pattern and quantitation observed for the dot blots (Figs. 2-5, 2-6).

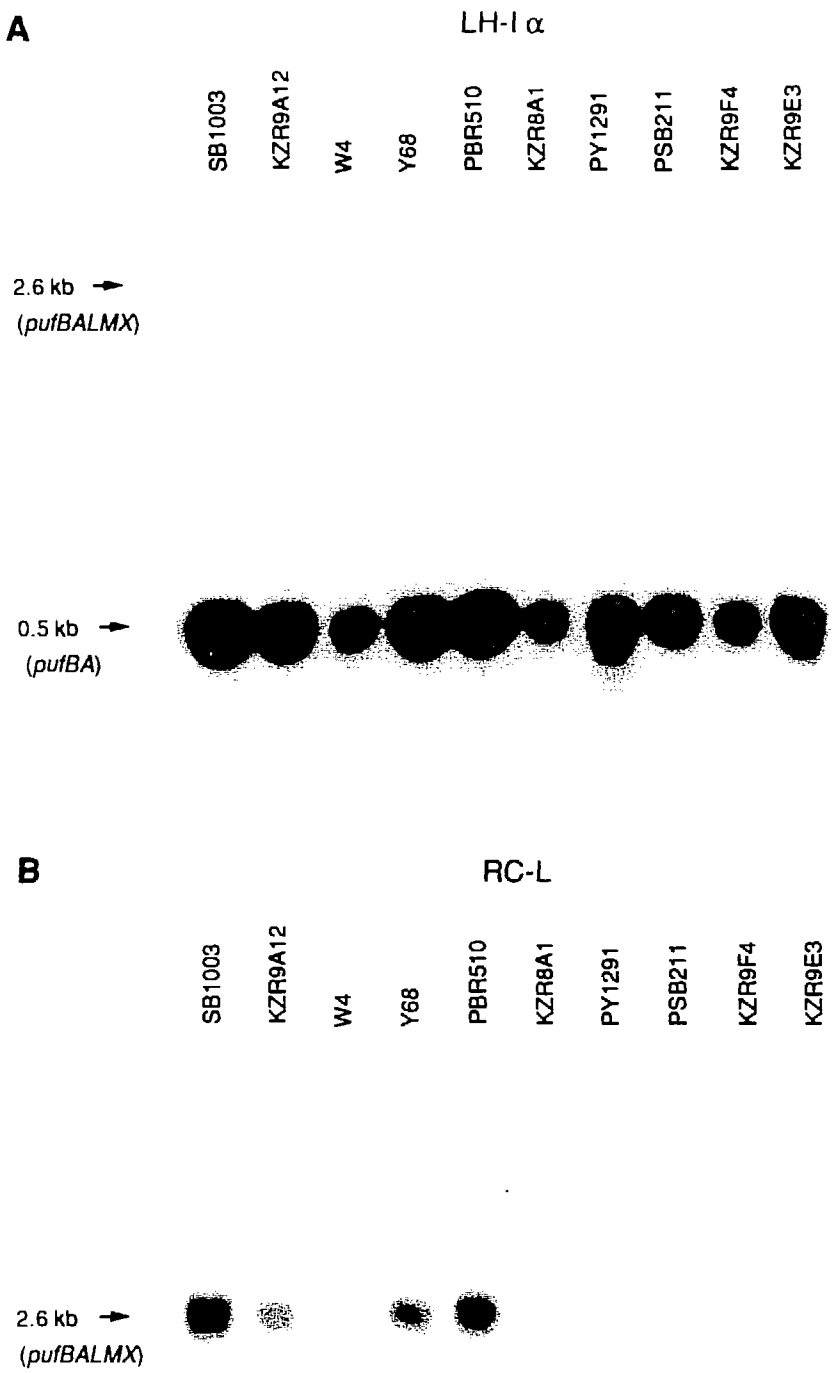
A
LH-I α
SB1003
KZR9A12
W4
Y68
PBR510
KZR8A1
PY1291
PSB211
KZR9F4
KZR9E3
2.6 kb
(pufBALMX)
0.5 kb
(pufBA)
B
RC-L
SB1003
KZR9A12
W4
Y68
PBR510
KZR8A1
PY1291
PSB211
KZR9F4
KZR9E3
2.6 kb
(pufBALMX)

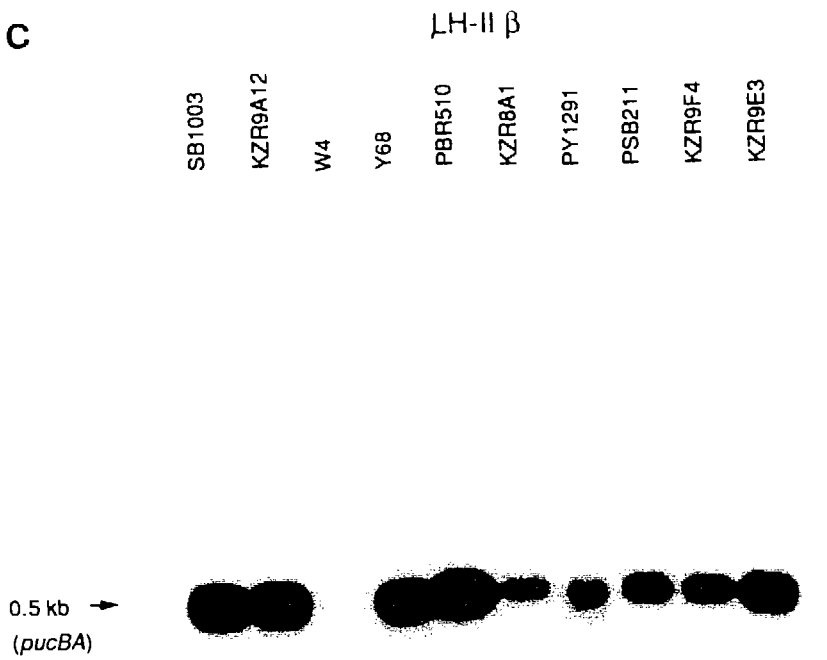
C
LH-II β
SB1003
KZR9A12
W4
Y68
PBR510
KZR8A1
PY1291
PSB211
KZR9F4
KZR9E3
0.5 kb
(pucBA)

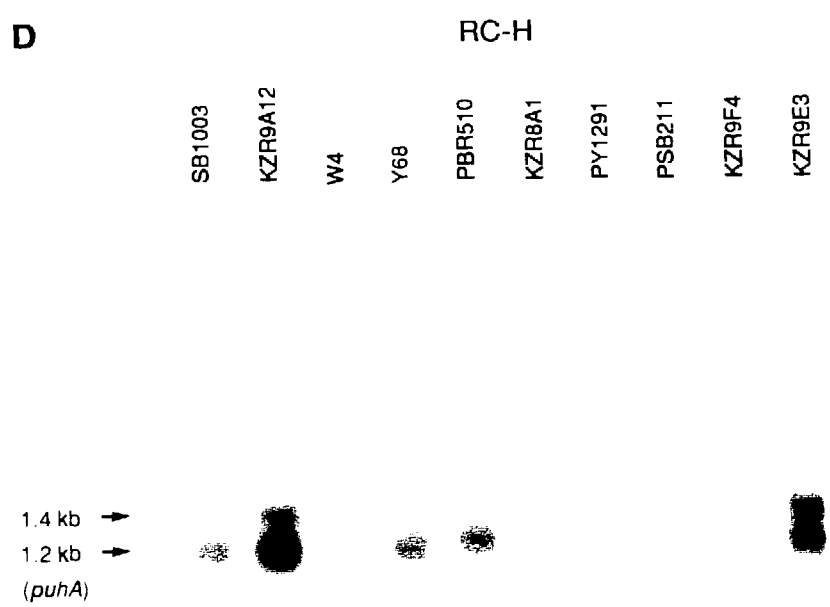
D
RC-H
SB1003
KZR9A12
W4
Y68
PBR510
KZR8A1
PY1291
PSB211
KZR9F4
KZR9E3
1.4 kb
1.2 kb
(puhA)

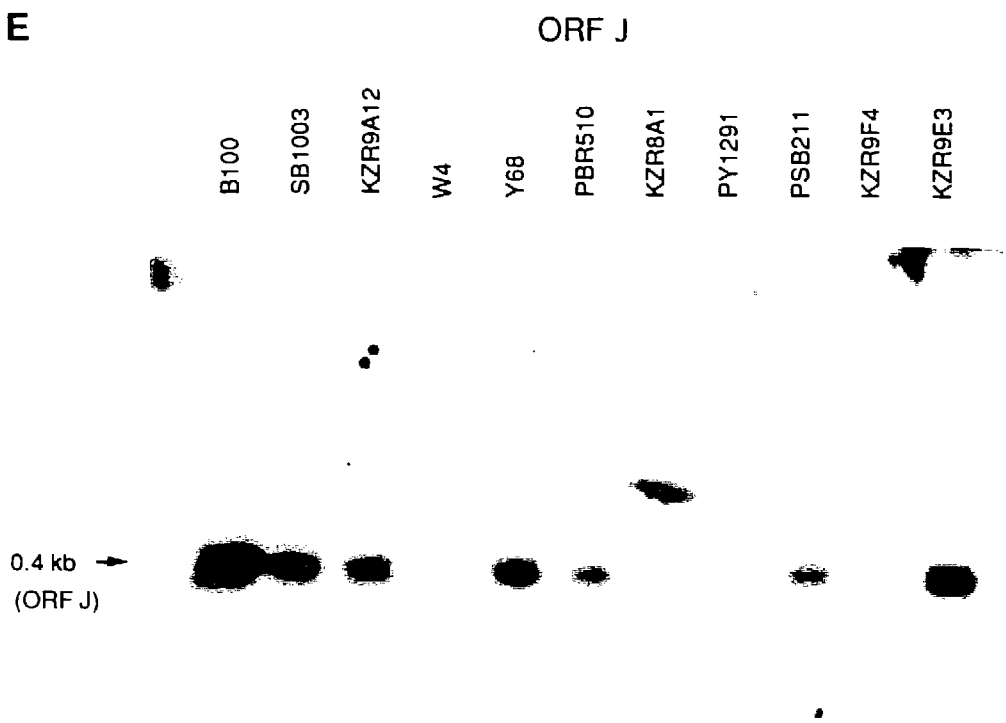
E
ORF J
B100
SB1003
KZR9A12
W4
Y68
PBR510
KZR8A1
PY1291
PSB211
KZR9F4
KZR9E3
0.4 kb
(ORF J)

Figure 2-5. Dot blot quantitation of mRNA species derived from the puf, puh, puc, or ORF J operons using probes located within the indicated genes (shown below the gene products at the top). 2 μg total RNA were used for each dot. Strains and their genotypes are shown at the left. Autoradiography exposure times differ between sets of dot blots. Duplicate dots were simultaneously probed in each case to minimize errors due to loading. Probes hybridize to the mRNA species described in Fig. 2-4, except for the probe for pufQ mRNA. This probe is located 5' to the coding region of pufQ (Zhu and Hearst, 1988) but lies within the transcribed non-coding region 3' to the pufQ promoter, from which transcription of the pufQBALMX operon originates (Bauer et al., 1988; Adams et al., 1989). Subsequent to autoradiography the dot blots were quantitated (Fig. 2-6).

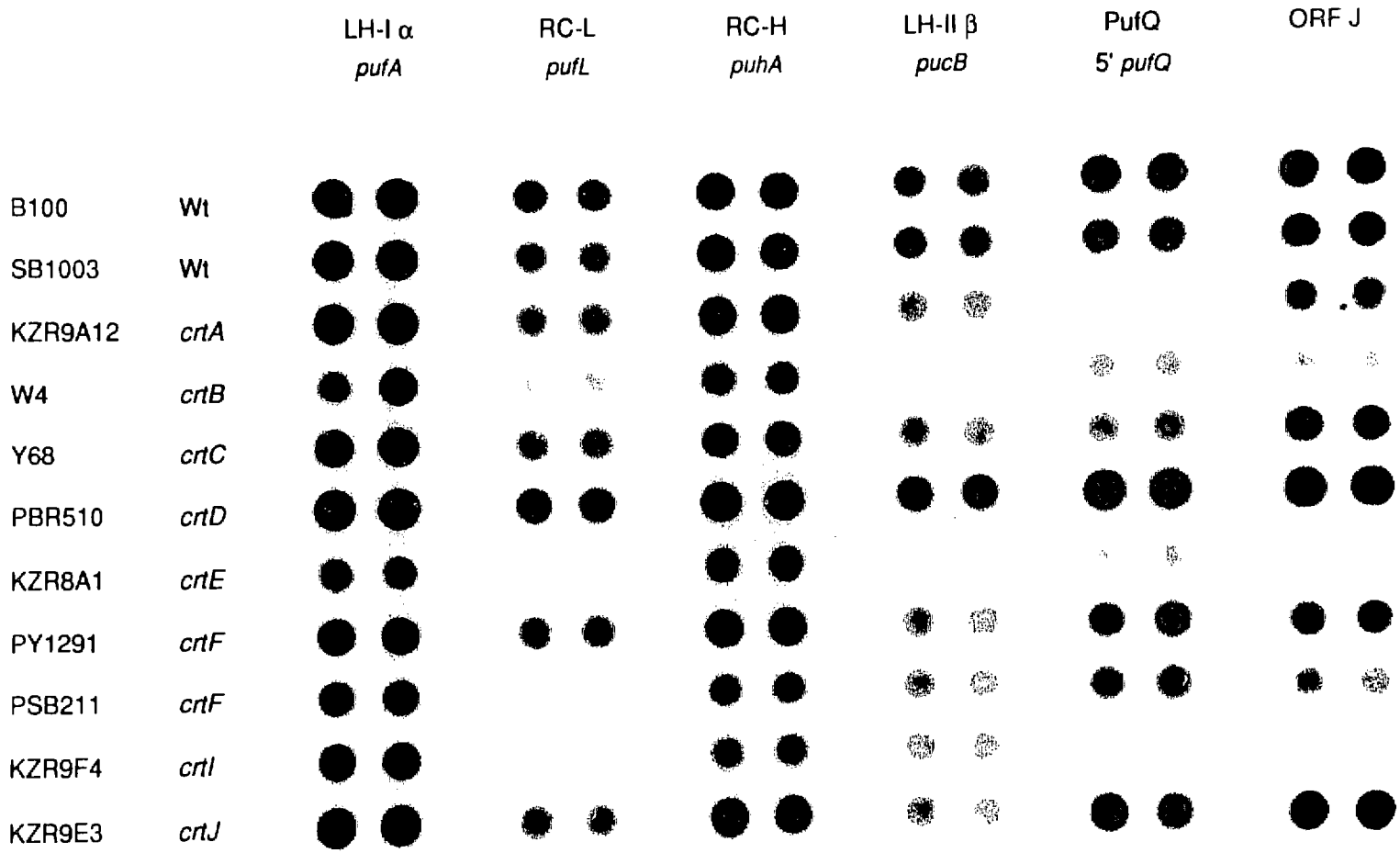
LH-I α
pufA
RC-L
pufL
RC-H
puhA
LH-II β
pucB
PufQ
5' pufQ
ORF J
B100
Wt
SB1003
Wt
KZR9A12
crtA
W4
crtB
Y68
crtC
PBR510
crtD
KZR8A1
crtE
PY1291
crtF
PSB211
crtF
KZR9F4
crtI
KZR9E3
crtJ

Figure 2-6. Bar graph comparison of dot blot hybridizations. Quantitation was performed by cutting out dots and liquid scintillation counting. Densitometric tracings of the autoradiograms gave similar results (data not shown). Data are normalized to hybridization obtained with RNA from strain SB1003. Both the Rif^r (SB1003) and Rif^s (B100) wildtype carotenoid strains gave similar hybridization results for all probes tested. The variation in hybridization results with these two strains gives an indication of the uncertainties involved in the quantitation shown here.

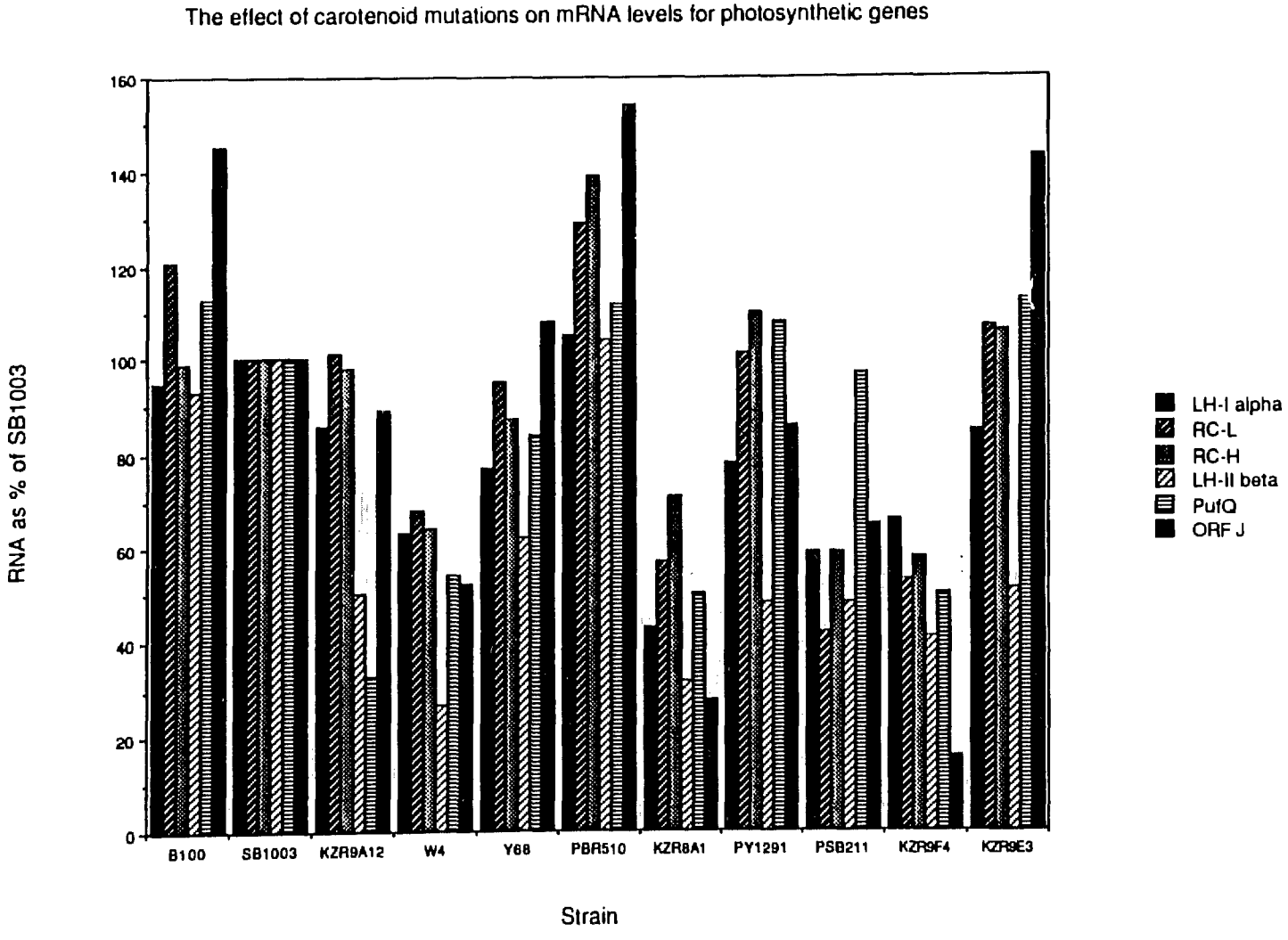
The effect of carotenoid mutations on mRNA levels for photosynthetic genes
RNA as % of SB1003
160
140
120
100
80
60
40
20
0
B100
SB1003
KZR9A12
W4
Y68
PBR510
KZR8A1
PY1291
PSB211
KZR9F4
KZR9E3
Strain
LH-I alpha
RC-L
RC-H
LH-II beta
PufQ
ORF J

In addition, dot blots were also probed for pufQ and ORF J mRNAs. According to recent results, pufQ is the proximal gene in the pufQBALMX operon (Bauer et al., 1988; Adams et al., 1989). PufQ is required for Bchl biosynthesis and has been proposed to be either a Mg tetrapyrrole-binding polypeptide (Bauer and Marrs, 1988) or a Bchl-binding polypeptide associated with a minor absorption band at 868 nm (Klug and Cohen, 1988). ORF J is located at one end of the crt gene cluster (Fig. 3-7) and may be part of an operon required for Bchl biosynthesis (Chapters 3, 4). pufQ mRNA is accumulated at unusually low levels in the crtA mutant KZR9A12, relative to the accumulation of 3' portions of puf transcript. ORF J mRNA accumulation is drastically reduced in the crtI mutant KZR9F4 (Figs. 2-4, 2-5, 2-6).

For dot blot hybridization experiments both rifampicin resistant (Rif^r) and rifampicin-sensitive (Rif^s) strains with wildtype pigmentation were used as controls (Table 2-1). Although to our knowledge the frequently used Rif^r 'wildtype' strain SB1003 has no other phenotypic differences from the Rif^s strain B100, the mutation conferring Rif^r is known to map to RNA polymerase in E. coli (Wehrli et al., 1968). Therefore, to exclude the possibility of differences in mRNA accumulation between the Rif^r and Rif^s crt mutants based solely on differential initiation of transcription, we probed RNA from both SB1003 and B100. In no case was a dramatic variation in mRNA levels observed between these strains (Figs. 2-5, 2-6).

IV. Discussion

A. Lack of a functional LH-II complex increases photosynthetic doubling time and cellular light scattering

We have observed a pronounced impairment of the photosynthetic growth rates, and reductions in both the Bchl:carotenoid ratio in whole cells and the accumulation of a stable LH-II complex with bound Bchl in the photosynthetic membrane as the result of mutations in all crt genes tested, with the exception of crtD. The impairment of growth rates in the carotenoid mutants either lacking or having reduced amounts of LH-II in the membrane (Table 2-4) is probably due to the reduction in the Bchl and carotenoid light harvesting cross-section of the photosynthetic antenna, rather than to a gross metabolic defect caused by the carotenoid mutations. KZR8A1, the crtE mutant, showed the longest photosynthetic doubling time and in fact may have suffered a reduction in the normally fixed ratio of LH-I:RC, as evidenced by the RC absorption maximum visible in chromatophore preparations from this strain (Table 2-3). The growth of this strain is thus impaired not only by the loss of the LH-II antenna and carotenoid light harvesting function, but by a reduction in the amount of LH-I, relative to the other blue-green mutants. The cause of this particular effect is unknown. Sistrom et al. (1956) observed that a blue-green phytoene-accumulating mutant of R. sphaeroides showed a reduced photosynthetic growth rate in comparison to the wildtype, although both strains showed identical growth rates during dark aerobic growth. Kiley et al. (1988) have shown that an R. sphaeroides blue-green mutant lacking the LH-II complex exhibited a doubling time roughly twice that of the wildtype strain when cultures were illuminated at 10 W/m^2. The specific Bchl content of the mutant was 2 to 3-fold less than that of the wildtype, although the wildtype LH-I:RC stoichiometry was preserved.

Striking observations have recently been made by Hunter et al. (1988) and Kiley et al. (1988), who have proposed that the LH-II (B800-850) complex is required for the

Table 2-4. Light scattering at 680 nm versus viable cell number, correlated with the ratio of LH-II:LH-I

Strain[a]	Ratio of LH-II:LH-I complex[b]	CFU[c] per OD at 680 nm ± mean S.D.
B100	Not determined	$1.3 \times 10^9 \pm 3.1 \times 10^8$
SB1003	Wildtype	$1.2 \times 10^9 \pm 2.7 \times 10^7$
KZR9A12	Wildtype[d]	$7.1 \times 10^8 \pm 1.1 \times 10^8$
W4	No LH-II	$2.7 \times 10^8 \pm 2.6 \times 10^7$
Y68	Reduced	$6.1 \times 10^8 \pm 1.2 \times 10^8$
PBR510	Wildtype	$1.1 \times 10^9 \pm 2.8 \times 10^8$
KZR8A1	No LH-II	$6.1 \times 10^8 \pm 1.1 \times 10^8$
PY1291	Reduced	$3.7 \times 10^8 \pm 5.6 \times 10^7$
KZR9F4	No LH-II	$5.4 \times 10^8 \pm 1.4 \times 10^8$
KZR9E3	No LH-II	$8.1 \times 10^8 \pm 5.1 \times 10^7$

[a] genotypes are given in Table 2-1
[b] see Fig. 2-2 and Table 2-3 for spectroscopic data
[c] CFU (colony forming units/ml) based on 3 or 4 independent sets of cell platings (see Materials and methods)
[d] although the LH-II:LH-I ratio is wildtype, the amount of LH-II per µg of total chromatophore protein is reduced in this strain (Fig. 2-2)

maturation of the intracytoplasmic membrane in R. sphaeroides. Hunter et al. (1988) observed in electron micrographs of thin sections of bacterial cells that a RC^+ LH-I^+ LH-II^- mutant with wildtype carotenoids produced long tubular internal membranes, rather than the normal vesicular membranes produced by the wildtype or by a RC^- LH-I^- LH-II^+ mutant. The tubular membranes synthesized in the LH-II^- strain were sometimes observed to stretch between two cells apparently interrupted in the process of division. A partial revertant of the LH-II^- strain, synthesizing a small amount of LH-II, showed mixed tubular and vesicular membranes. These authors concluded that absence of the LH-II complex alone is necessary and sufficient to cause the abnormalities in the photosynthetic membrane. Kiley et al. (1988) made similar observations in a blue green carotenoidless mutant also lacking the LH-II Bchl and both of the LH-II apoproteins (although the R. capsulatus LH-II contains α, β and γ polypeptides, the R. sphaeroides LH-II complex has only the former two proteins). On the other hand, these authors reported that a mutant lacking LH-II Bchl but synthesizing wildtype carotenoids showed an abnormal intracytoplasmic membrane, but did not produce the long tubular structures. Both mutants showed a similar pattern of chromatophore proteins, except for the synthesis of reduced amounts relative to wildtype of a polypeptide which was completely absent in the blue-green carotenoidless strain. Kiley et al. (1988) have suggested that either the loss of the LH-II pigment-binding polypeptides, the loss another non-pigmented component of the chromatophore membrane, or the absence of a functional LH-II complex produces the unusual membrane morphology.

Table 2-4 and Fig. 2-2 show that those R. capsulatus carotenoid mutants with cell titers per OD 680 substantially lower than that of wildtype either lack a spectroscopically detectable LH-II antenna (W4, KZR8A1, KZR9F4, KZR9E3), show reductions in the normal LH-II:LH-I ratio (PY1291), or show an overall reduction in the amount of LH-II as a fraction of total chromatophore protein (KZR9A12). We suggest that the increase in light scattering on a per cell basis in these strains is caused by the complete or partial

inhibition of vesicular membrane formation, leading to defects in cellular division, and alterations in membrane morphology and cell size of varying degrees of severity. The differences in the degree of light scattering by the blue-green mutants, all of which lack functional LH-II, may arise from differences in the accumulation of some of the LH-II polypeptides in the membrane (Tadros et al., 1984; Klug et al., 1984; data not shown) or of some other associated component required for normal membrane development. It would clearly be of interest to study intracytoplasmic membrane morphology of the mutants described here, particularly those which synthesize carotenoids but show an altered LH-II:LH-I ratio.

B. Carotenoid mutations affect the amount of LH-II in the photosynthetic membrane but do not abolish LH-II mRNA accumulation

Alterations in the LH-II:LH-I ratio in the photosynthetic membrane probably cause the observed differences in the Bchl:carotenoid ratio in extracted pigments from whole cells of certain carotenoid mutants (Table 2-2). Golecki et al. (1980) found in photosynthetic cultures of R. capsulatus that high light grown cells containing almost exclusively LH-I had a Bchl:carotenoid molar ratio of 0.91:1, while in low light cells in which LH-II was the dominant antenna complex the ratio was 1.85:1. Similarly, Sistrom (1978) has shown that Bchl:carotenoid molar ratios in the R. sphaeroides green strain Ga, which accumulates crtD carotenoids (Scolnik et al., 1980a), are about 1:1 in cells with a low specific Bchl content (equivalent to high light) and approach a limiting ratio of 2:1 in cells with a high Bchl content (equivalent to low light). Finally, recent data from whole cells pigment extractions of R. sphaeroides wildtype, LH-I$^-$ and LH-II$^-$ mutants have determined the respective Bchl:carotenoid ratios to be 1.54:1, 1.88:1 and 1.14:1 (Hunter et al., 1988). We stress the similarities between the Bchl:carotenoid ratios observed under similar conditions for both R. capsulatus and R. sphaeroides. Uncertainties in the ratio of Bchl:carotenoid in the isolated LH-II and LH-I complexes, and differences in the ratios

reported between R. capsulatus and R. sphaeroides make comparisons to these values less meaningful (see Chapter 1 and below). The ratio of 1.48:1 observed in the R. capsulatus wildtype (Table 2-2) drops to 0.87-0.35:1 in crtF mutants, thus indicating a reduction in the LH-II:LH-I ratio. The 0.35:1 ratio for strain PY1291 is, however, lower than the predicted minimal ratio of 1:1 in the extreme case of no LH-II complex in the membrane. Perhaps this crtF mutant synthesizes excess carotenoids which are inserted into sites other than the normal pigment-protein complexes, in the absence of the normal complement of LH-II. crtF mutants may lack the normal complement of LH-II because the complex may not readily bind carotenoids with a tertiary hydroxy group.

Changes in the ratio of LH-II:LH-I are more obvious in the spectra of chromatophores from all of the crt mutants, except for the crtA and crtD strains (Fig. 2-2). We have shown that strains W4, KZR8A1 and KZR9E3 (the crtB, E and J mutants described in this chapter) accumulate pyrophosphate precursors of phytoene (Chapter 4). The complete absence of LH-II complex in the phytoene-accumulating crtI mutant KZR9F4 (Chapter 4) and the presence of the LH-II complex in the crtC mutant Y68, which accumulates neurosporene, suggests a relationship between the stability or assembly of LH-II and the structure of the carotenoid species present. Whether or not the phytoene accumulated in crtI mutants is incorporated into the RC and LH-I pigment complexes has not, to our knowledge, been determined. We propose that the intermediate neurosporene (or possibly phytofluene or 7, 8, 11 12-tetrahydrolycopene), has a structure which permits the incorporation of a stable LH-II complex into the photosynthetic membrane. The exact basis of this structural effect may relate to the conformations of specific carotenoids in the LH-II complex. The conformation of phytoene, which has only 3 conjugated double bonds, would be expected to be considerably more flexible compared to neurosporene with 9 conjugated double bonds. Such changes in conformational flexibility could lead to the destabilization of the minimal LH-II unit. It has been determined recently that the stoichiometry of Bchl to carotenoid in the LH-II complex of R. sphaeroides is 2:1 (Evans

et al., 1988). The R. capsulatus LH-II ($\alpha\beta$) monomer is thought to contain three Bchl (Drews, 1985) and the Bchl to carotenoid ratio is now also proposed to be 2:1 (Evans et al., 1988), implying that each carotenoid molecule must be shared between monomers in a higher order structure. These data support a model in R. sphaeroides which proposes the minimal unit of LH-II to be a dimer containing 6 Bchl and 3 carotenoid molecules (Kramer et al., 1984), and also agree both with pigment extractions from the isolated R. sphaeroides LH-II complex and with the total pigment content of a mutant which synthesizes only LH-II (Hunter et al., 1988). The partial loss of the LH-II complex in crtF mutants may result from poor binding of the accumulated hydroxycarotenoids, as suggested above, and destabilization of the LH-II apoproteins not complexed with carotenoid.

Klug et al. (1984, 1985) have shown that two carotenoidless R. capsulatus strains accumulated puc mRNAs but not the LH-II complex. Our data modify their proposal that carotenoids are required for the stability and/or the assembly of the LH-II complex, by defining the type of carotenoid molecule required for the accumulation of LH-II. No functional LH-II complex exists in mutants accumulating phytoene or its precursors, and reduced amounts of LH-II are present in mutants accumulating demethylspheroidene as the major carotenoid. A possible scenario for LH-II instability in the absence of the proper carotenoid involves the incorporation of LH-II polypeptides into the photosynthetic membrane and their subsequent degradation as the result of conformational instability, as has been explicitly suggested for LH polypeptides in mutants lacking Bchl (Tadros et al., 1984; Klug et al., 1985). A difference in protein stability of the R. rubrum B890 antenna complex in the presence and absence of carotenoids has been clearly demonstrated (Brunisholz et al., 1986). In a carotenoidless mutant, the N-terminus of the α-apoprotein is sensitive to proteinase K digestion, in comparison to the wildtype carotenoid-containing complex. The α-apoproteins from both strains have identical primary structures, indicating that the destabilization of the complex is a direct consequence of a conformational change

in the absence of carotenoid binding. An R. capsulatus mutant containing reduced amounts of LH-II complex in the absence of carotenoids has recently been described (Dörge et al., 1987). The phenotype of this mutant is complex, however. The mutant fails to accumulate any LH-II under chemoheterotrophic conditions, in contrast to the wildtype, and synthesizes reduced amounts of LH-II which may be abnormally energetically coupled to LH-I during anaerobic photosynthetic growth. These authors speculate that the reduction in stably incorporated LH-II could be due to either reduced Bchl synthesis in the mutant, or the importance of carotenoids for the assembly and stability of LH-II. Other results indicate pleiotropic effects on the accumulation of stable LH-II polypeptides into the R. capsulatus photosynthetic membrane in the absence of colored carotenoids (Marrs, 1982; Zsebo and Hearst, 1984; Tadros et al., 1984; Klug et al., 1984).

At the level of gene expression, our data indicate that reductions or loss of spectroscopically detectable LH-II complex are correlated with reductions in puc operon mRNA accumulation. Whether these changes result from differential transcription initiation or variations in mRNA stability between strains remains to be determined. In none of the crt mutants tested was puc mRNA completely absent, even in mutants completely lacking a functional LH-II antenna. We therefore conclude that absence of the LH-II complex cannot be due solely to depression of the puc operon mRNA levels, but more likely is the result of decreased stability of LH-II complexes lacking the proper carotenoid. Thus, regulation of the accumulation of the LH-II complex in the photosynthetic membrane occurs at several levels. In support of our results, Klug et al. (1984, 1985) have examined the expression of the puc operon in two carotenoidless mutants of R. capsulatus during a reduction of oxygen tension in the medium. These authors found differences in the induction of puc mRNA in the two mutants although, unfortunately, the nature of the carotenoid mutations carried in these strains has not been defined. It would be interesting to examine the expression of the puc operon, using the

four well-characterized blue-green mutants described in this chapter, in a growth shift experiment of the type described in Chapter 6. The relationship between carotenoid deficiency and LH-II mRNA accumulation in R. capsulatus should be contrasted with that of mRNA accumulation for LHCP, the PS II antenna. LHCP mRNA accumulation in maize seedlings depends on the presence of carotenoids at high light fluences. In this case, however, the dependency probably results from photooxidative damage to the chloroplast caused by photosensitizing Chl in the absence of carotenoids (Burgess and Taylor, 1988).

Although mRNA levels for LH-I α, RC-L and RC-H are reduced up to 2-fold, the effect is less pronounced than in the case of the 2 to 4-fold reductions in LH-II mRNA. Of the four mutants tested which lack colored carotenoids, the crtJ mutant KZR9E3 shows almost wildtype levels of LH-I α, RC-L and RC-H mRNAs. We conclude that although some carotenoid mutations may reduce the accumulation of mRNAs encoding the RC and LH-I, this effect is not directly correlated with the absence of colored carotenoids. Klug et al. (1985) similarly concluded in kinetic experiments that the regulation of RC and LH-I mRNA accumulation and assembly of these complexes was normal in a strain of R. capsulatus lacking carotenoids. mRNA levels for the RC and LH-I are not coordinated with LH-II mRNA in certain crt mutants, reinforcing the conclusion that the transcription of the genes encoding the LH-II and LH-I complexes is regulated differentially (Klug et al., 1985; Zhu and Hearst, 1986; Zhu et al., 1986), as is the accumulation of the protein complexes (Drews and Oelze, 1981). While colored carotenoids are not absolutely required for the accumulation of LH-II mRNA, their absence or the presence of an abnormal carotenoid complement may modestly reduce LH-II mRNA levels.

C. PufQ and ORF J mRNAs are not coordinately accumulated with RC and LH-I mRNAs

The crtA mutant KZR9A12 shows a reduced growth rate without any change in the

wildtype ratio of LH-II to LH-I, but with a reduction in the amount of pigment-protein complexes as a fraction of total chromatophore protein, which can now be explained in light of more recent discoveries. The crtA mutant shows the most severe reduction (3-fold) of pufQ mRNA accumulation for all strains tested, a result which does not agree with the pattern of coordinate mRNA accumulation in other carotenoid mutants between the puf and puh operons. PufQ has been shown to be required for the biosynthesis of Bchl and has been postulated to be involved in the transport of Bchl precursors during the synthesis of Bchl (Bauer and Marrs, 1988). Thus, reduction of pufQ mRNA levels in the crtA mutant might reduce the pool of Bchl available for photosynthetic pigment-protein complexes without altering the final ratio of these components in the photosynthetic membrane. The mechanism for the reduction of pufQ mRNA levels as the result of a crtA mutation remains obscure. Recent evidence indicates that pufQ is the proximal gene of the pufQBALMX operon (Bauer et al., 1988; Adams et al., 1989), although steady-state pufQ mRNA levels are considerably lower than those for the downstream pufBA segment of the operon. 0.5 kb pufBA mRNAs appear to be long-lived albeit translationally functional processing products of 2.6 kb pufBALMX mRNAs (Chen et al., 1988), the molar ratio of the former to the latter species being 9:1 (Belasco et al., 1985). The results placing pufQ as the proximal gene of the puf operon indicate that pufBALMX mRNAs are also processing products of intact 3.4 kb transcripts (Adams et al., 1989). The discoordination of pufQ and pufBA mRNA accumulation in the crtA mutant, relative to the wildtype, may reflect a differential stability in the 5' end of puf transcripts in the mutant. Whatever the mechanism of mRNA discoordination may be, we postulate that the 3-fold reduction in pufQ mRNA leads to reduced levels of PufQ in KZR9A12, causing the observed 3-fold reduction in LH-I and LH-II Bchl accumulation without changing the ratio of the two antenna complexes.

The level of ORF J mRNA is severely depressed in KZR9F4 (crtI), but not in other crt mutants (Fig. 2-6). Evidence indicates that ORF J may be part of an operon required for

Bchl biosynthesis (Giuliano et al., 1988; Chapter 3). crtI encodes phytoene dehydrogenase (Giuliano et al., 1986; Chapters 3, 4), a key carotenoid biosynthetic enzyme. The striking 6 to 9-fold reduction in ORF J mRNA (compared to both wildtype strains) suggests a possible linkage between the expression of genes for carotenoid and Bchl biosynthesis. Further experiments are needed to clarify whether such a linkage exists. The 0.4 kb ORF J mRNA is not long enough to represent the intact transcript for the entire ORF (Fig. 2-3C) and, by analogy to the differential stability of segments of puf operon transcripts, probably represents a stable processing product of a longer, possibly polycistronic transcript. Whether the 0.4 kb mRNA species is translationally active is at present not known.

D. The crtD mutation does not affect the photosynthetic phenotype

The green crtD mutant PBR510 displays an essentially wildtype phenotype with respect to photosynthetic growth rate, pigment-protein complexes and mRNA accumulation. This suggests that the wildtype strain possesses some subtle and undetected advantage over a crtD mutant during photosynthetic or some other growth mode. Studies of pigment-protein complexes isolated from R. sphaeroides mutants and reconstitution experiments using carotenoidless RC preparations indicate no obvious differences in the physical properties of these complexes containing either crtD-type or wildtype carotenoids (Cogdell and Frank, 1987). Perhaps the difference in structure between the nonaene chromophore carotenoids accumulated in crtD mutants (neurosporene, methoxyneurosporene, and hydroxyneurosporene) and the major wildtype decaene carotenoid accumulated during photosynthetic growth (spheroidene) contributes to a small difference in photosynthetic growth rates not detected within the range of error in the experiments described in this chapter (Table 2-1). Cohen-Bazire et al. (1957) observed no differences in anaerobic photosynthetic growth rates or in the absorption spectra of pigment-protein complexes from whole cells of the green mutant Ga of R. sphaeroides versus a strain with wildtype

carotenoids. Griffiths and Stanier (1956) have reported that green mutants of R. sphaeroides similar to R. capsulatus crtD mutants occasionally arise spontaneously from wildtype cultures. These data suggest that at least under laboratory growth conditions wildtype Rhodobacter possesses only a marginal selective advantage over crtD mutants.

IV. Summary

In summary, none of the crt mutants tested showed the complete abolition of mRNA accumulation for the photosynthetic genes examined (pufL, pufA, puhA, pucB, pufQ, ORF J), demonstrating that carotenoid synthesis is not an absolute requirement for the expression of any of these genes. On the other hand, some of the more significant changes in mRNA levels in certain mutants using specific probes indicate that crt mutations in some cases affect the level of expression of these genes. Both the loss of LH-II antenna complex in blue-green carotenoid mutants lacking visibly absorbing carotenoids and the reductions in the LH-II:LH-I ratio in some mutants accumulating colored carotenoids are probably due primarily to a reduced stability of the LH-II complex in the absence of the proper carotenoid. A secondary effect may result from a pleiotropic reduction of puc operon mRNA accumulation. We postulate that the structure of the carotenoids accumulated thus has a direct effect on the stability of LH-II. In contrast, we believe that the decrease in accumulation of both antenna complexes in crtA mutants is due to the reduction of mRNA levels for PufQ, a probable Mg tetrapyrrole-binding carrier polypeptide (Bauer and Marrs, 1988; Klug and Cohen, 1988). Other effects observed in the carotenoid mutants, such as the reduction in ORF J mRNA in a crtI mutant and the differences in light scattering properties of mutant cell cultures require further investigation.

Chapter 3: Subcloning, nucleotide sequence and organization of the R. capsulatus carotenoid genes

I. Introduction

Marrs (1981) originally isolated the R-prime plasmid pRPS404 containing a portion of the chromosome from R. capsulatus. The R. capsulatus DNA insert carried on this plasmid complemented all known point mutation defects in photosynthesis, suggesting that the genes encoding structural photosynthetic polypeptides as well as the enzymes involved in carotenoid and Bchl biosynthesis were clustered on the chromosome (Fig. 1-4). The genes encoding the RC and LH-I polypeptides were subsequently localized to the two ends of this 46 kb cluster, flanking the pigment biosynthesis genes, by marker rescue experiments (Youvan et al., 1983; Taylor et al., 1983). The genes encoding the LH-II pigment binding polypeptides have more recently been shown to be unlinked to the photosynthesis gene cluster (Youvan and Ismail, 1985). The genes encoding the RC subunits, LH-I (Youvan et al., 1984a) and LH-II (Youvan and Ismail, 1985) have been sequenced. No DNA sequences have been published for either the carotenoid (crt) or Bchl (bch) biosynthetic enzymes, however. This statement holds true, in fact, not only for R. capsulatus, but for all other organisms as well. Thus, it is of paramount interest to determine the organization and sequence of the these genes as a prelude to further studies of the gene products on one hand, and the regulation of pigment biosynthetic genes on the other hand. We focus in this chapter on the characterization of a subcluster of genes, within the photosynthesis gene cluster, devoted to the synthesis of carotenoid pigments.

Seven of the eight previously identified R. capsulatus crt genes were known to be clustered on the BamHI-H, -G, -M, and -J fragments of pRPS404 in the order crtA, I, B, C, D, E, F from left to right (Taylor et al., 1983; Zsebo and Hearst, 1984; Giuliano et al.,

1986, 1988). These studies established that mutations causing Bchl$^-$ phenotypes map at both ends of the crt gene cluster within these four BamHI fragments. crtJ, identified by a Tn5.7 insertion (Zsebo and Hearst, 1984) and separated from the other crt genes by about 12 kb (Fig. 1-4), was not examined in the work described in this chapter.

We have determined the nucleotide sequence of an 11039 bp region encompassing the BamHI-H, -G, -M, and -J fragments of pRPS404, and present here a comprehensive analysis of the DNA sequence, the gene organization, and the identification of regulatory signals for the initiation and termination of transcription within this region. The nucleotide sequence reveals the presence of a new gene, crtK, not described in previous studies. We have also identified regions of exceptional amino acid similarity between CrtI and CrtD, the two dehydrogenases of the R. capsulatus carotenoid biosynthetic pathway.

II. Materials and methods

Bacterial strains

E.coli strains HB101 (Maniatis et al., 1982) and JM103 (Messing et al., 1981) were used as hosts for the pBR-derived plasmids, and recombinant M13 phage, respectively. HB101 and JM103 were cultured using LC broth (Marrs, 1981) or M9 minimal growth media (Maniatis et al., 1982). Ampicillin was used at a concentration of 50 mg/ml to select for pBR-derived plasmids, while 50 mg/ml kanamycin was used to select for pRPS404 (Marrs, 1981).

Cloning

Plasmids pBR322, pBR325, and restriction enzymes obtained from various commercial suppliers were used in accordance with specifications provided and standard recombinant DNA protocols (Maniatis et al., 1982). pRPS404 was partially digested with BamHI and the resulting fragments shotgun cloned into the BamHI site of pBR325. Recombinant plasmids containing the BamHI-J, -M, -G, -H fragments (Fig. 3-7), designated pFL227, pFL268, pFL104, and pFL103, respectively, were isolated (Table 3-1; courtesy F. Leach). The BglII-A/XhoI-D and BglII-D/XhoI-D fragments of pRPS404 were isolated from an agarose gel and cloned into SalI/BamHI-restricted pBR322, generating pGABX1 and pGABX2 (Table 3-1). These two plasmids overlap all of the BamHI sites within the crt gene cluster. The BamHI inserts from pFL227, pFL268, pFL104 and pFL103 were isolated from low-melting agarose (Maniatis et al., 1982) and either cloned directly or further restricted prior to shotgun cloning into M13mp18 or M13mp19 vectors (Yanisch-Perron et al., 1985).

DNA isolation and sequencing

Plasmid DNAs were isolated and purified by centrifugation through a CsCl gradient

according to standard procedures (Maniatis et al., 1982). Sequencing of the M13 subclones was performed by the chain termination dideoxy method (Sanger et al., 1977), with a commercial primer. Additional oligonucleotide primers were synthesized (courtesy of David Koh) using an Applied Biosystems 381A DNA synthesizer. The sequences of these oligonucleotides (5' to 3') and their locations (Fig. 3-7) are as follows: GCCCGTCCACCTCTTCCG (bp 3964-3947), GGACCGGACCAAGGTGGCGC (bp 6264-6245), GCATCCCCTCGCGGATCGCCC (bp 7649-7668), GGCGGGCAGATCGTCATGC (bp 8717-8699). These primers were used for supercoil sequencing (Chen and Seeburg, 1985) with plasmids pGABX1 and pGABX2 as templates.

Chemicals and Enzymes

Antibiotics were obtained from Sigma Chemical Co. Enzymes used in DNA cloning and sequencing, cloning vectors, the M13 primer and CsCl were obtained from New England Biolabs or Bethesda Research Laboratories. 5'-[α-^{32}P] dATP (400 Ci/mmol) was supplied by Amersham, while unlabelled dNTPs and ddNTPs were obtained from P. L. Biochemicals. Low melting point and normal agarose were supplied by Bio-Rad Laboratories. Bacteriological supplies were obtained from Difco.

DNA sequence analysis

Homology matrix search programs were used to perform nucleotide sequence comparisons (Pustell and Kafatos, 1982). The stabilities of putative secondary structures (Fig. 3-10) were calculated as previously described (Youvan et al., 1984a). Analysis of percentage AT content throughout the DNA sequence was also performed using programs described Pustell and Kafatos (1982).

III. Results

A. Subcloning of fragments from pRPS404 and alignment of the nucleotide sequence with genetic-physical maps

Isolation and cloning of the BglII-A/XhoI-D and BglII-D/XhoI-D fragments of pRPS404 is detailed in Figs. 3-1, 3-2. The resulting clones, pGABX1 and pGABX2, were used as described below (see also Materials and methods) to establish the contiguous nature of the four BamHI fragments. The identity of the inserts carried in pGABX1 and pGABX2 was confirmed by Southern blotting as shown in Fig. 3-3.

The DNA sequencing and M13 subcloning described in this section (see also Materials and methods) were performed by M. Alberti (U. of California, Berkeley). The complete nucleotide sequence of the BamHI-H, -G, -M and -J fragments of pRPS404 was determined using M13 subclones derived from pFL227, pFL268, pFL104 and pFL103 (Table 3-1). Sequencing across the BamHI sites on pGABX1 and pGABX2 (Table 3-1) demonstrated that the four BamHI fragments are indeed contiguous. Possible translational reading frames free of stop codons are shown in Fig. 3-4. Fig. 3-5 shows a portion of the 11039 base pair (bp) sequence determined. Because pRPS404 carries the crtD223 point mutation (Marrs, 1981), the nucleotide and deduced polypeptide sequences presented here reflect this deviation from the R. capsulatus wildtype sequences.

The bias in R. capsulatus against codons ending in A or T provides a powerful criterion for the identification of genes from a collection of possible ORFs preceded by ribosome binding sites (see next section). Potential ribosome binding sites (Fig. 3-6), and codon usage (Table 3-2), were evaluated by comparison to other sequenced R. capsulatus genes known to encode proteins. Our assignment of specific ORFs to the crt loci was based on the alignment of the rough genetic-physical maps with the nucleotide sequence, and with the phenotypes and insertion sites of Tn5.7 mutants (Chapter 4) and interposon mutants (Giuliano et al., 1988).

Figure 3-1. Scheme for subcloning of the BglII-D/XhoI-D and BglII-A/XhoI-D fragments of pRPS404. The location of the IS21 elements bordering the photosynthesis gene cluster (shown by arrows) and the location of the crt genes are indicated on the circular map of pRPS404. The XhoI-D restriction fragment is indicated by a solid arc. Both the BglII-D/XhoI-D and BglII-A/XhoI-D fragments were isolated from a double digest of pRPS404 and ligated into BamHI/SalI doubly restricted pBR322. Recombinants were selected by resistance to ampicillin (Amp) and screened for tetracycline (Tet) resistance. Analysis of clones yielded pGABX1 and pGABX2 (see Fig. 3-2 for details). Restriction sites indicated on the plasmids are as follows: x, XhoI; b, BglII; B or (B), BamHI; S or (S), SalI. (B) or (S) indicate restriction sites on pBR322 lost in the final products due to the cloning.

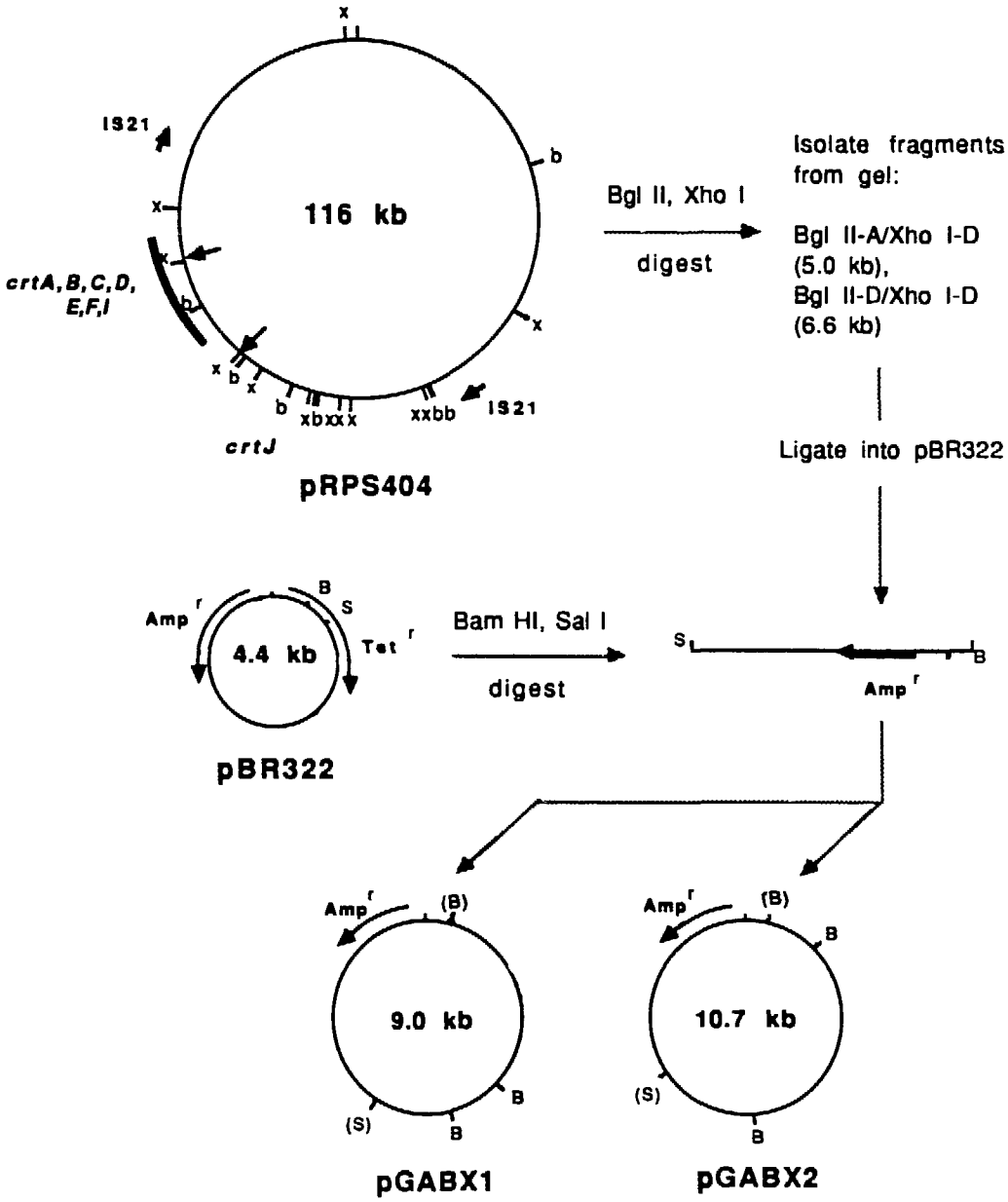
x
IS21
b
x
116 kb
x
crtA,B,C,D,
E,F,I
b
x
x b x b xbxxx xxbb IS21
crtJ
pRPS404
Bgl II, Xho I
digest
Isolate fragments
from gel:
Bgl II-A/Xho I-D
(5.0 kb),
Bgl II-D/Xho I-D
(6.6 kb)
Ligate into pBR322
Amp r
B
S
4.4 kb
Tet r
pBR322
Bam HI, Sal I
digest
S
B
Amp r
Amp r
(B)
9.0 kb
B
(S)
B
pGABX1
Amp r
(B)
B
10.7 kb
(S)
B
pGABX2

Figure 3-2. Detail of pGABX1 and pGABX2. These plasmids carry the BglII-A/XhoI-D and BglII-D/XhoI-D fragments of pRPS404, respectively. Abbreviations for restriction sites are as in Fig. 3-1. The R. capsulatus genes carried on these plasmids are indicated with their directions of transcription shown by arrows, based on previous genetic-physical mapping studies (Taylor et al., 1983; Zsebo and Hearst, 1984) and the DNA sequence of the crt gene cluster (Fig. 3-5). pGABX1 contains the 3' portion of crtB, all of crtC, crtD, crtE and the 5' portion of crtF. pGABX2 contains the 5' end of crtB, and all of crtI and crtA. crtK (located between crtB and crtC) and portions of ORFs bordering the crt genes are not shown here.

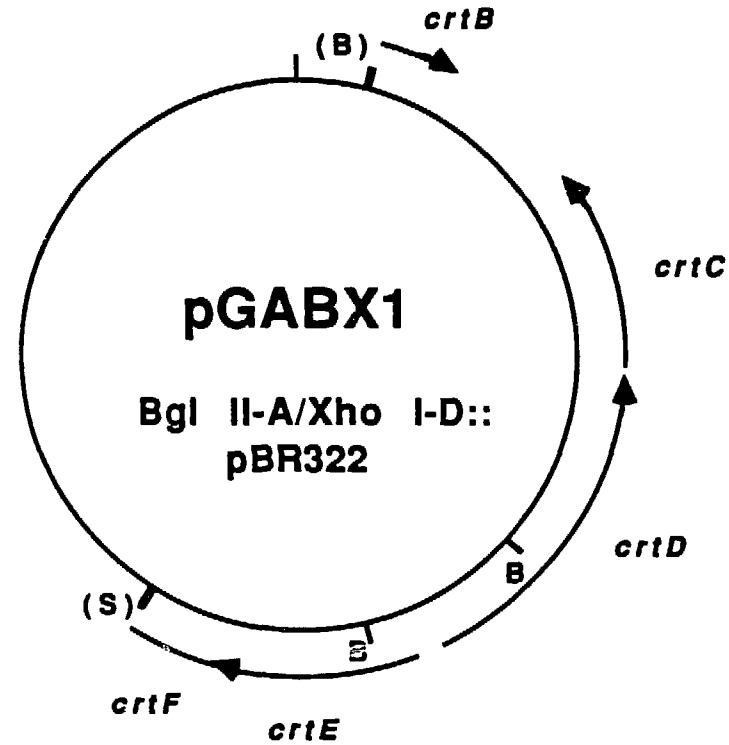
crtB
(B)
crtC
pGABX1
Bgl II-A/Xho I-D::
pBR322
crtD
B
(S)
crtF
crtE

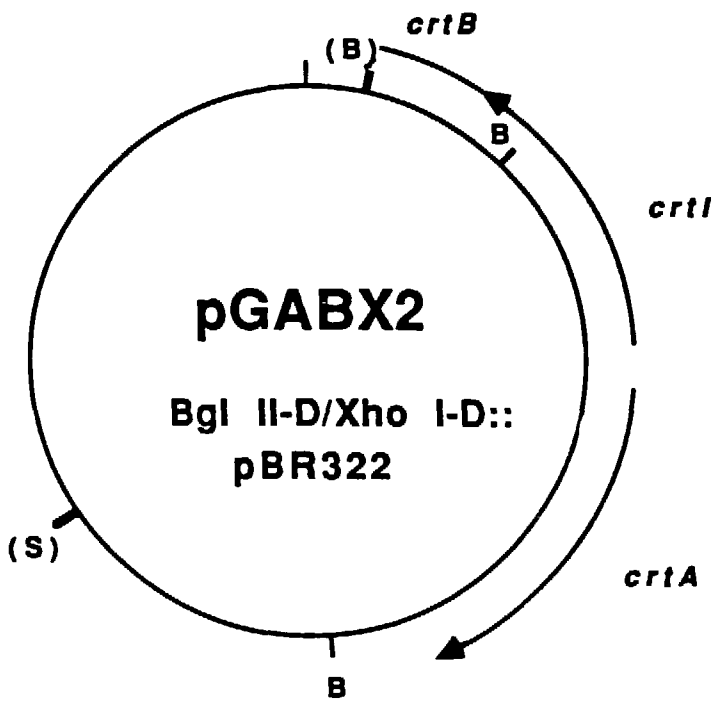
crtB
(B)
B
crtI
pGABX2
Bgl II-D/Xho I-D::
pBR322
(S)
crtA
B

Figure 3-3. Southern blot confirming the identity of the inserts carried on pGABX1 and pGABX2. Restriction digests of pGABX1 and pGABX2 were probed with pFL268 or pBR322 in the former case, and pFL103 or pBR322 in the latter case. Inserts carried in the probes are indicated in Table 3-1. Sizes of molecular weight standards in kb are indicated at the right and left borders of the blot. Restriction enzymes used were as follows: lanes 1 and 3, BamHI/EcoRI; lanes 2 and 4, SalI/EcoRI; lanes 5 and 7, BamHI/PstI; lanes 6 and 8, EcoRI/PstI. Fragments of 817 bp (lane 1) and 2298 bp (lane 2) hybridize to pFL268, containing the BamHI-M fragment of pRPS404, but not to the vector alone (lanes 3 and 4). Since the BamHI-M fragment lies within the BglII-A/XhoI-D fragment (Table 3-1, Fig. 3-7), both the hybridization pattern and the fragment sizes from the ethidium bromide-stained gel (data not shown) confirm the identity of the insert. Similarly, fragments of 515, 1289 and 2104 bp (lane 5), and 515, 1430 and ~2800 bp (lane 6) hybridize to pFL103, containing the BamHI-H fragment of pRPS404, but not to the vector (lanes 7 and 8). The 2104 bp fragment in (lane 5) overlaps a pBR322 fragment of similar size. A 349 bp hybridizing fragment in lane 6 is visible upon longer exposure times (data not shown). The BamHI-H fragment lies within the BglII-D/XhoI-D fragment (Table 3-1, Fig. 3-7), confirming again by hybridization and fragment sizes the identity of the insert. The size of the ~2800 bp fragment indicates that a PstI restriction site must be located about 700 bp to the left of the BamHI-E/BamHI-H junction (Figs. 3-7, 4-2).

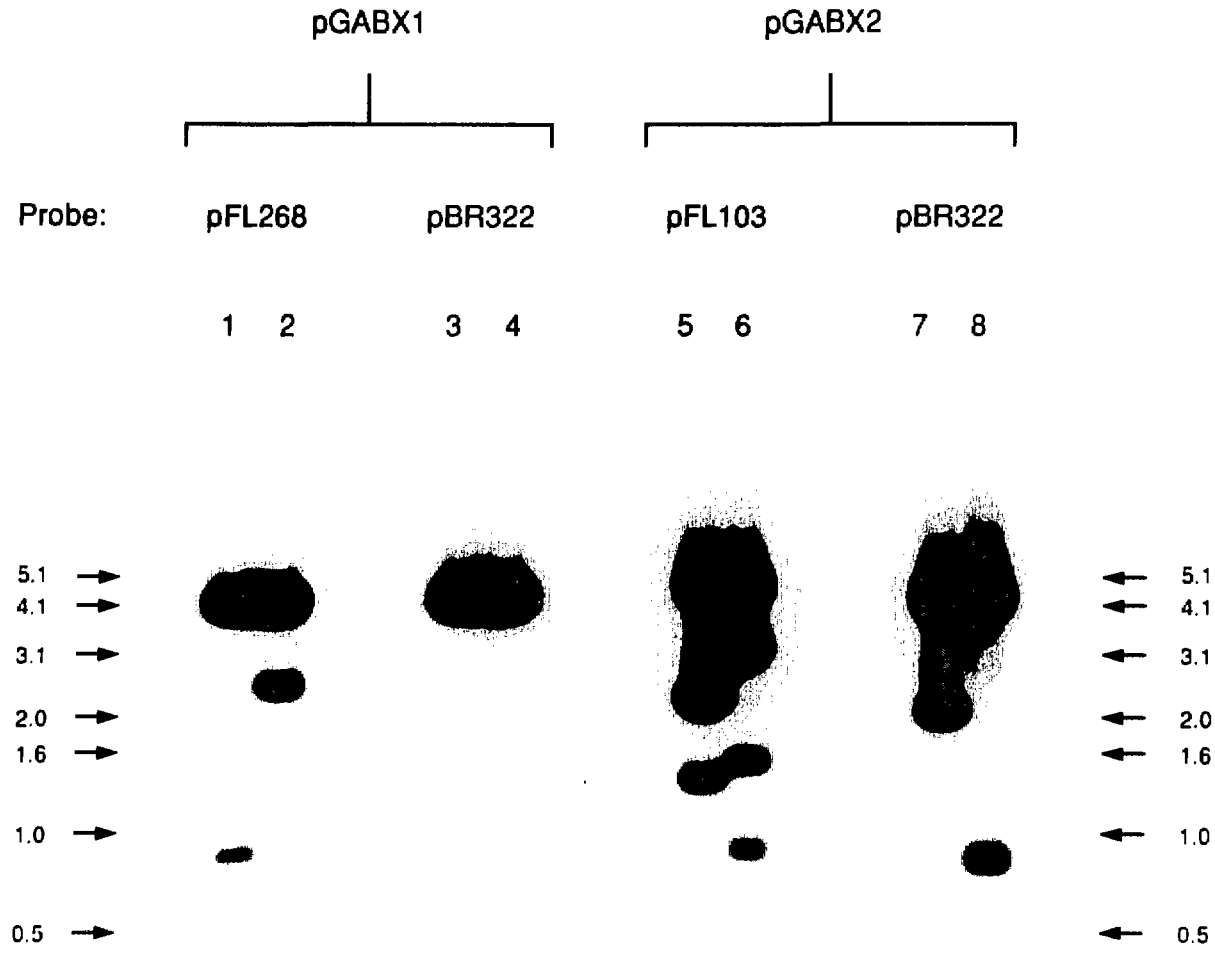
pGABX1
pGABX2
Probe:
pFL268
pBR322
pFL103
pBR322
1 2
3 4
5 6
7 8
5.1
4.1
3.1
2.0
1.6
1.0
0.5
5.1
4.1
3.1
2.0
1.6
1.0
0.5

Table 3-1. Plasmids used in this study

Plasmid	Insert carried	Location[a]	References
pBR322			Bolivar et al. (1977)
pBR325			Bolivar (1978)
pRPS404	*R. capsulatus* photosynthetic gene cluster		Marrs (1981)
pFL103	pRPS404 *Bam*HI-H fragment in pBR325	1-3908	This work
pFL104	pRPS404 *Bam*HI-G fragment in pBR325	3909-7776	This work
pFL227	pRPS404 *Bam*HI-J fragment in pBR325	8588-11039	This work
pFL268	pRPS404 *Bam*HI-M fragment in pBR325	7777-8587	This work
pGABX1	pRPS404 *Bgl*II-A/*Xho*I-D fragment in pBR322	4850-9797	This work
pGABX2	pRPS404 *Bgl*II-D/*Xho*I-D fragment in pBR322	1-4849[b]	This work

[a]numbers given refer to nucleotide positions (Fig. 3-7)
[b]also includes the *Bam*HI-E/*Xho*I-D fragment (Fig. 3-7)

Figure 3-4. Distribution of translational stop codons in all six potential reading frames of the BamHI-H, -G, -M and -J fragments of pRPS404. Stop codons are indicated by vertical lines through boxes representing each of the three forward and three reverse reading frames deduced from the DNA sequence (Fig. 3-5). Regions free of translational stops were further examined by other criteria described in the text in order to identify the crt genes (shown by light shading, internal letters indicate the specific gene) and the flanking ORFs (shown by dark shading, internal letters giving the ORF designation).

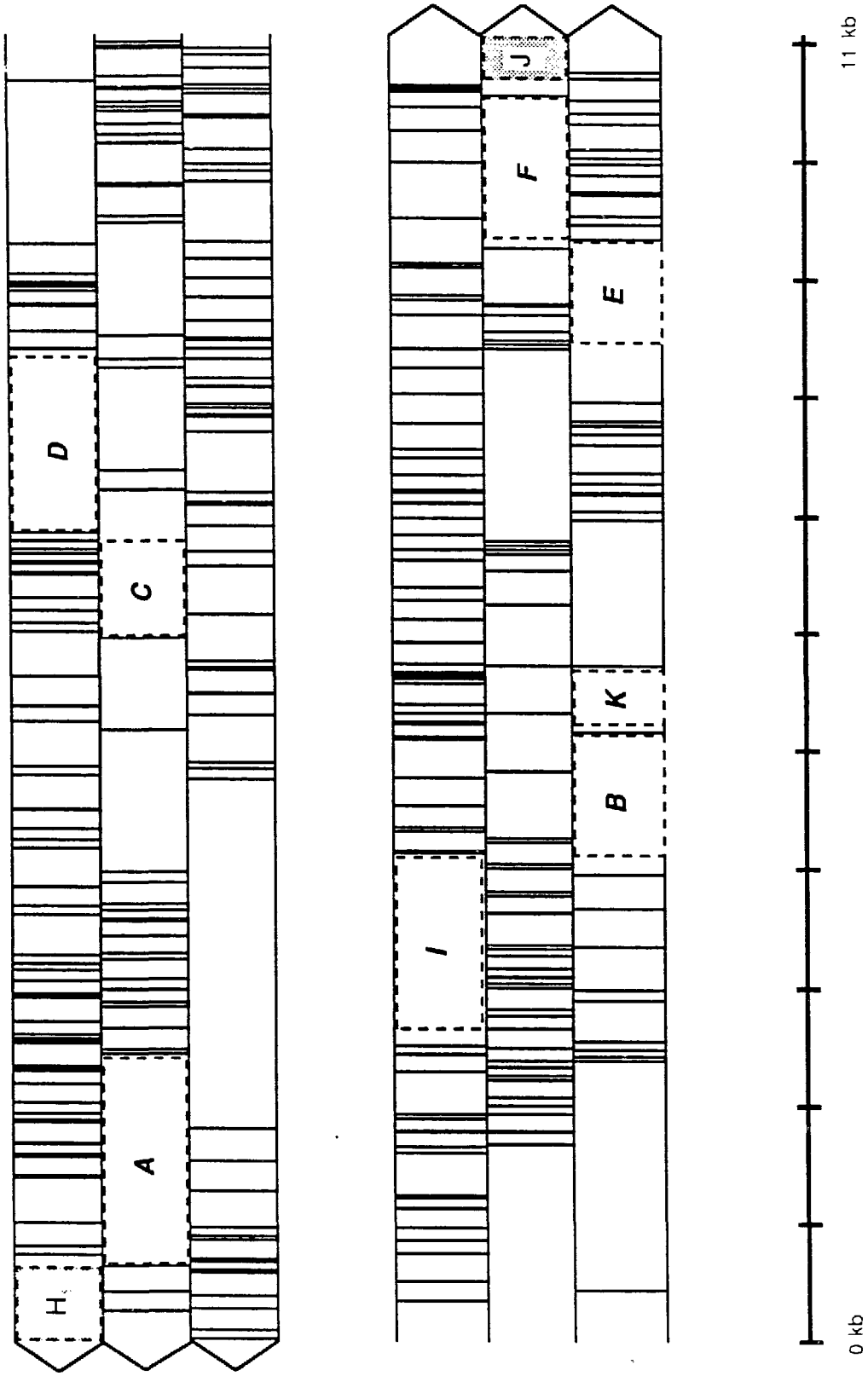
H
A
D
C
J
F
E
K
B
I
11 kb
0 kb

Figure 3-5. Nucleotide and deduced amino acid sequences of the crtA, B, C, D, E, F, I and K genes and gene products as determined by M. Alberti. The nucleotide sequence shown extends from the stop codon of crtA (bp 617) to the start codon of ORF J (bp 10684) (Fig. 3-7). The deduced single letter amino acid translation of the crt genes is given; arrows above the start codons show directions of transcriptions. Putative ribosome binding sites preceding the start codons are underlined. Possible E. coli-like promoters (Fig. 3-9) are indicated by (*) above the antisense strand. Putative palindromic regulatory sites (Fig. 3-10A) are shown by (+) between the two strands, below nucleotides which are complementary in both halves of the palindrome. Possible rho-independent terminators (Fig. 3-11) are indicated by pairs of converging arrows above complementary nucleotides in the antisense strand.

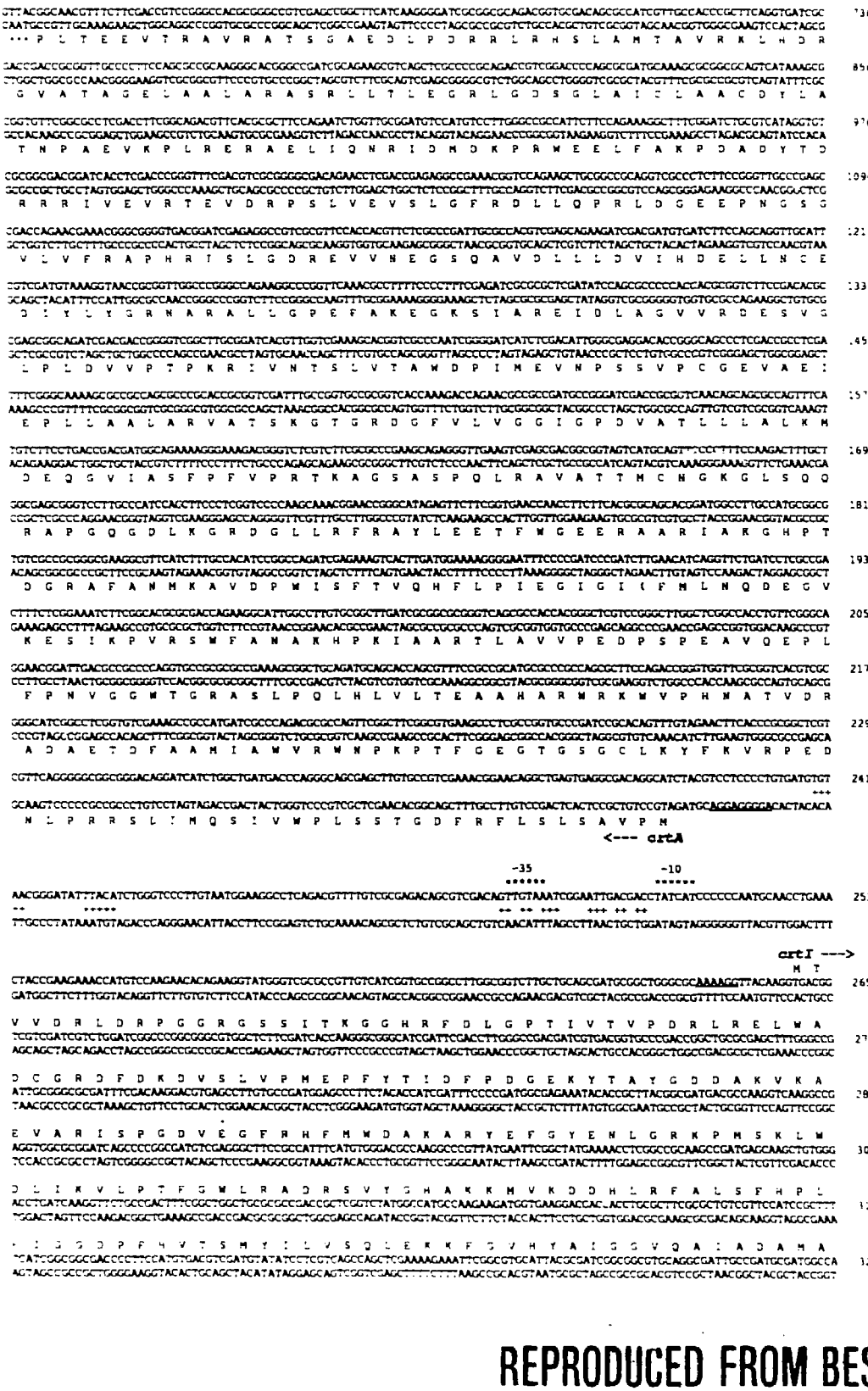

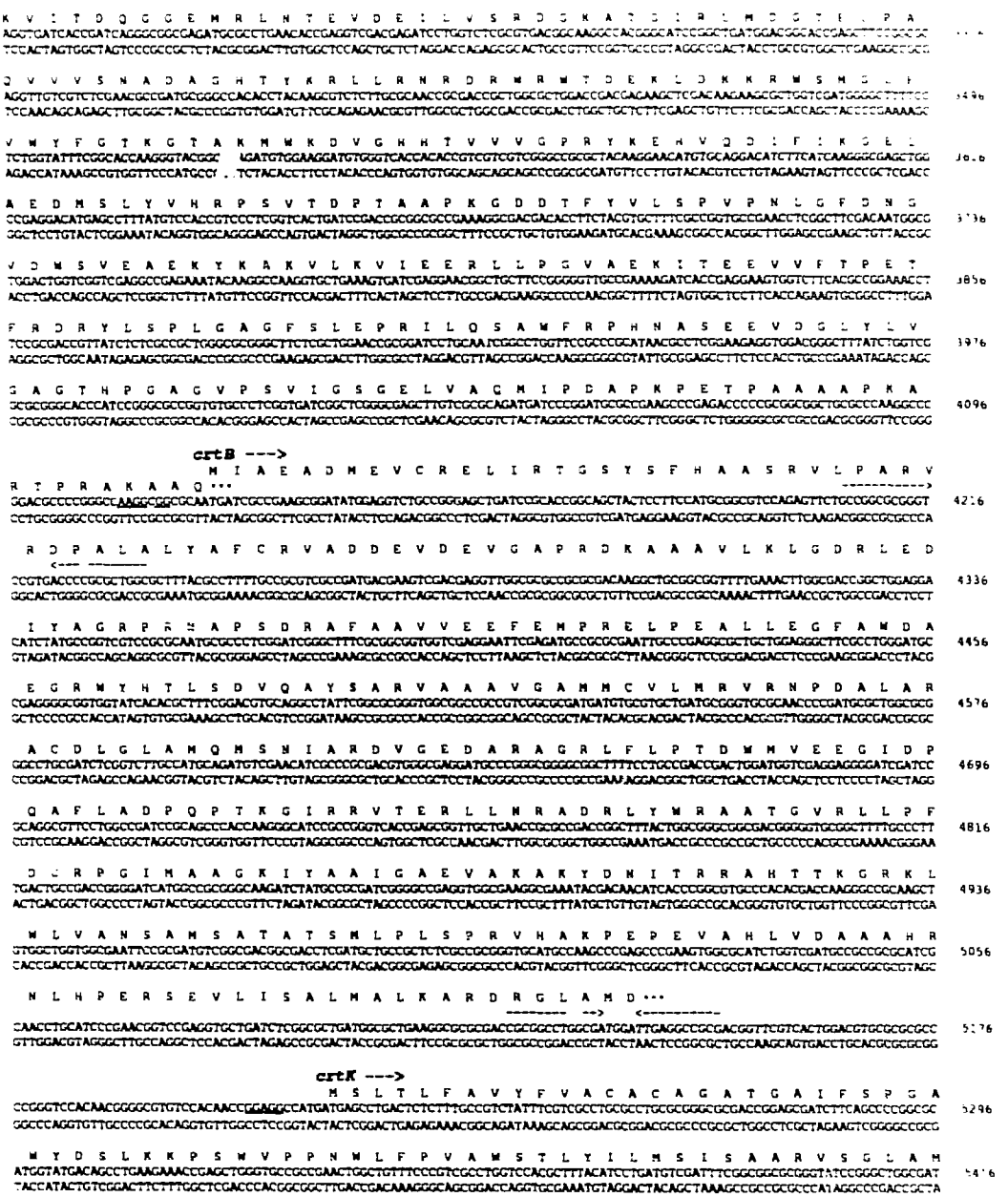

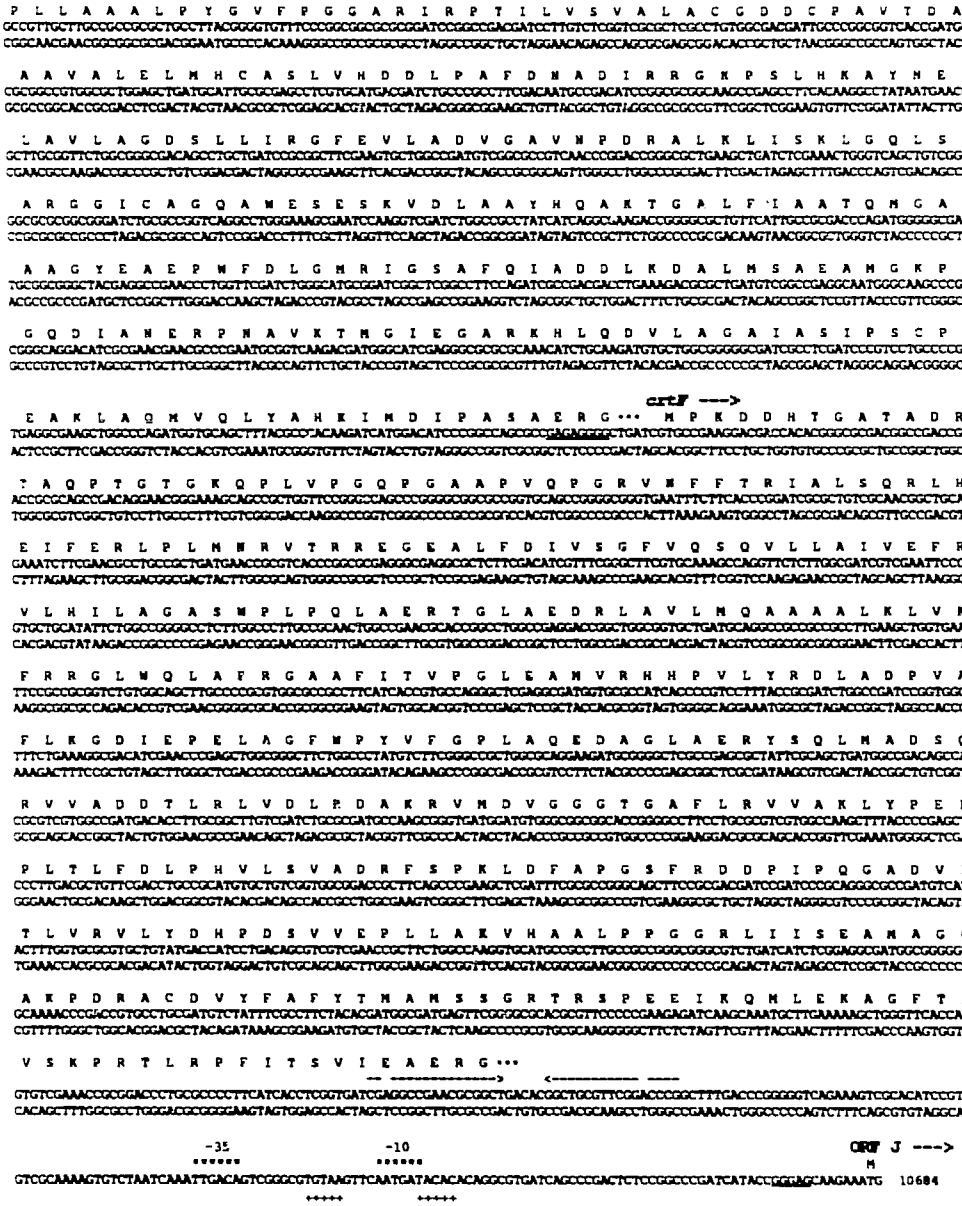

Figure 3-6 A, B. Characteristics of the crt gene translational initiation sites and gene products. (**A**) Sequences to the left of the ATG/GTG start codons contain purine-rich stretches (underlined), including nucleotides matching the predicted ribosome binding site (uppercase). The length of the gene product in amino acids and its calculated molecular weight in daltons are given to the right. (**B**) shows the predicted ribosome binding site (above) as the DNA complement of the 3' end of the R. capsulatus 16 S rRNA (below) (Youvan et al. 1984b).

A

Gene	5'	3'	Residues	MW
crtA	tcacaggGGAGGactgag	ATG	591	64761
crtB	ccgggccAAGGcGGcgca	ATG	339	37299
crtC	ggcgaAAAGGccttctcg	ATG	281	31855
crtD	tgcgtgcgGGAGcgagcg	ATG	494	52309
crtE	gcagcGGAGGgctctgtc	ATG	289	30004
crtF	cgccgaGAGGgGctgact	GTG	393	43004
crtI	ggcgcaAAAGGttacaag	GTG	491	54755
crtK	ccacaaccGGAGGccatg	ATG	160	17607

B

5' AGAAAGGAGGTGAT..3'

$3'_{HO}$UCUUUCCUCCACUA..5'

Table 3-2. Percent codon usage comparison of the carotenoid genes and other *R. capsulatus* genes

Amino Acid	Codon	% in *crt*[a]	% in Other[b]	Amino Acid	Codon	% in *crt*[a]	% in Other[b]	Amino Acid	Codon	% in *crt*[a]	% in Other[b]
Phe	UUU	0.63	0.50	Pro	CCU	0.26	0.25	Gln	CAA	0.49	0.45
	UUC	3.4	4.1		CCC	2.6	1.8		CAG	1.6	2.4
					CCA	0.07	0.10				
Leu	UUA	0.0	0.0		CCG	4.0	3.6	Asn	AAU	0.49	0.30
	UUG	0.79	0.35						AAC	1.2	2.7
	CUU	1.9	0.96	Thr	ACU	0.26	0.20				
	CUC	1.2	2.4		ACC	2.6	3.5	Lys	AAA	0.82	1.3
	CUA	0.0	0.0		ACA	0.07	0.03		AAG	3.2	3.0
	CUG	6.1	4.9		ACG	2.1	1.2				
								Asp	GAU	2.5	1.4
Ile	AUU	0.30	0.35	Ala	GCU	0.46	0.83		GAC	3.6	3.7
	AUC	3.7	5.4		GCC	5.5	5.6				
	AUA	0.0	0.0		GCA	0.43	0.28	Glu	GAA	2.5	3.2
					GCG	6.3	4.4		GAG	3.2	2.5
Met	AUG	2.6	3.0								
				Tyr	UAU	1.0	1.3	Arg	CGU	1.0	0.85
Val	GUU	0.69	0.73		UAC	0.86	2.0		CGC	3.4	3.3
	GUC	3.2	3.7						CGA	0.26	0.15
	GUA	0.03	0.0	Cys	UGU	0.10	0.10		CGG	2.9	1.1
	GUG	3.8	3.3		UGC	0.92	1.2		AGA	0.10	0.08
									AGG	0.07	0.13
Ser	UCU	0.23	0.08	Trp	UGG	2.0	2.4				
	UCC	0.59	0.50					Gly	GGU	0.69	1.1
	UCA	0.07	0.05	His	CAU	1.3	0.73		GGC	4.9	6.0
	UCG	2.5	2.6		CAC	1.0	1.5		GGA	0.33	0.18
	AGU	0.13	0.10						GGG	2.4	1.3
	AGC	1.1	1.2								

[a] *crtA*, *crtB*, *crtC*, *crtD*, *crtE*, *crtF*, *crtI*, *crtK* (This work)(total 3038 codons = 100%)

[b] *cycA* (Daldal et al., 1986), *fbcB*, *fbcC*, *fbcF* (Gabellini and Sebald, 1986; Davidson and Daldal, 1987), *nifA* copy I, *nifB* copy I (Masepohl et al., 1988), *nifD*, *nifH* (Schumann et al., 1986), *pufA*, *pufB*, *pufL*, *pufM*, *puhA* (Youvan et al., 1984a), *pufQ* (B[illegible]uer et al., 1988), *pucA*, *pucB* (Youvan and Ismail, 1985) (total 3979 codons = 100%)

The sequenced region contains three additional ORFs, designated crtK, ORF H and ORF J, distinct from any of the previously described crt genes. Interposon mutations introduced at SalI (bp 5583) and NruI (bp 6723) sites (Fig. 3-7) have both been proposed to lie within crtC because they result in the accumulation of neurosporene, a CrtC$^-$ phenotype (Giuliano et al., 1988). Based on the DNA sequence, however, the interposons interrupt two distinct genes, which cannot be cotranscribed because of their convergent transcriptional orientations. Because both mutants are phenotypically similar, it is not clear with which locus previously described crtC point mutants are actually associated (Yen and Marrs, 1976; Scolnik et al., 1980a). Genetic-physical maps (Taylor et al., 1983; Zsebo and Hearst, 1984) have shown crtC to be bounded by crtB and crtD, with a gap left between crtB and crtC. On the basis of these studies, we designate the previously undetected gene located in this gap as crtK (Fig. 3-7).

An interposon insertion at an EcoRV site (bp 1303) and a transposon insertion (between bp 999-1244) cause Bchl$^-$ phenotypes, although both of these mutations lie within the 3' end of the crtA gene (Giuliano et al., 1988; Chapter 4). Mutations at the 5' end of crtA cause a CrtA$^-$ phenotype but do not affect Bchl synthesis. The most likely explanation for these effects is the polar inactivation of ORF H (Fig. 3-7) in the insertion mutants, by disruption of ORF H transcriptional regulatory signals overlapping the 3' coding region of crtA. A similar overlap between promoters 5' to pufQ and the 3' coding region of an upstream gene has recently been proposed in Rhodobacter (Kiley and Kaplan, 1988; Bauer et al., 1988). ORF H, which extends into the adjacent BamHI-E fragment (Fig. 3-7), may thus be part of an operon required for Bchl biosynthesis. A mutant bearing an interposon insertion at an ApaI site (bp 10713) within ORF J exhibits a Bchl$^-$ phenotype, suggesting that this ORF may also be part of an operon required for Bchl biosynthesis (Giuliano et al., 1988). ORF J terminates within the adjacent BamHI-C fragment (Fig. 3-7, M. Alberti, unpublished data).

Figure 3-7. Organization of the carotenoid biosynthetic gene cluster. Directions of transcription are indicated with arrows and putative transcriptional regulatory sites (Fig. 3-10) are indicated by (•). Numbers above the genes show the putative nucleotide positions of translational starts and stops. Restriction sites referred to here or in previous genetic-physical mapping studies are indicated below the genes. B, BamHI; E, EcoRI; Bg, BglII; X, XhoI. Boxes containing a letter indicate specific restriction fragments from the photosynthesis gene cluster of pRPS404 (Zsebo and Hearst, 1984), while the IS21 elements derived from the vector are indicated to the left and right. The locations of photosynthesis genes outside the crt gene cluster are shown above the boxes. Only the BglII-D/XhoI-D and BglII-A/XhoI-D fragments of pRPS404 are shown (indicated by boxes containing D/D and A/D). The pufB, A, L and M genes encode the LH-I β, α and the RC-L, RC-M polypeptides, respectively, while the puhA gene encodes the RC-H polypeptide (Youvan et al. 1984a). Regions containing Bchl biosynthetic genes are indicated by bch. The location of crtJ relative the other crt genes is shown.

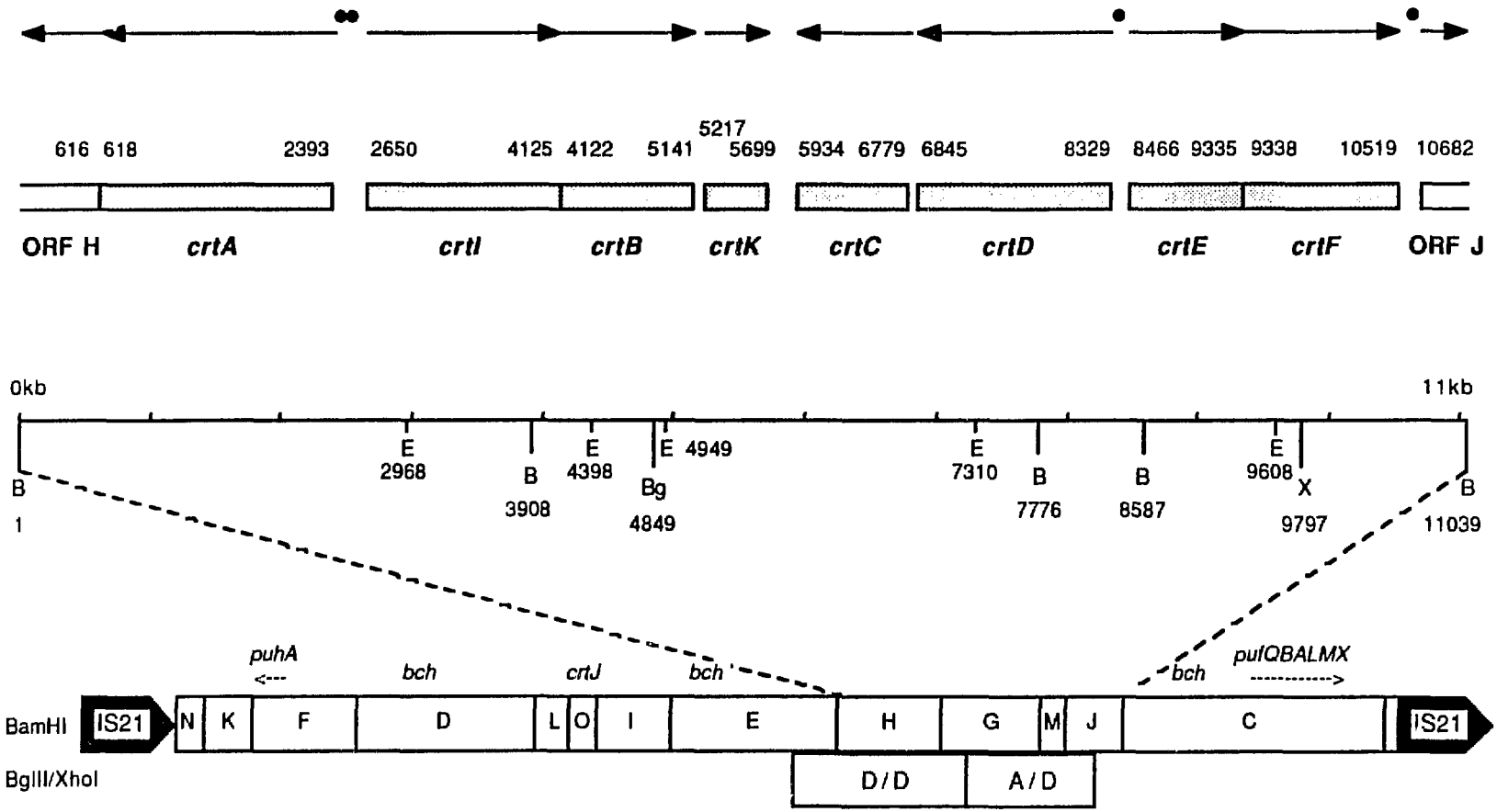
616 618
2393
2650
4125 4122
5141
5217
5699
5934 6779
6845
8329
8466 9335
9338
10519
10682
ORF H
crtA
crtI
crtB
crtK
crtC
crtD
crtE
crtF
ORF J
0kb
11kb
E 2968
B 3908
E 4398
E 4949
Bg 4849
E 7310
B 7776
B 8587
E 9608
X 9797
B 1
B 11039
puhA
bch
crtJ
bch
bch
pufQBALMX
BamHI
IS21
N
K
F
D
L
O
I
E
H
G
M
J
C
IS21
BglII/XhoI
D/D
A/D

B. Ribosome binding sites, translational starts and codon usage of the carotenoid genes

Youvan et al. (1984a) originally observed a strong bias against codons having an A or T in the third position in the R. capsulatus genes encoding RC-H, RC-L, RC-M, and the LH-I β, α polypeptides. This pattern of codon bias is maintained in all other sequenced R. capsulatus genes encoding proteins (Table 3-2). Among the 3979 codons from previously sequenced R. capsulatus genes, the triplets ATA, CTA, GTA and TTA, for example, are never used.

The proposed amino acid sequences of the crt gene products (Fig. 3-5) and the ORFs (data not shown) correspond to the longest possible translations of ORFs possessing Shine-Dalgarno ribosome binding sites (Shine and Dalgarno, 1974) and typical R. capsulatus codon usage, located in the appropriate regions of the crt gene cluster. Translation of the nucleotide sequence in any of the alternative forward or reverse reading frames, with respect to a given gene, results in the frequent appearance of stop codons (Fig. 3-4); the few alternative ORFs which do have ribosome binding sites show atypical codon usage (data not shown). ATA, CTA and TTA are never found among the 3038 predicted crt codons, while GTA (Val) appears only once, within crtK (Table 3-2, Fig. 3-5).

All of the translational starts proposed for the crt genes are preceded by purine-rich stretches containing possible ribosome binding sites (Fig. 3-6A) showing strong complementarity to the 3' end of the R. capsulatus 16 S rRNA (Fig. 3-6B) (Youvan et al., 1984b). The start codons of all previously sequenced genes known to encode proteins in R. capsulatus (Table 3-2) are preceded by similar ribosome binding sites. One exception to this is nifA copy I (Masepohl et al., 1988). We note that a possible ribosome binding site, GAGG, is centered 10 bp upstream from the GTG encoding Val-49 in the deduced amino acid sequence of NifA copy I. No ATG starts preceded by ribosome binding sites were observed for ORFs located in the regions genetically mapped to crtF and crtI.

Possible ribosome binding sites followed by a GTG, however, exist for both of these genes (Fig. 3-6A), leading us to propose that crtF and crtI use GTG for translational initiation. GTG start codons have been previously observed in about 8% of E. coli genes (Stormo, 1986). In addition, both the fbcF gene from R. capsulatus, encoding the Rieske Fe-S protein of the cytochrome bc_1 complex (Gabellini and Sebald, 1986; Davidson and Daldal, 1987), and the pucB gene of Rhodobacter sphaeroides, encoding the β subunit of the LH-II antenna complex (Kiley and Kaplan, 1987), use GTG for translational initiation.

C. Organization of the carotenoid gene cluster

The crt genes must form at least four distinct operons because of the inversions of transcriptional orientation which occur between crtA-crtI, crtK-crtC, and crtD-crtE (Fig. 3-7). crtA cannot be cotranscribed with the other crt genes because of its divergent orientation at one end of the gene cluster. As discussed earlier, mutations in the 5' end of crtA yield a $CrtA^-$ phenotype while those at the 3' end cause a $Bchl^-$ phenotype, suggesting that crtA is not cotranscribed with ORF H, although the promoter(s) for ORF H may overlap crtA. Groups of genes which could also form operons are crtIBK, crtDC and crtEF. ORF J (Fig. 3-7), located downstream from crtF, is not transcribed as part of an operon including crt genes (Chapter 4).

The coding regions of the crt genes are closely spaced. The maximum gap between adjacent genes (crtA and crtI) is 257 bp. Neighboring genes transcribed in the same direction tend to be grouped very tightly. In the most extreme case the TGA stop codon of crtI overlaps the putative ATG start of crtB. This situation is reminiscent of the three codon overlap between the 3' coding region of the R. capsulatus pufL gene and the 5' coding region of the pufM gene (Youvan et al., 1984a). An alternative crtB ATG start preceded by a potential ribosome binding site is found at bp 4407 (Fig. 3-5), in the same frame as our predicted start at bp 4122 (Fig. 3-6A). The downstream ATG would eliminate the overlap with crtI. Our provisional assignment of the upstream ATG as the

crtB start codon is based on the conservation of codon bias between bp 4122-4407. We cannot, however, rule out the possibility that the downstream ATG is used for translational initiation because either start codon would be consistent with the current genetic-physical mapping of crtB. Absolute confirmation of the deduced amino acid sequences will require the isolation of the gene products.

D. Asymmetry of percentage AT content in noncoding and coding regions

Fig. 3-8 illustrates the extreme asymmetry in % AT content within the region encoding the crt gene cluster. Although the entire genome of R. capsulatus has an average AT content of 34 % (Trüper and Pfennig, 1978), we have found the 5' flanking regions of crtA-crtI, crtD-crtE and ORF J to be unusually AT-rich, ranging up to 53 % in AT content averaged over a 151 bp window. These AT-rich regions contain DNA sequences which may bind transcriptional regulatory factors or serve as E. coli-like σ^{70} promoters (see below). The presence of these AT-rich islands in the 5' control regions of genes from an organism with a low average AT content suggests a compelling selective pressure for the preservation of the nucleotide bias. Non-coding regions surrounding prokaryotic transcription initiation and termination points are enriched in A and T residues compared to the coding regions, as determined using a data base composed predominantly of E. coli genes (Nussinov et al., 1987). Specific structural features due to the AT content of certain chromosomal regions, such as bending or ease of melting of double-stranded DNA may help alert DNA-binding proteins to the presence of potential sites of action (Nussinov et al., 1987).

E. E. coli-like σ^{70} promoter sequences

We have located three regions similar to the σ^{70} consensus promoter, TTGACA N_{15-19} TATAAT (N = any nucleotide) used by the major RNA polymerase of E. coli (McClure, 1985). The R. capsulatus sequences, found 5' to crtI, crtD and ORF J, are compared to the canonical E. coli promoter in Fig. 3-9. Additional nucleotides in the

Figure 3-8. Average A + T nucleotide content within the carotenoid gene cluster. Locations and polarities of the genes are indicated at the top. ORF H and ORF J extend beyond the boundaries of the region shown. Nucleotide positions are as in Fig. 3-7. Percentage AT content was calculated by averaging over a 151 bp window using 10 bp increments, and values exceeding 40 % were plotted (average genomic percentage AT content is 34 %). Note the unusually high mean AT content in 5' flanking regions of genes.

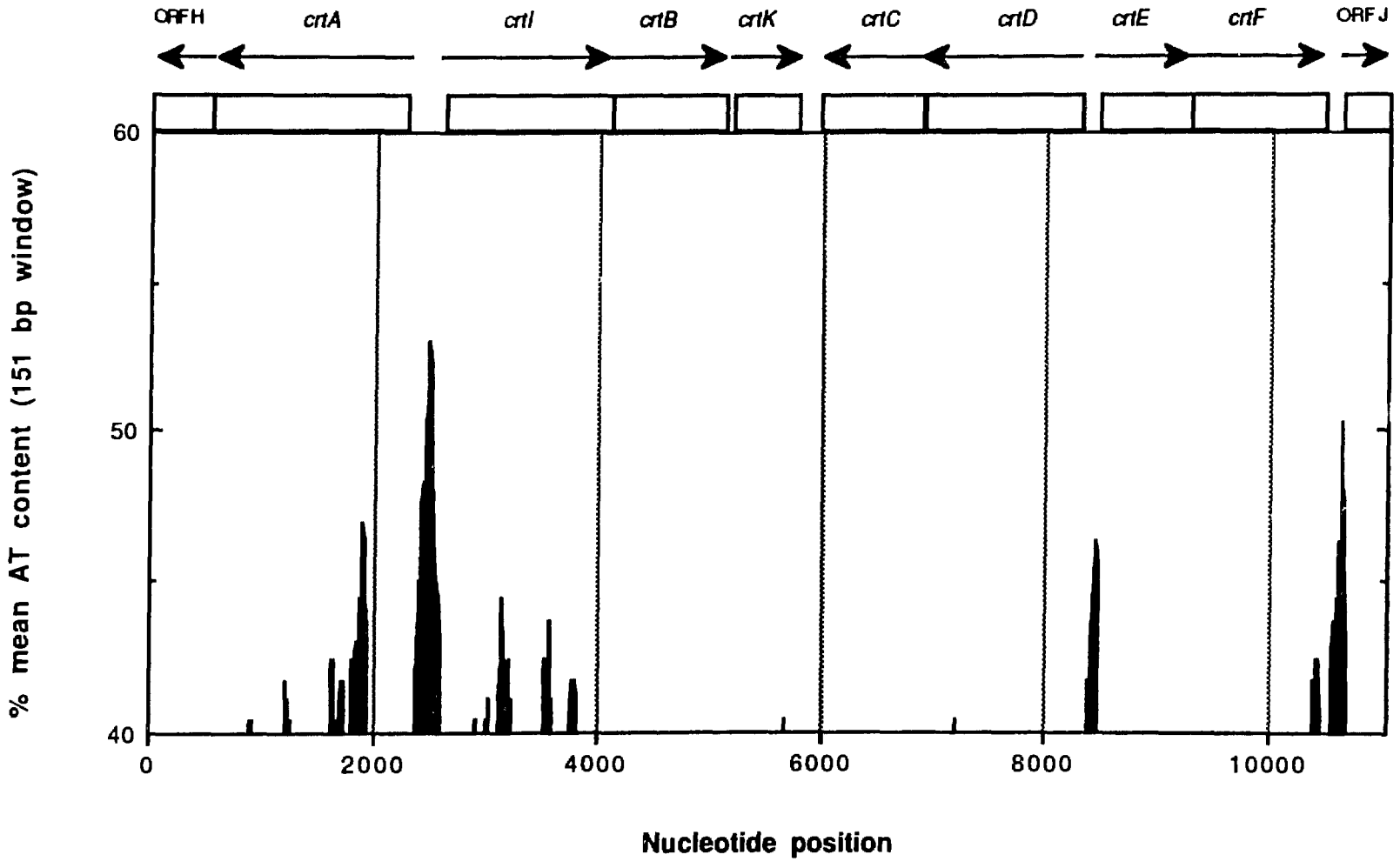
ORF H
crtA
crtI
crtB
crtK
crtC
crtD
crtE
crtF
ORF J
60
50
40
% mean AT content (151 bp window)
0
2000
4000
6000
8000
10000
Nucleotide position

Figure 3-9. Comparison of sequences found 5' to crtI, crtD and ORF J with the E. coli σ^{70} consensus promoter. The numbers at left indicate the position of the 5' nucleotide of each sequence (Fig. 3-5). The distance in bp from each putative promoter to the start codon of the 3' gene is shown at the right. The consensus E. coli promoter is shown below with the six most highly conserved nucleotides underlined (McClure, 1985). Putative -35 and -10 regions (above) are indicated in boldface, and uppercase letters show matches to the E. coli consensus. Gaps (-) were placed between these regions to maximize the nucleotide alignment. Nucleotides which are absolutely conserved in all three R. capsulatus sequences are indicated by (*).

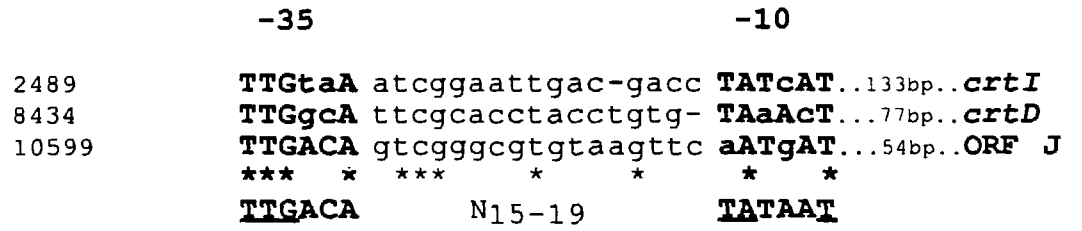
-35
-10
2489 TTGtaA atcggaattgac-gacc TATcAT..133bp..crtI
8434 TTGgcA ttcgcacctacctgtg- TAaAcT...77bp..crtD
10599 TTGACA gtcgggcgtgtaagttc aATgAT...54bp..ORF J
*** * *** * * * *
TTGACA N15-19 TATAAT

spacer between the -35 and -10 regions are also conserved in the R. capsulatus sequences. An optimal spacing of 17 bp is observed between the -35 and -10 regions in E. coli (McClure, 1985). The putative crtD and crtI promoters show spacings of 16 bp, while the putative ORF J promoter has a spacing of 17 bp. No other sequences with a total of nine or more nucleotide matches to the E. coli σ^{70} consensus promoter, including five of the six most conserved nucleotides (Fig. 3-9), were found within the crt gene cluster (Fig. 3-7). We allowed a variable spacing of N_{15-19} between the -35 and -10 regions for these homology searches.

F. A highly conserved palindromic motif homologous to a recognition site for DNA-binding regulatory proteins

We have identified a highly conserved palindromic nucleotide sequence, found four times in 5' flanking regions within the crt gene cluster. This motif occurs twice in the crtA-crtI 5' flanking region, and once each in the crtD-crtE and ORF J 5' flanking regions (Figs. 3-7, 3-5). A search among other published R. capsulatus gene sequences (Table 3-2) also revealed the presence of this palindrome 5' to the puc operon (Youvan and Ismail, 1985). Based on these five examples, the consensus sequence is TGTAART N_3 A N_2 TTACAC (R = purine) (Figs. 3-10B). The palindromes are centered anywhere from 162 bp (pucB) to 29 bp (crtA) from the start codon of the nearest gene (Fig. 3-10A). Each of the three putative E. coli-like promoters located within the crt gene cluster overlaps one of the palindromes (Fig. 3-5). We have searched for further examples of the palindromic site in the coding and flanking regions of other published R. capsulatus nucleotide sequences encoding proteins (Table 3-2), as well as from the 5' end of ORF J to the 5' end of the pufQ gene (Fig. 3-7) (M. Alberti, unpublished data). No additional palindromic sites were found when we required matches to each absolutely conserved nucleotide in the consensus (Fig. 3-10B).

Hyphenated twofold (palindromic) symmetry is a characteristic of the recognition sites

Figure 3-10 A-C. Comparison of a palindromic motif found 5' to photosynthesis genes with a consensus regulatory protein binding site. **(A)** The genes flanking each palindrome are indicated to the left and right, respectively. Arrows show the directions of transcription. Numbers above each sequence show the nucleotide positions (as in Fig. 3-5, except for pucB (see Youvan and Ismail 1985)) of the 5' ends of the flanking genes (or the 3' end in the case of crtF), and the location of the palindrome. Possible puc operon transcription initiation signals (Zucconi and Beatty 1988) are indicated by (•). Complementary nucleotides in the two halves of the palindromes are underlined. **(B)** Nucleotides which match the R. capsulatus consensus are given in uppercase, while those that occur in positions defined by the consensus are shown in boldface. (+) indicates an absolutely conserved nucleotide in the palindrome. **(C)** The R. capsulatus consensus sequence is compared to a consensus derived from the recognition sites of the transcriptional regulatory factors NifA, AraC, CAP, LacI, GalR, LexA, TnpR, LysR and λ cII. Nucleotides conserved between the two consensuses are indicated by (|) between the sequences.

A

2650	2434	2410	2393
<--*crtI*	aga**TGTAAAT**atcccg**TTACAC**atc		*crtA*-->
2393	2487	2511	2650
<--*crtA*	agt**TGTAAAT**cgg**A**at**TgACga**cct		*crtI*-->
8329	8394	8418	8466
<--*crtD*	ggg**TGTAAGT**ttc**A**gt**TTACAC**agg		*crtE*-->
10520	10610	10634	10682
-->*crtF*	gcg**TGTAAGT**tca**A**tg**aTACAC**aca		ORF J-->
	24	58	198
	cag**TGTAAGcccg**A**ct**TTACAC**ttg		*pucB*-->

B **TGTAARTN$_3$ANTTACAC**

C **TGTGT** N$_{6-10}$ **ACACA**

for oligomeric DNA-binding regulatory proteins (Gicquel-Sanzey and Cossart, 1982; Gussin et al., 1986). The R. capsulatus consensus palindrome also shows strong similarity to a consensus sequence, TGTGT N_{6-10} ACACA, derived from the recognition sites of a group of prokaryotic transcriptional regulatory factors containing examples of both positive and negative regulators (Fig. 3-10C) (Gicquel-Sanzey and Cossart, 1982; Buck et al., 1986). We propose that the R. capsulatus palindromic motif represents the binding site for a transcriptional regulatory factor.

G. Rho-independent transcription termination signals

The DNA sequence shown in Fig. 3-5 was searched, using homology matrix programs, for regions of dyad symmetry with the potential to form stem-loop structures in RNA. Possible secondary structures found between crtK and crtC include two GC-rich stem-loops, one 3' to crtK (centered at bp 5727) and the other 3' to crtC (centered at bp 5815), each followed by a run of three thymidines (Figs. 3-5, 3-11). Single regions of dyad symmetry followed by thymidine-rich stretches were found 3' to the crtI, B and F genes, centered at bp 4219, 5136 and 10520, respectively (Figs. 3-5, 3-11). The combination of a GC-rich dyad symmetrical region, followed by several thymidine residues is characteristic of rho-independent transcriptional terminators in bacteria (reviewed in Platt, 1986). Possible rho-independent termination signals are found close to the 3' ends of the R. capsulatus puf and puc operon mRNAs as mapped by nuclease protection experiments (Zucconi and Beatty, 1988; Chen et al., 1988). As few as four consecutive thymidines following a GC-rich stem-loop region have been observed to terminate transcription very efficiently in vivo (Chen et al., 1988). The sequence CTTT (Fig. 3-11) was found once 3' to the crtC, F and K stem-loops and twice 3' to the crtI stem-loop. The putative terminators 3' to crtB and crtF each overlap the translational stop codons of these genes (Fig. 3-5). The putative terminator 3' to crtI lies within the 5' coding region of crtB, assuming our proposed crtB start at bp 4122.

Figure 3-11. Possible rho-independent transcriptional terminators. Nucleotide positions (Fig. 3-5) of the stem-loops are shown on the left and right. The 5' gene and the stability of each hairpin are indicated to the right of each structure. AT or GC base pairs, and GT base pairs are indicated by (-) and (~), respectively. Underlined nucleotides indicate a thymidine-rich sequence found 3' to the stem-loops.

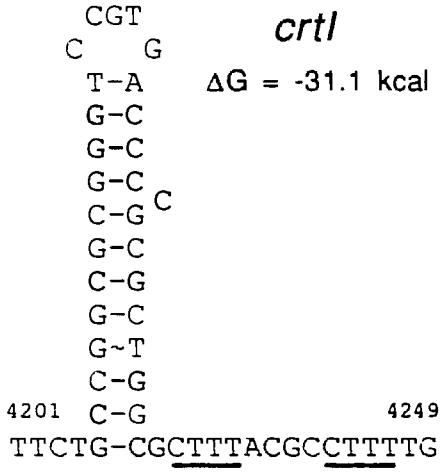

crtI

ΔG = -31.1 kcal

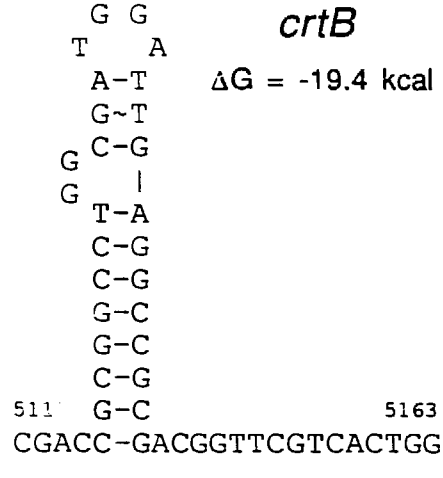

crtB

ΔG = -19.4 kcal

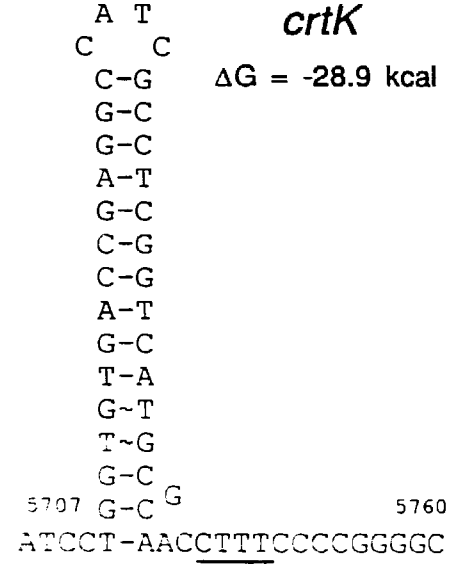

crtK

ΔG = -28.9 kcal

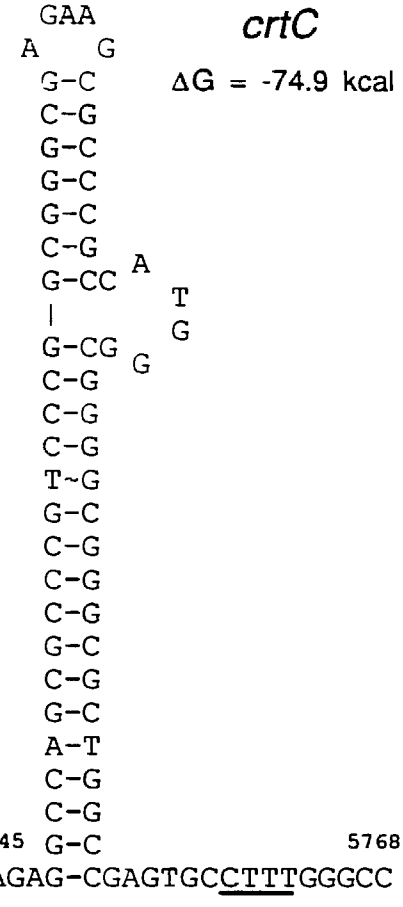

crtC

ΔG = -74.9 kcal

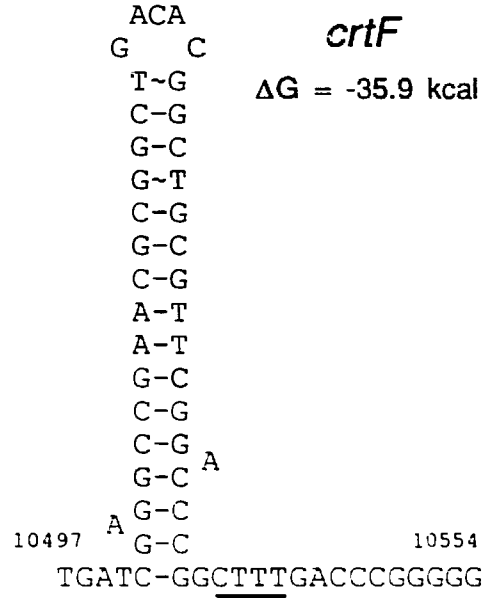

crtF

ΔG = -35.9 kcal

IV. Discussion

A. Operon structure and codon usage of the carotenoid genes

The clustering of eight of the nine identified R. capsulatus carotenoid genes (crtA, B, C, D, E, F, I and K) suggests a potential for their coordinate regulation. This regulation could be assisted by segregation of the genes on one domain of the bacterial chromosome. Studies in R. sphaeroides, a closely related photosynthetic bacterium, indicate a similar clustering of the crtA, B, C, D, E and F genes, although the exact gene order remains to be determined (Pemberton and Harding, 1986). Previous data have shown the R. capsulatus crt gene cluster to be bounded by genetic loci required for Bchl biosynthesis (Fig. 1-4; Taylor et al., 1983; Zsebo and Hearst, 1984). The correspondence of these loci with specific ORFs has not yet been established, although mutations within ORF J and 5' to ORF H in the 3' end of crtA (Fig. 3-7) cause Bchl$^-$ phenotypes (Giuliano et al., 1988; Chapter 4). We propose that ORF J and ORF H are part of two operons which include genes required for Bchl but not carotenoid biosynthesis, and which are transcribed outwards away from the crt gene cluster.

The directions of transcription of all genes shown in Fig. 3-7 have been confirmed using single-stranded DNA probes (Figs. 6-3, 6-4). Our results are in agreement with the directions of transcription proposed by Giuliano et al. (1988), except in the case of the tentative proposal of these authors for crtD. Confirming our transcriptional data are the complete nucleotide sequence of the crtD region (Fig. 3-5), the codon usage of open reading frames on both DNA strands (data not shown), and the regions of strong amino acid similarity observed between CrtD and CrtI (Chapter 7, Fig. 7-1), all of which indicate that crtD is transcribed from right to left in Fig. 3-7. Giuliano et al. (1988) did not identify crtK as a discrete gene by interposon mutagenesis, presumably because of the similarity of CrtC$^-$ and CrtK$^-$ phenotypes and the fact that crtC and crtK are adjacent. The minimum four operons in the crt gene cluster are crtA, crtIBK, crtDC and crtEF based on

the orientation of the genes. A crtDC operon, however, seems unlikely because polar Ω interposon insertions within crtD at ApaI and EcoRI sites (bp 8163 and 7310, respectively) produce CrtD$^-$ rather than CrtC$^-$ phenotypes (Giuliano et al., 1988). Possible rho-independent transcriptional terminators have been found 3' to the crtI, B, K, C and F genes (Fig. 3-11). If termination occurs 3' to crtI and crtB in vivo, the operon organization of the crt gene cluster would be even more complex.

In R. capsulatus we observe no major differences between codon usage in highly expressed structural protein genes (puf, puh and puc, for example), and the crt genes. 17% of the 3038 predicted crt codons end in A or T, compared to 15.5% of the 3979 codons from all other R. capsulatus genes. Extensive studies of codon usage in E. coli have also shown that codon bias is preserved from genes encoding very highly expressed ribosomal proteins to genes encoding rarely expressed regulatory proteins (Sharp and Li, 1986). The triplets ATA, CTA and TTA have not yet been observed in the 7017 codons from R. capsulatus genes described here or in previous studies (Table 3-2), providing the most extreme example of the strong bias against codons ending in A or T.

B. Nucleotide sequences which may be involved in transcription initiation and regulation of the crt genes, ORF J and the puc operon

E. coli-like σ^{70} promoter signals have never been observed in Rhodobacter (Kiley and Kaplan, 1988), nor have detailed data on any R. capsulatus promoters been available until recently. We have, however, found possible E. coli-like σ^{70} promoters (McClure, 1985) 5' to crtI, crtD and ORF J (Fig. 3-9). Within the constraints of our homology search (see Results), no other E. coli-like promoter sequences were found within the crt gene cluster, although the gene organization suggests that there must be promoter signals in the 5' flanking regions of crtA and crtE (Fig. 3-7). We note, however, that positively controlled promoters often deviate more strongly than do unregulated promoters from the E. coli σ^{70} consensus sequence (McClure, 1985) and may not have been detected in our homology

search. Another possibility is that R. capsulatus uses multiple σ factors to control the expression of different classes of genes (Reznikoff et al., 1985). Sequences similar to NtrA (σ^{60}) promoters, which control the expression of anaerobically induced nitrogen fixation (nif) genes (reviewed in Gussin et al., 1986), have been recently described in R. capsulatus (Masepohl et al., 1988; Bauer et al., 1988).

Photosynthetic pigments (Bchl and carotenoid) do not accumulate in E. coli strains harboring the R. capsulatus photosynthesis gene cluster carried on pRPS404 (Marrs, 1981). Johnson et al. (1986) have suggested that E. coli does not transcribe the R. capsulatus photosynthesis genes. Our observation that the R. capsulatus crtD and crtI genes may have E. coli-like σ^{70} promoters, thus, was not anticipated. Pemberton and Harding (1987) have, however, recently shown that transfer of the R. sphaeroides crt gene cluster to several species of phylogenetically related nonphotosynthetic bacteria results in the production of carotenoids. Lack of carotenoid production in E. coli may occur because of lack of recognition of at least one crt gene promoter, absence of the proper transcriptional regulatory factors required for crt gene expression, or because of differences in post-transcriptional regulation between the two species.

We have found five examples of a conserved nucleotide motif (Fig. 3-10A) in the 5' flanking regions of R. capsulatus photosynthesis genes. This motif shows strong sequence similarity to a derived consensus binding site for a series of prokaryotic DNA-binding proteins including NifA, AraC, CAP, LacI, GalR, LexA, TnpR, LysR and λ cII (Gicquel-Sanzey and Cossart, 1982; Buck et al., 1986), which function as repressors and/or activators of transcription (reviewed in Raibaud and Schwartz, 1984). The R. capsulatus motif is palindromic, as are the binding sites for known dimeric or tetrameric regulatory factors (Gicquel-Sanzey and Cossart, 1982; Gussin et al., 1986). The two halves of the consensus palindrome (Fig. 3-10B) are separated by 12 nucleotides center to center. Such a spacing would allow a dimeric regulatory factor to bind cooperatively to two sites on the same face of the DNA helix separated by about one helical turn.

One example of the R. capsulatus palindromic motif occurs 5' to the puc operon (Fig. 3-10A), which encodes the LH-II antenna polypeptides. Zucconi and Beatty (1988) have mapped the 5' triphosphate ends of puc operon mRNAs by nuclease protection experiments and have suggested that a direct repeat of ACACTTG, located 5' to each of the two mapped mRNA start sites, may be involved in transcription initiation. We note that the palindrome overlaps the upstream ACACTTG sequence (Fig. 3-10A). The two 5' ends of the puc mRNAs are located ~35 and ~50 nucleotides downstream from the center of the palindrome. Three other examples of the palindrome overlap the putative E. coli-like promoter sequences found 5' to crtI, crtD and ORF J (Figs. 3-5, 3-10). We propose a regulatory function for the palindrome because of the extraordinary conservation of the motif, its presence in the 5' flanking regions of four crt genes, ORF J and the puc operon, and its overlap with putative E. coli-like promoters in the above three cases.

Overlap of the putative R. capsulatus regulatory site with promoter sequences could be consistent with either positive or negative gene regulation. The regulatory sites may also be widely separated from the promoters with which they interact. Regulatory factors such as AraC, NtrC, λ cI and CAP may function as either activators or repressors of transcription (for examples of reviews see Raibaud and Schwartz, 1984; Gussin et al., 1986). AraC, MalT, and λ cI bind immediately upstream of the -35 region of positively regulated E. coli promoters and λ cII binds within the -35 flanking regions, while NifA may bind more than 100 bp upstream of the anaerobically induced nif promoters (Buck et al., 1986). Negative regulation mediated by repressors often occurs through overlap of the repressor binding site with the regulated promoter (Reznikoff et al., 1985). Formation of a DNA loop between two separate protein binding sites, as in the cases of AraC, GalR and possibly NifA, serves as an additional mechanism for gene regulation (Gussin et al., 1986). Further experiments will be necessary to define the interaction between the R. capsulatus putative regulatory palindromes and sequences involved in transcription initiation.

The puc operon is known to be highly regulated at the transcriptional level in response to oxygen tension (Klug et al., 1985). We have recently shown that expression of several crt genes is strongly induced during a shift from aerobic to photosynthetic growth (Chapter 6), while Giuliano et al. (1988) have found an increase in the steady-state levels of 5' ends from crtA, C and E mRNAs in anaerobic versus aerobic cultures. The common feature of anaerobic gene induction could explain the unexpected presence of identical transcriptional regulatory signals 5' to both the puc and crt operons. These regulatory sequences are not, however, found close to the puf and puh operons (Fig. 3-7), whose expression is also induced by reduction of the oxygen tension (Clark et al., 1984; Klug et al., 1985). Whether a linkage exists between the expression of the puc operon and the regulated crt genes remains to be tested. The palindromes (Fig. 3-10A) may thus bind a transcriptional factor involved in the regulation of a subset of the R. capsulatus photosynthesis genes. ORF J is also preceded by a putative regulatory site and may be part of an operon required for Bchl biosynthesis (see Results). It will be interesting to determine if similar regulatory palindromes exist 5' to the bch genes previously reported to be regulated by oxygen tension (Biel and Marrs, 1983; Zhu and Hearst, 1986; Zhu et al., 1986).

IV. Summary

The work described in this chapter provides the necessary basis for the genetic, biochemical and immunological dissection of the R. capsulatus carotenoid biosynthetic pathway. We have determined the first DNA and deduced amino acid sequences for carotenoid biosynthesis genes and gene products, and have also identified possible promoter, terminator and transcriptional regulatory signals which govern crt gene expression. Previous studies of crt gene regulation in R. capsulatus have been hampered by the lack of gene-specific probes (Clark et al., 1984; Klug et al., 1985; Zhu and Hearst, 1986; Zhu et al., 1986). The work presented here will facilitate an examination of the regulation of individual crt genes. R. capsulatus will, no doubt, continue to prove a valuable model system from which to extend studies of carotenoid biosynthesis to other photosynthetic and nonphotosynthetic organisms.

Chapter 4: Construction of new R. capsulatus carotenoid mutants, and determination of mutant phenotypes and genotypes

I. Introduction

Nine carotenoid biosynthesis (crt) genes have been identified in R. capsulatus and all are contained in the 46 kb photosynthesis gene cluster (Yen and Marrs, 1976; Scolnik et al., 1980a; Zsebo and Hearst, 1984; Chapter 3). We have determined the nucleotide sequence of an 11 kb subcluster encoding eight of the nine genes, providing the first sequence information for carotenoid genes from any organism (Chapter 3). The ninth gene, crtJ, is separated from the other crt genes by about 12 kb (Zsebo and Hearst, 1984). The crt gene cluster is flanked by genetic loci denoted bch which are involved in bacteriochlorophyll (Bchl) biosynthesis (Zsebo and Hearst, 1984; Giuliano et al., 1988).

R. capsulatus carotenoid biosynthesis mutants are available and are photosynthetically viable (Yen and Marrs, 1976; Scolnik et al., 1980; Zsebo and Hearst, 1984; Giuliano et al., 1986, 1988). Genetic lesions in four loci within the R. capsulatus photosynthetic gene cluster, crtB, crtE, crtI and crtJ, produce a blue-green phenotype resulting from the loss of visibly absorbing carotenoids and the continued synthesis of Bchl (Yen and Marrs, 1976; Zsebo and Hearst, 1984). None of these lesions would be expected to block the general isoprenoid biosynthetic pathway before the intermediate GGPP (Fig. 1-5) because this compound is required for the synthesis of the phytyl or geranylgeranyl side chain of chlorophylls in bacteria and plants (Goodwin, 1980). crtB and crtE were originally defined by point mutations (Yen and Marrs, 1976), while crtI and crtJ were identified by Tn5.7 mutagenesis (Zsebo and Hearst, 1984). Giuliano et al. (1986) have recently shown that crtI point mutants accumulate phytoene, which can be converted in vitro to later carotenoids by a mixture of crude cell-free extracts from crtI and crtB mutants. These

authors have proposed that CrtI is the phytoene dehydrogenase. We have recently shown that the deduced amino acid sequence of the R. capsulatus crtD gene product, which also encodes a carotenoid dehydrogenase, shows substantial amino acid similarity to the crtI gene product (Chapter 7). No functions for the crtB, crtE and crtJ gene products have been proposed, however, as information on the in vivo or in vitro accumulation of intermediates in mutants has been lacking. The construction and characterization of several R. capsulatus Tn5.7 mutants blocked in carotenoid biosynthesis have been previously described (Zsebo and Hearst, 1984). Strains KZR8A1, KZR9F4, KZR9E3 contain crtE, crtI and crtJ mutations, respectively. KZR9A12 has a yellow-brown phenotype and is a crtA mutant. KZR8D7 contains a Tn5.7 insertion mapped to the bchI locus, at one end of the crt gene cluster, and is bacteriochlorophyll-minus ($Bchl^-$) (Zsebo and Hearst, 1984).

We have produced six new R. capsulatus mutants containing Tn5.7 insertions within the crt gene cluster and have mapped to high resolution the insertion sites of Tn5.7 in the four previously described mutants and the six new mutants. The phenotypes of the Tn5.7 mutants have been correlated with the sites of the mutations they carry. We also present in this chapter the first evidence for the biochemical functions of the crtB and crtE gene products using a new cell-free in vitro system for incorporation of ^{14}C into carotenoid pyrophosphate precursors and phytoene. The combination of genetic and biochemical data from the Tn5.7 mapping results and the in vitro system allow us to present a revised R. capsulatus carotenoid biosynthetic pathway and scheme for the operon organization of the crt gene cluster, as well as to define to high resolution the DNA sequences required for transcription initiation from the divergent crtA and crtI operons.

II. Materials and methods

Media, cultivation and manipulation of bacterial strains

The bacterial strains and plasmids used are described in Table 4-1. E. coli strains were grown on LC medium (Marrs, 1981). R. capsulatus strains were grown in liquid culture aerobically on a rotary shaker at 200 rpm either on rich PYE medium (Marrs, 1981) or on minimal RCV medium (Weaver et al., 1975). For steady-state photosynthetic growth prior to DNA isolation or pigment extraction, aerobic cultures were inoculated into filled 15 ml screwtop test tubes containing RCV, supplemented with 10 µg/ml L-tryptophan for strain Y68 (Yen and Marrs, 1976), and the test tubes were left in darkness for 12 hours. Cultures were then illuminated at an intensity of 5 W/m^2 by a bank of Lumiline lamps (General Electric Co.), at a constant temperature of 32°C. Blue-green mutants are photosynthetically viable but are susceptible to photooxidative killing for a short period following a shift from dark aerobic growth to the light because they lack colored carotenoids (Sistrom et al., 1956; Yen and Marrs, 1976). The dark period permitted the blue-green mutants to exhaust the remaining oxygen in the medium prior to illumination, thus allowing them to avoid photooxidative killing. Photosynthetic cultures were harvested by centrifugation at early stationary phase. Strain KZR8D7 which lacks Bchl was grown under dark anaerobic conditions in RCV supplemented with dimethyl sulfoxide, glucose and sodium pyruvate (Yen and Marrs, 1977).

Procedures for conjugal matings between E. coli KZE strains (NECO100 derivatives carrying Tn5.7-mutated pRPS404 plasmids) and R. capsulatus SB1003, selection for transfer of the mutated pRPS404 plasmids to SB1003, subsequent integration of Tn5.7 into the chromosome and repurification of the resulting KZR Tn5.7 mutant strains have been previously described (Zsebo and Hearst, 1984). Strain PBR510 (courtesy of P. O'Brien) was constructed by conjugation of E. coli strain BEC404 with SB1003, selection for kanamycin resistance to assure the transfer of pRPS404, and subsequent repurification

of green colonies arising from the recombination of the crtD223 lesion carried on pRPS404 (Marrs, 1981) into the chromosomal copy of crtD in SB1003. Matings between KZE strains and SB1003 gave rise to two classes of transconjugants, depending on whether the double recombination event incorporated both Tn5.7 and the crtD223 allele or only Tn5.7 into the chromosome. Strains carrying the crtD223 point mutation are green due to the accumulation of yellow carotenoids and Bchl, except in cases of mutants also carrying mutations blocking carotenoid biosynthesis before the substrates used by the crtD gene product or those mutants failing to synthesize Bchl. When possible, we selected transconjugants which had recombined only the Tn5.7 based on the color phenotype of the colonies. This was not possible in all cases (Table 4-1, see Results). The plasmid pLAFR1 (Friedman et al., 1982) was conjugated from E. coli strain NECO205 into certain R. capsulatus Tn5.7-containing strains (Table 4-1), using pRK2013 supplied by strain NECO200 as a helper plasmid (Ditta et al., 1980), as previously described (Zsebo and Hearst, 1984). This procedure was used to cure strains of partially deleted pRPS404 derivatives remaining after the recombination of Tn5.7 into the chromosome. Antibiotics were obtained from Sigma Chemical Co. and bacteriological supplies from Difco.

Pigment extraction and characterization

Total pigments were extracted from photosynthetically grown cells carrying out all possible manipulations in darkness or dim light at 4ºC. 15 ml of cells were pelleted by centrifugation and extracted three times with 1 ml of dimethyl sulfoxide. Extracts were centrifuged each time to pellet the cellular debris. Carotenoids and Bchl were fractionated by several extractions of the dimethyl sulfoxide phase with equal volumes of petroleum ether. The petroleum ether fraction containing the carotenoids was back-extracted with an equal volume of dimethyl sulfoxide to remove traces of Bchl and the petroleum ether then evaporated to dryness under a stream of dry nitrogen. Pigment extracts from previously uncharacterized R. capsulatus strains were analyzed by silica gel thin layer

chromatography using a solvent system of acetone:petroleum ether (5:95). Standards for compounds of known structure (Scolnik et al., 1980a) were obtained by extraction of carotenoids from characterized R. capsulatus crt mutants and the wildtype (Table 4-1).

In vitro carotenoid biosynthesis assay and analysis of the products

The experimental procedures of this section were developed and carried out by A. Schmidt (U. of Konstanz, West Germany). Bacteria were grown aerobically in the dark in 200 ml PYE rich medium until early stationary phase. Cells were harvested by centrifugation, resuspended in 2 ml of 0.4 M Tris-HCl (pH 8.0), 5 mM DTT, and lysed in a French pressure cell at 8000 psi. To 0.8 ml of the cell-free extract were added 50 µl $NADP^+$ (25 mM), 50 µl ATP (150 mM) and 10 µl of a $MnCl_2$ (0.6 M)/$MgCl_2$ (0.4 M) solution. The reaction was started with 5 µl [1-^{14}C]IPP (0.5 µCi) and the mixture was incubated in the dark for 2 hours at 33ºC. The pyrophosphates were extracted according to the method of Qureshi et al. (1973). After addition of 9 ml of 1-butanol, the extract was centrifuged for 1 minute in a Hettich centrifuge at maximum speed. The butanol layer was dried by rotary evaporation and the residue redissolved 2 ml of ethanol. 250 µl of HCl (25%) were added and the pyrophosphates hydrolysed for 15 minutes at 37ºC. After the addition of 100 µl ammonia (25%) and 200 µl EDTA (0.25 M) the resulting alcohols were extracted into 5 ml hexane and dried under a stream of dry nitrogen. This extraction procedure also yielded quantitative amounts of phytoene. The alcohols and pigments were redissolved in 25 µl acetone and separated on a Spherisorb C-18 reversed phase HPLC column, using acetonitrile: methanol: 2-propanol (85:10:5). Absorbance readings were monitored with a Jasco Intelligent Spectrophotometer BT 8200 and radioactivity was determined directly with a Raytest Radio-Monitor-Analyzer Ramona LS. [1-^{14}C]IPP was obtained from Amersham Buchler (Frankfurt, Federal Republic of Germany). ^{14}C-labelled HPLC standards for prephytoene alcohol and phytoene were isolated from mutants of the fungi Neurospora crassa (al-2) (Bramley and Mackenzie, 1988) and Phycomyces blakesleeanus

(C5) (Sandmann and Bramley, 1985), respectively. The identity of both standards was confirmed by mass spectroscopy. Pure [^{14}C]geranylgeraniol was a kind gift of Dr. W. Rüdiger (University of Munich, Federal Republic of Germany).

Chromosomal DNA isolation and restriction, preparation of M13 probes, and Southern hybridizations

Total cellular DNA from 15 ml cultures was isolated as described below. Cells were lysed by three freeze-thaw cycles between a 37ºC bath and dry ice. After a 20 minute incubation at 37ºC, DNA was extracted once with phenol:chloroform:isoamyl alcohol (25:24:1) and twice with chloroform:isoamyl alcohol (24:1). Nucleic acids were precipitated with ethanol and resuspended in 0.5 ml TES buffer (50 mM Tris-HCl, pH 7.5, 50 mM NaCl, 10 mM EDTA). RNAse A digestion (30 µg/ml) for 15 minutes at 37ºC was followed by proteinase K digestion (50 µg/ml) for 30 minutes at 55ºC. Samples were again extracted with phenol:chloroform:isoamyl alcohol and chloroform:isoamyl alcohol followed by ethanol precipitation. DNA was resuspended to a concentration of 67 ng/µl and digested with the restriction enzyme(s), PstI, BamHI, PstI plus BamHI, AvaII, or BanII (3-5 units enzyme/µg DNA). Restriction digests were then ethanol precipitated, resuspended, and 10 µg DNA/lane separated on agarose gels (0.8 to 1.2 %) run in 1 x TBE buffer (Maniatis et al., 1982). Southern blots were performed by transferring the DNA to nitrocellulose (Schleicher and Schuell) according to standard procedures (Maniatis et al., 1982). Single-stranded M13 phage generated during the sequencing of the crt genes (Chapter 3) were used to synthesize radioactively labelled probes by primer extension for hybrizations to determine the transposon insertion sites (Table 4-4). M13 probes were labelled as described in Zhu and Hearst (1986) using 50 µCi 5'-[α-^{32}P]dATP (400 Ci/mmol), except that the reaction was carried out for 15 minutes and the probes were digested with HpaII restriction endonuclease subsequent to separation of the unincorporated [α-^{32}P]dATP from the labelled probe. Southern hybridizations were performed according to standard

procedures. [α-^{32}P]dATP was obtained from Amersham. Restriction enzymes, Klenow fragment of DNA polymerase I, and reagents for labelling of DNA were obtained and used according to protocols supplied by the manufacturers (Bethesda Research Laboratories, New England Biolabs, P. L. Biochemicals).

III. Results

A. Construction of Tn5.7 mutated strains and phenotypic characterization of the mutants

We constructed six new R. capsulatus strains (Table 4-1) carrying Tn5.7 insertions within the crt gene cluster by conjugation of Tn5.7-mutated pRPS404 derivatives, originally described by Zsebo and Hearst (1984), from E. coli to R. capsulatus, followed by selection for recombination of the transposon into the bacterial chromosome. The color phenotypes of the new strains (KZR8B3, KZR9D10, KZR9F12, KZR8F6, KZR3H3, KZR8F2) are given in Table 4-1. The carotenoid content was examined by extraction of pigments from photosynthetic cultures (Table 4-2). All of the newly characterized Tn5.7 insertion mutants continued to produce Bchl and could be grown photosynthetically (data not shown).

KZR8B3 accumulates wildtype carotenoids and forms reddish-brown colonies on agar plates as does the wildtype strain. Thus, the Tn5.7 insertion in KZR8B3 does not inactivate any crt gene, although two flanking insertions in strains KZR9A12 and KZR9F4 (Table 4-1) cause CrtA$^-$ and CrtI$^-$ phenotypes, respectively (Zsebo and Hearst, 1984). KZR9D10 and KZR9F12 have a green phenotype and accumulate neurosporene (Fig. 1-5), consistent with the inactivation of either crtC or crtK (Chapter 3). KZR8F6 is blue-green and accumulates no colored carotenoids.

Matings to generate strains KZR3H3 and KZR8F2 gave rise to stable green transconjugants and sectoring muddy-brown transconjugants. Mutations in crtF have been observed to be unstable and lead to stabilizing secondary mutations causing earlier blockages in carotenoid biosynthesis or completely abolishing development of the photosynthetic apparatus (ie. mutations in Bchl biosynthesis and structural photosynthetic genes) (Taylor et al., 1983). We suspected that the Tn5.7 insertions in KZR3H3 and KZR8F2 were located within crtF and therefore purified only the green transconjugants

Table 4-1. Bacterial strains used in this study[a]

Strain	Genotype[b]	Relavent Phenotype[c]	References
E. coli[d,e]			
BEC404	HB101 [pRPS404]	Km^r	Marrs, 1981
NECO100	*leu⁻ thr⁻ thi⁻ trp⁻ recA⁻ lacY⁻*	Rif^r	Youvan *et al.*, 1982
NECO200	HB101 [pRK2013]	Km^r	Ditta *et al.*, 1980
NECO205	HB101 [pLAFR1]	Tc^r	Friedman *et al.*, 1982
KZE8F2	NECO100 [pRPS404Ω(33.4::Tn5.7)]		Zsebo and Hearst, 1984
KZE3H3	NECO100 [pRPS404Ω(33.7::Tn5.7)]		Zsebo and Hearst, 1984
KZE8F6	NECO100 [pRPS404Ω(33.8::Tn5.7)]		Zsebo and Hearst, 1984
KZE9F12	NECO100 [pRPS404Ω(36.4::Tn5.7)]		Zsebo and Hearst, 1984
KZE9D10	NECO100 [pRPS404Ω(36.8::Tn5.7)]		Zsebo and Hearst, 1984
KZE8B3	NECO100 [pRPS404Ω(40.2::Tn5.7)]		Zsebo and Hearst, 1984
R. capsulatus[e]			
KZR8F2	*crtF*Ω(33.4::Tn5.7) *crtD223 rif*-10	Green	This work
KZR3H3	*crtF*Ω(33.7::Tn5.7) *crtD223 rif*-10	Green	This work
KZR8F6[f,g]	*crtE*Ω(33.8::Tn5.7) *rif*-10	Blue-green	This work
KZR8A1[f]	*crtE*Ω(34.6::Tn5.7) *rif*-10	Blue-green	Zsebo and Hearst, 1984
KZR9F12[f,g]	*crtC*Ω(36.4::Tn5.7) *rif*-10	Green-brown	This work
KZR9D10[f]	*crtC*Ω(36.8::Tn5.7) *rif*-10	Green-brown	This work
KZR9F4[f]	*crtI*Ω(39.8::Tn5.7) *rif*-10	Blue-green	Zsebo and Hearst, 1984
KZR8B3[g]	Ω(40.2::Tn5.7) *rif*-10	Wildtype pigments	This work
KZR9A12	*crtA*Ω(41.0::Tn5.7) *rif*-10	Yellow-brown	Zsebo and Hearst, 1984
KZR8D7	*bchI*Ω(41.6::Tn5.7) *crtD223 rif*-10	Yellow, $BchI^-$	Zsebo and Hearst, 1984
KZR9E3[f]	*crtJ*Ω(53.5A::Tn5.7) *rif*-10	Blue-green	Zsebo and Hearst, 1984
PBR510	*crtD223 rif*-10	Green, SB1003 derivative	This work
PY1291	*crtF129*	Muddy brown	Scolnik *et al.*, 1980
SB1003	*rif*-10	Wildtype pigments	Yen and Marrs, 1976
W4	*crtB4*	Blue-green	Yen and Marrs, 1976
Y68	*crtC68 str-2 trpA20*	Green, Str^r, Trp^-	Yen and Marrs, 1976

[a] abbreviations used in this table are: Km, kanamycin; Rif, rifampicin; Sp, spectinomycin; Str, streptomycin; Tc, tetracycline; Tm, trimethoprim; Trp, tryptophan

[b] nomenclature for KZE and KZR strains was developed in Zsebo and Hearst (1984)

[c] color phenotypes reflect aerobic growth on agar plates; wildtype pigmentation is reddish-brown under these conditions and yellow-brown under anaerobic photosynthetic conditions

[d] strains containing a pRPS404 derivative are Km^r

[e] strains containing Tn5.7 are Sp^r, Str^r and Tm^r; strains carrying the *rif*-10 allele are Rif^r

[f] these strains may carry the *crtD223* allele masked by an earlier blockage in carotenoid biosynthesis

[g] strains into which pLAFR1 was conjugated

Table 4-2. Major carotenoids accumulated in the new *R. capsulatus* Tn5.7 mutants compared to the wildtype and characterized point mutants

Strain[a]	Carotenoids accumulated in anaerobic photosynthetic cultures[b]
KZR8F2	neurosporene, hydroxyneurosporene
KZR3H3	neurosporene, hydroxyneurosporene
KZR8F6	no visibly absorbing carotenoids
KZR9F12	neurosporene
KZR9D10	neurosporene
KZR8B3	spheroidene, hydroxyspheroidene
SB1003	spheroidene, hydroxyspheroidene
PY1291	demethylspheroidene
PBR510	neurosporene, hydroxyneurosporene, methoxyneurosporene
Y68	neurosporene

[a] genotypes are given in Table 4-1

[b] R_f values (average of two plates) for silica gel thin layer chromatography in the solvent system of acetone:petroleum ether (5:95) were as follows: 0.91 for neurosporene, 0.77 for methoxyneurosporene, 0.71 for spheroidene, 0.21 for hydroxyneurosporene, 0.19 for demethylspheroidene, 0.17 for hydroxyspheroidene. Small amounts of the keto-derivatives of spheroidene-type carotenoids also accumulate

which had recombined both the Tn5.7 insertion and the crtD223 mutation, derived from pRPS404 (Marrs, 1981), into the chromosome (Materials and Methods). The green derivatives of KZR8F2 and KZR3H3 accumulate neurosporene and hydroxyneurosporene as the major carotenoids (Table 4-2, Fig. 1-5) and maintain a stable phenotype during repurification and growth. The accumulation of carotenoid intermediates in these strains is consistent with the simultaneous inactivation of both crtF and crtD.

KZR strains carrying mutations earlier than crtD in the carotenoid biosynthetic pathway (Fig. 1-5) may also carry the crtD223 mutation (Table 4-1), masked by the phenotype due to the earlier biosynthetic blockage. No gross phenotypic differences other than the change in carotenoid composition distinguish strain PBR510, carrying the crtD223 mutation, and SB1003 wildtype with respect to photosynthetic growth, chromatophore spectra of the light harvesting I and II pigment-protein complexes, or expression of the genes encoding these complexes (Chapter 2). Thus, the phenotypes of Tn5.7 mutants which also carry the crtD223 mutation result from the transposon insertion.

B. Determination of carotenoid precursors accumulated by blue-green carotenoid mutants using a new *in vitro* system

The experiments in this section were performed in collaboration with A. Schmidt (U. of Konstanz, West Germany). We wanted to characterize the compounds accumulated in crtB, crtE and crtJ blue-green mutants because the carotenoid biosynthetic blockages of these strains have not been previously determined and no functions have been assigned to the products of these genes. We also wished to determine whether the crtI Tn5.7 insertion carried in strain KZR9F4 was polar on the downstream crtB gene. If crtI and crtB were on the same operon, as has been suggested both on the basis of the DNA sequence of this region (Chapter 3) and the phenotypes of interposon insertion mutants (Giuliano et al., 1988), one would expect the same compound to be accumulated in both a crtB mutant and the crtI Tn5.7 mutant.

In order to define the biochemical functions of the early crt gene products we developed an in vitro carotenoid biosynthesis system. Label is added to a cell-free extract in the form of [^{14}C]IPP, a five carbon compound which is incorporated into all isoprenoids, including phytoene and its pyrophosphate precursors (Fig. 1-5). The efficiency of in vitro incorporation of [^{14}C]IPP was comparable in cellular extracts from the wildtype strain SB1003 and the crt mutants. Table 4-3 shows that strain W4 (CrtB$^-$) accumulates GGPP but neither PPPP nor phytoene, while KZR8A1 (CrtE$^-$) accumulates PPPP but not phytoene. Based on these results we propose that the crtE gene encodes phytoene synthetase, while crtB encodes the PPPP synthetase. The assignment of these enzymatic functions is reflected in the revised R. capsulatus carotenoid biosynthetic pathway shown in Fig. 1-5. The low levels of PPPP accumulated in comparison to GGPP or phytoene may reflect the lability of this compound (A. Schmidt, personal communication).

KZR9E3 (CrtJ$^-$) accumulates GGPP (Table 4-3) and small amounts of another unidentified compound which is not one of the intermediates shown in Fig. 1-5 (A. Schmidt, personal communication). Although CrtJ may be directly involved in the conversion of GGPP to PPPP, if would be premature to propose an enzymatic function for the gene product until the identity of the unknown compound can be established. Alternatively, crtJ may encode a factor required for the activation of the carotenoid biosynthetic pathway at the level of the crtB gene or gene product, thus leading to accumulation of GGPP in the crtJ mutant.

The in vitro system described here does not convert phytoene into later carotenoids. This may be due to dissociation of the phytoene synthetase from the membranes containing the later carotenoid biosynthetic enzymes under the conditions used (A. Schmidt, personal communication) or because the isomer of phytoene produced in the in vitro system is not recognized as a substrate by the phytoene dehydrogenase (see below). Because the in vitro system did not allow us to unequivocally demonstrate that no

Table 4-3. *In vitro* incorporation of [^{14}C]IPP in cell-free extracts and *in vivo* accumulation of phytoene in *R. capsulatus* blue-green mutants

Strain[a]	GGPP made *in vitro*[b,c]	PPPP made *in vitro*[b,c]	Phytoene made *in vitro*[b]	Phytoene found *in vivo*[d]
SB1003	66182	808	6900	143.4
KZR9F4	28339	1140	7776	2149.1
KZR8A1	30998	6720	- - - -	- - - - -
W4	40418	- - - -	- - - -	- - - - -
KZR9E3[e]	43096	- - - -	- - - -	- - - - -

[a] genotypes are given in Table 4-1

[b] [^{14}C]IPP incorporated in dpm/ml cell-free extract, dashes indicate the compound was not detected

[c] pyrophosphates were converted to their corresponding alcohols for HPLC analysis (Materials and Methods)

[d] accumulation in ng/ml cell-free extract, dashes indicate the compound was not detected

[e] this strain also incorporates a small amount of ^{14}C into another unidentified compound (data not shown)

carotenoids beyond phytoene were synthesized in KZR9F4 (CrtI$^-$) we also quantitated the in vivo accumulation of phytoene in this strain (Table 4-3). The mutant accumulates approximately 15-fold more phytoene than the wildtype in vivo. Both dark chemoheterotrophic and anaerobic photosynthetic cultures of R. capsulatus KZR9F4 accumulate all-trans and 15-cis phytoene in approximately 1:1 ratios (A. Conner and G. Britton, personal communication). The nature of the phytoene isomer produced in the in vitro system remains to be determined, however.

C. High resolution mapping of Tn5.7 insertion sites

The rough mapping of the Tn5.7 insertion sites within mutated pRPS404 derivatives has been previously reported (Zsebo and Hearst, 1984). We have taken advantage of the structure of Tn5.7 to map to high resolution (25-267 bp) the chromosomal insertion sites of Tn5.7 mutations within the R. capsulatus crt gene cluster. Tn5.7 is a hybrid transposon containing the IS50 elements from Tn5 and the antibiotic resistances of Tn7 (Zsebo et al., 1984). The IS50 elements flanking the antibiotic resistance region of Tn5.7 are 1.5 kb in length and are identical in sequence, with the exception of a single nucleotide difference (Auerswald et al., 1980). In addition, during the construction of Tn5.7 the terminal BglII restriction site found in IS50R was lost from IS50L (Zsebo et al., 1984). Transposon insertion sites were mapped by digestion of chromosomal DNA from an R. capsulatus Tn5.7-containing strain with a restriction enzyme which cuts at least once in the IS50 elements, followed by Southern blotting and hybridization with radiolabelled M13 probes. A digest of Tn5.7 mutant DNA probed an M13 subclone overlapping the insertion point of the transposon hybridizes to two restriction fragments, reflecting the net appearance of a single new restriction site resulting from the mutation. The two hybrid restriction fragments in the mutant are formed partially from the interrupted wildtype fragment and partially from the IS50 elements of Tn5.7. Use of small DNA probes overlapping the Tn5.7 insertion site, and various combinations of restriction digests thus

yields high resolution map data.

For the transposon mapping we used the enzymes PstI and BanII, which cut after bp 684 and bp 437, respectively of the IS50 elements (Auerswald et al., 1980). AvaII, which was also used in the Tn5.7 mapping, cuts only within the portion of Tn5.7 derived from Tn7 but not within the IS50 elements. BamHI, which was used in some cases in combination with PstI to generate readily resolvable doubly-digested chromosomal fragments, does not cut within Tn5.7 (Zsebo et al., 1984). Table 4-4 shows a detailed list of the M13 probes used to determine the Tn5.7 insertion sites and the results of Southern hybridizations. Fig. 4-1 shows representative Southern hybridizations used to localize the Tn5.7 insertion sites. Fig. 4-2 shows the locations of the transposon insertions relative to the locations of the crt genes.

KZR8D7 (BchI$^-$) carries a Tn5.7 insertion between bp 999-1244, within the 3' end of the crtA gene and upstream of the proposed ORF H translational start at bp 616. KZR9A12 carries a Tn5.7 insertion between bp 1651-1862, within the 5' coding region of crtA. The phenotypes of these two crtA insertions are, however, dissimilar as KZR9A12 produces Bchl and spheroidene (data not shown), as expected for a CrtA$^-$ strain, while KZR8D7 is Bchl$^-$ (Zsebo and Hearst, 1984). KZR8B3 contains an insertion in the common 5' control region of crtA and crtI, between bp 2437-2481, but accumulates wildtype carotenoids (Table 4-2). The insertion in KZR9F4 lies between bp 2755-2915, at the 5' end of the crtI gene. Both KZR9D10 and KZR9F12 contain Tn5.7 insertions within the crtC gene, between bp 6037-6203 and bp 6567-6773, respectively. The KZR8A1 Tn5.7 is inserted between bp 8461-8485, either within the 5' crtE coding region or less than five nucleotides 5' to the ATG start. KZR8F6 bears a Tn5.7 insertion between bp 8948-9047, also within crtE, which is consistent with the blue-green phenotype of this strain (Table 4-1). Both KZR3H3 and KZR8F2 carry Tn5.7 insertions within crtF, between bp 9334-9600 and bp 9601-9835, respectively.

Table 4-4. Positioning of Tn5.7 insertions by Southern hybridization using M13 probes[a]

		<----------Tn5.7 mutants[b]---------->									
Probe	Insert[a]	8D7	9A12	8B3	9F4	9D10	9F12	8A1	8F6	3H3	8F2
BSp31	1-226	L[c]									
SpSa25	227-569	L[c]									
TT70	660-871	L[c]									
TT88	872-994	L[d]									
XX46	1244-999	+[d]									
TT68	1298-1382	R[d]									
TT71	1650-1494		L[c]								
TT41	2194-1651		+[c]								
TT93	1863-2194		R[c]								
PP18	2619-2105		R[c]	+[e]	L[c]						
SpSa27	2133-2481			+[c]							
TT69	2195-2359			L[c]							
PSa133	2619-2482			R[c]	L[c]						
HH128	2678-2598			R[c]	L[c]						
PE23	2620-2968		R[c]		+[c]						
HH122	2754-2679			R[c]	L[c]						
HH121	2915-2755				+[c]						
ESa116	2969-3301				R[c]						
BaS2	3302-3908		R[c]		R[c]						
SpSp84	6892-6037					+[d]	+[d]				
SS112	6295-6231					R[d]					
SS101	6231-6409					R[d]					
SS114	6410-6566					R[d]	L[d]				
SS103	6773-6410						+[d]				
XB20	8101-7777							L[d]			
XB14	8364-8102							L[d]			
TS10	8485-8300							+[d]			
XB2	8365-8587							+[f, d]			
TS11	8486-8587							R[d]			
TB4	8818-8588							R[d]	L[d]		
TT25	8875-8947								L[d]		
TSp3	8875-9059								+[d]		
TT10	8875-9187								+[d]	L[d]	L[d]
SS40	9047-8909								+[d]		
SS41	9600-9334								R[d]	+[d]	L[d]
SS35	9835-9601									R[d]	+[d]
TT4	9873-9799									R[d]	R[d]

[a] all nucleotide positions in this table refer to Fig. 4-2, orientations of the inserts represent the ^{32}P-labelled strand

[b] + means hybridization to two chromosomal fragments indicating a Tn5.7 insertion, L or R means hybridization to only one chromosomal fragment located to either the left or the right of the Tn5.7 insertion (Fig. 4-2), and spaces denote combinations not tested

[c] PstI/BamHI chromosomal digest

[d] PstI chromosomal digest

[e] AvaII chromosomal digest; PP18 hybridizes to wildtype AvaII fragments extending from bp 1731-2436 and bp 2437-3015, the latter of which is interupted by the Tn5.7

[f] BanII chromosomal digest; XB2 hybridizes to wildtype BanII fragments extending from bp 8164-8460 and bp 8461-9798, the latter of which is interrupted by the Tn5.7

Figure 4-1 A-D. Southern blots showing the mutation sites in the Tn5.7 insertion strains KZR8B3, KZR9F4, KZR8A1 and KZR8F6. Locations of M13 probes are given in Table 4-4 and probes used are indicated across the top of each panel. The restriction enzymes used for the chromosomal digests were PstI plus BamHI in (**A**) for KZR8B3 and (**B**) for KZR9F4, and PstI in (**C**) for KZR8A1 and (**D**) for KZR8F6. The SB1003 wildtype (Wt) digest is shown in the left lane and the mutant digest in the right lane for each probe. BamHI does not cut within Tn5.7. In the mutants, a PstI restriction digest leaves 684 bp from the end of each IS50 element fused to both segments of the interrupted wildtype fragment resulting from the Tn5.7 insertion. Probes not overlapping the Tn5.7 insertion site hybridize to only one mutant fragment of altered size. Restriction digests were selected in order to distinguish between hybrid chromosomal fragments located to the left and right of the Tn5.7 insertion (Table 4-4) based on size. Probes overlapping the Tn5.7 insertion site hybridize to two mutant fragments. The sum of the measured sizes of the two mutant fragments (given in bp at the right of each panel) agrees closely with the prediction from the combination of the wildtype fragment size (shown at the left of each panel in bp; Fig. 4-2) plus the contribution from the two IS50 elements.

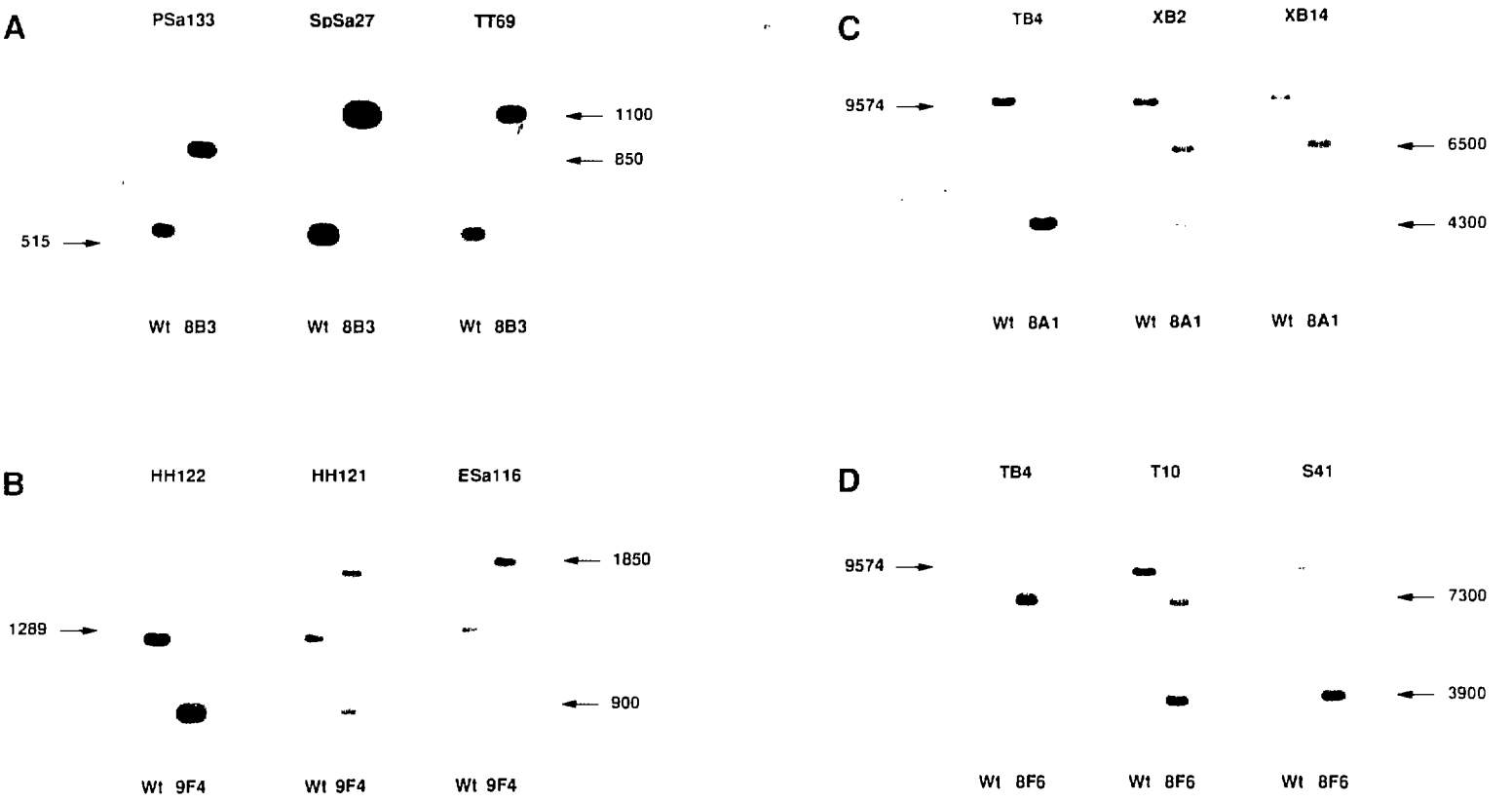
A
PSa133
SpSa27
TT69
1100
850
515
Wt 8B3
Wt 8B3
Wt 8B3
C
TB4
XB2
XB14
9574
6500
4300
Wt 8A1
Wt 8A1
Wt 8A1
B
HH122
HH121
ESa116
1850
1289
900
Wt 9F4
Wt 9F4
Wt 9F4
D
TB4
T10
S41
9574
7300
3900
Wt 8F6
Wt 8F6
Wt 8F6

Figure 4-2. Location of Tn5.7 insertions within the crt gene cluster. Numbers across the top indicate the nucleotide positions of translational starts and stops for the crt genes and neighboring open reading frames (ORFs). Arrows above the genes indicate the directions of transcription. Triangles and solid bars below denote the regions of Tn5.7 insertions in different R. capsulatus KZR mutants based on the hybridization results in Table 4-4. Nucleotide locations of the insertion regions are given in the text. Solid circles show the locations of palindromic sequences proposed to be involved in the regulation of transcription (Chapter 3). Restriction sites important to the mapping of Tn5.7 insertions are shown below (B = BamHI, P = PstI, A = AvaII, Bn = BanII). All BamHI and PstI sites are shown, while only those AvaII and BanII sites relevant for Tn5.7 mapping in strains KZR8B3 and KZR8A1, respectively, are shown. Flanking PstI sites not shown in this figure are located approximately 700 bp to the left of bp 1 (as determined in Fig. 3-3) and 1154 bp to the right of bp 11039 (M. Alberti, unpublished data).

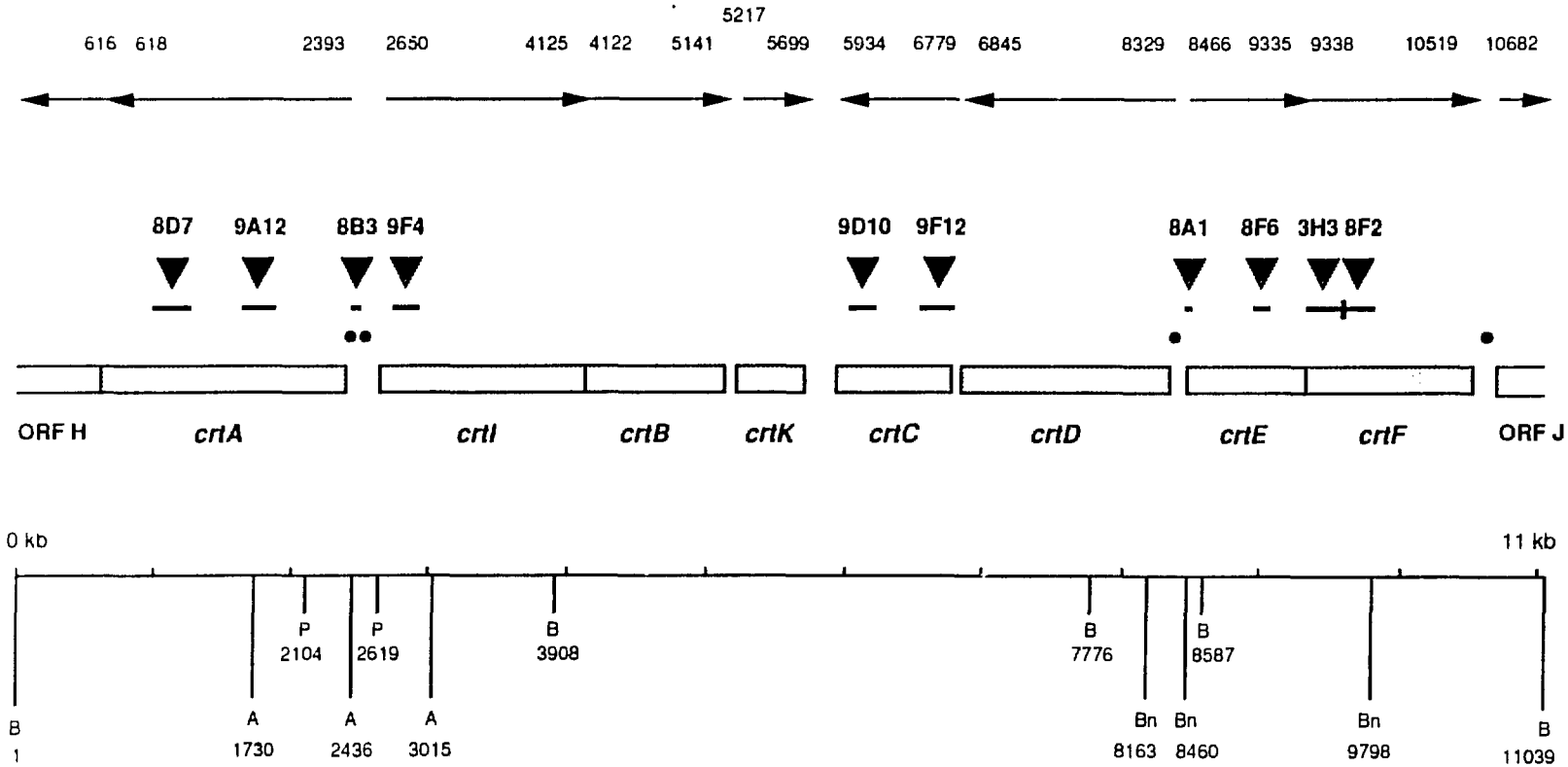
5217
616 618 2393 2650 4125 4122 5141 5699 5934 6779 6845 8329 8466 9335 9338 10519 10682
8D7 9A12 8B3 9F4 9D10 9F12 8A1 8F6 3H3 8F2
ORF H crtA crtI crtB crtK crtC crtD crtE crtF ORF J
0 kb 11 kb
B 1
A 1730
P 2104
P 2619
A 2436
A 3015
B 3908
B 7776
Bn 8163
B 8587
Bn 8460
Bn 9798
B 11039

IV. Discussion

A. Tn5.7 mapping and operon structure of the crt genes

Tn5 insertions are polar, thus inactivating both the interrupted gene and any downstream genes on the same operon (Berg et al., 1980). The transposon interrupts transcription from external promoters because its sequence contains transcription termination signals. The polarity of transposon insertions has allowed us to refine the operon structure of the crt gene cluster using Tn5.7 mutants. We have recently proposed that the crt genes form a minimum of four operons, crtA, crtIBK, crtDC and crtEF, based on the complete nucleotide sequence and the organization of the crt gene cluster (Fig. 3-7). Giuliano et al. (1988) have proposed that the crtA, C, D, E and F genes each constitute separate operons, and that crtI and crtB may be on the same operon. These conclusions were based on the carotenoid intermediates accumulated in interposon mutants and on complementation analyses.

Each of the Tn5.7 insertions in strains KZR9A12, KZR9F4, KZR9D10, KZR9F12, KZR8A1, KZR8F6, KZR3H3 and KZR8F2 lies within the coding region of one of the crt genes (Fig. 4-2) and the phenotypes of these mutants (Tables 4-2, 4-3) correlate directly with the proposed biosynthetic function of the interrupted gene. The Tn5.7 insertions in strains KZR8D7 and KZR8B3 are exceptions.

The transposon in KZR8D7 lies within the 3' coding region of crtA although this mutant lacks Bchl. We have recently suggested that this phenotype is due to polar inactivation of a downstream gene, possibly ORF H, which is part of an operon required for Bchl synthesis (Chapter 3) and whose transcription initiation signals overlap the 3' coding region of crtA. Taylor et al. (1983) have determined that the BamHI-H fragment of pRPS404 (bp 1-3908 in Fig. 4-2) complements the bchD1008 point mutation, suggesting that most or all of the bchD gene is contained in this region. Although the mutation in KZR8D7 was originally assigned to a newly defined bchI locus on the basis of

complementation analysis (Zsebo and Hearst, 1984), Giuliano et al. (1988) have observed that an interposon insertion at bp 1303 leads to a BchlD$^-$ phenotype. The interrelationships between ORF H, and the bchI and bchD genetic loci remain to be determined. Because KZR9A12 produces Bchl while KZR8D7 is Bchl$^-$, we conclude that crtA and ORF H are not cotranscribed. As KZR8D7 also carries the crtD223 point mutation (Table 1), which blocks carotenoid biosynthesis before the reactions mediated by CrtA, we do not know if this strain is also CrtA$^-$.

The Tn5.7 insertion in strain KZR8B3 lies in the crtA-crtI 5' flanking region. This transposon causes no change in the wildtype carotenoid pigmentation and must hence lie between the minimal promoter and regulatory signals required for the expression of the crtA and crtI genes. An unlikely alternative explanation for the KZR8B3 wildtype phenotype would be the fortuitous creation of a promoter at the Tn5.7 insertion site. We do not favor this explanation because an interposon inserted in the same area at a NruI site (bp 2471) also has no effect on pigmentation (Giuliano et al., 1988). The transposon is inserted in the region between bp 2437-2481 (Figs. 4-2, 4-3, Table 4-4). A promoter for crtA cannot therefore be located farther to the right than bp 2481, while a promoter for crtI cannot be placed farther to the left than bp 2437. Using the additional result of the NruI insertion phenotype, we can further define the boundaries of the crtA and crtI control sequences. A crtA promoter must lie between bp 2471-2393, while a promoter for crtI must lie between bp 2472-2650 (Fig. 4-3). This mapping is consistent with our proposal (Chapter 3) that an E. coli-like σ^{70} recognition sequence located from bp 2489-2516 may function as a promoter for crtI. These results also place severe constraints on the location of the unidentified promoter sequences for crtA. For the divergent crtA and crtI operons either overlapping or face-to-face promoter geometries (reviewed in Beck and Warren, 1988) appear to be excluded by our results.

The observation that KZR9F4 accumulates phytoene is significant in light of the fact that Giuliano et al. (1986, 1988) have reported that crtI point mutants accumulate phytoene

Figure 4-3. The 5' flanking region of the divergent crtA and crtI operons. Nucleotide positions are indicated at the left and right from the start codon of crtA to the start codon of crtI. Nucleotides between bp 2537-2649 have been omitted (indicated by dashes 5' to the crtI start codon). The black bar indicates the region within which the Tn5.7 insertion of strain KZR8B3 lies. Underlined restriction sites shown correspond to enzyme cutting after bp 2436 (AvaII), bp 2471 (NruI), and bp 2481 (SalI). A possible crtI promoter sequence similar to the consensus E. coli σ^{70} promoter is indicated by (*) above the -35 and -10 regions. Boxes indicate the locations of conserved palindromic sequences (shown by arrows below) which we have proposed to be the recognition sites for the binding of a transcriptional factor.

while interposon mutants do not. These authors concluded that the interposons likely exerted a polar effect on the downstream crtB gene, and that crtB and crtI may form a single operon. The transposon mutation in KZR9F4 lies between bp 2755-2915 (Fig. 4-2, Table 4-4), 5' to the two interposon insertions at sites now known to correspond to bp 2968 and bp 3301.

We offer two possible explanations to account for the discrepancy in the phenotypes of the crtI mutants. If crtB and crtI are contained on two distinct operons, the transcription initiation signals for crtB may substantially overlap the 3' coding region of crtI. The distal interposon insertions, but not the proximal transposon insertion, may lie between the crtB transcriptional regulatory signals and the coding region of the crtB. Thus, only the crtI interposons would show a polar effect on crtB expression. If, alternatively, crtI and crtB are part of the same operon, the Tn5.7 insertion in KZR9F4 may fortuitously activate a cryptic promoter at the insertion site, thus allowing for continued expression of crtB. We have previously reported the presence of a possible rho-independent transcription termination signal 3' to crtI (Fig. 3-11). In addition, Zsebo and Hearst (1984) originally identified crtI as a locus distinct from the neighboring crtB locus because a plasmid bearing the Tn5.7 insertion in KZR9F4 complemented two separate crtB point mutants, including strain W4 which we have shown to accumulate GGPP in vitro (Table 4-3). These data support the first proposal and lead us to conclude that crtI and crtB are not cotranscribed. We note the analogy between the proposed overlap of cis-acting elements for ORF H with the 3' coding region of crtA, and the overlap of cis-acting elements for crtB with the 3' coding region of crtI.

An interposon insertion in ORF J, 3' to crtF, has been shown to produce a Bchl$^-$ phenotype (Giuliano et al., 1988), while crtF transposon insertions (Fig. 4-2) do not abolish Bchl biosynthesis. We have also located a possible rho-independent transcription terminator in the DNA sequence 3' to crtF and a possible σ^{70} promoter sequence 5' to ORF J (Fig. 3-9). All of these data strongly suggest that crtF and ORF J are not

cotranscribed. Taylor et al. (1983) have proposed that crtF mutants accumulate secondary mutations as the result of selection rather than an enhanced mutation rate. crtF mutants accumulate demethylspheroidene as the major carotenoid under anaerobic photosynthetic conditions (Scolnik et al., 1980a). The stability of the phenotypes of the crtFcrtD223 double mutants KZR3H3 and KZR8F2 suggests that demethylspheroidene and perhaps demethylspheroidenone, are responsible for the observed selection against crtF mutants, while the hydroxyneurosporene accumulated in the double mutants has no deleterious biological effect. The basis of the selection against the accumulation of these compounds remains to be determined.

In summary, our data indicate that neither crtA and ORF H, nor crtF and ORF J are cotranscribed. Similarly, crtI and crtB do not appear to be cotranscribed. Giuliano et al. (1988) have shown that interposon insertions in crtD are not polar on crtC, indicating that these genes are on separate operons. Thus, we now propose a minimal operon structure for the crt gene cluster of crtA, crtI, crtBK, crtC, crtD and crtEF. Whether or not crtB and crtK, or crtE and crtF form operons remains to be demonstrated, although evidence presented in Chapter 6 suggests that the former two genes are not cotranscribed.

B. Biochemical functions of the CrtB and CrtE enzymes in the carotenoid biosynthetic pathway

In R. capsulatus we propose that two distinct enzymes (CrtB and CrtE) and possibly a third factor (CrtJ), are required for the conversion of GGPP to phytoene via PPPP. A bifunctional phytoene synthetase enzyme catalyzing both the formation of PPPP from two molecules of GGPP, and the subsequent formation of phytoene from PPPP has recently been purified from Capsicum (red pepper) chromoplasts (Dogbo et al., 1988). This is the first reported purification to homogeneity of an enzyme involved in the synthesis of PPPP or phytoene. Both biosynthetic activities are kinetically coupled and are associated with a single polypeptide of apparent molecular weight 47.5 kDa determined by SDS-PAGE.

For comparison, the molecular weights of the R. capsulatus CrtB and CrtE enzymes deduced from the DNA sequence are 37 kDa and 30 kDa, respectively (Fig. 3-6). These data suggest that the PPPP synthetase and phytoene synthetase enzymatic activities may have been fused into a single polypeptide during the course of evolution from photosynthetic bacteria to higher plants. The accumulation of GGPP in strain W4 (Table 4-3) and our proposal that CrtB is the PPPP synthetase are consistent with earlier observations that a mixture of cell-free extracts from W4, which was known at the time to accumulate no carotenoids, and a crtI phytoene-accumulating point mutant complemented the biochemical defect of the crtI mutant in vitro (Giuliano et al., 1986). The in vivo accumulation of phytoene in KZR9F4 confirms that the crtI gene product is required for phytoene dehydrogenation. In addition, recent evidence indicates that antibodies raised against an R. capsulatus CrtI fusion protein inhibit the dehydrogenation of phytoene in vitro using a solubilized membrane fraction from the cyanobacterium Aphanocapsa (Schmidt et al., submitted).

V. Summary

The data presented in this chapter have allowed us to correlate the phenotypes of ten Tn5.7 insertion mutants in R. capsulatus crt biosynthesis gene cluster with the genotypes by a combination of high resolution mapping of the mutation sites and characterization of the carotenoids accumulated. Development of a new in vitro assay for the synthesis of phytoene and its pyrophosphate precursors has allowed us for the first time to examine the enzymatic blockages in crtB, crtE, and crtJ blue-green mutants. We propose that CrtB is the PPPP synthetase and that CrtE is the phytoene synthetase based on the accumulation of phytoene precursors in the in vitro system, and present a revised R. capsulatus carotenoid biosynthetic pathway incorporating these results. The combination of Tn5.7 mapping and in vivo accumulation of phytoene in a crtI Tn 5.7 mutant suggests that crtI and crtB are not cotranscribed. We also propose that neither crtA and ORF H, nor crtF and ORF J are cotranscribed, indicating a minimal operon structure for the crt gene cluster of crtA, crtI, crtBK, crtC, crtD and crtEF.

Chapter 5: Erwinia herbicola pigment genes resident in Escherichia coli as a model system for carotenoid biosynthesis in a nonphotosynthetic bacterium

I. Introduction

Erwinia herbicola is a phytopathogenic bacterium and is often associated with aerial plant parts. Perry et al. (1986) have recently prepared a Escherichia coli cosmid library of total DNA from E. herbicola strain Eho10 (ATCC 39368) using the cosmid pHC79. Eho10 is a yellow pigmented strain isolated from apple leaves obtained in Fresno, California. Clones from the cosmid library which directed the synthesis of the yellow pigments in E. coli were characterized. A 12.4 kb chromosomal fragment, which contains all the necessary genetic information for yellow pigment synthesis, was isolated on plasmid pPL376 by partial deletion of one of the cosmid clones. The pigment synthesis genes appear to be present in a single chromosomal copy in E. herbicola Eho10. Other strains of E. herbicola loose their pigmentation when cured of endogenous plasmids, although this is not true for Eho10 (Gantotti and Beer, 1982; Perry et al., 1986). Perry et al. (1986) found the accumulation of yellow pigments in E. coli to be under cyclic AMP (cAMP) control. Glucose is known to inhibit cAMP synthesis (Makman and Sutherland, 1965) and its addition to the growth medium represses yellow pigment production. In addition, no pigment was synthesized in a strain of E. coli unable to produce cAMP. In E. coli minicells (Meagher et al., 1977), the E. herbicola DNA insert in pPL376 codes for the synthesis of seven polypeptides of molecular weights 84, 69, 56, 53, 50, 43 and 37 kDa. The synthesis of the 84, 56 and 43 kDa proteins was repressed by the addition of glucose to the medium. Both colony pigmentation and inhibition of pigment production by glucose were variable in different strains of E. herbicola examined (Perry et al., 1986).

Further work to define the nature of the yellow pigments and to evaluate their possible protective effects in E. coli against phototoxic molecules has been recently described (Tuveson et al., 1988). The three major yellow pigments produced in E. coli strain HB101 containing pPL376 (hereafter designated HB101 [pPL376]) have visible absorption spectra similar to that of β-carotene. These compounds are, however, more polar than β-carotene in TLC and HPLC analysis suggesting that they may be xanthophylls. The production of the putative carotenoids in E. coli conferred resistance to exogenous photosensitizing molecules activated by near-UV (320-400 nm) or visible light but not far-UV (200-300 nm), and which damage cellular membranes. E. coli synthesizing the carotenoids were also protected from the harmful effects of near-UV alone, although the nature of the endogenous photosensitizing molecule is not known in this case. Photosensitizers in other carotenogenic nonphotosynthetic organisms include porphyrins such as cytochromes and protoporphyrin IX (Tuveson et al., 1988).

Assuming that the yellow pigments produced by in E. coli carrying the E. herbicola crt genes were xanthophylls derived from a C_{40} backbone, we reasoned that the E. herbicola carotenoid biosynthetic pathway would proceed via the dehydrogenation of phytoene and the production of cyclic carotenes from lycopene or neurosporene (Fig. 1-2), prior to xanthophyll formation. Diphenylamine (DPA) and nicotine are two frequently used and well characterized inhibitors of carotenoid biosynthesis, effective in a variety of organisms (reviewed in Goodwin, 1980). DPA is known to inhibit carotenoid biosynthesis by blocking the dehydrogenation of phytoene in many bacteria, both nonphotosynthetic and photosynthetic, and in fungi. Nicotine inhibits both the hydration of the C-1, 2 and C-1', 2' carotenoid double bonds in members of the family Rhodospirillaceae and the cyclization of lycopene to carotenes (Fig. 1-2) in nonphotosynthetic bacteria and fungi, two mechanistically similar reactions (Patel et al., 1983). We have thus undertaken to demonstrate that E. herbicola yellow pigment genes direct the synthesis of carotenoids in E. coli by inhibitor studies with DPA and nicotine.

II. Materials and methods

Growth and maintenance of bacterial strains

E. coli HB101 containing either pPL376, a plasmid bearing the E. herbicola pigment biosynthesis genes cloned into the cosmid vector pHC79 (Perry et al., 1986), or pHC79 alone as a negative control were used in the studies described here. These strains are hereafter designated HB101 [pPL376] and HB101 [pHC79]. E. coli strains were grown in LC rich medium (Marrs, 1981) at 37°C in the presence of 100 μg/ml ampicillin, as both pHC79 and pPL376 confer resistance to this drug. For measurement of growth curves the cells were cultured in 15 ml screw top tubes containing 5 ml of medium, shaken sideways at 200 rpm on a rotary shaker. Optical density measurements at 660 nm were taken using a Bausch and Lomb Spectronic 21 colorimeter. After preliminary experiments to establish inhibitor concentrations which did not impair cellular growth, final concentrations of 70 μM DPA and 5 mM nicotine were selected for successive experiments. DPA and nicotine were obtained from Sigma Chemical Co. DPA was added to the growth medium from a 0.35 M stock prepared in ethanol, while nicotine was added directly. For pigment isolations, 100 ml of LC medium in a 1 liter flask was innoculated with 1 ml of stationary phase cells and the appropriate amount of inhibitor. Cultures were grown at 37°C on a rotary shaker at 200 rpm and were harvested by centrifugation at early stationary phase.

Pigment extractions, thin layer chromatography, and UV-visible spectroscopy

All possible pigment extraction manipulations were carried out on ice in dim light. Lyophilized cell pellets were extracted three times with 1 ml of dimethyl sulfoxide, followed by three extractions with 1 ml of petroleum ether. The dimethyl sulfoxide fraction was reextracted once with 3 ml of petroleum ether. The petroleum ether fractions containing the non-polar pigments were pooled and dried under a stream of dry nitrogen.

The dimethyl sulfoxide fraction containing the polar pigments was centrifuged to remove debris and spectra of the total polar pigment mixture were recorded. The dried petroleum ether fraction was resuspended in petroleum ether and the spectrum recorded as above. Concentrations of pigments were normalized prior to recording of the spectra on the basis of equivalent dry cell pellet weights. The non-polar pigment fractions from all samples were subsequently dried under a stream of nitrogen, resuspended in a small volume of petroleum ether and chromatographed on a silica gel Si500F TLC plate containing a 254 nm fluorescent indicator (J. T. Baker). Pigments were separated using a solvent system of acetone:petroleum ether (5:95). UV fluorescing material was visualized directly on the TLC plate during chromatography using a hand held Mineralight UVSL-25 UV lamp (Ultra-violet Products, Inc.) on the long wavelength UV setting. Large amounts of UV fluorescing material migrating close to the solvent front (R_f of 0.91) could be seen in the extracts from DPA- and nicotine-inhibited cultures, small amount in the uninhibited culture, and none in the pHC79 control. Several pigment bands unique to extracts from HB101 [pPL376], including the UV absorbing material, were purified by scrapping the silica gel off of the plate and extraction of the samples with petroleum ether. Spectra of the purified non-polar pigments in petroleum ether were subsequently recorded. All spectra were taken using a Varian 2300 spectrophotometer.

III. Results

A. The effect of carotenoid biosynthesis inhibitors on the growth of E. coli

We initially wanted to determine whether DPA and nicotine were effective as inhibitors of carotenogenesis in cultures of E. coli carrying the cloned E. herbicola carotenoid genes, and if so what concentrations of inhibitors would suffice to alter culture pigmentation without inhibiting cellular growth. To achieve this goal we cultured E. coli HB101 [pPL376] in the presence of a range of concentrations of each inhibitor and measured light scattering at 680 nm to monitor cellular growth. Addition of DPA to the medium did not cause appreciable inhibition of cellular growth until a concentration of 175 μM (Fig. 5-1). A concentration of 70 μM DPA resulted in the obvious loss of yellow pigmentation in centrifuged pellets of E. coli, without inhibiting growth. In the case of nicotine, addition of concentrations of 10 mM or higher in the growth medium inhibited growth, preventing growth entirely at 50 mM. 5 mM nicotine resulted in a slight reddening of the E. coli cell pellets, relative to the color of the uninhibited cell pellets, with little effect on cellular growth.

B. Characterization of compounds found in E. coli bearing the E. herbicola pigment genes, grown in the presence and absence of inhibitors

The cell-free growth medium from a stationary phase culture of HB101 [pPL376] had a deep yellow color in contrast to the medium from the control culture of HB101 [pHC79], whose genetic makeup is identical except for the absence of the E. herbicola pigment genes. The cell-free growth medium of HB101 [pPL376] cultured in the presence of 5 mM nicotine was also deep yellow, while the supernatant of HB101 [pPL376] cultured in the presence of 70 μM DPA was similar to that of HB101 [pHC79]. Spectra of the growth medium from these samples revealed that HB101 [pPL376] synthesized pigments

Figure 5-1 A, B. Effects of DPA and nicotine on cellular growth of E. coli. HB101 [pPL376] was cultured in the presence of the indicated concentrations of the carotenoid biosynthesis inhibitors. Concentrations of DPA of 70 μM or less (**A**), or nicotine concentrations of 5 mM or less (**B**) have little effect on cellular growth.

A

Effect of DPA on E. coli growth

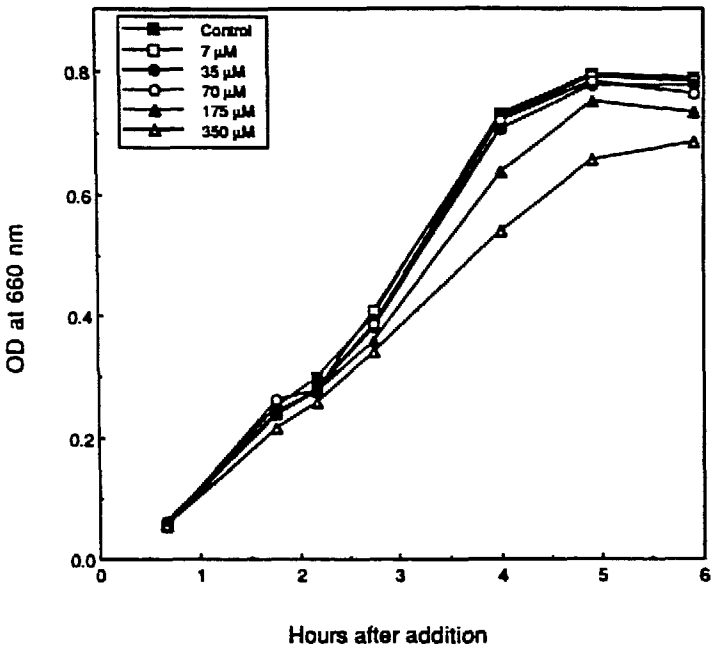

B

Effect of nicotine on E. coli growth

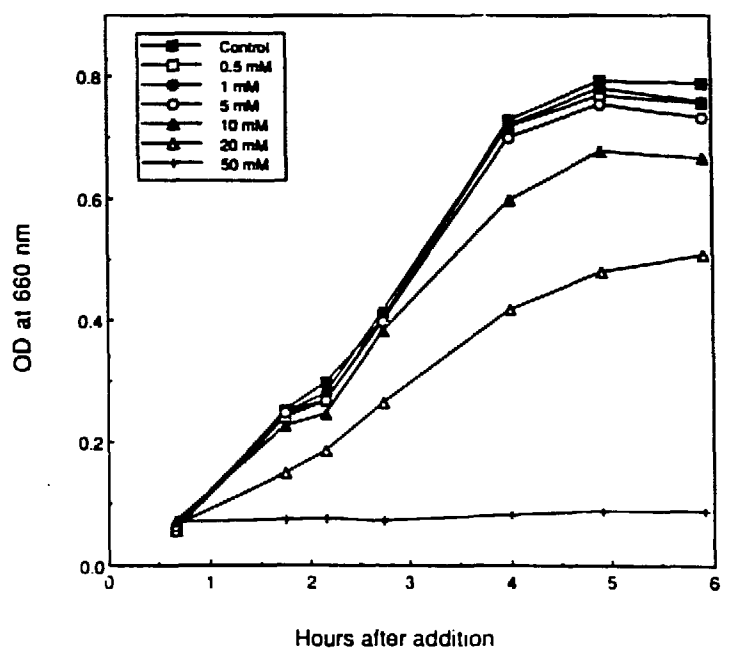

with absorption maxima at 436, 460, 490 nm while HB101 [pHC79] did not (Fig 5-2A). Growth with 5 mM nicotine led to a slight red-shifting of the absorption maxima to 440, 462, 496 nm and less than a 2-fold reduction in pigment accumulation, while growth with 70 μM DPA drastically reduced pigment accumulation (Fig. 5-2B). The question of whether the growth medium contains free water soluble pigment or pigment complexed with protein remains to be addressed.

Polar and non-polar pigments from HB101 [pPL376], HB101 [pPL376] plus 70 μM DPA, HB101 [pPL376] plus 5 mM nicotine, and HB101 [pHC79] were fractionated as described (Materials and methods). The bulk of the yellow pigments in HB101 [pPL376] extracts from either inhibited or uninhibited cultures were polar and partitioned into the dimethyl sulfoxide phase. The concentration of total polar visibly absorbing pigments, normalized by dry cell weight, was less than 2-fold reduced in the nicotine-treated culture, but was dramatically reduced (about 15-fold) in the DPA-treated culture (Fig. 5-3). Both uninhibited and DPA-treated cultures showed similar polar pigment absorption maxima (Table 5-1), while nicotine-treated cultures showed slightly red-shifted absorption maxima relative to HB101 [pPL376]. No visibly absorbing pigments were apparent in the spectrum from HB101 [pHC79].

The visible spectra of the non-polar pigment fractions showed that HB101 [pPL376] accumulated a small amount of non-polar pigment, relative to the polar pigments, in the absence of inhibitor. The nicotine-inhibited culture accumulated several-fold more non-polar pigment, the bulk of which exhibits maxima red-shifted with respect to the uninhibited sample (Fig. 5-4). The multitude of absorption peaks in the visible spectrum indicates the accumulation of several new pigments. The DPA-inhibited culture accumulated roughly as much visibly absorbing non-polar pigment as did the uninhibited culture, although the presence of DPA led to a pronounced blue-shifting of the maxima for the accumulated material (Table 5-1) which appeared to be a mixture of compounds. The control extract, from HB101 [pHC79], showed no visibly absorbing pigments.

Figure 5-2 A, B. Spectra of the growth medium. (**A**) shows the spectra of the growth medium from HB101 [pPL376] and HB101 [pHC79]. (**B**) shows similar spectra from nicotine- and DPA-inhibited HB101 [pPL376] cultures. Samples were collected at the time cell pellets were harvested for pigment extractions. The vertical hairline indicates the maximal absorption wavelength in the HB101 [pPL376] sample.

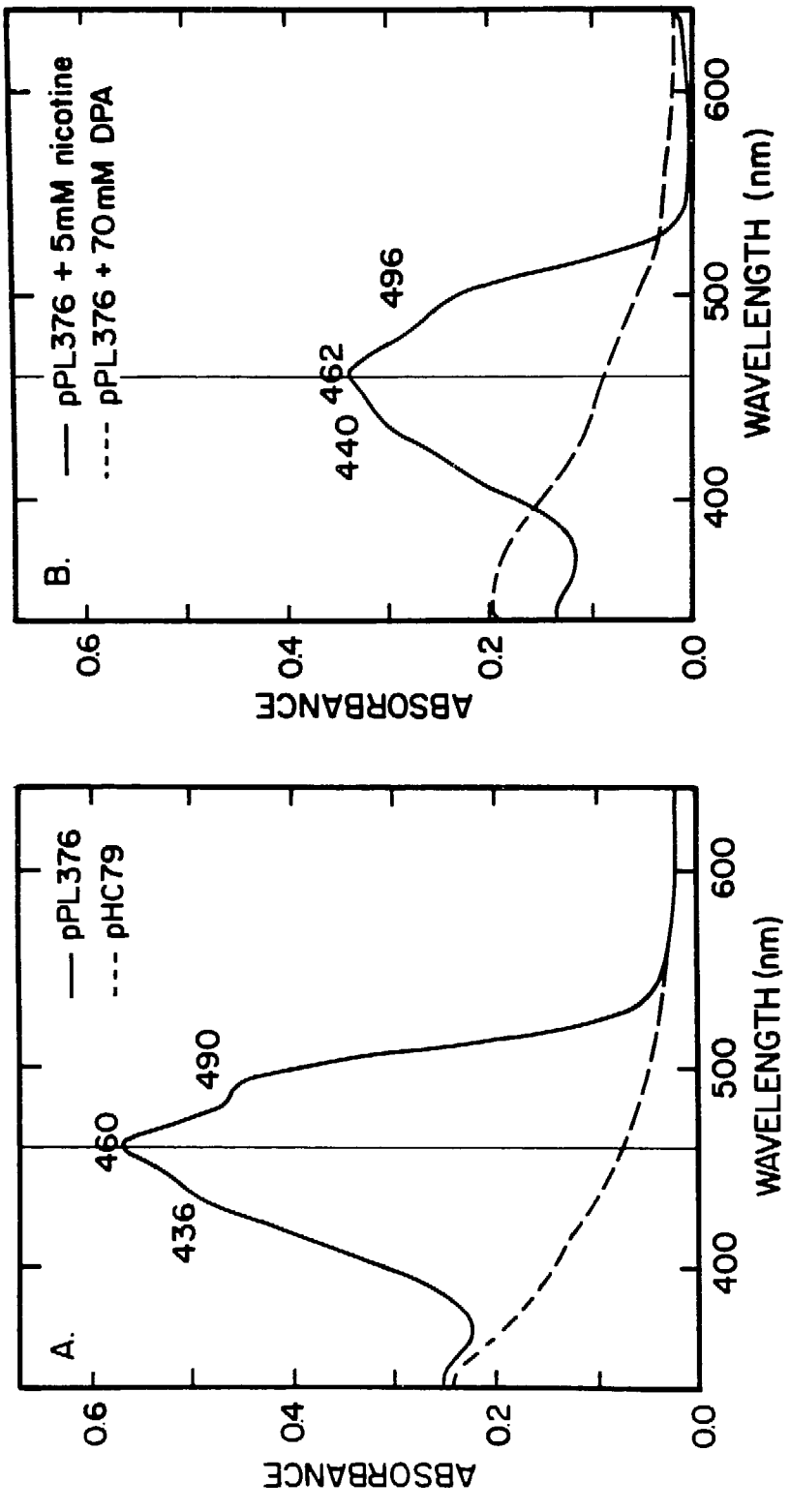
A.
pPL376
pHC79
460
490
436
ABSORBANCE
WAVELENGTH (nm)
B.
pPL376 + 5mM nicotine
pPL376 + 70mM DPA
462
496
440
ABSORBANCE
WAVELENGTH (nm)

Figure 5-3. Spectra of the total polar pigment fraction from cell pellets of HB101 [pPL376], both inhibited and uninhibited, and HB101 [pHC79], recorded in dimethyl sulfoxide. Concentrations of pigments were normalized on the basis of equivalent dry weights of the bacterial cell pellets. The vertical hairline indicates the maximal absorption wavelength in the HB101 [pPL376] sample. Absorption maxima are given in Table 5-1.

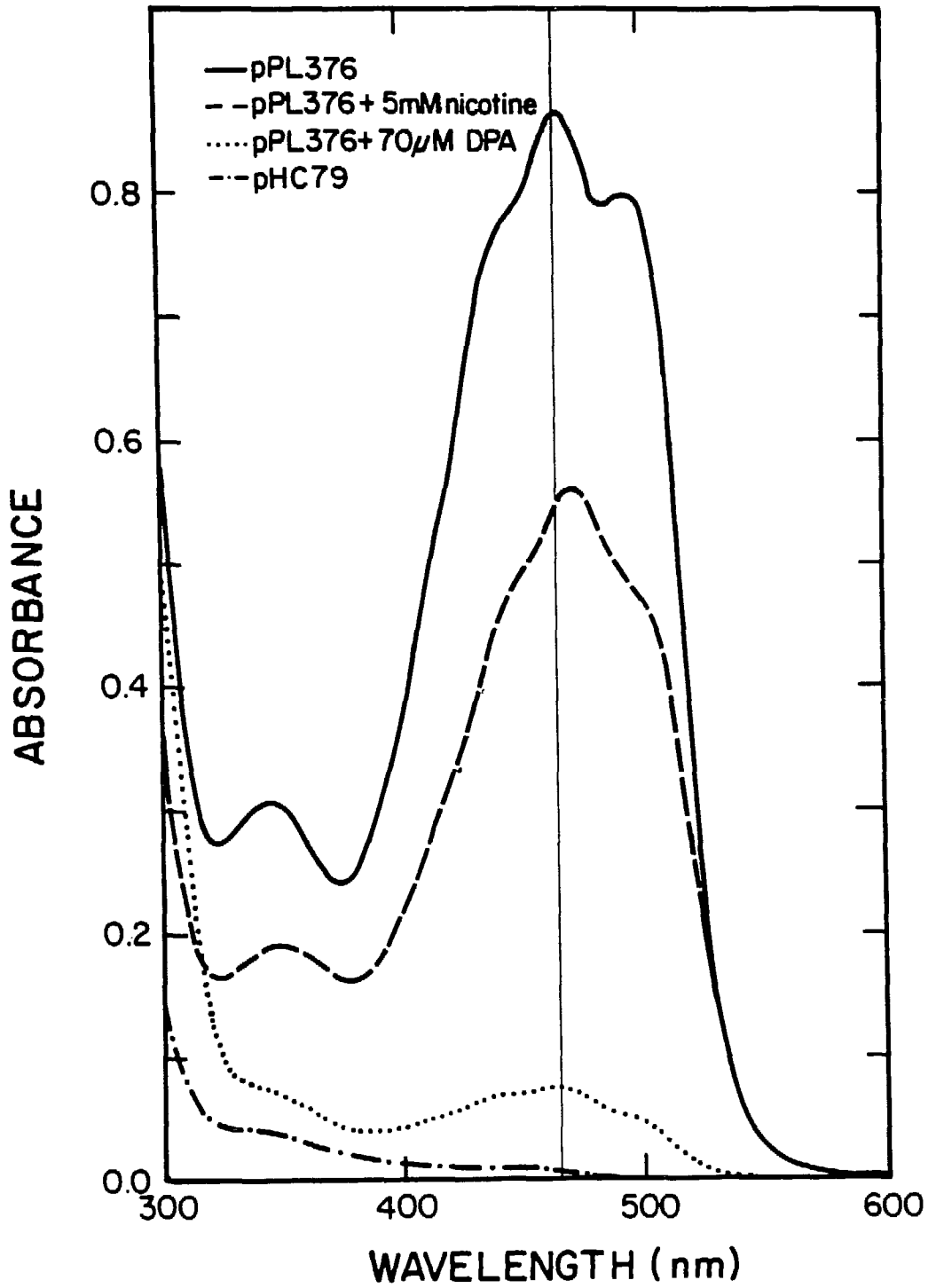
pPL376
pPL376 + 5mM nicotine
pPL376+70μM DPA
pHC79
ABSORBANCE
0.0
0.2
0.4
0.6
0.8
300
400
500
600
WAVELENGTH (nm)

Table 5-1. Visible absorption maxima and shoulders of polar and nonpolar pigment fractions

Sample	Inhibitor	Nonpolar pigment maxima (nm)[a]	Polar pigment maxima (nm)[b]
HB101 [pPL376]	-----	390, 420, 444, 472	440, 465, 494
HB101 [pPL376]	70 μM DPA	328, 344, 366, 394, 418, 462,	440, 464, 495
HB101 [pPL376]	5 mM nicotine	330, 345, 368, 395, 420, 434, 461, 491	446, 470, 503
HB101 [pHC79][c]	-----	no maxima	no maxima
γ-carotene[d]	-----	437, 462, 494	-----
α-carotene[d]	-----	422, 444, 473	-----

[a] in petroleum ether (Fig. 5-4)

[b] in dimethyl sulfoxide (Fig. 5-3)

[c] control plasmid containing the vector portion of pPL376 carrying no E. herbicola DNA

[d] from Britton (1985), maxima in petroleum ether

Figure 5-4. Spectra of the total nonpolar pigment fraction from cell pellets of HB101 [pPL376], both inhibited and uninhibited, and HB101 [pHC79], recorded in petroleum ether. Concentrations of pigments were normalized on the basis of equivalent dry weights of the bacterial cell pellets. The vertical hairline indicates the maximal absorption wavelength in the HB101 [pPL376] sample. Absorption maxima are given in Table 5-1.

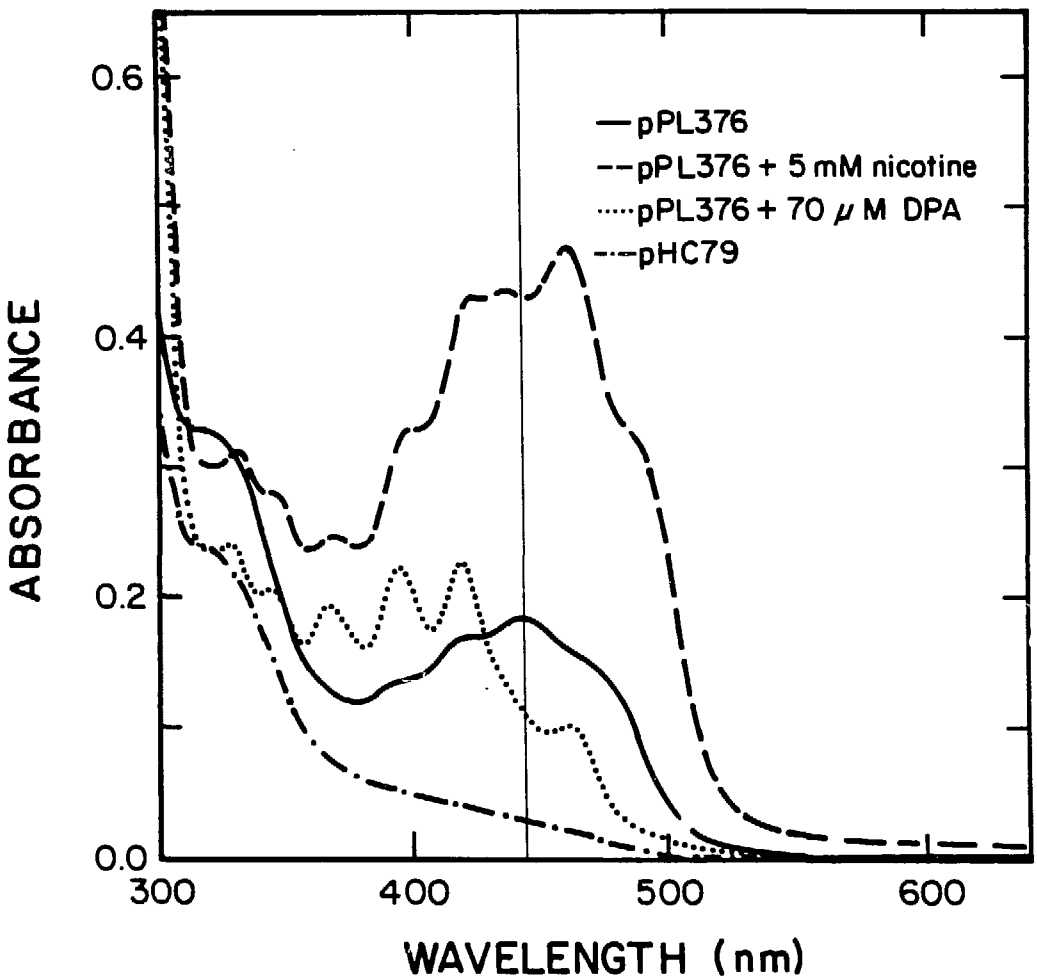
0.6
0.4
0.2
0.0
ABSORBANCE
300
400
500
600
WAVELENGTH (nm)
—pPL376
--pPL376 + 5 mM nicotine
·····pPL376 + 70 μ M DPA
-·-pHC79

Non-polar pigment extracts from both nicotine- and DPA-inhibited cultures showed large increases in absorption in the ultraviolet, indicated by the absorption shoulder visible at 300-305 nm (Fig. 5-4). The non-polar pigment fraction was further characterized by thin layer chromatography, followed by isolation of both visibly and UV absorbing pigment bands. Yellow pigment bands were apparent in extracts from untreated HB101 [pPL376] or inhibited samples, but too little material was obtained for further characterization. On the other hand, large amounts of UV-absorbing material showing a violet fluorescence were present in both inhibited extracts. Smaller amounts of this material were present in the untreated extract and no UV fluorescing material was visible in the control extract (HB101 [pHC79]). Phytoene is known to exhibit a characteristic violet fluorescence under UV (Britton, 1985). The purified UV absorbing pigment shows an absorbance spectrum (Fig. 5-5) identical to that of phytoene (Grumbach, 1983 (see Fig. 1-1); Britton, 1985; Giuliano et al., 1986).

HB101 [pPL376] was cultured in both the dark and the light to test whether light is required for pigment accumulation in E. coli. The pigmentation of either dark or light-grown HB101 [pPL376] cultures was qualitatively similar, indicating that light is not required for pigment accumulation, at least in the heterologous host.

Figure 5-5. Spectrum of purified phytoene in petroleum ether, isolated from DPA inhibited HB101 [pPL376] cells. A similar spectrum was obtained from a UV absorbing pigment purified from nicotine-inhibited HB101 [pPL376] cells (data not shown). The absorption maxima agree with literature values for phytoene in the same solvent (Britton, 1985).

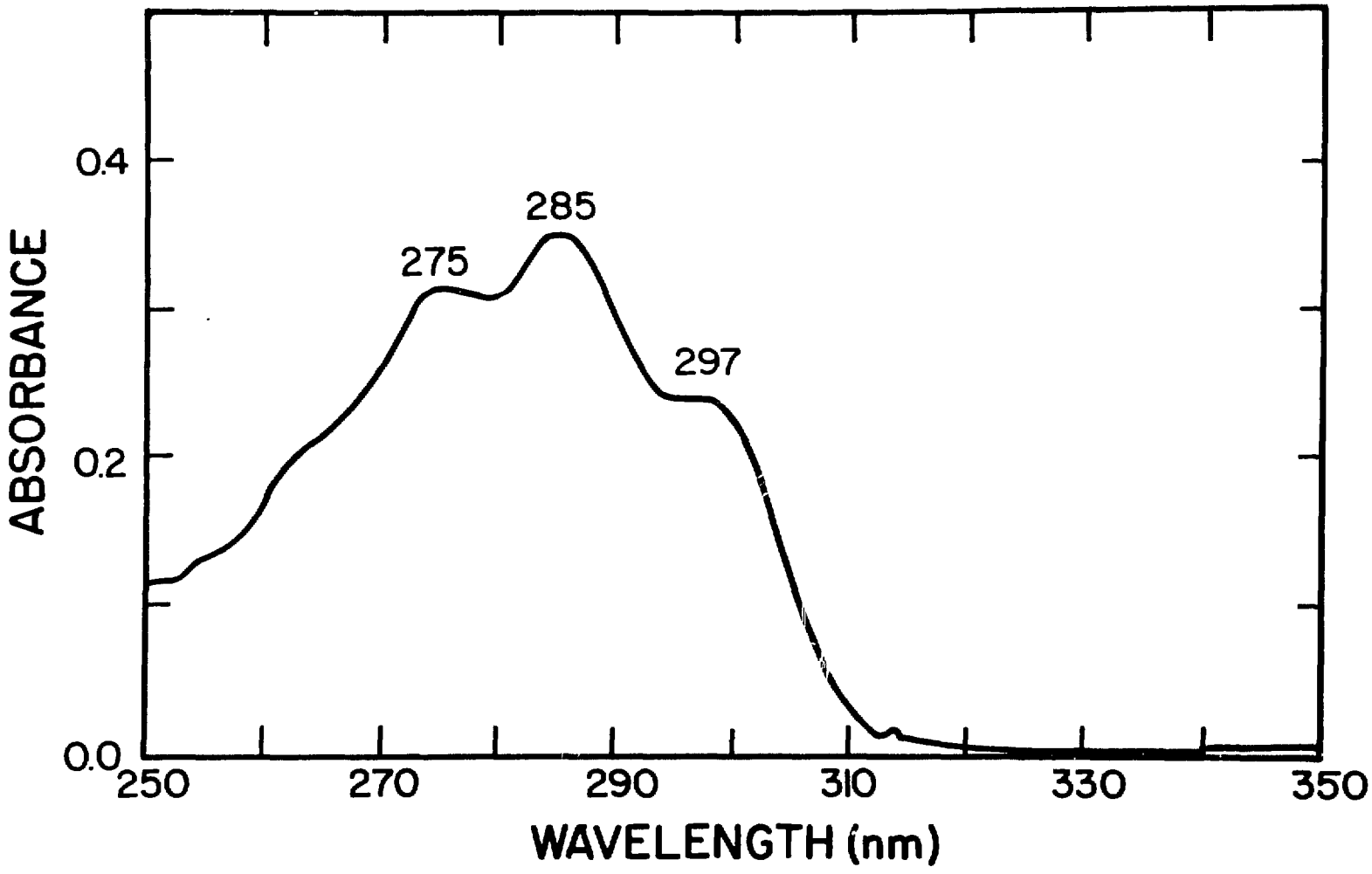
ABSORBANCE
0.4
0.2
0.0
285
275
297
250
270
290
310
330
350
WAVELENGTH (nm)

IV. Discussion

Tuveson et al. (1988) reported that the pigments extracted from HB101 [pPL376] with acetone:methanol (7:2) showed absorption maxima in this solvent mixture of 425, 453 and 478 nm due to a mixture of several yellow compounds, possibly xanthophylls, with β-carotene-like chromophores. Our observation of changes in pigmentation in cultures of E. coli containing the E. herbicola pigment genes cultured in the presence of two well characterized carotenoid biosynthesis inhibitors supports the proposal that the yellow pigmentation of E. herbicola arises from carotenoids. Furthermore, based on the predicted sites of action of the inhibitors, we have evidence that carotenoid biosynthesis in E. herbicola proceeds through the intermediate phytoene and probably involves a carotene cyclization reaction (Fig. 1-2), prior to xanthophyll formation.

Growth of HB101 [pPL376] in the presence of DPA led to a dramatic reduction in pigments present in the medium (Fig. 5-2), polar pigment accumulation in cells (Fig. 5-3), and a blue-shifting of absorption maxima for visibly absorbing nonpolar pigments accompanied by a large increase in the accumulation of UV absorbing pigments (Figs. 5-4, 5-5; Table 5-1). These results are consistent with the almost complete inhibition of phytoene dehydrogenation by DPA.

In the case of nicotine inhibition, although a small decrease in the accumulation of visibly absorbing pigments was observed, the most striking result was a red-shifting of the absorption maxima of pigments excreted into the growth medium (Fig. 5-2), and of the pigments accumulated in both the polar and non-polar pigment fractions (Figs. 5-3, 5-4, Table 5-1). These changes in the absorption spectra indicate that the action of nicotine inhibits a reaction which would shorten the effective length of the polyene chromophore of the pigments, an observation consistent with the inhibition of carotene cyclization (Fig. 1-2). Lycopene, for example, shows a red-shifted absorption spectrum in comparison to cyclic carotenes with the same number of conjugated double bonds (ie. γ-carotene and β-

carotene) (compare Figs. 1-1, 1-2 and Table 5-1). This effect arises from a shortening of the effective chromophore length in the latter compounds, due to steric hindrance and twisting of the rings (Britton, 1983). Lycopene also absorbs at longer wavelengths than do cyclic carotenes with fewer conjugated double bonds (ie. δ-carotene, ε-carotene and α-carotene) (Table 5-1, Fig. 1-2). The visibly absorbing pigments accumulated in the nicotine-inhibited samples remain to be identified. The major absorption maxima of the bulk nonpolar pigments from nicotine-inhibited and uninhibited cells do, however, closely resemble that of γ-carotene and α-carotene, respectively (Table 5-1).

Finally, the UV absorption spectrum obtained from a compound purified from DPA and nicotine-inhibited cultures (Fig. 5-5) matches that of phytoene purified from R. capsulatus crtI mutants (Giuliano et al., 1986) and is consistent with data given in the literature for phytoene (Grumbach, 1983; Britton, 1985). A mass spectrum of the compound purified from the DPA-inhibited E. coli cultures matches that of phytoene (Z. Ma, unpublished data). Thus, we have shown that E. coli HB101 carrying the E. herbicola pigment genes synthesizes carotenoids derived from the C_{40} compound phytoene.

E. coli does not normally synthesize carotenoids. As few carotenoprotein complexes which do not contain chlorophylls have been characterized in detail, it will be of interest to determine both the binding sites of the E. herbicola carotenoids accumulated inside E. coli cells and those released into the medium. A carotenoprotein complex containing spirilloxanthin bound to an 11 kDa polypeptide has been isolated from chromatophores of Rhodospirillum rubrum (Schwenker et al., 1973). A water soluble carotenoprotein complex binding about 44 molecules of carotenoid per homodimer has recently been isolated from the cyanobacterium Anacystis nidulans (Diverse-Pierluissi and Krogmann, 1988). Bullerjahn and Sherman (1986) have described a carotenoprotein complex found in cyanobacterial cytoplasmic membranes. Carotenoid glycosides are polar enough to be water soluble and are widely distributed among nonphotosynthetic bacteria and

cyanobacteria (Britton, 1983). Whether the carotenoids found in the growth medium of E. coli HB101 [pPL376] cultures are excreted as free pigments, such as carotenoid glycosides, or as pigment-protein complexes remains to be established.

Although light is required for the large scale synthesis of carotenoids in higher plants, certain fungi and nonphotosynthetic bacteria (reviewed in Bramley and Mackenzie, 1988), this is not the case for E. coli carrying the E. herbicola carotenoid genes. cAMP has been shown to be required for the accumulation of yellow pigments in HB101 [pPL376] and appears necessary for the expression of 84, 56 and 43 kDa polypeptides encoded by the E. herbicola carotenoid gene cluster (Perry et al., 1986). Interestingly, a negative correlation between cAMP content and carotenoid accumulation has been observed in the fungus Neurospora crassa (Kritsky et al., 1982). The determination of the DNA sequence of the E. herbicola carotenoid biosynthesis gene cluster will ultimately shed light not only on the structures of the gene products, but also on the nature of the regulatory signals encoded in the DNA.

The contrasting expression of E. herbicola (Perry et al., 1986) but not R. capsulatus (Marrs, 1981) carotenoid biosynthesis genes in an E. coli host is probably due to the degree of evolutionary divergence between R. capsulatus and E. coli (Fig. 1-7). Although two of the nine identified R. capsulatus carotenoid biosynthesis genes are preceded by possible E. coli-like σ^{70} promoter sequences (Fig. 3-9), the failure of the E. coli transcriptional machinery to recognize a single promoter for an early R. capsulatus carotenoid gene would be sufficient to prevent colored carotenoid synthesis. The production of the yellow carotenoids of E. herbicola in the E. coli host implies, on the other hand, a recognition of transcriptional initiation signals encoded in the E. herbicola DNA by the E. coli RNA polymerase. Pemberton and Harding (1987) have shown that transfer of a large piece of DNA containing all of the known R. sphaeroides carotenoid biosynthesis genes resulted in carotenoid production in several closely related species of nonphotosynthetic bacteria, including Agrobacterium tumifaciens and Paracoccus

denitrificans. These data support the view that the evolutionary distance between R. capsulatus and E. coli prevents the production of carotenoids in the latter species. It is interesting to note that in the three systems from which carotenoid biosynthesis genes have actually been isolated (R. capsulatus, R. sphaeroides, and E. herbicola) all of determinants known to be required for pigment synthesis are clustered. The functional significance of this observation is not known, although it might be a feature important for coregulation of these genes.

V. Summary

In summary, the E. herbicola carotenoid biosynthesis genes carried in E. coli provide an exceptionally well defined system for future biochemical and genetic studies of carotenoid biosynthesis in a nonphotosynthetic system. We have now identified phytoene, the first C_{40} carotenoid, as a compound present in HB101 [pPL376] cultures. The likely conservation between E. herbicola and R. capsulatus of at least the early portion of the carotenoid biosynthesis pathway up to phytoene suggests an obvious starting point for comparison of protein sequence similarities between these two organisms.

Chapter 6: Regulation of the carotenoid and other photosynthesis genes by oxygen and light in R. capsulatus

I. Introduction

The expression of individual carotenoid biosynthesis genes has not been previously studied in any organism, because neither gene sequences nor amino acid sequences of carotenoid biosynthetic enzymes have been available. Carotenogenesis is photoregulated in organisms as diverse as fungi, nonphotosynthetic bacteria, algae and higher plants (Harding and Shropshire, 1980; Bramley and Mackenzie, 1988). The regulation by oxygen and light of intracytoplasmic membrane, Bchl, carotenoid and pigment-protein complex synthesis in purple non-sulfur bacteria has been reviewed by Drews and Oelze (1981). The simultaneous elimination of oxygen and the illumination of a dark grown culture, or a downshift in light intensity under conditions of anaerobiosis stimulates carotenoid accumulation in cultures of Rhodobacter capsulatus (Golecki et al., 1980; Kaufmann et al., 1982) and in the closely related purple non-sulfur photosynthetic bacterium, R. sphaeroides (Cohen-Bazire et al., 1957). A decrease of oxygen tension in dark grown aerobic cultures produces a similar result in R. capsulatus (Schumacher and Drews, 1978; Biel and Marrs, 1985). Previous studies have, however, indicated little or no regulation of transcription of carotenoid biosynthesis (crt) genes in this organism during the shift from aerobic respiratory to anaerobic photosynthetic growth (Clark et al., 1984; Klug et al., 1985), and only small changes between steady-state photosynthetic and aerobic crt mRNA levels (Zhu and Hearst, 1986). The interpretation of these results is, however, complicated by the fact that gene specific probes were not used in these experiments (see Discussion). Recent S1 nuclease protection experiments show higher levels of the 5' ends of mRNAs mapped roughly to crtA, E and C in steady-state anaerobic

photosynthetic versus aerobic cultures illuminated at the same light intensity (Giuliano et al., 1988). Unfortunately, because illuminated aerobic cultures of purple photosynthetic bacteria may use both photosynthetic and respiratory growth modes simultaneously (Cohen-Bazire et al., 1957; Keister, 1978), the growth conditions of this experiment were not well defined. We recently determined the DNA sequence of a cluster of eight carotenoid genes from R. capsulatus (Chapter 3). We report here the first detailed studies of carotenoid gene regulation by oxygen and light using gene specific probes for all eight carotenoid genes and two flanking open reading frames (ORFs), which may be Bchl biosynthesis (bch) genes (Figs. 1-4, 3-7).

II. Materials and methods

Growth and cultivation of bacterial strains

R. capsulatus wildtype strain SB1003 (Yen and Marrs, 1976) was used for growth shift experiments described below. SB1003 was grown in 150 ml of RCV minimal medium (Weaver et al., 1975) in a 250 ml side-arm flask at 32ºC. Chemoheterotrophic aerobic cultures were sparged in the dark in foil covered flasks with a mixture of N_2:O_2:CO_2 (80:20:2). Photosynthetic cultures were illuminated at 15 W/m^2 by a bank of Lumiline lamps (General Electric) and sparged with a mixture of N_2:CO_2 (80:2). Gas flow and composition were controlled using a Matheson Gas Products Multiple Dyna-blender, Model 8219. Growth rates were monitored at 680 nm on a Bausch and Lomb Spectronic 21 colorimeter. At time zero of the growth shift experiments the gas mixture was changed, eliminating O_2 from the sparged medium. In a separate experiment to determine the effect of light on gene expression during the transition from anaerobic to anaerobic growth, duplicate cultures were simultaneously switched from the aerobic to the anaerobic gas mixture as noted above, with one culture exposed to the light at the time of the shift.

Collection of time points and isolation of RNA

Cells from the growth shift experiments were collected at various times by removal of a 6 ml aliquot of the culture. Cells were immediately mixed with an equal volume of ice cold buffer A (80 mM Tris-chloride, pH 7.5, 10 mM $MgCl_2$) containing 200 µg/ml chloramphenicol, 25 mM sodium azide and 10 mM β-mercaptoethanol (Zhu and Kaplan, 1985), cooled for 15 seconds in a dry ice-ethanol bath, and dispensed into 1.5 ml Eppendorf tubes. Samples were centrifuged for 2 minutes, the medium aspirated, and the pellets resuspended in RNA lysis buffer containing proteinase K. Time points were frozen on dry ice and stored at -70ºC until isolation of the RNA. The entire procedure required about 8 minutes for each time point. RNA was extracted using a scaled-down

version of the Zhu and Kaplan (1985) procedure designed for 6 ml of cell culture.

Preparation of RNA dot blots, M13 probes, and nucleic acid hybridizations

Equal amounts of purified RNA, 5 μg per time point, were spotted onto a Gene Screen nylon membrane (New England Nuclear Corp.) using a Minifold dot blot apparatus (Schleicher and Schuell), following the procedure of Schloss et al. (1984). These samples were probed for mRNAs as described below. In order to normalize results from hybridizations for mRNAs, we prepared dot blots using about 3 ng of total RNA per time point and hybridized these with either pRC1 (courtesy G. Drews), containing cloned R. capsulatus rRNA genes (Yu et al., 1982), or with total R. capsulatus chromosomal DNA. The dot blot time courses were probed with M13 subclones labelled by primer extension across the insert region with the Klenow enzyme. Because only one strand of the M13 phage was labelled by this procedure it was possible to confirm the predicted transcriptional orientations of the crt genes and the ORFs by hybridization. Labelling reactions were performed as described in (Chapter 4) except that reactions were carried out using 50 μCi 5'-[α-^{32}P]dCTP (3000 Ci/mmol). Gene-specific M13 probes which hybridize to puf, or puh transcripts are described in Chapter 2 (Materials and methods) and were generated during the sequencing of these genes (Youvan et al., 1984a). M13 probes for the crt genes, ORF J and ORF H were generated during the sequencing of these regions (Chapter 3) and their locations are shown in Fig. 6-5. All M13 probes were specific for the coding region of a single gene. The probe for the R. capsulatus fbc operon, which encodes the cytochrome bc_1 complex (Gabellini and Sebald, 1986), was plasmid pDC100 (courtesy of D. Cook), derived from pRSF1 (courtesy of N. Gabellini) by deletion of those BamHI fragments not encoding the fbc genes. pDC100 and pRC1 were labelled with 50 μCi [α-^{32}P]dCTP (3000 Ci/mmol) by nick-translation using a Bethesda Research Laboratories kit. RNA dot blot hybridizations were carried out using standards techniques and the dots quantitated by scintillation counting as described in

Chapter 2. In cases where hybridization signals were very weak, as for the crtC and crtD probes, autoradiograms were also quantitated by densitometry using a Hoefer Scientific Instruments scanning densitometer, Model GS 300. Raw hybridization data for all probes were normalized by dividing by the hybridization obtained with pRC1 as the internal control in order to determine the relative levels of gene expression. Similar results were obtained using total chromosomal DNA as the normalization probe. The original dot hybridizations are shown in the autoradiograms in Figs. 6-1, 6-2, 6-3 and 6-4, while normalized data for selected probes is plotted in the former two figures.

III. Results

A. Expression of the carotenoid biosynthesis genes, ORF J and ORF H, in response to a reduction of the oxygen tension in the presence of light

Dot blots (Figs. 6-1, 6-2, 6-3) show mRNA accumulation from the crt genes, the puf (RC-L, RC-M) and puh (RC-H) operons, and ORF J and ORF H during the shift from dark aerobic (respiratory) to light anaerobic (photosynthetic) growth. Dots prior to the shift show a constant level of expression for all probes tested. During the first hour of the shift, cellular growth ceases (Fig. 6-1A) as cells prepare to resume growth under photosynthetic conditions. Fig. 6-1B shows the approximately 6 to 8-fold induction of mRNAs from the puf and puh operons, which encode the RC and LH-I structural photosynthetic polypeptides, with the maximal mRNA accumulation occurring about 90 minutes post-shift. The crt genes (Figs. 6-2, 6-3) fall into three classes, depending on their response to this change in environmental conditions. crtA, crtK, crtE, crtF and ORF H are strongly induced (5 to 10-fold), crtC, crtD and ORF J are moderately induced (2 to 5-fold), while crtB and crtI are uninduced during the entire time course. All of the induced crt genes and the ORFs show peak mRNA accumulation about 45 to 60 minutes after the removal of oxygen from the medium. Thus, the crtA, C, D, E, F, K genes, and ORFs J and H are coordinately expressed during the adaptation to photosynthetic growth, although the levels of gene induction range from 2 to 10-fold (summarized in Fig. 6-5). The fbc operon, which encodes the subunits of the cytochrome bc_1 electron transport complex, was not induced during the duration of the shift (Fig. 6-1A). The cytochrome bc_1 complex is present during both dark aerobic and photosynthetic growth.

B. Effect of light on the expression of an inducible carotenoid gene

Accumulation of carotenoids depends on light in many photosynthetic and nonphotosynthetic organisms (Harding and Shropshire, 1980; Bramley and Mackenzie,

Figure 6-1 A-C. Growth of R. capsulatus strain SB1003 during the shift from dark aerobic growth to anaerobic photosynthetic growth, and expression of genes encoding the RC (pufLM and puhA) and cytochrome bc_1 (fbc) complexes during the shift. At time zero the cultures were shifted from dark aerobic growth to anaerobic photosynthetic growth (indicated by arrows). Cell division ceased for about one hour, as shown in (**A**) for two separate cultures (open diamonds and black circles) shifted at different initial cell densities. Normalized mRNA levels, relative to an arbitrary value of one at time zero of the shift, are plotted in (**B**) using probes for pufLM (black diamonds), puhA (open squares) and the fbc operon (open diamonds). The actual dot hybridizations, shown in (**C**), were normalized by comparison to the hybridization obtained using an rRNA probe (Fig. 6-3). The accumulation of puhA and pufLM mRNAs peaks about 90 minutes subsequent to the shift and shows a 6 to 8-fold induction over the pre-shift levels. Similar results were obtained using a probe for pufA, encoding the LH-I α subunit (data not shown). fbc mRNA is expressed constitutively during the course of the experiment. Note that the level of expression of all genes prior to the shift remains essentially constant. Autoradiogram exposure times vary depending on the probe used. Collection of time point samples was performed with the technical assistance of D. Cook (U. of California, Berkeley). This figure is taken from Cook et al., submitted.

A

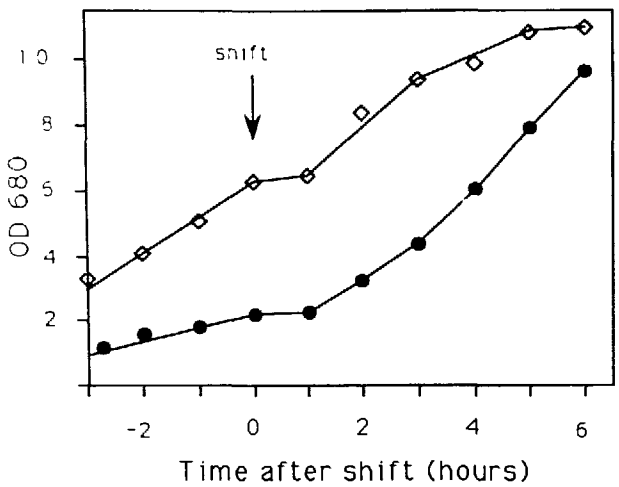
shift
OD 680
10
8
6
4
2
-2
0
2
4
6
Time after shift (hours)

B

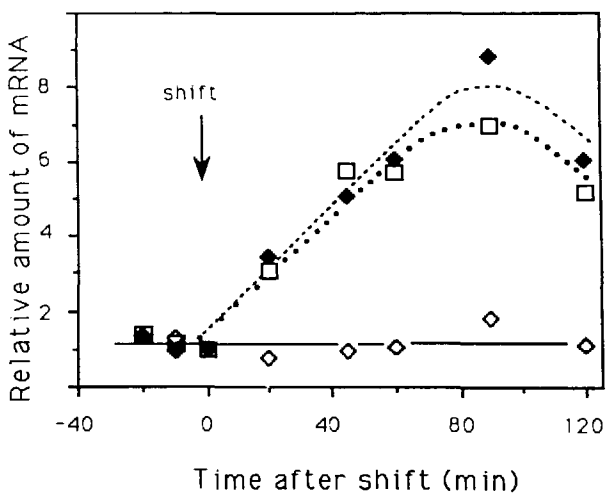
shift
Relative amount of mRNA
8
6
4
2
-40
0
40
80
120
Time after shift (min)

C

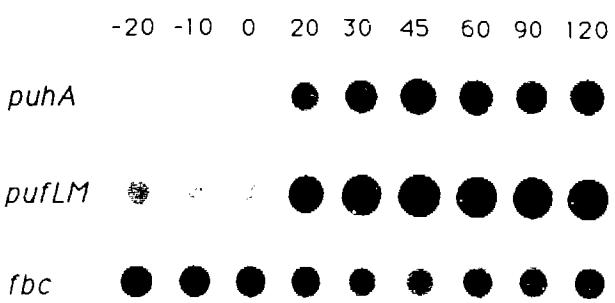
-20 -10 0 20 30 45 60 90 120
puhA
pufLM
fbc

Figure 6-2 A, B. Dot blot time courses showing the expression patterns of examples of inducible and constitutive crt genes. crtA (open squares) and crtI (black squares) gene expression during the time course of the growth shift is plotted in (**A**), normalized as described in Fig. 6-1. The actual dot hybridizations with probes to these genes are shown in (**B**). The probe for crtI was BSa6 (Fig. 6-5). A similar hybridization pattern was obtained using probe HH121 for crtI (data not shown). Although crtI is expressed constitutively during the shift, crtA expression increases approximately 9-fold during the same period, with maximal expression peaking at 45 to 60 minutes post-shift.

A

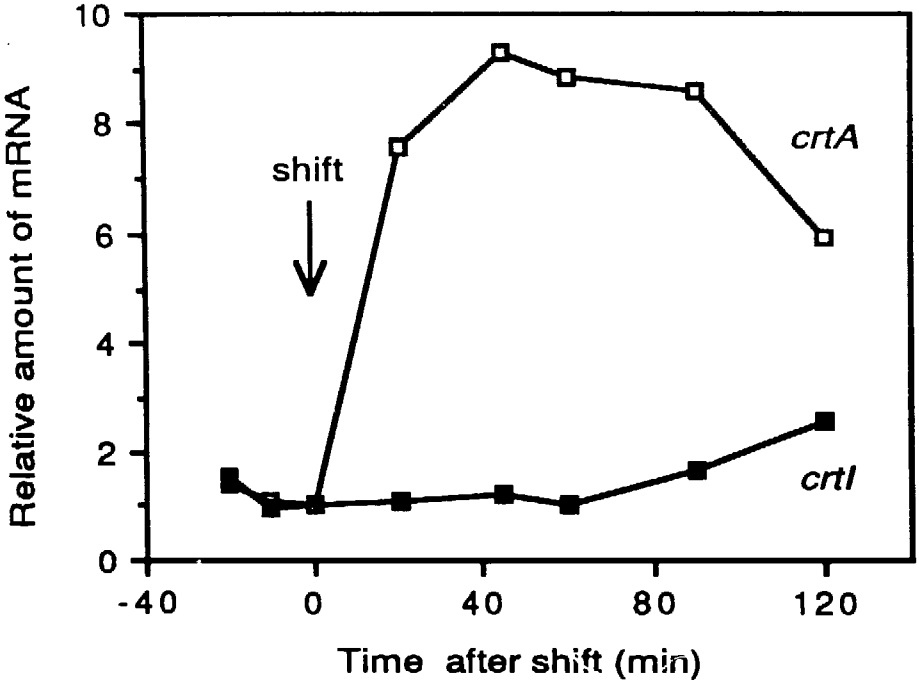
Relative amount of mRNA
10
8
6
4
2
0
shift
crtA
crtI
-40
0
40
80
120
Time after shift (min)

B

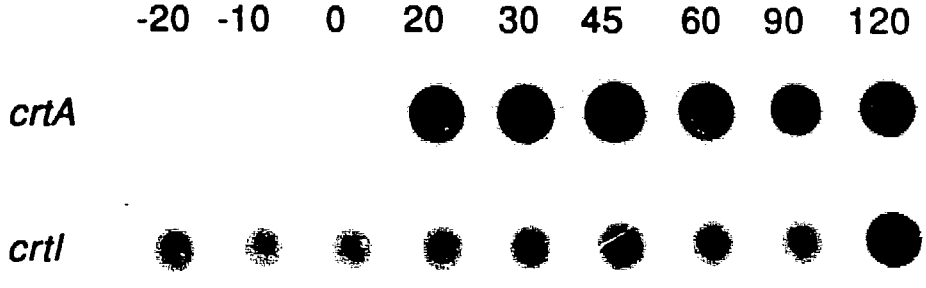
-20 -10 0 20 30 45 60 90 120
crtA
crtI

Figure 6-3 A, B. Dot blot time courses of the expression of crtB, C, B, E, F, K , ORF J and ORF H during the shift from dark aerobic growth to anaerobic photosynthetic growth. Results from these dot blot hybridizations and Fig. 6-2 show that the crt genes and the ORFs fall into three classes, strongly induced (5 to 10-fold), moderately induced (2 to 5-fold) and constitutively expressed. mRNA induction was estimated by scintillation counting of the dots, combined with densitometry of the autoradiograms in the cases of the weak hybridizations with the crtC, crtD and ORF H probes. (**A**) shows that crtE, crtF, crtK and ORF H are strongly induced, while crtC, crtD, crtF and ORF J are moderately induced, and crtB remains uninduced. All inducible genes show a maximal mRNA accumulation between 45 to 60 minutes post-shift. The intensity of the hybridization in the 120 minute time point is exaggerated due to either to underestimation of the RNA concentration, or to a small constant amount of contaminating DNA, not detected on ethidium bromide stained agarose gels of the RNA stocks following DNAse treatment during the RNA purification. Although autoradiogram exposure times vary depending on the probe used, crtK, crtB, crtD and crtC blots were exposed for the same amount of time, as were crtE and crtF blots. The intensities of hybridization for individual probes are functions of the autoradiogram exposure time, the length of the DNA probe, and the amount of hybridizing mRNA. (**B**) shows the hybridization to rRNA or total RNA during the time course of the shift experiment.

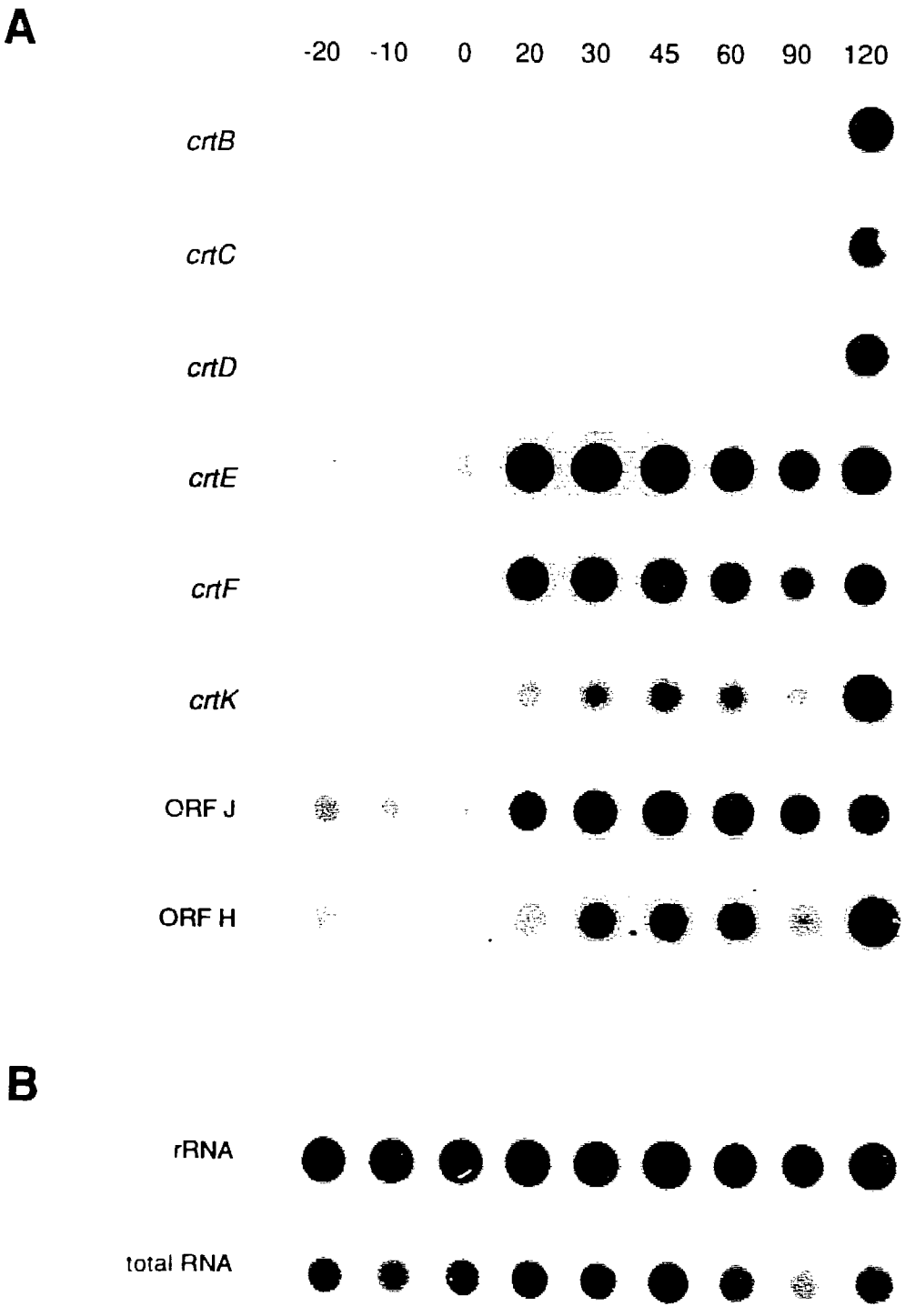
A
-20
-10
0
20
30
45
60
90
120
crtB
crtC
crtD
crtE
crtF
crtK
ORF J
ORF H
B
rRNA
total RNA

1988). Carotenoid accumulation in R. capsulatus can, on the other hand, be stimulated by a downshift in the oxygen tension in dark grown cultures (Schumacher and Drews, 1978; Biel and Marrs, 1985). Nevertheless, in order to explore the untested possibility that the R. capsulatus crt genes are transcriptionally regulated in response to light we performed the following experiment. We examined crt gene expression during the shift from dark aerobic to either dark anaerobic or anaerobic photosynthetic conditions using the crtA gene as an example. In both shift experiments, crtA mRNA levels reached a maximum 30 to 60 minutes post-shift. Cells shifted in the presence of light showed roughly a 10-fold mRNA induction, while those shifted in the absence of light showed about a 5-fold induction. These experiments demonstrate that a reduction in the oxygen tension, independent of the presence of light, is qualitatively sufficient for the induction of the crtA gene (Fig. 6-4).

Figure 6-4. Expression of the crtA gene during a shift from dark aerobic growth to anaerobisis in the presence or absence of light. The kinetics of crtA mRNA induction are similar whether or not light is present after time zero of the shift, although there is approximately a 2-fold greater level of induction in the light (10-fold versus 5-fold).

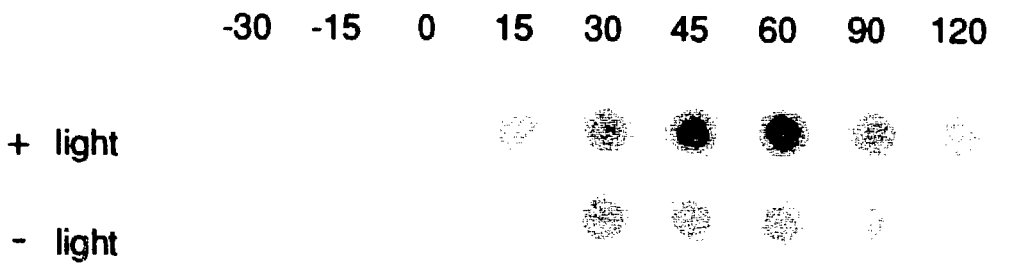
-30
-15
0
15
30
45
60
90
120
+ light
- light

IV. Discussion

A. Regulation of carotenoid gene expression in comparison to the genes encoding the RC and LH-I complexes

Several earlier studies with R. capsulatus indicated little or no regulation of the transcription of carotenoid biosynthesis genes. Thus, our result that six of the eight crt genes, crtA, C, D, E, F and K, are induced by a factor of 2-10 during the onset of photosynthetic growth was unexpected (Fig. 6-5). Several caveats must be made, however, in the comparison of this work with previous studies. First, shift and steady-state measurements of mRNA levels by Clark et al. (1984), Klug et al. (1985), Zhu and Hearst (1986) and Zhu et al. (1986) monitored the expression of crt genes using DNA probes containing several genes. Thus, any conclusion reached about the level of crt gene induction would reflect some average of mRNA accumulated by both induced and uninduced crt genes, weighted by the relative abundances of the specific mRNAs. This may account for some of the differences in levels of crt gene expression between our results and the previous studies. Second, in none of these experiments was a shift done to rigorously anaerobic conditions (0% O_2), thus complicating a direct comparison between our results and previous studies. With these cautions in mind, Clark et al. (1984) found no increase in mRNA accumulation for carotenoid biosynthesis genes during a reduction of oxygen tension in the medium which caused a 40-fold increase in puf operon mRNA. Klug et al. (1985), using experimental conditions similar to those of Clark et al. (1984), measured approximately a 16-fold increase in puf operon mRNA, but found only a 2-fold increase in expression of carotenoid biosynthesis genes. Zhu and Hearst (1986) found no more than 2-fold differences in expression of carotenoid genes between steady-state cultures grown under high versus low light, or high versus low oxygen tension, for all but one of the probes used. Although the argument was made that crt genes were upregulated by increases in oxygen tension or light intensity, possibly as part of a photooxidative

Figure 6-5. Map of the R. capsulatus carotenoid biosynthesis gene cluster. Orientations of the genes and ORFs are as indicated. The scale at the bottom shows the nucleotide positions of the translational starts and stops for the genes (vertical numbers), as well as the locations of BamHI restriction sites denoted by (B). The ORFs extend into the flanking regions (indicated by the detached arrowheads). Gene-specific single-stranded M13 probes used to detect crt mRNAs are indicated above the genes, with arrows showing the direction of the synthesized probe and the length of the M13 insert. The locations of the M13 probes used are as follows: SpSa25 (ORF H), 227-569; TT93 (crtA), 1863-2194; HH121 (crtI), 2755-2915; BSa6 (crtI), 3302-3908; XSp54 (crtB), 5008-5176; E*Sa90 (crtK), 5584-5650; SS110 (crtC), 6204-6409; EB96 (crtD), 7311-7776; TB4 (crtE), 8588-8818, SS41 (crtF), 9334-9600; XX6 (ORF J), 10752-10843. The summarized pattern of gene regulation during the shift to anaerobic photosynthetic growth is indicated by shading of the genes and ORFs: black, 5 to 10-fold induction; gray, 2 to 5-fold induction; white, no induction. Black circles indicate sites for binding of a putative transcriptional regulator. The BamHI fragments of the photosynthesis gene cluster shown here are, from left to right, the BamHI-H, -G, -M and -J.

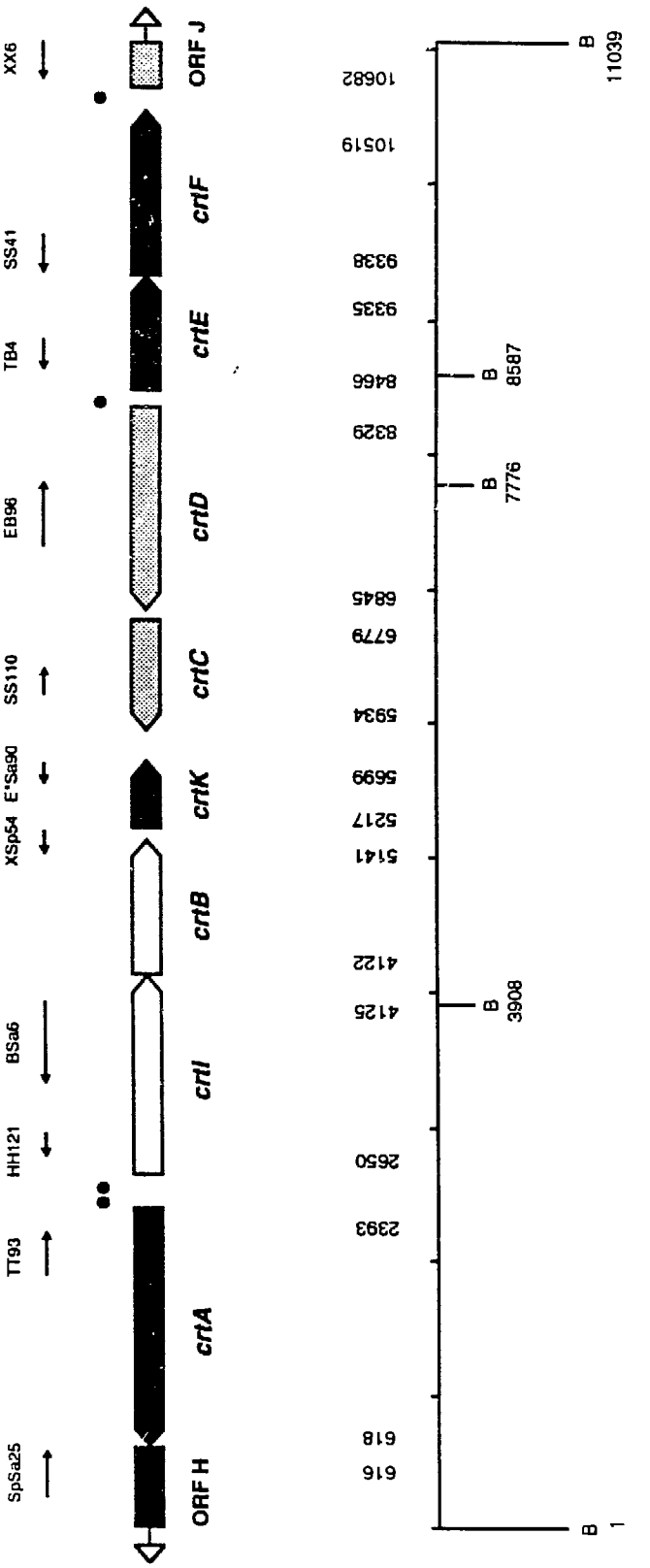
SpSa25
TT93
HH121
BSa6
XSp54
E*Sa90
SS110
EB96
TB4
SS41
XX6
ORF H
crtA
crtI
crtB
crtK
crtC
crtD
crtE
crtF
ORF J
B
1
616
618
2393
2650
4125
4122
5141
5217
5699
5934
6779
6845
7776
8329
8466
8587
9335
9338
10519
10682
11039
3908

protection mechanism (Zhu and Hearst, 1986; Zhu et al., 1986), the small changes in gene expression observed in these studies suggested that the transcription of the R. capsulatus crt genes, in contrast to the that of the puf operon, was not highly regulated either by light or by oxygen tension.

It has also been suggested that oxygen does not directly regulate the biosynthesis of carotenoids based on measurements of carotenoid accumulation in Bchl$^-$ mutants and the R. capsulatus wildtype grown under steady-state high and low oxygen tensions and in a shift experiment (Biel and Marrs, 1985). Carotenoid accumulation in the wildtype was about 3-fold greater in steady-state cultures grown in low rather than high oxygen tension, while Bchl$^-$ mutants showed less than 2-fold increases in carotenoid content. Similarly, the increase in rate of carotenoid synthesis upon reduction of the oxygen tension in the medium was substantially reduced in a Bchl$^-$ strain. These differences in carotenoid accumulation were proposed to be the consequence of a requirement for the synthesis of Bchl or some other photosynthetic component, rather than a direct effect of oxygen. It was argued that no evidence for enhanced carotenoid turnover in the absence of the pigment-protein complexes exists in R. capsulatus (Scolnik and Marrs, 1987), although there is thought to be substantial carotenoid turnover in mature chloroplasts (Bramley and Mackenzie, 1988). The erroneous inference was drawn from the results of Biel and Marrs (1985) that the carotenoid biosynthetic genes are not regulated (Giuliano et al., 1986). The former study did not, however, directly examine expression of crt genes.

Our data clearly indicate a coordinated regulation of mRNA accumulation for five crt genes, occurring either at the level of transcription initiation or mRNA stability. Induction of crt gene expression requires a reduction of oxygen tension, but is qualitatively independent of light, at least in the case of the strongly induced crtA gene (Fig. 6-4). Whether oxygen itself is the direct signal for gene induction will be discussed later. Our results are not, however, necessarily in conflict with the model of Biel and Marrs (1985), as these authors examined only carotenoid pigment accumulation and not gene expression.

Recent results have suggested that the steady-state levels of the 5' ends of crtC, crtA and crtE mRNAs are higher under anaerobic versus aerobic conditions using constant illumination, while the level of crtI 5' mRNA ends was not (Giuliano et al., 1988). Under aerobic conditions plus light, however, R. capsulatus may be using photosynthetic and respiratory growth modes simultaneously (Cohen-Bazire et al., 1957; Keister, 1978), making these growth conditions poorly defined for a study of crt gene expression. Despite this potential complication, our data from the growth shift experiments agree with the qualitative results of Giuliano et al. (1988), although we did not follow the expression of the crt genes beyond two hours post-shift, at which point steady-state mRNA levels had not yet been reached.

The most striking contrast between our results and the previous literature comes in the comparison of the level of induction of RC and LH-I mRNAs (pufL, pufA, puhA) with that of the carotenoid genes. The 5 to 10-fold magnitude of induction of mRNA for crtA, E, F and K reported here matches that observed for the puf, and puh operons (6 to 8-fold) during the same shift experiment under our growth conditions (Figs. 6-1, 6-2, 6-3). These results contrast sharply with the large increases in puf operon mRNA accumulation reported by Clark et al. (1984) and Klug et al. (1985), versus the low level or lack of induction of mRNA for the crt genes. This discrepancy may be due to variation in the experimental techniques or growth conditions used, or could alternatively be an artifact of the failure to use gene-specific probes for the crt mRNAs in the previous studies.

B. crtB and crtK mRNA accumulation is not coordinated

We recently offered as a possibility that a crtIBK operon might exist based on the organization of these genes (Chapter 3). More recent evidence indicates that crtI and crtB are probably not cotranscribed because of the phenotype of a polar insertion in crtI (Chapter 4). The observation made here that crtK is strongly upregulated during the shift from aerobic to photosynthetic growth, while crtI and crtB are not, suggests that crtK and

crtB also form two distinct operons. An alternative explanation would be the differential regulation of mRNA stability between two portions of the same transcript as in the case of the puf operon (Chen et al., 1988; Adams et al., 1989). Nevertheless, we favor the interpretation that crtB and crtK are not cotranscribed. Thus, of the eight crt genes and two flanking ORFs shown in Fig. 6-5, all of them, with the possible exception of crtE and crtF, form monocistronic operons.

C. Regulation and possible functions of ORF J and ORF H

Both ORF J and ORF H are upregulated in analogous fashion to the crt genes during the time course of our shift to photosynthetic growth. We have suggested that these ORFs may be required for Bchl biosynthesis (Chapters 3, 4), and we discuss further evidence here. The 5' end of ORF J is located in the BamHI-J fragment of pRPS404, and the ORF extends 586 bp into the adjacent BamHI-C fragment (Figs. 2-3C, 6-5) before reaching a translational termination codon (M. Alberti, unpublished data). Taylor et al. (1983) used marker-rescue techniques to map the bchC Bchl biosynthesis gene roughly to this region. One bchC point mutation was not complemented by a clone containing the BamHI-J, but could be rescued by recombination with this fragment. These data indicated that part but not all of the bchC gene was probably carried on the BamHI-J fragment. Most point mutations genetically mapped to bchC have a BchC$^-$ phenotype, but one mutant has a BchA$^-$ phenotype indicating a polar effect on the bchA gene and suggesting that bchCA form an operon (Biel and Marrs, 1983). These authors have determined by lacZ (β-galactosidase) gene fusions that bchB, bchC, bchG and bchH (see Figs. 1-4, 1-6) are upregulated 2 to 3-fold under low versus high oxygen tensions. Giuliano et al. (1988) have recently observed that an interposon insertion 3' to crtF, now known to lie within the 5' coding region of ORF J (Chapter 3), produces a BchA$^-$ phenotype. We have shown a 3-fold induction of ORF J mRNA during the shift to photosynthetic growth (Fig. 6-3). All of these data are consistent with the hypothesis that ORF J encodes either BchC or a

gene product required for BchC expression and that bchCA form an operon. At the opposite end of the crt gene cluster (Fig. 6-5), ORF H is also upregulated about 6-fold during the shift to photosynthetic growth conditions (Fig. 6-3). Data from our laboratory (Chapters 3, 4; Zsebo and Hearst, 1984; M. Alberti, unpublished data) and the data of Giuliano et al. (1988) suggest that ORF H corresponds to either bchD or bchI, or encodes a gene product required for the expression of one of these genes.

D. Constitutively expressed mRNAs and rRNA

We have shown that the fbc operon is not induced during the shift from aerobic to photosynthetic growth described here (Fig. 6-1B, C) and hence provides a valuable constitutively expressed control gene. crtI and crtB are also constitutively expressed during this shift. These genes may be useful as internal controls in future experiments.

The amounts of total RNA used in dot blots of the growth shift time course experiments were normalized by hybridization with an R. capsulatus rRNA probe, pRC1 (Yu et al., 1982). Normalization by hybridization using total DNA as a probe also gave the same results (data not shown). This was expected because rRNA accounts for the vast majority of total cellular RNA (Scolnik and Marrs, 1987). Dark grown chemoheterotrophic R. capsulatus cultures shifted to low oxygen tension, which induces the synthesis of the photosynthetic apparatus, have been claimed to increase their rRNA content 7-fold during the first 140 minutes of the shift (Klug et al., 1984). Cellular growth was negligible during this period. We have not observed an appreciable increase in total RNA isolated on a per cell basis during the time course of our growth shift experiments (data not shown). In fact, if an increase in rRNA were actually occurring, one would have to argue that the fbc , crtI and crtB mRNAs must also be coordinately induced with the rRNA genes in order to account for the apparently constitutive expression pattern observed for these mRNAs (Cook et al., submitted; Figs. 6-1, 6-2, 6-3). Our results are in agreement with the work of Gray (1967) who showed that cultures of R.

sphaeroides shifted from dark aerobic to photosynthetic anaerobic growth underwent a 90 minute adaptation phase during which there were no net increases in cell number, cell mass, total RNA, DNA or cellular protein content. Specifically induced mRNAs, such as those encoded by the crt, puf or puh operons, do not contribute significantly to total RNA content due to the molar excess of rRNA.

E. Rationale for the coordinate induction of crt genes during the adaptation to photosynthetic growth

A linkage between the induction of certain crt genes and the puf, puh and puc operons can be rationalized in the following manner. Each of these operons encode gene products which are structural polypeptides of the photosynthetic apparatus and which bind both carotenoid and Bchl pigment cofactors. The normal molar stoichiometry of Bchl specific to LH-II and LH-I per RC complex is approximately 80-40:20:1 (Drews, 1985). Under our growth conditions LH-II is both the predominant pigment-protein complex and carotenoid binding site in the photosynthetic membrane (see Chapter 2). An intriguing possibility is that the same transcriptional factor postulated in Chapter 3 may regulate transcription of both the pucBA and certain crt operons (Fig. 3-10), thereby balancing the levels of LH-II complex with the supply of carotenoid biosynthetic enzymes. A similar rationale could be used to explain the induction of genes encoding Bchl biosynthetic enzymes (possibly ORF J and ORF H). The shift from chemoheterotrophic to photosynthetic metabolism (Fig. 6-1A), causes cell division of R. capsulatus cultures to cease for roughly a one hour period before the resumption of cellular growth. During this lag, the cells must adapt to a photosynthetic lifestyle by the synthesis of carotenoids, Bchl, pigment-binding polypeptides and an intracytoplasmic membrane system containing these components (Drews and Oelze, 1981). Previous results indicating a rapid increase in the rates of carotenoid and Bchl synthesis during the lag in resumption of cellular growth were originally obtained in the classic study of Cohen-Bazire et al. (1957) in R. sphaeroides,

and subsequently by Schumacher and Drews (1978) in R. capsulatus. We have shown that crtA, E, F and K genes and ORF H are strongly induced, the crtC, D and ORF J genes are moderately induced, and the crtB and I genes are expressed constitutively. One mechanism for a rapid and transient increase in carotenoid production to meet the demands of the cell would be to induce those crt genes encoding enzymes governing rate-limiting biosynthetic reactions. Additional post-transcriptional mechanisms may also regulate carotenogenesis in Rhodobacter, thus allowing the induction of the carotenoid biosynthetic activities which are not controlled at the level of transcription.

In the shift experiment described here mRNAs for the puf and puh operons were induced 6 to 8-fold and accumulated to a maximum level about 90 minutes subsequent to removal of oxygen from the medium. All of the induced crt genes and the ORFs reached the pinnacle of induction about 45 to 60 minutes after the shift. This result may indicate a sequential expression of genes involved in photosynthetic pigment synthesis, followed by the genes encoding the pigment-binding polypeptides. The motivation for such an expression pattern is clear since the stable assembly of the pigment-protein complexes depends in most cases on the presence of all of the individual components (Zsebo and Hearst, 1984; Tadros et al., 1984; Klug et al., 1985; Klug et al., 1986; Chapter 2). It will be of interest to determine the expression pattern of the puc operon (LH-II) mRNA during the growth shift time course. Klug et al. (1985) have previously followed the expression of the genes encoding the RC, LH-I, and LH-II complexes during a reduction of oxygen tension in dark grown cultures. They observed the sequential expression and assembly of the RC plus LH-I, followed by LH-II. Our data extends the model for sequential expression to photosynthetic pigment synthesis genes. Because mRNA for these genes is already substantially induced 15-20 minutes after the shift (Fig. 6-2, 6-3, 6-4), the regulatory factors governing gene expression must act very rapidly in response to the lowering of oxygen tension.

In R. sphaeroides, Cohen-Bazire et al. (1957) reported that introduction of oxygen

into a continuously illuminated anaerobic culture was sufficient to cause the cessation of carotenoid synthesis, while Schumacher and Drews (1978) showed that a reduction of oxygen tension in dark grown R. capsulatus cultures led to an increase in the rate of carotenoid synthesis. These results indicate that light is not absolutely required for carotenoid synthesis and also does not substantially modify the regulation by oxygen tension. Whether light influences the expression of crt genes has not been previously addressed with gene-specific probes. Our results following the expression of the crtA gene during growth shifts from either dark aerobic to dark anaerobic or photosynthetic anaerobic growth demonstrate for the first time that light is not required for the qualitative induction of crt gene expression in photosynthetic bacteria. Recent studies using inhibitors of transcription and translation in the fungus Aspergillus giganteus suggest that certain carotenoid enzyme activities are photoinduced and that transcription is required for this process (El-Jack et al., 1988). A similar conclusion has been reached in studies of the nonphotosynthetic bacterium Myxococcus xanthus, using chromosomal lacZ gene fusions (Balsalobre et al., 1987). Although etioplasts contain small amounts of carotenoids, light is required for the large scale coordinated synthesis of carotenoids and Chl during chloroplast development in higher plants, while most algae synthesize carotenoids even in dark grown cultures (Bramley and Mackenzie, 1988). The mechanisms governing the upregulation of carotenoid production in higher plants remain unknown, however. Thus, the details of the regulation of carotenogenesis by oxygen tension, light or other factors such as cAMP (Chapter 5) depend on the organism studied.

The obvious question arises whether the induction of particular carotenoid biosynthesis genes (crtA, C, D, E, F and K) during the shift to photosynthetic growth relates only to an overall induction of the carotenoid biosynthetic apparatus or to the specific roles of certain gene products. Manwaring et al. (1978) have observed increases in both the levels of spheroidene, spheroidenone and demethylspheroidenone subsequent to a shift from dark aerobic growth to anaerobic photosynthesis. Addition of both

transcriptional and translational inhibitors prevented this increase in the cases of spheroidene and spheroidenone, but not demethylspheroidenone. The stimulation of spheroidenone accumulation during the shift to photosynthetic growth is consistent with the 9-fold induction of the crtA gene. The induction of crtA during the shift from aerobic to photosynthetic growth (Fig. 6-2) is of particular interest since this gene appears to be induced 2-fold during the reverse shift from photosynthetic to aerobic growth (Zhu et al., 1986). It would be worthwhile to reexamine this observation with the benefit of a gene-specific probe for crtA. crtA encodes an oxygenase which uses molecular oxygen as a substrate in the conversion of spheroidene to spheroidenone (Shneour, 1962). The biological function of this reaction (Fig. 1-5) is unknown. We have, however, observed a reduction in the accumulation of the LH-II and LH-I complexes in a crtA mutant (Chapter 2).

Carotenoid intermediates with a terminal hydroxy group have been observed to transiently accumulate in cells of R. capsulatus undergoing a shift from dark aerobic to anaerobic photosynthetic growth (Manwaring et al., 1978). These results have been taken as an indication that the methylation of the terminal hydroxy group of carotenoids mediated by crtF may be inhibited during the dark-to-light transition (Scolnik et al., 1980a). Inhibition of methylation could be accounted for by the roughly 45 minute lag before the maximal induction of the crtF gene during the shift experiments (Fig. 6-3). Manwaring et al. (1978) observed, however, that the accumulation of unmethylated carotenoids was insensitive to the addition of inhibitors of either transcription or translation, indicating that inhibition of methylation is a post-translational effect. Further conclusions regarding the significance of the induction of specific crt genes await a better understanding, both of the functions of the carotenoid gene products (crtK, for example) and the roles and accumulation patterns of specific carotenoid species during the development of the photosynthetic membrane.

F. Mechanisms for regulation of genes in the Rhodobacter capsulatus photosynthesis gene cluster

We have shown here that some genes for carotenoid and possibly Bchl biosynthesis are induced by a reduction of oxygen tension in the growth medium. This is also the case for the genes encoding structural photosynthetic proteins (pufB, pufA, pufL, pufM, puhA, pucB, pucA) as shown here, under our growth conditions, and in previous experiments (Clark et al., 1984; Klug et al., 1985). It is not known, however, whether the mechanisms of regulation for all of the members of the photosynthesis genes cluster (Figs. 1-4, 3-7) are similar. All of the approximately 30 genes needed for photosynthetic growth in R. capsulatus, except for the LH-II genes, are clustered on a 46 kb region of the chromosome (Marrs, 1981). This clustering makes attractive models involving coregulation of the entire gene cluster by the same mechanism.

One version of this type of model involves a change in chromosomal superhelicity affecting expression of the inducible photosynthesis genes. Zhu and Hearst (1988) have recently shown that the activity of DNA gyrase is required for the accumulation of mRNAs from the puf and puh operons, and bch biosynthesis genes, but not for the fbc operon or the crt genes, although crt or bch gene-specific probes were not used. The differential dependence on gyrase activity does not result, however, from a stable segmental difference in chromosomal superhelicity in the regions encoding any of these genes, but may reflect a requirement for topoisomerases (gyrase and topoisomerase I) to relieve torsional stress in heavily transcribed regions of the chromosome (Cook et al., submitted). Gyrase activity may not be required for crt gene expression because of the relatively low level of expression of these genes (unpublished observations), or because their particular arrangement on the chromosome serves to reduce the buildup of torsional stress.

A second example suggesting multiple forms of regulation in the photosynthesis gene cluster involves a palindromic nucleotide motif, which we propose to represent the binding site for a trans-acting factor (Chapter 3). Palindromes were found in the crtA-crtI, crtD-

crtE and ORF J 5' flanking regions (Fig. 3-5), as well as 5' to the puc operon (Fig. 3-10), but not immediately 5' or 3' to the puf or puh operons. We hypothesize that these palindromic sites are involved in the regulation of transcription of some inducible crt genes, ORF J, and the puc operon, but not the puf and puh operons, and that the regulation is mediated by the binding of a trans-acting factor. Putative palindromic regulatory sites are found between pairs of divergently transcribed crt genes, crtA-crtI and crtD-crtE (Fig. 6-5). In these cases, one gene of each pair is strongly induced while the other is not. Since the expression of crtI is constitutive and crtD is only weakly induced (about 2-fold), one would argue that the crtA and crtE genes are the likely targets of action for the trans-acting regulator. Two simplistic models involve either the binding of a trans-acting factor to repress transcription during aerobic growth, or the binding of a factor to stimulate transcription during the shift to photosynthetic growth. We have previously observed that crtI and crtD are preceded by nucleotide sequences with strong similarity to the E. coli σ^{70} consensus promoter (Figs. 3-5, 3-9). This may explain the constitutive or near-constitutive expression of these genes. crtA and crtE, on the other hand, are not preceded by recognizable E. coli-type promoters. These genes may utilize a different class of promoters, whose expression is controlled by transcriptional factors assisting RNA polymerase in the activator model. We have, in Chapter 4, defined to high resolution the region containing crtA promoter signals. In the case of crtE, Giuliano et al. (1988) have roughly mapped either one or two stable mRNA 5' ends in S1 nuclease protection experiments, using RNA from steady-state illuminated aerobic or anaerobic cultures, respectively. A qualitative increase in the levels of these mRNAs under the latter condition was due almost entirely to a new mRNA species about 20 nucleotides longer than the single species detected under aerobic conditions. Unfortunately, the low resolution of the S1 mapping does not allow us to draw any meaningful correlations between the 5' ends of these mRNA species and the nucleotide sequence of the crtE 5' flanking region (Fig. 3-5). These results are, however, consistent with the existence of crtE promoters, one

constitutive and the other highly inducible. We have located a possible E. coli σ^{70} promoter 5' to ORF J, which is induced about 3-fold during the shift. The relatively low magnitude of the induction of mRNA from this ORF, in comparison to the respective 9-fold and 6-fold inductions of crtA and crtE mRNAs (Figs. 6-2, 6-3), may result from a reasonably high basal level of expression driven by the constitutive σ^{70} promoter. The binding of a trans-acting factor to the putative regulatory palindrome 5' to ORF J could stimulate expression from a second inducible promoter, by analogy to crtE.

What might be the nature of the trans-acting transcriptional factor and is it likely to be directly regulated by oxygen? One particularly analogous prokaryotic system involves the Fnr protein of E. coli. Fnr is a transcriptional regulatory factor required for expression of anaerobic respiratory metabolism genes (reviewed in Stewart, 1988). The gene encoding Fnr is itself, however, not regulated by oxygen tension (Pascal et al., 1986). The transcriptional regulation mediated by Fnr is rather proposed to occur through a redox-induced conformational change in the protein (Unden and Guest, 1985), perhaps by binding of a redox-sensitive effector (Shaw et al., 1983) or by direct interaction with a component of the aerobic respiratory chain (Stewart, 1988), thereby altering Fnr activity as a transcriptional activator. In either of these scenarios, oxygen itself is not directly the redox effector. An Fnr-like redox-sensitive regulatory protein could serve as an effective means of regulating anaerobically-induced photosynthesis genes in Rhodobacter. In such a fashion, oxygen could exert an indirect effect on gene expression by the modulation of the redox state of a particular cellular component.

Bauer and Marrs (1988) have recently suggested that PufQ, a putative Bchl precursor-binding protein, may also bind quinones and that the redox state of the quinone pool may provide a means for the observed repression of Bchl biosynthesis by oxygen (Drews and Oelze, 1981). Whether this hypothetical mode of regulation could be acting directly at the level of expression of the anaerobically inducible bch genes (Biel and Marrs, 1983; this Chapter) remains to be tested.

Because six of the eight crt genes in the gene cluster are induced to some degree, and regulatory palindromes are not found 5' to all of the inducible genes (Fig. 6-5), other as yet unidentified promoter and regulatory sequences involved in crt gene expression are likely to exist. The mechanism of regulation of the inducible puf and puh operons also remains to be determined. All of the data discussed in this section suggests that several distinct and perhaps overlapping mechanisms may be required for the coordinated regulation of several different classes of anaerobically induced photosynthesis genes in R. capsulatus.

V. Summary

We conclude, based on the evidence presented in this chapter, that six of the eight studied carotenoid biosynthesis genes of R. capsulatus, and two ORFs flanking these eight clustered genes, are induced (2 to 10-fold) by a shift from dark aerobic to anaerobic photosynthetic growth. Light is not required for the qualitative induction of the crtA gene. In a striking contrast to previous studies, we observed that the magnitude of the induction of the crt genes is comparable to or even exceeds the 6 to 8-fold induction of the genes encoding the RC and LH-I complexes. Furthermore, the maximal accumulation of crt gene mRNAs precedes that of the RC and LH-I mRNAs (45 to 60 minutes, versus 90 minutes). We therefore propose a model in which sequential induction of pigment biosynthesis genes precedes that of the genes encoding structural photosynthetic polypeptides. All of the crt genes may not be induced due either to post-transcriptional steps regulating some carotenoid biosynthetic activities or because only the enzymes governing rate-limiting biosynthetic reactions need be upregulated. We have previously proposed that a palindromic motif found in the 5' flanking regions of crtA-crtI and crtD-crtE might be involved in transcriptional regulation (Chapter 3). We have now directly shown that the crtA and crtE genes are strongly regulated by the shift to photosynthetic growth, while the crtI gene is constitutively expressed and the crtD gene is only weakly induced (2-fold), and therefore propose that the former two genes are targets for the proposed trans-acting protein factor, which we hypothesize may be redox-sensitive, by analogy to the E. coli Fnr protein. Other factors may also be involved in the regulation of the inducible crt genes.

Chapter 7: Properties of the carotenoid gene products from R. capsulatus

I. Introduction

None of the enzymes involved in carotenoid biosynthesis from GGPP onwards (Fig. 1-5) has been purified from R. capsulatus. With one exception, noted in the Discussion, this statement also holds true in all organisms for the enzymes involved in β-carotene synthesis (Fig 1-2). The examination of the deduced protein sequences of the R. capsulatus carotenoid enzymes thus provides valuable information as a starting point for prediction of structural features of these proteins.

Protein similarities between the structural polypeptides of the reaction centers of purple photosynthetic bacteria and the PS II reaction center of cyanobacteria, algae and higher plants have provided important insights into the structure and evolution of the photosynthetic reaction center (reviewed in Michel and Deisenhofer, 1988). The comparison of protein sequences for carotenoid biosynthetic enzymes from R. capsulatus with sequences to be determined from other photosynthetic and nonphotosynthetic prokaryotes and eukaryotes should provide structural, functional and evolutionary information. Almost all carotenoid synthesizing organisms follow a similar pathway to that used by R. capsulatus, at least through the intermediate neurosporene. Thereafter, the pathways of Rhodobacter and general carotene biosynthesis diverge (compare Figs. 1-2, 1-5). Thus, the R. capsulatus enzymes involved in the synthesis of compounds up to neurosporene might be expected to have analogs in other carotenogenic organisms.

This chapter describes features of the deduced amino acid sequences of the R. capsulatus carotenoid biosynthesis enzymes which may be related to their structure or function.

II. Materials and methods

Protein sequence analysis

Homology matrix search programs were used to perform protein sequence comparisons between the carotenoid enzymes (Pustell and Kafatos 1982). Mean hydropathy values for proteins (Table 7-1) were calculated using the consensus hydrophobicity scale of Sweet and Eisenberg (1983). Hydropathy plots were performed by averaging the hydrophobicity of individual amino acids over a 19 amino acid residue window to define potential hydrophobic membrane spanning regions (Kyte and Doolittle, 1982).

III. Results

A. Protein homologies

CrtI and CrtD, both of which catalyze dehydrogenations (Fig. 1-5), show extraordinary amino acid similarity in two regions (Fig. 7-1). In the C-terminus of each protein, 21 of 39 consecutive residues (54%) are conserved. From Gly-438 to Pro-453 of CrtI and Gly-457 to Pro-472 of CrtD 14 of 16 residues (87.5%) match exactly. The two amino acid substitutions from CrtI to CrtD are Ala to Val and Gly to Ala, both conservative changes. The N-termini of CrtI and CrtD show matches in 18 of 44 consecutive residues (41%), with conservation of spacing between the homologous amino acids. Pairwise comparisons of the Crt biosynthetic enzymes revealed no other regions of such significant amino acid similarity. The amino acid sequence of CrtD deduced in Chapter 3 (Fig. 3-5) and discussed in this chapter represents the translation product of the crtD223 allele originally carried on pRPS404 (Marrs, 1981). The high degree of similarity between CrtI and CrtD argues that the crtD223 point mutation is probably a missense mutation, rather than a frameshift mutation which might effect a gross alteration in the deduced amino acid sequence of CrtD, with respect to the wildtype protein.

B. Mean hydrophobicity and hydropathy plots of the carotenoid gene products

The predicted molecular weights of the crt gene products range from 18 kDa (kDa) for CrtK to 65 kDa for CrtA (Fig. 3-5). Mean hydropathy values (Table 7-1) of the crt gene products were calculated by averaging the hydrophobicities of individual amino acids over the length of the protein. Hydrophobicity values for the individual amino acids range from -2.5 for arginine to +1.4 for isoleucine (Sweet and Eisenberg, 1983). The mean hydropathy thus reflects the overall hydrophobicity or hydrophilicity of a protein. Abundant evidence exists in the literature that many of the later carotenoid enzymes are

Figure 7-1. Amino acid similarity between CrtI and CrtD. The N- and C- termini of each protein (residues are indicated at the left and right) have been aligned to generate the highest percentage match. Conserved amino acids are shown by (*). The C-terminal region of greatest similarity is shown in boldface, separated by spaces from the adjacent sequence. CrtI and CrtD are 491 and 494 amino acids in length, respectively (see Fig. 3-6).

```
CrtI    Thr-2     TVVDRLDRPGGRGSSITKGGHFRDLGPTIVTVPDRLRELWADCG  Gly-45
CrtD    Thr-31    TVVEAGDAPGGKARAVPTPGGPADTGPTVLTMRHVLDALFAACG  Gly-74
                  ***   * ***         *   * ***  *    *  * * **

CrtI    Ala-425   AWFRPHNASEEVD GLYLVGAGTHPGAGVP SVIGSGELVA   Ala-463
CrtD    Ala-444   ATFRRPLARTGLK GLYLAGGGTHPGAGVP MALTSGTHAA   Ala-482
                  * **   *       **** * ********** **   *
```

Table 7-1. Mean hydropathies of the carotenoid gene products and other membrane-bound *R. capsulatus* gene products

Crt gene products	Mean hydropathy[a]	Other gene products[b]	Mean hydropathy[a]
CrtK	+0.482	PucA, (LH-II α)	+0.408
CrtE	+0.151	PufA, (LH-I α)	+0.403
CrtD	+0.112	PufL, (RC-L)	+0.378
CrtF	+0.077	PufM, (RC-M)	+0.338
CrtA	+0.010	PufB, (LH-I β)	+0.303
CrtI	+0.009	PucB, (LH-II β)	+0.257
CrtB	-0.015	PuhA, (RC-H)	+0.014
CrtC	-0.040		

[a] values arranged from most hydrophobic (+) to most hydrophilic (-)
[b] see Chapter 1 and Fig. 3-7 legend for a further description

membrane-bound or membrane-associated (see Discussion). For comparison we also determined the mean hydropathies for the membrane-bound R. capsulatus RC, LH-I and LH-II polypeptides. The mean hydropathies of the crt gene products range from +0.482 for CrtK to -0.040 for CrtC and, with the exception of CrtK, are not particularly hydrophobic compared to other known R. capsulatus proteins (Table 7-1). CrtK, however, is more hydrophobic than any of the polypeptides in the RC, LH-I or LH-II complexes.

Fig. 7-2A-H show the mean hydropathy plots of the R. capsulatus carotenoid biosynthesis enzymes averaging over a 19 amino acid membrane-spanning window. As no other determined or deduced amino acid sequences are available for carotenoid biosynthetic enzymes, a direct comparison of the features of the R. capsulatus enzymes with enzymes from other systems is not possible, thus making the assignment of possible transmembrane helical regions highly speculative. A few salient features emerge from the hydropathy plots, however. Comparison of the mean hydropathies for the N-terminal and C-terminal regions of similarity between the CrtI and CrtD dehydrogenases (regions I and II in Fig. 7-2B, Fig. 7-2C, respectively) shows that the local hydropathy of the C-terminal region is conserved between both enzymes. This similar region includes a stretch of amino acids at the start of a potential transmembrane helix. In contrast, the N-terminal region does not show a conservation of local hydropathy. Both CrtD and CrtI share a central hydrophilic domain spanning about 30 amino acids, centered at about residue 250 in CrtD and residue 265 in CrtI. CrtK, overall the most hydrophobic of all of the carotenoid enzymes, shows an extended hydrophilic region only at the C-terminus which may thus be exposed to solvent.

Figure 7-2 A-H. Hydropathy plots of the deduced amino acid sequences of the R. capsulatus carotenoid biosynthesis gene products averaging over a 19 amino acid window. Hydrophobicity values for individual amino acids range from -2.5 for arginine to +1.4 for isoleucine. Mean hydropathies calculated over the length of the entire protein (see Table 7-1) correspond to the y-axis value indicated by the dotted horizontal line, while the dashed horizontal line indicates a hydropathy value of zero, for reference. Regions I and II of amino acid similarity between CrtD and CrtI (Fig. 7-1) are indicated by brackets in plots (**B**) and (**C**). The four largest carotenoid enzymes, CrtA, CrtD, CrtI and CrtF (**A - D**) are plotted using a different amino acid residue x-axis, than the smaller enzymes, CrtB, CrtE, CrtC and CrtK (**E - H**). Deduced lengths of the proteins in amino acid residues and their molecular weights are given in Fig. 3-6.

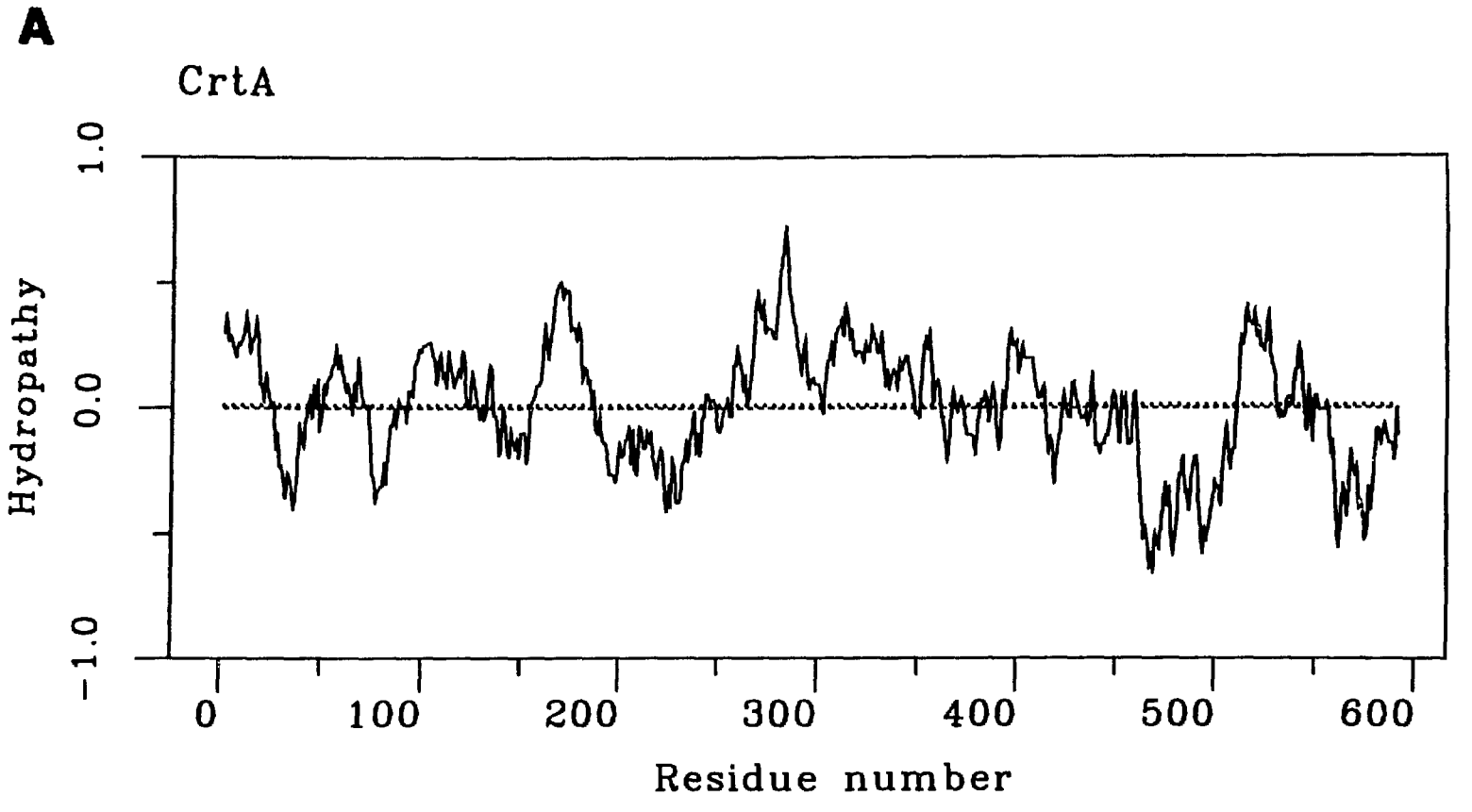
A
CrtA
Hydropathy
1.0
0.0
-1.0
0
100
200
300
400
500
600
Residue number

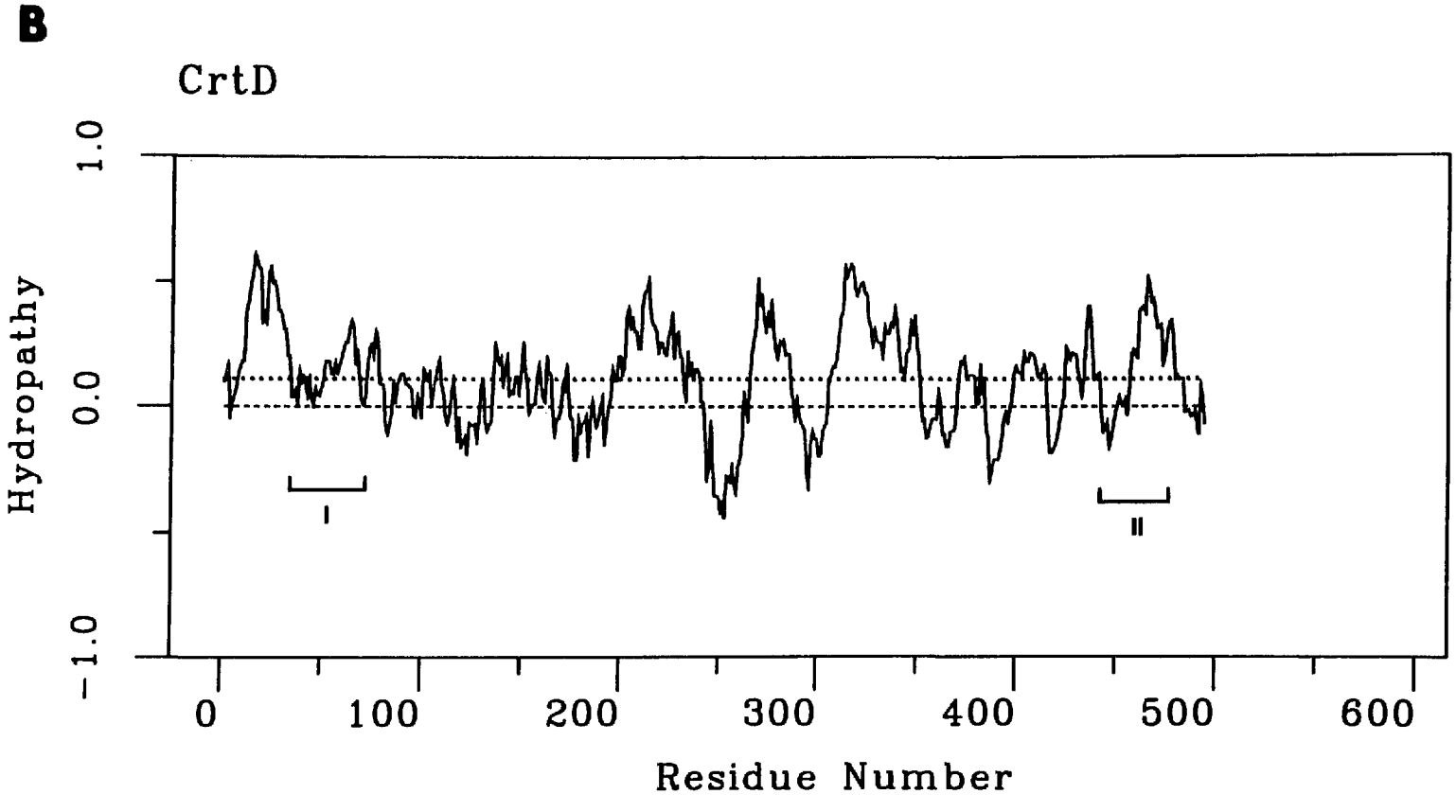
B
CrtD
Hydropathy
1.0
0.0
-1.0
0
100
200
300
400
500
600
Residue Number
I
II

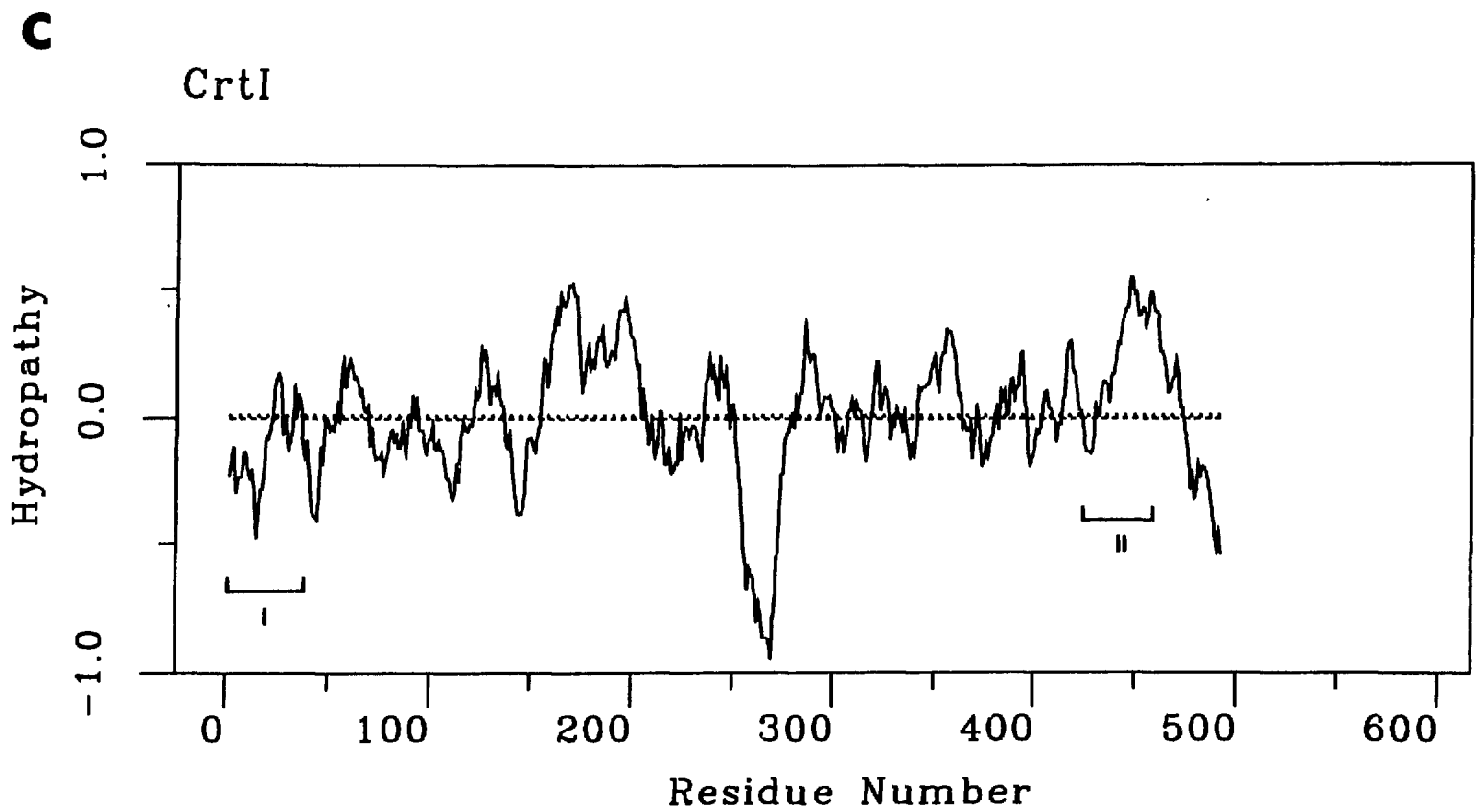
c
CrtI
Hydropathy
1.0
0.0
-1.0
0
100
200
300
400
500
600
Residue Number
I
II

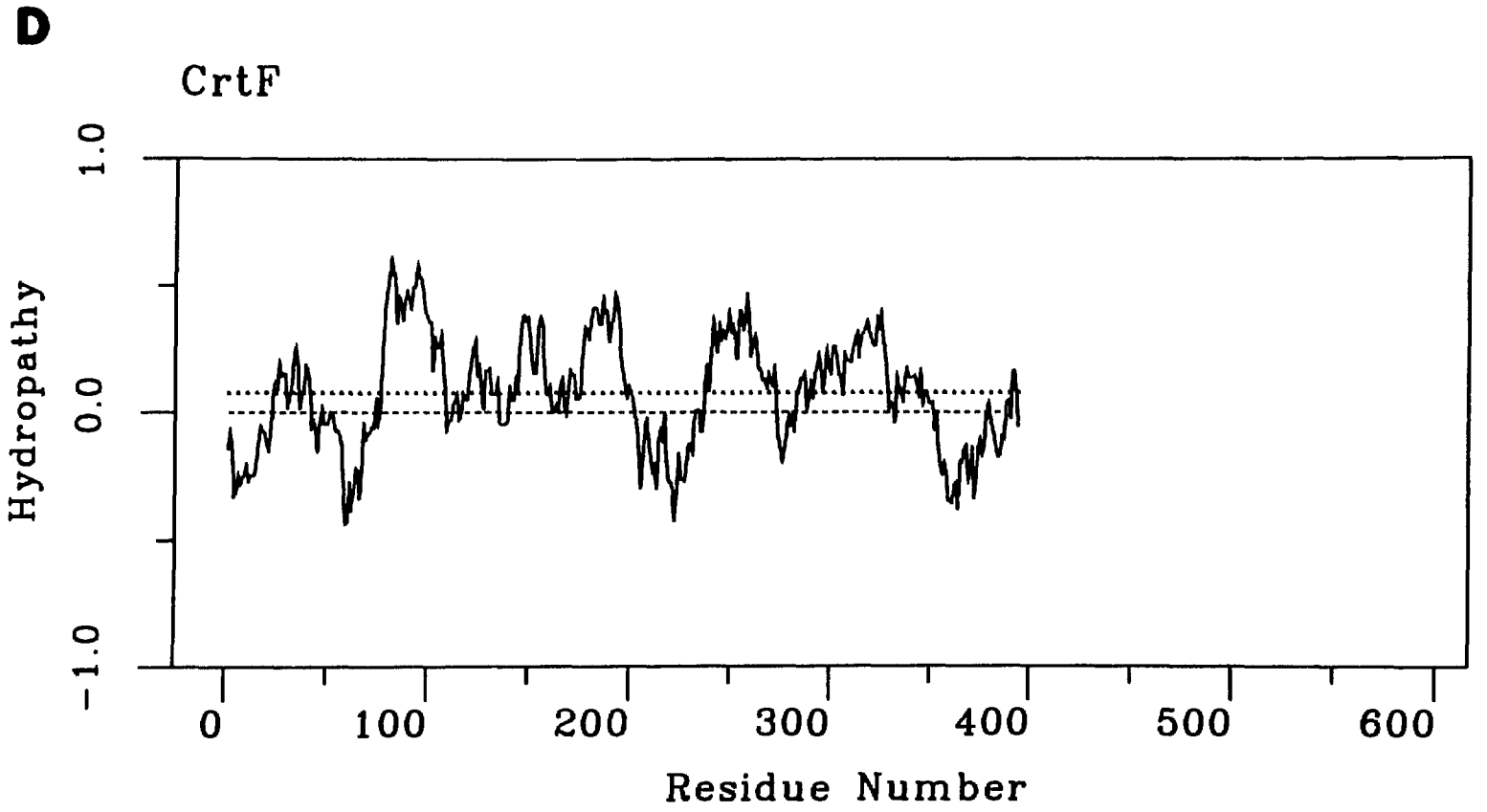
D
CrtF
Hydropathy
1.0
0.0
-1.0
0
100
200
300
400
500
600
Residue Number

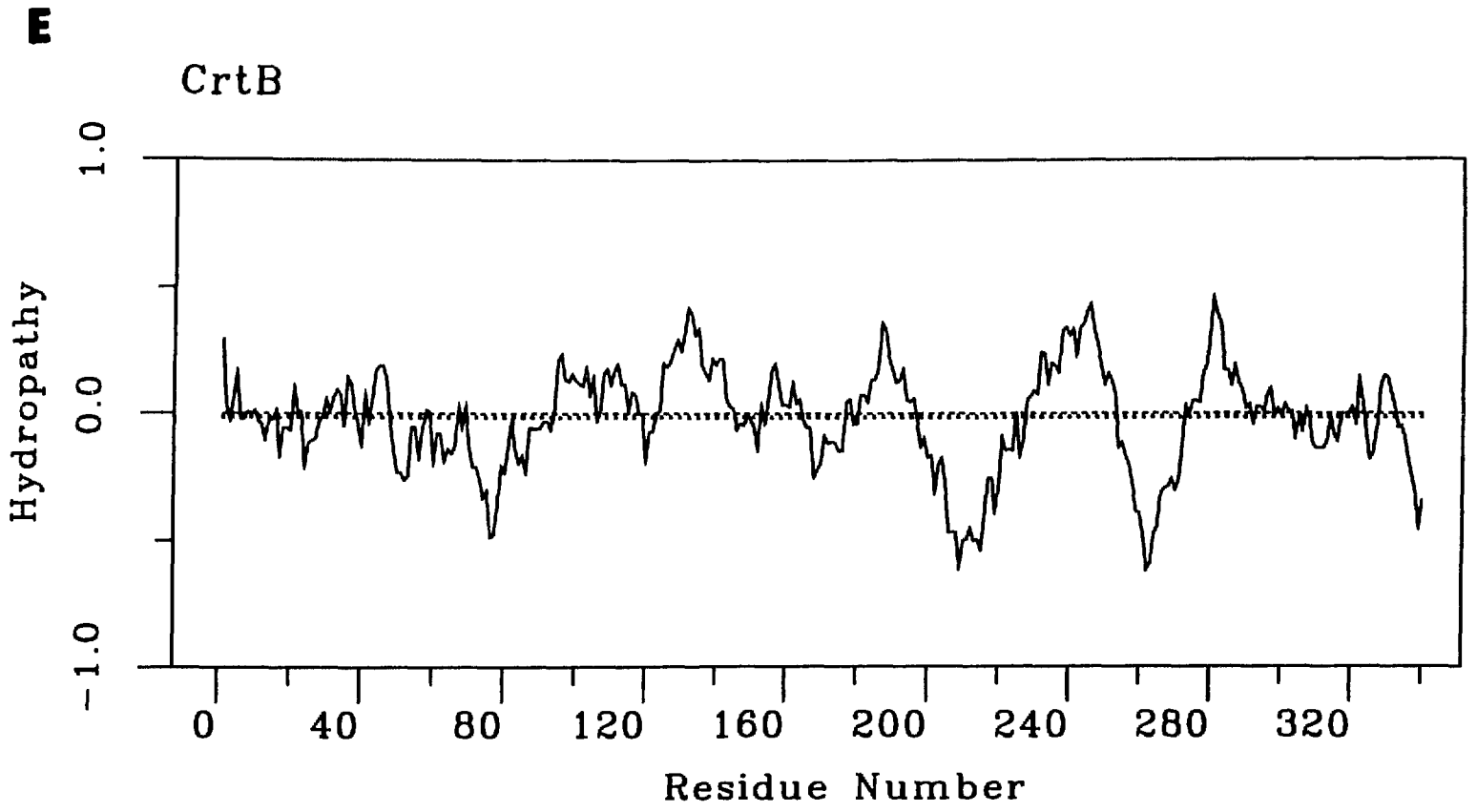
E
CrtB
Hydropathy
1.0
0.0
−1.0
0
40
80
120
160
200
240
280
320
Residue Number

F

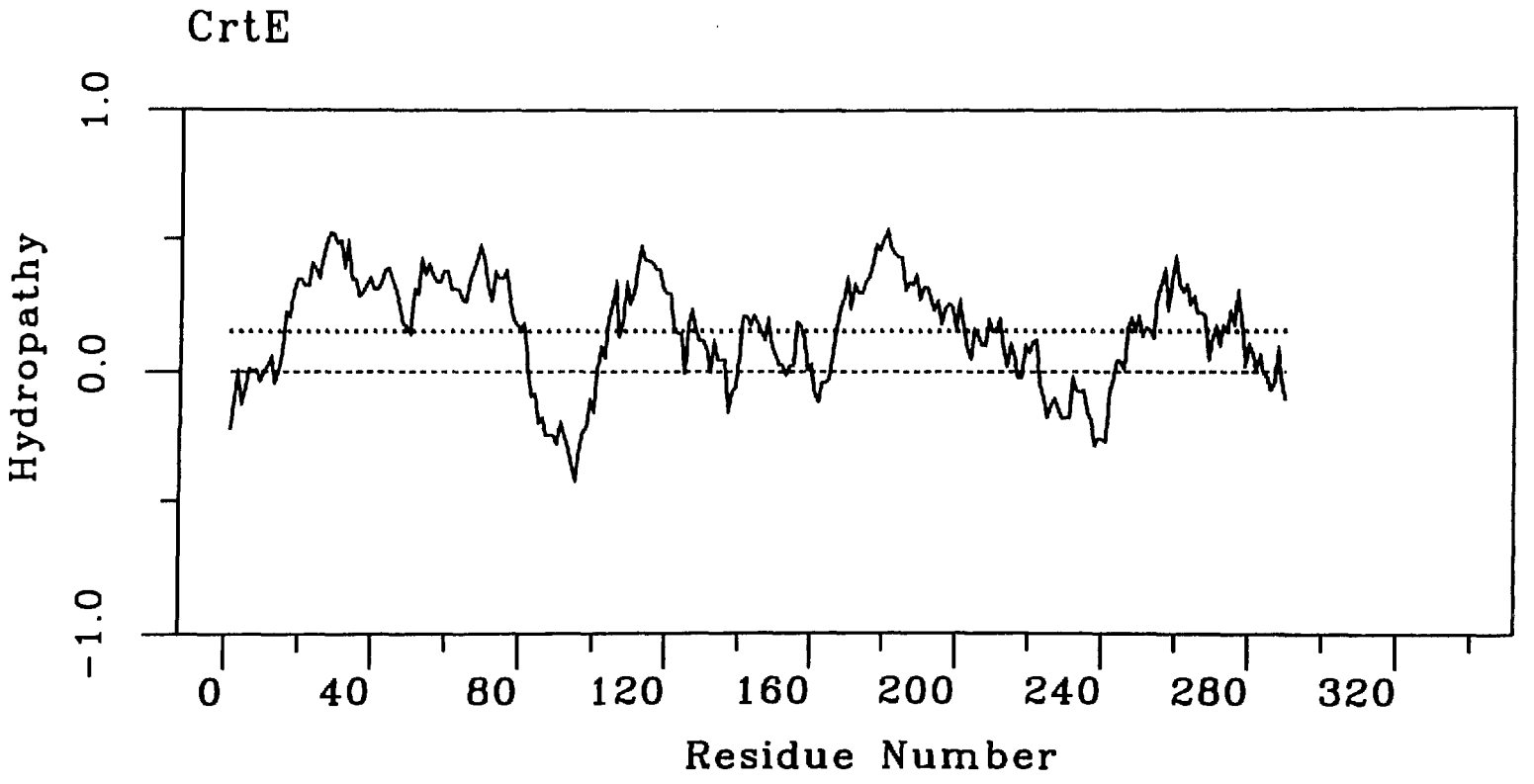
CrtE
Hydropathy
1.0
0.0
-1.0
0
40
80
120
160
200
240
280
320
Residue Number

G

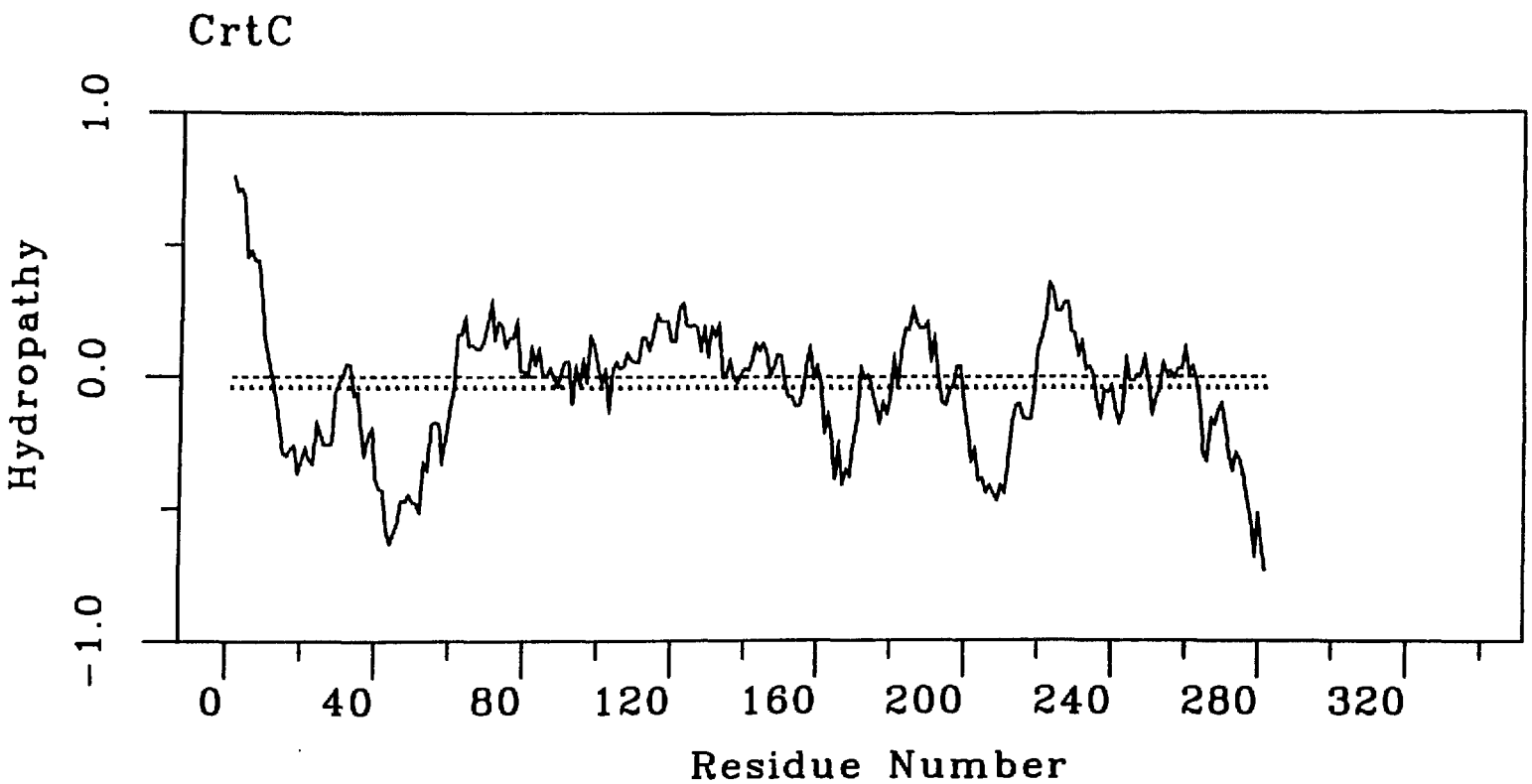
CrtC
Hydropathy
1.0
0.0
-1.0
0
40
80
120
160
200
240
280
320
Residue Number

H

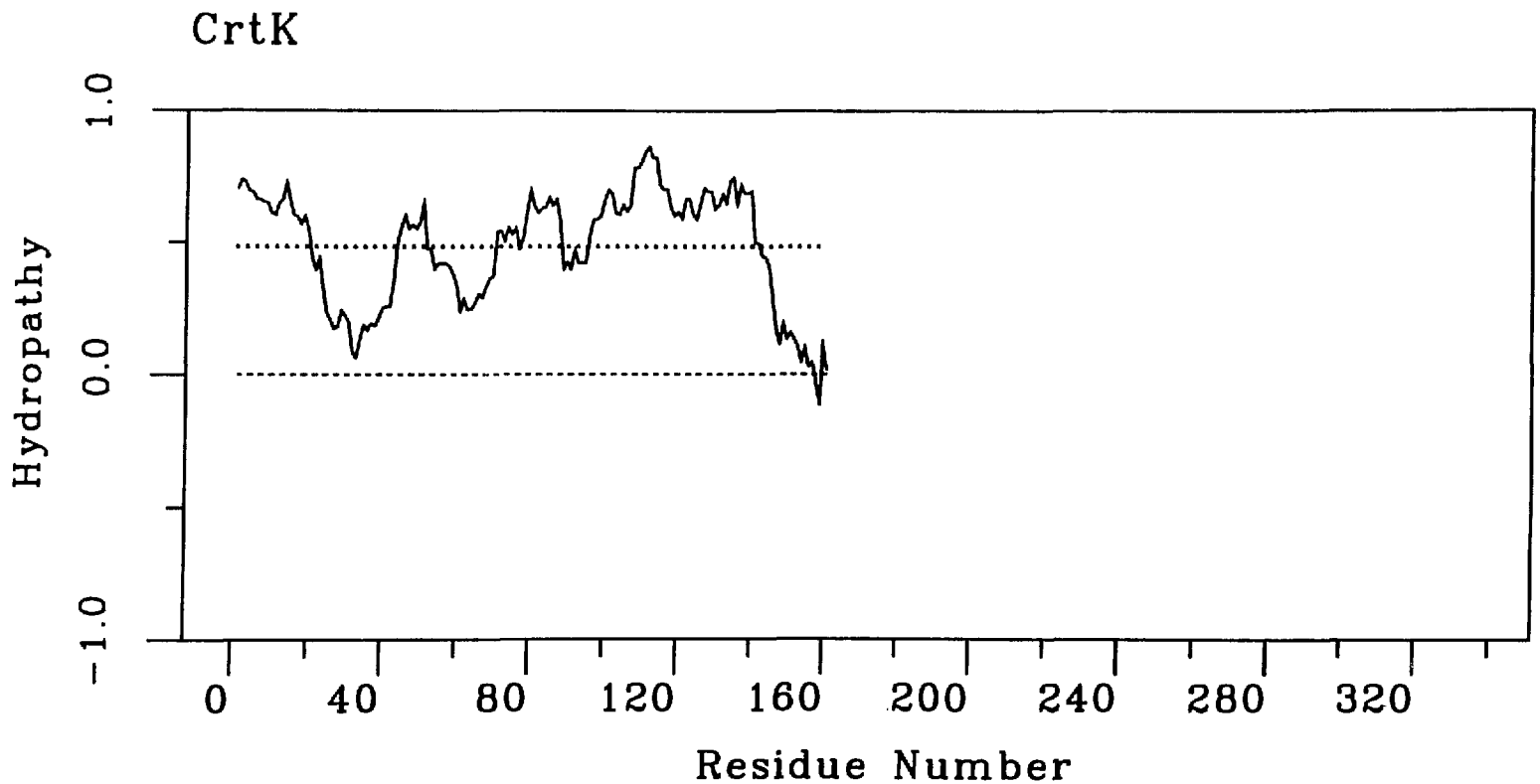
CrtK
Hydropathy
1.0
0.0
-1.0
0
40
80
120
160
200
240
280
320
Residue Number

IV. Discussion and summary

Carotenoid biosynthesis may be divided roughly into early and late reactions. The early reactions leading to production of neurosporene (Fig. 1-5) are common to many organisms, while the later reactions diverge widely depending on the final carotenoid product(s) (Goodwin, 1980). The consecutive reactions mediated by CrtB, CrtE (Chapter 4) and CrtI (Giuliano et al., 1986) are early reactions (Fig. 1-5). These enzymes might thus be expected to show the greatest similarities to carotenoid biosynthetic enzymes from other organisms. The later reactions mediated by CrtC, K, D, F and A in R. capsulatus produce more specialized carotenoids (Fig. 1-5) found only in certain photosynthetic bacteria (Goodwin, 1980).

Preliminary partial DNA and deduced amino acid sequences (M. Alberti, unpublished data) from the Erwinia herbicola carotenoid biosynthesis gene cluster (Chapter 5) have revealed substantial amino acid similarities between the R. capsulatus CrtB, CrtE and CrtI enzymes and potential open reading frames in the E. herbicola DNA. The examination of the complete nucleotide and deduced amino acid sequences may reveal additional similarities to other R. capsulatus carotenoid enzymes. In addition, a hybrid gene consisting of the C-terminal 921 bp of the R. capsulatus crtI gene fused to the N-terminal region of the E. coli lacZ gene, encoding β-galactosidase, has been used to synthesize a CrtI fusion protein for the production of polyclonal antisera (Schmidt et al., submitted). The CrtI fusion antibody reacts monospecifically with a protein of apparent molecular weight 64 kDa in R. capsulatus, and monospecifically with proteins from cyanobacteria, algae and higher plants, which range in size from 55 to 65 kDa. No cross-reaction was observed with an antibody specifically directed against β-galactosidase alone. The R. capsulatus fusion antibody also inhibited phytoene dehydrogenation in vitro, using solubilized membranes from the cyanobacterium, Aphanocapsa. Thus, these preliminary indications suggest similarities between prokaryotic and eukaryotic phytoene

dehydrogenases, although the nature of the heterologous cross-reacting proteins remains to be rigorously demonstrated.

A second rough division of the carotenoid pathway can be made based on the cellular localization of the biosynthetic enzymes. The condensation of carotenoid pyrophosphate precursors culminating in the formation of phytoene is conducted by soluble enzymes in tomato plastids (Jones and Porter, 1986) and in red pepper (Camara et al., 1982). Dogbo et al. (1988) have recently isolated and purified to homogeneity phytoene synthase from the stromal fraction of red pepper chromoplasts. This single bifunctional polypeptide of molecular weight 47.5 kDa catalyzes both the condensation of two molecules of GGPP to give PPPP, and the subsequent conversion of PPPP to phytoene. Phytoene synthetase is, however, a peripheral membrane protein in daffodil (Kreuz et al., 1982) and in the fungus Phycomyces (Bramley and Taylor, 1985). Phytoene dehydrogenase and later carotenoid biosynthetic enzymes are membrane-bound in the cyanobacterium Aphanocapsa (Sandmann and Bramley, 1985), Phycomyces (Bramley and Taylor, 1985) and in daffodil (Beyer et al., 1985).

In R. capsulatus one might thus, by analogy, suggest that CrtB and CrtE would be soluble or peripheral membrane proteins, while CrtI, C, K, D, F and A would be membrane-bound. Mean hydropathy values (Table 7-1) show that although CrtB is overall the most hydrophilic carotenoid enzyme, CrtE is relatively hydrophobic. None of the crt gene products is as hydrophobic as integral membrane polypeptides such as RC-L, RC-M, LH-I β, α and LH-II β, α (Table 7-1), with the exception of CrtK. The mean hydropathy values of the crt gene products thus do not suggest a simple model of enzyme localization. CrtK encodes a very hydrophobic polypeptide which may be required along with CrtC for the conversion of neurosporene to hydroxyneurosporene. Interestingly, an interposon mutation within the crtK gene produces an unstable phenotype with a high reversion rate (P. Scolnik, personal communication) (Fig. 1-5, see Results). Based on the data presented here and by Giuliano et al. (1988) it is not presently possible to determine

the relative roles of CrtC and CrtK in the hydration of neurosporene. Because CrtK is more hydrophobic than known R. capsulatus integral membrane polypeptides (Table 7-1) or the other Crt enzymes mentioned above, it could be membrane-bound or otherwise shielded from solvent, possibly serving as a membrane attachment point for an enzyme complex.

We interpret the observation of two regions of strong amino acid similarity between CrtI and CrtD (Fig. 7-1) in the following manner. Carotenoids accumulated in crtI and crtD mutants indicate that both gene products are probably carotenoid dehydrogenases (Scolnik et al., 1980a; Giuliano et al., 1986; Chapter 4). CrtI mediates the introduction of a double bond at the 11, 12 position of phytoene, while CrtD dehydrogenates either methoxyneurosporene or hydroxyneurosporene at the 3, 4 position (Fig. 1-5). We propose that the homologous amino acids represent conserved structural or functional features required for the interaction between Crt and the dehydrogenases. The most highly conserved region, in the C-terminal domain of each protein, contains a high number of hydrophobic amino acids (Fig. 7-1). The CrtF, C, K and A enzymes do not, however, share significant homology with either the conserved N-terminal or C-terminal domains of the dehydrogenases. This suggests that the conserved residues do not simply form a hydrophobic carotenoid binding pocket, but may also provide specific side chains uniquely required for the dehydrogenation reaction. The lack of obvious homology between the conserved region in the dehydrogenases and the residues in close proximity to the bound RC carotenoid molecule in the high resolution X-ray crystal structures of the R. sphaeroides (Komiya et al., 1988) and the R. viridis (Deisenhofer and Michel, 1988) RC complexes also illustrates that the conserved amino acids do not simply represent the carotenoid binding site. The C-terminal residues conserved between the two dehydrogenases form similar hydrophobic domains, as seen in the hydropathy plots of these enzymes (Fig. 7-2B, 7-2C, respectively). We note that the portion of the R. capsulatus crtI gene used to make the previously described gene fusion with lacZ (Schmidt

et al., submitted) includes the conserved C-terminal region and the very hydrophilic domain centered at residue 265, but not the conserved N-terminal domain (Fig. 7-2C).

The conversion of GGPP to phytoene by the purified phytoene synthetase of Dogbo et al. (1988) is inhibited by hydroxyphenylglyoxal, which specifically derivitizes arginine residues. Arginine has been implicated as a residue found in the binding sites of enzymes which handle anionic substrates (Riordan et al., 1977), and has thus been suggested to be important in binding the pyrophosphate moiety of GGPP and PPPP in the case of the red pepper phytoene synthetase (Dogbo et al., 1988). Thus, one of the arginines in the R. capsulatus CrtB and CrtE enzymes may also be essential for pyrophosphate binding. Since, however, the primary structure of the red pepper phytoene synthetase has not been determined, a direct comparison with the R. capsulatus sequences is not possible. The apparent fusion of the R. capsulatus PPPP synthetase and phytoene synthetase activities into a single polypeptide chain during the course of evolution from photosynthetic bacteria to higher plants has been proposed as a means of reducing substrate diffusion times between catalytic sites of different enzymes (Dogbo et al., 1988). It will be of exceptional interest to ultimately compare the features of enzymes involved in phytoene synthesis from R. capsulatus and E. herbicola, as representatives of photosynthetic and nonphotosynthetic prokaryotes, to higher plant and fungal enzymes.

Chapter 8: Summary and future directions

I. Summary and future directions

Although carotenoids comprise one of the most widely distributed classes of natural pigments, little is known about the enzymes involved in carotenoid biosynthesis, the genes encoding these enzymes, and the regulation of either gene expression or enzymatic activity. This work has described investigations into some of these areas, using primarily Rhodobacter capsulatus and, to a lesser extent, Erwinia herbicola carotenoid biosynthesis genes as model systems. In addition, this work has examined the consequences of mutations in carotenoid biosynthesis genes on the photosynthetic phenotype of R. capsulatus, including growth rate, cell size, pigment content, pigment-protein complexes, and the expression of the genes encoding these complexes.

Chapter 2 discusses the relationship between photosynthetic phenotype and carotenoid biosynthetic deficiencies. A major conclusion of this work is the definition of the carotenoid component needed for the stable incorporation and/or assembly of the LH-II antenna complex in the photosynthetic membrane. A carotenoid mutant accumulating phytoene (Fig. 1-5) has no functional LH-II complex, while a mutant accumulating neurosporene has substantial amounts of LH-II. Accumulation of demethylspheroidene, with a terminal hydroxy group, also reduces the amount of LH-II. Thus, the presence of specific types of carotenoids is required for the accumulation of a stable LH-II complex. It would be interesting to determine if the biosynthetic intermediates after phytoene but before neurosporene (ie. phytofluene, and 7, 8, 11, 12-tetrahydrolycopene) are sufficient to allow the formation of a stable LH-II complex. Unfortunately, mutants accumulating these compounds have not been described in R. capsulatus, nor are chemical inhibitors available for these steps in carotenoid biosynthesis. An alternative approach to this

question would be to attempt to reconstitute these carotenoids into isolated LH-II complexes containing no carotenoid, such as those from a mutant reported by Dörge et al. (1987) which accumulates an LH-II complex of reduced stability in the absence of colored carotenoids, and to assay the complexes for stability and spectral properties. A corollary would be to determine if the phytoene accumulated in R. capsulatus crtI mutants is actually incorporated into the RC and LH-I complexes in vivo. Carotenoids are normally present in these complexes, but are not required for their assembly and stability. The anionic pyrophosphate precursors of phytoene (Fig. 1-5), accumulated in R. capsulatus crtB, crtE and crtJ mutants, would not be expected to be incorporated into the integral membrane pigment-protein complexes.

None of the crt mutants we have studied completely lacked puc operon (LH-II) mRNA. Thus, the complete deficiency in functional LH-II complexes observed in blue-green mutants lacking colored carotenoids cannot be due solely to transcriptional effects, although reductions in LH-II mRNA levels were observed in these strains and in crtF mutants, which show reduced amounts of LH-II in the photosynthetic membrane. The experiments in Chapter 2 show that while mRNA levels for the genes encoding the RC and LH-I complexes vary between the different mutants, the pattern of mRNA accumulation among the strains is coordinated using RC-L, RC-H and LH-I α probes. On the other hand, mRNA levels for the genes encoding LH-II, PufQ (a possible Mg tetrapyrrole-binding polypeptide) and ORF J (a possible Bchl biosynthesis gene) are not coordinated with the LH-I and RC mRNAs, and show interesting deviations from the pattern of coordinate regulation in several cases (Figs. 2-5, 2-6). For example, although PufQ is encoded by the proximal gene of the puf operon, which also encodes RC-L, RC-M and the LH-I polypeptides, a crtA mutation causes the 3-fold reduction of PufQ mRNA without affecting the mRNA for the distal puf-encoded gene products. The crtA mutant is unable to convert spheroidene to spheroidenone (Fig. 1-5). This defect produces a reduced accumulation of LH-II and LH-I complexes, as well as an impairment in the

photosynthetic growth rate. As the function of the reaction catalyzed by CrtA is not understood, it might be of interest to determine whether the reduction in PufQ mRNA levels in the crtA mutants is due to reduced transcription initiation or decreased mRNA stability of the 5' portion of puf transcripts. Similar experiments would also be appropriate to investigate the 6 to 9-fold reduction in ORF J mRNA levels in a carotenoid mutant (crtI) blocked in phytoene dehydrogenation. As ORF J appears to be required for Bchl biosynthesis, there may exist a previously undetected link between the transcription of Bchl and carotenoid biosynthetic enzymes.

A further experimental result from Chapter 2 shows that increases in cellular light scattering, as a reflection of cell size, are correlated with the absence or partial loss of a functional LH-II complex among the carotenoid mutants. We propose that LH-II requires particular carotenoids for structural stability and/or assembly, and that a post-transcriptional consequence of most carotenoid mutations is the loss or reduction in the amount of LH-II in the photosynthetic membrane, accompanied by morphological defects in membrane formation and partial inhibition of cell division. Abnormal membrane morphologies have been observed in certain R. sphaeroides mutants completely deficient in the LH-II complex (Hunter et al., 1987; Kiley et al., 1988). It would be worthwhile to verify our proposal for the R. capsulatus mutants studied in Chapter 2 by electron microscopy of thin sections of bacterial cells, particularly for the mutants showing only partial loss of the LH-II complex and accumulating colored carotenoids (crtF strains, for example).

As an aside to the main focus of Chapter 2, we have detected a stable 0.4 kb mRNA species, mapped to the 5' end of ORF J (Fig. 2-3C), which is not of sufficient length to encode the entire ORF J gene product. We conclude, by analogy to the puf operon (Adams et al., 1989), that this mRNA represents a relatively stable processing product of a longer, rapidly processed transcript. Based on the high resolution of our mapping of the mRNA species, it should be possible to identify the determinants which confer stability

upon the 3' end of the 0.4 kb mRNA, protecting it from 3' to 5' exonucleolytic degradation. It would also be interesting to test whether the 0.4 kb mRNA directs the synthesis of a functional gene product.

Experiments described in Chapters 3, 4 and 6 have examined the nucleotide sequence and organization of the R. capsulatus carotenoid biosynthesis genes, the phenotype and genotypes of carotenoid biosynthesis mutants, and the regulation of these genes by oxygen tension and light during the shift from dark aerobic to anaerobic photosynthetic growth. Most of the work described in Chapter 3 and a portion of Chapter 7 has been accepted for publication (Armstrong et al., in press), while a portion of Chapter 6 has been submitted for publication (Cook et al., submitted). Chapter 3 describes the nucleotide sequence of a gene cluster containing eight of the nine known R. capsulatus crt genes. The characterization of the ninth gene, crtJ, awaits further studies. A crtJ mutant is blocked before phytoene synthesis (Chapter 4), but we have not yet proposed a biochemical function for the gene product because the mutant accumulates one compound which has not been identified. Biochemical functions have been proposed for the CrtB and CrtE enzymes based on the accumulation of pyrophosphate precursors of phytoene in these strains, as determined using an in vitro phytoene biosynthesis system (Chapter 4). CrtB is proposed to encode the PPPP synthetase, while CrtE is proposed to encode the phytoene synthetase. Chapter 6 examines the regulation of the crt genes.

As neither published carotenoid gene sequences, nor carotenoid enzyme amino acid sequences, are yet available from any other organism, Chapter 3 is perhaps the single most significant portion of the thesis in terms of information that it provides about the carotenoid biosynthetic pathway. Because information from other systems is not available for comparison, one must consider the predicted amino acid sequences of the crt gene products as provisional. Recent results, mentioned briefly in Chapter 7, provide evidence confirming our predicted amino acid translations at least in the cases of the crtB, crtE and crtI gene products, however. Similarly, no other gene sequences are available for

comparison of nucleotide homologies.

The cumulative results of the experiments described in Chapters 3, 4 and 6 suggest the eight genes of the crt gene cluster form at least six operons, crtA, crtI, crtB, crtK, crtDC and crtEF. The results of Giuliano et al. (1988) appear to rule out a crtDC operon, thus leaving crtEF as the only possible polycistronic operon in this region. The ORFs flanking the crt gene cluster may be involved in Bchl biosynthesis and are not cotranscribed with crt genes. The results of Chapter 4 indicate that the transcriptional control sequences for ORF H may overlap substantially with the 3' coding region of crtA. A similar situation may exist with possible overlapping transcription units for crtI and crtB. Possible E. coli-like rho-independent transcription terminators have been found in the nucleotide sequence of the crt gene cluster 3' to crtI, crtK, crtC and crtF. The location of these putative terminators is consistent with the predicted operon structure, although some crt genes may utilize other types of transcription terminators.

The nucleotide sequence of the crt gene cluster identifies a new gene, crtK, which may be involved in the hydration of neurosporene (Fig. 1-5) although this assignment is tentative, and awaits the further characterization of a mutant described by Giuliano et al. (1988). The nucleotide sequence also identifies unusually AT-rich areas at the 5' ends of genes. These regions contain two interesting types of sequences probably involved in transcription: possible E. coli-like σ^{70} promoters 5' to crtD, crtI and ORF J, and a highly conserved palindrome found in the 5' regions of the divergent crtA-crtI, crtD-crtE operons, ORF J and the unlinked puc operon. Very little is known about promoters in purple photosynthetic bacteria and E. coli-like σ^{70} promoters have never been observed 5' to other previously studied Rhodobacter genes (Kiley and Kaplan, 1988). Some of the crt genes may be transcribed by an RNA polymerase using a σ factor similar to that of the major polymerase of E. coli. Fusion of these putative crt promoters to promoter-less indicator genes and assaying for promoter activity, both in E. coli and R. capsulatus, may provide a useful means of assaying the importance of these sequences in transcription

initiation. Introduction of point and deletion mutations into the 5' flanking regions of various crt genes and subsequent conjugation of these constructs into R. capsulatus may also prove an effective method to localize the promoter sequences recognized in vivo.

The discovery of the conserved palindromes is extremely exciting from two standpoints. First, these sequences show very strong similarity to the consensus of the binding sites for a variety of prokaryotic transcriptional factors including both positive and negative regulators (Gicquel-Sanzey and Cossart, 1982). Second, the R. capsulatus crt genes have been repeatedly suggested to show little or no transcriptional regulation in response to environmental factors (Clark et al., 1984; Klug et al., 1985; Zhu and Hearst, 1986; Giuliano et al., 1986), a finding which does not agree with the results presented in Chapter 6. Experiments to assay the biological function of the palindrome could be conducted as described above for the analysis of possible promoter sequences. As we hypothesize that the palindromic motif interacts with a transcriptional factor, an obvious set of experiments, currently in progress in the laboratory, is to identify the protein factor binding to a duplex synthetic oligonucleotide probe corresponding to the consensus palindrome. In vitro studies with the purified protein factor could address the issue of determinants required for protein binding, while in vivo footprinting studies with dimethylsulfate could be used to observe the overall pattern of protein binding in regulatory regions of the crt gene cluster, particularly during the shift from dark aerobic to anaerobic photosynthetic growth. Such a shift, as documented in Chapter 6, leads to the coordinate 2 to 10-fold induction of crtA, crtC, crtD, crtE, crtF, crtK, ORF J and ORF H about 45 to 60 minutes after the shift. We suggest that the observed induction of at least crtA, crtE and ORF J may be partially or wholly mediated by the interaction of a protein factor with the palindromic sequences found 5' to these genes. Although we have not identified the promoter for the strongly regulated crtA gene, we have defined the region within which this promoter must lie by the high resolution mapping of a Tn5.7 insertion mutation located in the crtA-crtI intergenic region, which has no effect on carotenoid

biosynthesis (Chapter 4; Fig. 4-3). The crtA gene has been shown in Chapter 6 to be induced by a reduction of oxygen tension in the growth medium, either in the presence or absence of light. It would also be interesting to identify the role of the palindrome found 5' to the puc operon, encoding the LH-II polypeptides. As LH-II is ultimately the major binding site of carotenoids in the photosynthetic membrane, it is intriguing to speculate that the transcription of the genes encoding certain carotenoid enzymes and the LH-II complex might be regulated by the same transcriptional factor.

The work described in Chapter 6 not only forces a reevaluation of statements in the literature concerning carotenoid gene regulation, but also reveals that under our growth shift conditions the crt genes are induced to the same extent as the genes encoding the RC and LH-I complexes during the adaptation to photosynthetic growth. On the other hand, previous studies have not used gene specific probes to examine crt gene expression. We propose that pigment biosynthesis genes are coordinately induced as a means of rapidly boosting pigment accumulation during the initial stages of photosynthetic development, preceding the maximal induction of the genes encoding pigment-protein complexes. Since not all crt genes are induced, it remains to be shown how the induction of mRNA levels for certain enzymes correlates with the individual enzymatic activities and with the biosynthetic capacity of the entire carotenoid pathway. Some of the future approaches mentioned in the following summary and discussion of Chapter 7 may be helpful in addressing these questions. Our model of temporal regulation of induction for different classes of photosynthesis genes can also be tested by future experiments using probes for known Bchl biosynthesis genes. Our results showing the induction of ORF J and ORF H provide tantalizing evidence that Bchl biosynthesis genes may indeed be transcriptionally regulated, but confirmation awaits a thorough investigation of the functions of the gene products of these ORFs.

Chapter 5 describes the preliminary characterization of the Erwinia herbicola pigment synthesis genes expressed in Escherichia coli, as a second model system for carotenoid

biosynthesis. Prior to the work reported here, it had been speculated but not conclusively demonstrated that the yellow pigments synthesized by E. coli carrying the E. herbicola gene cluster were actually C_{40} carotenoids. We have shown that two well-characterized carotenoid biosynthesis inhibitors, diphenylamine and nicotine, inhibit yellow pigment production in a predictable fashion. Inhibition with either diphenylamine, which blocks phytoene dehydrogenation, or nicotine, which increases the accumulation of hydrocarbon carotenoids, led to the accumulation of a UV absorbing pigment identified by absorption and mass spectroscopy as phytoene, the first C_{40} carotenoid species and an intermediate common to all carotenogenic organisms (Fig. 1-2). The later intermediates and final products of the E. herbicola carotenoid biosynthetic pathway remain to be identified. The detection of pigments in the medium of uninhibited cultures suggests, however, the excretion of either water soluble carotenoproteins or polar carotenoid glycosides, a type of carotenoid derivative often found in nonphotosynthetic bacteria and cyanobacteria (Britton, 1983).

The full exploitation of the E. herbicola model system will provide a wealth of information, and suggests a prodigious number of possible experiments. Perhaps the most valuable experiments will be based on the comparison of amino acid homologies between the R. capsulatus and E. herbicola carotenoid biosynthetic enzymes (see the summary of Chapter 7). On the other hand, preliminary experiments would provide crucial genetic and biochemical support for hypotheses based solely on sequence homologies. For example, since the carotenoid genes are clustered (as in R. capsulatus) and expressed in E. coli (unlike R. capsulatus), it would be a simple procedure to mutagenize the E. herbicola crt gene cluster at specific restriction sites by antibiotic cartridge mutagenesis and to screen the resulting mutants by color phenotype and pigment accumulation. Because E. coli does not normally produce carotenoids, none of the mutations would be expected to be lethal. This approach would probably prove to be the most straightforward route to an elucidation of the E. herbicola carotenoid biosynthetic

pathway. Accumulation of large amounts of intermediates in the mutants should simplify the chemical identification of the pigments. Another useful set of experiments would be to characterize the biochemical defects of the mutants using a cell-free in vitro carotenoid biosynthesis system, as has been done with R. capsulatus (Chapter 4). A further step toward biochemical characterization of the E. herbicola gene products would be the over-expression of the carotenoid biosynthetic enzymes in E. coli, as a means of obtaining purified proteins for production of antibodies or for use in in vitro reconstitution studies. Provided that a full complement of E. herbicola crt mutants can be generated, a particularly interesting set of experiments would involve inter-species in vivo complementation using E. coli strains carrying both R. capsulatus and E. herbicola crt genes simultaneously. Although the R. capsulatus photosynthesis gene cluster carried in E. coli does not direct carotenoid or Bchl pigment synthesis (Marrs, 1981), it is not known whether the pigment biosynthetic genes are actually transcribed. We have shown in Chapter 3 that the crtD and crtI genes, and ORF J are preceded by sequences similar to the consensus E. coli σ^{70} promoter. The transcription of these genes in E. coli can now be tested by, for example, simultaneously introducing both the E. herbicola crt gene cluster with a mutated crtI, and an intact R. capsulatus crtI gene into the same strain of E. coli. Results of the complementation assay would be easily monitored simply by inspection of colony pigmentation.

Chapter 7 describes the properties of the R. capsulatus carotenoid biosynthetic enzymes, based on the amino acid sequences deduced from the nucleotide sequences of the gene (Chapter 3). The most significant finding of this chapter is the amino acid similarity between the CrtI (phytoene dehydrogenase) and CrtD (neurosporene dehydrogenase) enzymes in two regions. The respective N- and C-termini of each protein show 41 and 54 % amino acid similarity over stretches of about 40 amino acids in each case, the most highly conserved region being a hydrophobic domain at the C-terminus. We propose that this region represents a conserved structural or functional feature related

to the carotenoid-dehydrogenase interaction, but not solely to carotenoid binding. In most carotenogenic systems, the enzymatic activities which synthesize phytoene are soluble or peripherally membrane-associated (reviewed in Bramley, 1985). The later activities, from the dehydrogenation of phytoene onwards, are thought to be membrane-bound. The mean hydropathy values of the carotenoid gene products from R. capsulatus do not, however, allow a simple proposal of enzyme organization to be made. Further studies on the isolated enzymes will be necessary to address questions of enzyme localization. The availability of nucleotide and deduced amino acid sequences of the R. capsulatus enzymes now provides a new avenue for their biochemical and immunological characterization, as extensive purification of carotenoid enzymes, particularly those localized on membranes, has to date met with little success. Over-expression of the R. capsulatus enzymes in E. coli should provide large quantities of the proteins for either reconstitution studies to try to assemble a carotenogenic enzyme complex in vitro by mixing the purified components, or for the production of antisera for the immunological characterization of the R. capsulatus enzymes. Possible immunological studies include the inhibition of in vitro carotenoid biosynthesis with antibodies, and the determination of the localization and expression pattern of the enzymes. Because we have shown in Chapter 6 that six of eight carotenoid genes are transcriptionally induced during the adaptation to photosynthetic growth, it would be of interest to follow the accumulation of the gene products using antibodies.

The characterization of both the R. capsulatus and E. herbicola carotenoid biosynthetic enzymes should provide a foundation for studies of eukaryotic carotenogenesis. Preliminary experiments using an antibody raised against an R. capsulatus CrtI (phytoene dehydrogenase) fusion protein suggest that some structural features of this enzyme may be conserved in cyanobacteria, algae and higher plants (Schmidt et al., submitted). Such also appears to be the case not only for the phytoene dehydrogenase, but also for the two preceding enzymes in the carotenoid biosynthetic pathway, PPPP synthetase (CrtB) and phytoene synthetase (CrtE), in a preliminary comparison between deduced amino acid

sequences from R. capsulatus and E. herbicola. Data obtained from these two systems will propel the exploration of eukaryotic carotenoid biosynthesis using the types of approaches mentioned above. By analogy to the relationship between the bacterial photosynthetic RC and the PSII RC of oxygen-evolving photosynthetic organisms, the purple bacterial model system is likely to serve as a stepping stone for the genetic and biochemical characterization of carotenoid biosynthesis in higher organisms.

References

Aagaard J, Sistrom WR (1972) Control of synthesis of reaction center bacteriochlorophyll in photosynthetic bacteria. Photochem Photobiol 15:209-225

Adams CW, Forrest ME, Cohen SN, Beatty JT (1989) Structural and functional analysis of transcriptional control of the Rhodobacter capsulatus puf operon. J Bacteriol 171:473-482

Allen JP, Feher G, Yeates TO, Komiya H, Rees DC (1987a) Structure of the reaction center from Rhodobacter sphaeroides R-26: the cofactors. Proc Nat Acad Sci USA 84:5730-5734

Allen JP, Feher G, Yeates TO, Komiya H, Rees DC (1987b) Structure of the reaction center from Rhodobacter sphaeroides R-26: the protein subunits. Proc Nat Acad Sci USA 84:6162-6166

Allen JP, Feher G, Yeates TO, Komiya H, Rees DC (1988) Structure of the reaction center from Rhodobacter sphaeroides R-26: protein-cofactor (quinones and Fe^{2+}) interactions. Proc Nat Acad Sci USA 85:8487-8491

Armstrong GA, Alberti M, Leach F, Hearst JE (1989) Nucleotide sequence, organization, and nature of the protein products of the carotenoid biosynthesis gene cluster of Rhodobacter capsulatus. Mol Gen Genet, in press

Auerswald EA, Ludwig G, Schaller H (1980) Structural analysis of Tn5. Cold Spring Harbor Symp Quant Biol 45:107-113

Balsalobre JM, Ruiz-Vazquez RM, Murillo FJ (1987) Light induction of gene expression in Myxococcus xanthus. Proc Nat Acad Sci USA 84:2359-2362

Bauer CE, Young DA, Marrs, BL (1988) Analysis of the Rhodobacter capsulatus puf operon. J Biol Chem 263:4820-4827

Bauer CE, Marrs BL (1988) Rhodobacter capsulatus puf operon encodes a regulatory protein (PufQ) for bacteriochlorophyll biosynthesis. Proc Nat Acad Sci USA 85:7074-7078.

Beck CF, Warren RAJ (1988) Divergent promoters, a common form of gene organization. Microbiol Rev 52:318-326

Belasco JG, Beatty JT, Adams CW, Von Gabain A, Cohen SN (1985) Differential expression of photosynthesis genes in R. capsulata results from segmental differences in stability within the polycistronic rxcA transcript. Cell 40:171-181

Berg DE, Weiss A, Crossland L (1980) The polarity of Tn5 insertion mutations in Escherichia coli. J Bacteriol 142:439-446

Beyer P, Weiss G, Kleinig H (1985) Solubilization and reconstitution of the membrane-bound carotenogenic enzymes from daffodil chromoplasts. Eur J Biochem 153:341-346

Biel AJ, Marrs BL (1983) Transcriptional regulation of several genes for bacteriochlorophyll biosynthesis in Rhodopseudomonas capsulata in response to oxygen. J Bacteriol 156:686-694

Biel AJ, Marrs BL (1985) Oxygen does not directly regulate carotenoid biosynthesis in Rhodopseudomonas capsulata. J Bacteriol 162:1320-1321

Bolivar F, Rodriguez RL, Greene PJ, Betlach MC, Heynecker HL, Boyer HW (1977) Construction and characterization of new cloning vehicles: II. A multipurpose cloning system. Gene 2:95-113

Bolivar F (1978) Construction and characterization of new cloning vehicles: III. Derivatives of plasmid pBR322 carrying the EcoRI sites for selection of EcoRI generated recombinant DNA molecules. Gene 4:121-136

Bramley P (1985) The in vitro biosynthesis of carotenoids. In: Paoletti R, Kritchensky D (eds) Advances in Lipid Research. vol 21, Academic Press, Orlando, Florida, pp 243-279

Bramley PM, Taylor RF (1985) The solubilization of carotenogenic enzymes of Phycomyces blakesleeanus. Biochim Biophys Acta 839:155-160

Bramley PM, Mackenzie A (1988) The regulation of carotenoid biosynthesis. In: Horecker BL, Stadtman ER (eds) Current Topics in Cellular Regulation. vol 29, Academic Press, London, United Kingdom, pp 291-343

Britton G (1983) The Biochemistry of Natural Pigments. Cambridge University Press, Cambridge, United Kingdom

Britton G (1985) General Carotenoid Methods. Methods Enzymol 111:113-149

Brunisholz RA, Zuber H, Valentine J, Lindsay JG, Woolley KJ, Cogdell RJ (1986) The membrane location of the B890-complex from Rhodospirillum rubrum and the effect of carotenoid on the conformation of its two apoproteins exposed at the cytoplasmic surface. Biochim Biophys Acta 849:295-303

Buck M, Miller S, Drummond M, Dixon R (1986) Upstream activator sequences are present in the promoters of nitrogen fixation genes. Nature 320:374-378

Bullerjahn GS, Sherman LA (1986) Identification of a carotenoid-binding protein in the cytoplasmic membrane from the heterotrophic cyanobacterium Synechocystis sp. strain PCC6714. J Bacteriol 167:396-399

Burgess DG, Taylor WC (1988) The chloroplast affects the transcription of a nuclear gene family. Mol Gen Genet 214:89-96

Camara B, Bardat F, Moneger R (1982) Sites of biosynthesis of carotenoids in Capsicum chromoplasts. Eur J Biochem 127:255-258

Cerda-Olmedo E (1987) Carotene. In: Cerda-Olmedo E, Lipson E (eds) Phycomyces. Cold Spring Harbor Laboratory Press, Cold Spring Harbor, New York, pp 199-222.

Chadwick BW, Frank HA (1986) Electron-spin resonance studies of carotenoids incorporated into reaction centers of Rhodobacter sphaeroides R26.1. Biochim Biophys Acta 851:257-266

Chen CY, Beatty JT, Cohen SN, Belasco JG (1988) An intercistronic stem-loop structure functions as an mRNA decay terminator necessary but insufficient for puf mRNA stability. Cell 52:609-619

Chen EY, Seeburg H (1985) Laboratory methods--supercoil sequencing: a fast and simple method for sequencing plasmid DNA. DNA 4:165-170

Clark WG, Davidson E, Marrs BL (1984) Variation of levels of mRNA coding for antenna and reaction center polypeptides in Rhodopseudomonas capsulata in response to changes in oxygen concentration. J Bacteriol 157:945-948

Clayton RK (1966) Spectroscopic analysis of bacteriochlorophylls in vitro and in vivo. Photochem Photobiol 5:669-677

Cogdell RJ, Frank HA (1987) How carotenoids function in photosynthetic bacteria. Biochim Biophys Acta 895:63-79

Cohen-Bazire G, Sistrom WR, Stanier RY (1957) Kinetic studies of pigment synthesis by non-sulfur purple bacteria. J Cell Comp Physiol 49:25-68

Cook DN, Armstrong GA, Hearst JE (1989) Induction of anaerobic gene expression in Rhodobacter capsulatus is not accompanied by a local change in chromosomal supercoiling as measured by a novel assay. J Bacteriol, submitted

Daldal F, Chen S, Applebaum J, Davidson E, Prince RC (1986) Cytochrome c_2 is not essential for photosynthetic growth of Rhodopseudomonas capsulata. Proc Nat Acad Sci USA 83:2012-2016

Davidson E, Daldal F (1987) fbc operon, encoding the Rieske Fe-S protein, cytochrome b, and cytochrome c_1 apoproteins previously described from Rhodopseudomonas sphaeroides, is from Rhodopseudomonas capsulata. J Mol Biol 195:25-29

Davies BH (1985) Carotenoid metabolism in animals: a biochemist's view. Pure Appl Chem 57:679-684

Deisenhofer J, Epp O, Miki K, Huber R, Michel H (1984) X-ray structure analysis of a membrane protein complex: electron density map at 3 Å resolution and a model of the chromophores of the photosynthetic reaction center from Rhodopseudomonas viridis. J Mol Biol 180:385-398

Deisenhofer J, Epp O, Miki K, Huber R, Michel H (1985) Structure of the protein subunits in the photosynthetic reaction centre of Rhodopseudomonas viridis at 3 Å resolution. Nature 318:618-624

Deisenhofer J, Michel H (1988) In: Breton J, Vermeglio A (eds) The Photosynthetic Bacterial Reaction Center NATO ASI Series A: Life Sciences. Plenum Press, New York, New York, pp 1-4

Ditta G, Stanfield S, Corbin D, Helinski DR (1980) Broad host range DNA cloning system for gram-negative bacteria: construction of a gene bank of Rhizobium meliloti. Proc Nat Acad Sci USA 77:7347-7351

Diverse-Pierluissi M, Krogmann DW (1988) A zeaxanthin protein from Anacystis nidulans. Biochim Biophys Acta 933:372-377

Dogbo O, Laferriere A, d'Harlingue A, Camara B (1988) Carotenoid biosynthesis: isolation and characterization of a bifunctional enzyme catalyzing the synthesis of phytoene. Proc Nat Acad Sci USA 85:7054-7058

Dörge B, Klug G, Drews G (1987) Formation of the B800-850 antenna pigment-protein complex in the strain GK2 of Rhodobacter capsulatus defective in carotenoid synthesis. Biochim Biophys Acta 892:68-74

Drews G (1985) Structure and functional organization of light-harvesting complexes and photochemical reaction centers in membranes of phototrophic bacteria. Microbiol Rev 49:59-70

Drews G, Oelze J (1981) Organization and differentiation of membranes of phototrophic bacteria. In: Rose AH, Morris JG (eds) Advances in Microbial Physiology. vol 22, pp 1-92

El-Jack M, Mackenzie A, Bramley PM (1988) The photoregulation of carotenoid biosynthesis in Aspergillus giganteus mut. alba. Planta 174:59-66

Evans MB, Cogdell RJ, Britton G (1988) Determination of the bacteriochlorophyll:carotenoid ratios of the B890 antenna complex of Rhodospirillum rubrum and the B800-850 complex of Rhodobacter sphaeroides. Biochim Biophys Acta 935:292-298

Frickel F (1985) Retinoids: an overview of some natural carotenoid metabolites and their synthetic analogs. Pure Appl Chem 57:709-716

Friedman AM, Long SR, Brown SE, Buikema WJ, Ausubel FM (1982) Construction of a broad host range cosmid cloning vector and its use in the genetic analysis of Rhizobium meliloti. Gene 18:289-296

Gabellini N, Sebald W (1986) Nucleotide sequence and transcription of the fbc operon from Rhodopseudomonas sphaeroides. Eur J Biochem 154:569-579

Gamble PE, Mullet JE (1986) Inhibition of carotenoid accumulation and abscisic acid biosynthesis in fluridone-treated dark-grown barley. Eur J Biochem 160:117-121

Gantotti BV, Beer SV (1982) Plasmid-borne determinants of pigmentation and thiamine prototrophy in Erwinia herbicola. J Bacteriol 151:1627-1629

Gicquel-Sanzey B, Cossart P (1982) Homologies between different procaryotic DNA-binding regulatory proteins and between their sites of action. EMBO J 1:591-595

Giuliano G, Pollock D, Scolnik PA (1986) The crtI gene mediates the conversion of phytoene into colored carotenoids in Rhodopseudomonas capsulata. J Biol Chem 261:12925-12929

Giuliano G, Pollock D, Stapp H, Scolnik PA (1988) A genetic-physical map of the Rhodobacter capsulatus carotenoid biosynthesis gene cluster. Mol Gen Genet 213:78-83

Golecki JR, Schumacher A, Drews G (1980) The differentiation of the photosynthetic apparatus and the intracytoplasmic membrane in cells of Rhodopseudomonas capsulata upon variation of light intensity. Eur J Cell Biol 23:1-5

Goodwin TW (1980) The Biochemistry of the Carotenoids, vol 1, Plants. Chapman and Hall, Ltd., New York, New York

Gray ED (1967) Studies on the adaptive formation of photosynthetic structures in Rhodopseudomonas spheroides: I. Synthesis of macromolecules. Biochim Biophys Acta 138:550-563

Griffiths M, Stanier RY (1956) Some mutational changes in the photosynthetic pigment system of Rhodopseudomonas spheroides. J Gen Microbiol 14:698-715

Grumbach KH (1983) Effect of phytochrome on the biosynthesis of acyclic and cyclic carotenoids in higher plants. Photochem Photobiol 38:717-721

Gussin GN, Ronson CW, Ausubel FM (1986) Regulation of nitrogen fixation genes. Annu Rev Genet 20:567-591

Harding RW, Shropshire W (1980) Photocontrol of carotenoid biosynthesis. Annu Rev Plant Physiol 31:217-238

Hunter CN, Pennoyer JD, Sturgis JN, Farrelly D, Niederman RA (1987) Oligomerization states and associations of light-harvesting pigment-protein complexes of Rhodobacter sphaeroides as analyzed by lithium dodecyl sulfate-polyacrylamide gel electrophoresis. Biochemistry 27:3459-3467

Hunter CN, Van Grondelle R, Olsen JD (1989) Photosynthetic antenna proteins: 100 ps before photochemistry starts. Trends Biochem Sci 14:72-76

Imhoff JF, Trüper HG, Pfennig N (1984) Rearrangements of the species and genera of the phototrophic 'purple nonsulfur bacteria'. Int J Syst Bacteriol 34:340-343

Johnson JA, Wong WKR, Beatty JT (1986) Expression of cellulase genes in Rhodobacter capsulatus by the use of plasmid expression vectors. J Bacteriol 167:604-610

Jones BL, Porter JW (1986) Biosynthesis of carotenes in higher plants. CRC Crit Rev Plant Sci 3:295-324

Jones OTG (1978) Biosynthesis of porphyrins, hemes, and chlorophylls. In: Clayton RK, Sistrom WR (eds) The Photosynthetic Bacteria. Plenum Press, New York, New York, pp 751-778

Kaufmann N, Reidl HH, Golecki JR, Garcia AF, Drews G (1982) Differentiation of the membrane system in cells of Rhodopseudomonas capsulata after transition from chemotrophic to phototrophic growth conditions. Arch Microbiol 131:313-322

Kaplan S, Marrs BL (1986) Proposed nomenclature for photosynthetic procaryotes. ASM News 52:242

Keister DL (1978) Respiration versus photosynthesis. In: Clayton RK, Sistrom WR (eds) The Photosynthetic Bacteria. Plenum Press, New York, New York, pp 849-856

Kiley PJ, Kaplan S (1987) Cloning, DNA sequence and expression of the Rhodobacter sphaeroides light-harvesting B800-850-α and B800-850-β genes. J Bacteriol 169:3268-3275

Kiley PJ, Kaplan S (1988) Molecular genetics of photosynthetic membrane biosynthesis in Rhodobacter sphaeroides. Microbiol Rev 52:50-69

Kiley PJ, Varga A, Kaplan S (1988) Physiological and structural analysis of light-harvesting mutants of Rhodobacter sphaeroides. J Bacteriol 170:1103-1115

Kläui H (1982) Industrial and commercial uses of carotenoids. In: Britton G, Goodwin TW (eds) IUPAC Carotenoid Chemistry and Biochemistry. Pergamon Press, Oxford, United Kingdom, pp 309-317

Klug G, Kaufmann N, Drews G (1984) The expression of genes encoding proteins of B800-850 antenna pigment complex and ribosomal RNA of Rhodopseudomonas capsulata. FEBS Lett. 177:61-65

Klug G, Kaufmann N, Drews G (1985) Gene expression of pigment-binding proteins of the bacterial photosynthetic apparatus: transcription and assembly in the membrane of Rhodopseudomonas capsulata. Proc Nat. Acad Sci USA 82:6485-6489

Klug G, Liebetanz R, Drews G (1986) The influence of bacteriochlorophyll biosynthesis of the formation of pigment-binding proteins and assembly of pigment protein complexes in Rhodopseudomonas capsulata. Arch Microbiol 146:284-291

Klug G, Cohen SN (1988) Pleiotropic effects of localized Rhodobacter capsulatus puf operon deletions on production of light-absorbing pigment-protein complexes. J Bacteriol 170:5814-5821

Komiya H, Yeates TO, Rees DC, Allen JP, Feher G (1988) Structure of the reaction center from Rhodobacter sphaeroides R-26 and 2.4.1: symmetry relations and sequence comparisons between different species. Proc Nat Acad Sci USA 85:9012-9016

Koyama Y, Kanaji M, Shimamura T (1988) Configurations of neurosporene isomers isolated from the reaction center and the light-harvesting complex of Rhodobacter sphaeroides G1C. A resonance Raman, electronic absorption, and ^{1}H-NMR study. Photochem Photobiol 48:107-114

Kramer HJM, Van Grondelle R, Hunter CN, Westerhuis WHJ, Amesz J (1984) Pigment organization of the B800-850 antenna complex of Rhodopseudomonas sphaeroides. Biochim Biophys Acta 765:156-165

Kreuz K, Beyer P, Kleinig H (1982) The site of carotenogenic enzymes in chromoplasts from Narcissus pseudonarcissus L. Planta 154:66-69

Krinsky NI (1979) Carotenoid protection against oxidation. Pure Appl Chem 51:649-660

Krinsky NI, Deneke SM (1982) Interaction of oxygen and oxy-radicals with carotenoids. J Nat Cancer Inst 69:205-209

Kritsky MS, Sokolovsky VY, Belozerskaya TA, Chernysheva EK (1982) Relationship between cyclic AMP levels and accumulation of carotenoid pigments in Neurospora crassa. Arch Microbiol 133:206-208

Kyte J, Doolittle RF (1982) A simple method for displaying the hydropathic character of a protein. J Mol Biol 157:105-132

Liaaen-Jensen S, Cohen-Bazire G, Stanier RY (1961) Biosynthesis of carotenoids in purple bacteria: a reevaluation based on considerations of chemical structure. Nature 192:1168-1172

Lutz M, Szponarski W, Berger G, Robert B, Neumann JM (1987) The stereoisomerism of bacterial, reaction-center-bound carotenoids revisited: an electronic absorption, resonance Raman and ^{1}H-NMR study. Biochim Biophys Acta 894:423-433

Makman RS, Sutherland EQ (1965) Adenosine 3', 5'-phosphate in Escherichia coli. J Biol Chem 240:1309-1314

Maniatis T, Fritsch EF, Sambrook, J (1982) Molecular Cloning, A Laboratory Manual. Cold Spring Harbor Laboratory Press, Cold Spring Harbor, New York

Manwaring J, Pullin CA, Evans EH, Britton G (1978) Alteration in concentration of carotenoids in Rhodopseudomonas capsulatus transferred from dark to light growth. Biochem Soc Trans 6:1041-1044

Marrs B (1981) Mobilization of the genes for photosynthesis from Rhodopseudomonas capsulata by a promiscuous plasmid. J Bacteriol 146:1003-1012

Marrs BL (1982) Genetic analysis of carotenogenesis in Rhodopseudomonas capsulata. In: Britton G, Goodwin, TW (eds) IUPAC Carotenoid Chemistry and Biochemistry. Pergamon Press, New York, New York, pp 273-277

Masepohl B, Klipp W, Pühler A (1988) Genetic characterization and sequence analysis of the duplicated nifA/nifB region of R. capsulatus. Mol Gen Genet 212:27-37

Mathews-Roth MM (1982) Antitumor activity of beta-carotene, canthaxanthin and phytoene. Oncology 39:33-37

Mathews-Roth MM (1987) Photoprotection by carotenoids. Federation Proc 46:1890-1893

McClure WR (1985) Mechanism and control of transcription initiation in prokaryotes. Annu Rev Biochem 54:171-204

Meagher RB, Tait RC, Betlach M, Boyer HW (1977) Protein expression in E. coli minicells by recombinant plasmids. Cell 10:521-536

Messing J, Crea R, Seeburg PH (1981) A system for shotgun DNA sequencing. Nucl Acids Res 9:309-321

Michel H, Epp O, Deisenhofer J (1986) Pigment-protein interactions in the photosynthetic reaction centre from Rhodopseudomonas viridis. EMBO J 5:2445-2451

Michel H, Deisenhofer J (1988) Relevance of the photosynthetic reaction center from purple bacteria to the structure of photosystem II. Biochemistry USA 27:1-7

Nelson MA, Morelli G, Carattoli A, Romano N, Macino G (1989) Molecular cloning of a Neurospora crassa carotenoid biosynthetic gene (albino-3) regulated by blue light and the products of the white collar genes. Mol Cell Biol 9:1271-1276

Nussinov R, Barber A, Maizel JV (1987) The distributions of nucleotides near bacterial transcription initiation and termination sites show distinct signals that may affect DNA geometry. J Mol Evol 26:187-197

Orser C, Staskawicz BJ, Panopoulos N, Dahlbeck D, Lindow S (1985) Cloning and expression of bacterial ice nucleation genes in Escherichia coli. J Bacteriol 164:359-366

Patel NJ, Britton G, Goodwin TW (1983) Use of deuterium labelling from deuterium oxide to demonstrate carotenoid transformations in photosynthetic bacteria. Biochim Biophys Acta 760:92-96

Pemberton JM, Harding CM (1986) Cloning of carotenoid biosynthesis genes from Rhodopseudomonas sphaeroides. Curr Microbiol 14:25-29

Pemberton JM, Harding CM (1987) Expression of Rhodopseudomonas sphaeroides carotenoid photopigment genes in phylogenetically related nonphotosynthetic bacteria. Curr Microbiol 15:67-71

Perry KL, Simonitch TA, Harrison-Lavoie KJ, Liu ST (1986) Cloning and regulation of Erwinia herbicola pigment genes. J Bacteriol 168:607-612

Pitt GAJ (1971) Vitamin A. In: Isler O, Gutmann H, Solms U (eds) Carotenoids. Birkheuser Verlag, Basel, Switzerland, pp 717-742

Platt T (1986) Transcription termination and the regulation of gene expression. Annu Rev Biochem 55:339-372

Pustell J, Kafatos F (1982) A convenient and adaptable package of DNA sequence analysis programs for microcomputers. Nucl Acids Res 10:51-59

Qureshi AA, Barnes FJ, Semmler EJ, Porter JW (1973) Biosynthesis of prelycopersene pyrophosphate and lycopersene by squalene synthetase. J Biol Chem 218:2755-2767

Pascal MC, Bonnefoy V, Fons M, Chippaux M (1986) Use of gene fusions to study the expression of fnr, the regulatory gene of anaerobic electron transfer in Escherichia coli. FEMS Microbiol Lett 36:35-40

Raibaud O, Schwartz M (1984) Positive control of transcription initiation in bacteria. Annu Rev Genet 18:173-206

Reznikoff WS, Siegele DA, Cowing DW, Gross C (1985) The regulation of transcription initiation in bacteria. Annu Rev Genet 19:355-387

Ridley SM (1982) Carotenoids and herbicide action. In: Britton G, Goodwin TW (eds) IUPAC Carotenoid Chemistry and Biochemistry. Pergamon Press, Oxford, United Kingdom, pp 353-369

Riordan JF, McElvaney KD, Borders CL, Jr. (1977) Arginyl residues: anion recognition sites in enzymes. Science 195:884-886

Sandmann G, Bramley P (1985) Carotenoid biosynthesis by Aphanocapsa homogenates coupled to a phytoene-generating system from Phycomyces blakesleeanus. Planta 164:259-263

Sanger F, Nicklen S, Coulson AR (1977) DNA sequencing with chain terminating inhibitors. Proc Nat Acad Sci USA 74:5463-5467

Schloss JA, Silflow CD, Rosenbaum JL (1984) mRNA abundance changes during flagellar regeneration in Chlamydomonas reinhardtii. Mol Cell Biol 4:424-434

Schmidt A, Sandmann G, Armstrong GA, Hearst JE, Böger P (1989) Expression of a fusion gene construct and immunological detection of phytoene desaturase in algae and higher plants. Eur J Biochem, submitted

Schmidt K (1978) Biosynthesis of carotenoids. In: Clayton RK, Sistrom WR (eds) The Photosynthetic Bacteria. Plenum Press, New York, New York, pp 729-750

Schultz JE, Weaver PF (1982) Fermentation and anaerobic respiration by Rhodospirillum rubrum and Rhodopseudomonas capsulata. J Bacteriol 149:181-190

Schumacher A, Drews G (1978) The formation of bacteriochlorophyll-protein complexes of the photosynthetic apparatus of Rhodopseudomonas capsulata during early stages of development. Biochim Biophys Acta 501:183-194

Schumann J, Waitches G, Scolnik P (1986) A DNA fragment hybridizing to a nif probe in Rhodobacter capsulatus is homologous to a 16 S rRNA gene. Gene 48:79-90

Schwenker U, St-Onge M, Gingras G (1974) Chemical and physical properties of a carotenoprotein from Rhodospirillum rubrum. Biochim Biophys Acta 351:246-260

Scolnik PA, Marrs BL (1987) Genetic research with photosynthetic bacteria. Annu Rev Microbiol 41:703-726

Scolnik PA, Walker MA, Marrs BL (1980a) Biosynthesis of carotenoids derived from neurosporene in Rhodopseudomonas capsulata. J Biol Chem 255:2427-2432

Scolnik PA, Zannoni D, Marrs BL (1980b) Spectral and functional comparisons between the carotenoids of the two antenna complexes of Rhodopseudomonas capsulata. Biochim Biophys Acta 593:230-240

Segen BJ, Gibson KD (1971) Deficiencies of chromatophore proteins in some mutants of Rhodopseudomonas spheroides with altered carotenoids. J Bacteriol 105:701-709

Sharp PM, Li W-H (1986) Codon usage in regulatory genes in Escherichia coli does not reflect selection for 'rare' codons. Nucl Acids Res 14:7737-7749

Shaw DJ, Rice DW, Guest JR (1983) Homology between CAP and Fnr, a regulatory protein of anaerobic respiration in Escherichia coli. J Mol Biol 166:241-247

Shine J, Dalgarno L (1974) The 3'-terminal sequence of Escherichia coli 16S ribosomal RNA: complementarity to nonsense triplets and ribosome binding sites. Proc Nat Acad Sci USA 71:1342-1346

Shneour EA (1962) The source of oxygen in Rhodopseudomonas spheroides carotenoid pigment conversion. Biochim Biophys Acta 65:510-511

Siefermann-Harms D (1985) Carotenoids in photosynthesis. I. Location in photosynthetic membranes and light-harvesting function. Biochim Biophys Acta 811:325-355

Sistrom WR (1978) Control of antenna pigment components. In: Clayton RK, Sistrom WR (eds) The Photosynthetic Bacteria. Plenum Press, New York, New York, pp 841-848

Sistrom WR, Griffiths M, Stanier RY (1956) The biology of a photosynthetic bacterium which lacks colored carotenoids. J Cell Comp Physiol 48:473-515

Stewart V (1988) Nitrate respiration in relation to facultative metabolism in Enterobacteria. Microbiol Rev 52:190-232

Stormo GD (1986) Translation initiation. In: Reznikoff W, Gold L (eds) Maximizing Gene Expression. Butterworths, Stoneham, Massachusetts, pp 195-224

Sunada KV, Stanier RY (1965) Observations of the pathway of carotenoid synthesis in Rhodopseudomonas. Biochim Biophys Acta 107:38-43

Sweet RM, Eisenberg D (1983) Correlation of sequence hydrophobicities measures similarity in three-dimensional protein structure. J Mol Biol 171:479-488

Tadros MH, Dierstein R, Drews G (1984) Occurrence of the bacteriochlorophyll-binding polypeptides B870α and B800-B850α in the mutant strains Y5 and Ala$^+$ of Rhodopseudomonas capsulata, which are defective in formation of the light-harvesting complexes B870 and B800-850, respectively. Z Naturforsch 39c:922-926

Taremi SS, Violette CA, Frank HA (1989) Transient optical spectroscopy of the reaction center from Rhodobacter sphaeroides. Biochim Biophys Acta 973:86-92

Taylor DP, Cohen SN, Clark WG, Marrs BL (1983) Alignment of the genetic and restriction maps of the photosynthesis region of the Rhodopseudomonas capsulata chromosome by a conjugation-mediated marker rescue technique. J Bacteriol 154:580-590

Trüper HG, Pfennig N (1978) Taxonomy of the Rhodospirillales. In: Clayton RK, Sistrom WR (eds) The Photosynthetic Bacteria. Plenum Press, New York, New York, pp 19-27

Tuveson RW, Larson RA, Kagan J (1988) Role of cloned carotenoid genes expressed in Escherichia coli in protecting against inactivation by near-UV light and specific phototoxic molecules. J Bacteriol 170:4675-4680

Unden G, Guest JR (1985) Isolation and characterization of the Fnr protein, the transcriptional regulator of anaerobic electron transport in Escherichia coli. Eur J Biochem 146:193-199

Weaver PF, Wall JD, Gest H (1975) Characterization of Rhodopseudomonas capsulata. Arch Microbiol 105:207-216

Webster GD, Cogdell RJ, Lindsay GJ (1980) The location of the carotenoid in the B800-850 light-harvesting pigment-protein complex from Rhodopseudomonas capsulata. FEBS Lett 111:391-394

Wehrli W, Knüsel F, Schmid K, Staehelin M (1968) Interaction of rifamycin with bacterial RNA polymerase. Proc Nat Acad Sci USA 61:667-673

Wilson AC, Ochman H, Prager EM (1987) Molecular time scale for evolution. Trends Genet 3:241-247.

Yanisch-Perron C, Vieira J, Messing J (1985) Improved M13 cloning vectors and host strains: nucleotide sequences of the M13mp18 and pUC19 vectors. Gene 33:103-119

Yeates TO, Komiya H, Rees DC, Allen JP, Feher G (1987) Structure of the reaction center from Rhodobacter sphaeroides R-26: membrane-protein interactions. Proc Nat Acad Sci USA 84:6438-6442

Yeates TO, Komiya H, Chirino A, Rees DC, Allen JP, Feher G (1988) Structure of the reaction center from Rhodobacter sphaeroides R-26 and 2.4.1: protein-cofactor (bacteriochlorophyll, bacteriopheophytin, and carotenoid) interactions. Proc Nat Acad Sci USA 85:7993-7997

Yen HC, Marrs B (1976) Map of genes for carotenoid and bacteriochlorophyll biosynthesis in Rhodopseudomonas capsulata. J Bacteriol 126:619-629

Yen HC, Marrs BL (1977) Growth of Rhodopseudomonas capsulata under anaerobic dark conditions with dimethylsulfoxide. Arch Biochem Biophys 181:411-418

Youvan DC, Elder JT, Sandlin DE, Zsebo K, Alder DP, Panopoulos NJ, Marrs BL, Hearst JE (1982) R-prime site-directed transposon Tn7 mutagenesis of the photosynthetic apparatus in Rhodopseudomonas capsulata. J Mol Biol 162:17-41

Youvan DC, Hearst JE, Marrs BL (1983) Isolation and characterization of enhanced fluorescence mutants of Rhodopseudomonas capsulata. J Bacteriol 154:748-755

Youvan DC, Bylina EJ, Alberti M, Begusch H, Hearst JE (1984a) Nucleotide and deduced polypeptide sequences of the photosynthetic reaction-center, B870 antenna, and flanking polypeptides from R. capsulata. Cell 37:949-957

Youvan DC, Alberti M, Begusch H, Bylina EJ, Hearst JE (1984b) Reaction center and light-harvesting genes from Rhodopseudomonas capsulata. Proc Nat Acad Sci USA 81:189-192

Youvan DC, Ismail S (1985) Light-harvesting II (B800-B850 complex) structural genes from Rhodopseudomonas capsulata. Proc Nat Acad Sci USA 82:58-62

Yu PL, Hohn B, Falk H, Drews G (1982) Molecular cloning of the ribosomal RNA genes of the photosynthetic bacterium Rhodopseudomonas capsulata. Mol Gen Genet 188:392-398

Zhu YS, Kaplan S (1985) Effects of light, oxygen, and substrates on steady-state levels of mRNA coding for ribulose-1,5-bisphosphate carboxylase and light-harvesting and reaction center polypeptides in Rhodopseudomonas sphaeroides. J Bacteriol 162:925-932

Zhu YS, Hearst JE (1986) Regulation of the expression of the genes for light-harvesting antenna proteins LH-I and LH-II; reaction center polypeptides RC-L, RC-M, and RC-H; and enzymes of bacteriochlorophyll and carotenoid biosynthesis in Rhodobacter capsulatus by light and oxygen. Proc Nat Acad Sci USA 83:7613-7617

Zhu YS, Cook DN, Leach F, Armstrong GA, Alberti M, Hearst JE (1986) Oxygen-regulated mRNAs for light-harvesting and reaction center complexes and for bacteriochlorophyll and carotenoid biosynthesis in Rhodobacter capsulatus during the shift from anaerobic to aerobic growth. J Bacteriol 168:1180-1188

Zhu YS, Hearst JE (1988) Transcription of oxygen-regulated photosynthesis genes requires DNA gyrase in Rhodobacter capsulatus. Proc Nat Acad Sci USA 85:4209-4213

Zsebo KM, Wu F, Hearst JE (1984) Tn5.7 construction and physical mapping of pRPS404 containing photosynthetic genes from Rhodopseudomonas capsulata. Plasmid 11:182-184

Zsebo KM, Hearst JE (1984) Genetic-physical mapping of a photosynthetic gene cluster from R. capsulata. Cell 37:937-947

Zucconi AP, Beatty JT (1988) Posttranscriptional regulation by light of the steady-state levels of mature B800-850 light-harvesting complexes in Rhodobacter capsulatus. J Bacteriol 170:877-882